THE ROLE OF Kv3.3 VOLTAGE-GATED POTASSIUM CHANNEL EXPRESSION IN CEREBELLAR PURKINJE CELLS IN MOTOR COORDINATION

APPROVED BY SUPERVISORY COMMITTEE

Rolf H. Joho, Ph.D.

David W. Self, Ph.D.

Ege T. Kavalali, Ph.D.

Joachim Herz, M.D.

DEDICATION

I would like to dedicate this work to those who have suffered with depression, addictions, or intractable pain and inspired me to devote my career, of which this work is a part, to eventually elucidate with precision the neural reward/aversion circuitry that underlies these afflictions to allow rational development of potent, specific, innovative molecular therapeutics to abolish them -and the societal ills that result. Liberated from these impediments, humanity can turn its attention to peacefully reaching its entelechy and enjoy life to the fullest.

ACKNOWLEDGMENTS

I thank my committee members, Drs. Joho, Kavalali, Self and Herz, previous Joho Lab members and those listed as coauthors or acknowledged in publications arising from this work. I also thank my first laboratory mentor at Columbia, Dr. Gareth Tibbs, for my initial training in electrophysiology, as well as Drs. Jay Gibson and Felipe Espinosa for further training at Southwestern. I thank Drs. Arvind Kumar, Gandham Mahendra, Richard Lu and Mr. Tao Yue for training in molecular biology. I thank my parents for their unerring, generous support of a high quality education as well as nurturing my interests in science, technological innovation and nature. I thank Annemarie and George Roeper for founding the humanistic Roeper School, which gave my education a solid foundation along with an equally important sense of responsibility to use that education to resolve challenging problems facing humanity.

THE ROLE OF Kv3.3 VOLTAGE-GATED POTASSIUM CHANNEL EXPRESSION IN CEREBELLAR PURKINJE CELLS IN MOTOR COORDINATION

by

EDWARD CLIFTON HURLOCK IV

DISSERTATION / THESIS

Presented to the Faculty of the Graduate School of Biomedical Sciences

The University of Texas Southwestern Medical Center at Dallas

In Partial Fulfillment of the Requirements

For the Degree of

DOCTOR OF PHILOSOPHY

The University of Texas Southwestern Medical Center at Dallas

Dallas, Texas

December, 2008

THE ROLE OF Kv3.3 VOLTAGE-GATED POTASSIUM CHANNEL EXPRESSION IN CEREBELLAR PURKINJE CELLS IN MOTOR COORDINATION

Edward Clifton Hurlock IV, Ph.D.

The University of Texas Southwestern Medical Center at Dallas, 2008

Rolf Hans Joho, Ph.D.

I examined the role of the Kv3.3 voltage-gated potassium channel (Kv) subunit encoded by the *Kcnc3* gene in cerebellar Purkinje cells in determining the properties of complex spikes and in motor coordination. Kv3 channels (Kv3.1-Kv3.4) enable high-frequency firing by activating and deactivating rapidly during and after action potentials, respectively. Kv3.3 subunits are expressed in distinct neuronal cell-types in regions throughout the CNS including the cerebellum, an area important for motor control. *Kcnc3*-null mice exhibit a reduced frequency and broadening of spikes in Purkinje cells as well as ataxia, as in spinocerebellar ataxia type 13 (*SCA13*) patients who carry mutations in *KCNC3*. In contrast to Purkinje cells, in other neuronal cell types Kv3.3 is co-expressed with

considerable levels of other Kv3 subunits that potentially complement the loss of Kv3.3, suggesting that Purkinje cellular Kv3.3 function may be important for motor coordination. I restored expression of the Kv3.3b splice variant specifically in Purkinje cells by crossing transgenic mice that express Kv3.3b under the control of the tetracycline transactivator with a line expressing the latter exclusively in Purkinje cells on a *Kcnc3*-null background. Whole-cell recordings in slices at the resting potential of complex spikes in Purkinje neurons revealed weakened bursts but lengthened simple spike pauses thereafter in *Kcnc3*-null mice. Restoration of Kv3.3 completely rescued all spike parameters and sufficed to rescue motor coordination measured by counting slips traversing a 1-cm beam and recording lateral deviation of gait on a force plate actometer. The *Kcnc3*-null mice heterozygous for *Kcnc1* were partially rescued. Gait analysis indicated the ataxia arises from hypermetria not gait ataxia. When *Kcnc1* alleles are additionally ablated gait ataxia appears. Spikes in large, glutamatergic deep cerebellar nuclear (DCN) neurons, which express all four Kv3 units, broaden concurrently, but remain largely normal in *Kcnc3*-null mice, suggesting functional redundancy here could underlie severe ataxia in *Kcnc1*/*Kcnc3* double-null mutants. Therefore, Kv3.3 function in Purkinje neurons is sufficient to account for the hypermetric *Kcnc3*-null phenotype and impaired complex spiking represents a potential underlying mechanism in addition to broadened, decelerated simple spiking. The behavioral rescue, fast spiking in DCN neurons and normal gait require *Kcnc1.*

TABLE OF CONTENTS

PUBLICATIONS

Hurlock EC, Bose M, Pierce G, Joho RH.
Rescue of motor coordination by Purkinje cell-targeted restoration of Kv3.3 channels in *Kcnc3*-null mice requires *Kcnc1*. (in preparation)

Joho RH, Hurlock EC.
The Role of Kv3-type Channels in Cerebellar Physiology and Behavior. Cerebellum (in press)

Hurlock EC, McMahon A, Joho RH.
Purkinje-cell-restricted restoration of Kv3.3 function restores complex spikes and rescues motor coordination in *Kcnc3* mutants.
J Neurosci. 2008 Apr 30;28(18):4640-8.

Hurlock EC, McMahon A, McKay BE**,** Turner RW and Joho RH. Purkinje cell-restricted restoration of Kv3.3 channel function rescues complex spikes and motor coordination in Kv3.3-mutant mice. *Proc. Soc. Neurosci.* 2007.

FIGURES

ABBREVIATIONS

+/+;+/+	Wildtype
+/+;+/-	*Kcnc3*-null allele heterozygote
+/+;-/-	*Kcnc3*-null mutant
+/-;-/-	*Kcnc3*-null mutant additionally lacking one *Kcnc1* allele
-/-;-/-	*Kcnc1*/*Kcnc3* double-null mutant
+/-;+/-	*Kcnc1*/*Kcnc3* double-null heterozygote
-/-;+/+	*Kcnc1*-null
aCSF	Artificial cerebrospinal fluid
ANOVA	Analysis of variance
4-AP	4-aminopyridine
BDS-I	Blood-depressing substance I
BK channel	Large conductance calcium-activated potassium channel
cM	Centimorgan
cc	Cubic centimeter
CMV	Cytomegalovirus
CNS	Central nervous system
COF	Center of force
DAB	Diaminobenzidine
D-AP5	D-(-)-2-amino-5-phosphonopentanoic acid
DCN	Deep cerebellar nuclear or nuclei
DKO	*Kcnc1*/*Kcnc3* double-null mutant
DNA	Deoxyribonucleic acid
DNQX	6,7-Dinitroquinoxaline-2,3-dione
DPBS	Dulbecco's phosphate-buffered saline
eGFP	Enhanced green fluorescent protein
E_{Cl}	Chloride equilibrium potential
eIPSC	Excitatory inhibitory postsynaptic current
eIPSP	Excitatory inhibitory postsynaptic potential
E_{K+}	Potassium equilibrium potential

EMG	Electromyography
E_{Na}	Sodium equilibrium potential
ER	Endoplasmic reticulum
EPSP	Excitatory postsynaptic potential
ES cells	Embryonic stem cells
F–I	Frequency as a function of injected current
GAD67	Glutamic acid decarboxylase 67
GAD65	Glutamic acid decarboxylase 65
GABA	γ-aminobutyric acid decarboxylase
HCN	Hyperpolarization-activated, cyclic-nucleotide gated, cation non-selective channels
HEPES	4-(2-hydroxyethyl)-1-piperazineethanesulfonic acid
Hz	Hertz
IC_{50}	Median inhibition concentration at which 50% inhibition occurs
I.D.	Inner diameter
IPSC	Inhibitory postsynaptic current
IPSP	Inhbitory postsynaptic potential
Kv	Voltage-gated potassium [channel]
LDI	Lateral deviation index
LTD	Long-term depression
LTP	Long-term potentiation
MΩ	Megaohms
MDCK	Madin-Darby canine kidney cells
mGluR1	Metabotropic glutamate receptor type-1
MiRP2	Mink-related peptide type 2
mOsm	Milliosmole
mRNA	Messenger ribonucleic acid
NBQX	2,3-dihydroxy-6-nitro-7-sulfamoyl-benzoquinoxaline-2,3-dione
NCBI	National Center for Biotechnology Information
O.D.	Outer diameter

pBI	pBIeGFP bicistronic vector
PCR	Polymerase chain reaction
PKA	Protein kinase A
PKC	Protein kinase C
RNA	Ribonucleic acid
ROR-α	Retinoid-related orphan receptor-α
RT-PCR	Reverse transcription-polymerase chain reaction
SCA	Spinocerebellar ataxia
SCA13	Spinocerebellar ataxia type 13
SCA3	Spinocerebellar ataxia type 3
SCA6	Spinocerebellar ataxia type 6
SCA8	Spinocerebellar ataxia type 8
SDS	Sodium dodecyl sulfate
SK channel	Small-conductance calcium-activated potassium channel
TBS-T	Tris-buffered saline with Tween20
TEA	Tetraethylammonium
TRE	Tetracycline-responsive element
tTA	Tetracycline transactivator
3'UTR	3' untranslated region
5'UTR	5' untranslated region

CHAPTER ONE
Introduction

1.1. KV3 CHANNELS

Ion channels are a diverse and vast class of proteins present across phylogeny vital at the systems and even cellular levels. Whenever cells must passively conduct ions through the plasma membrane ion channels are employed, with the notable exception of connexins that form gap junctions between apposed plasma membranes of adjacent cells for the direct exchange of ions and small organic solutes. Cells of every mammalian tissue express ion channel genes of some kind both for basic maintenance of a resting potential and ion exchange as well as in numerous tissues specialized functions such as filtering in the kidney, regulation of muscle contraction in myocytes, control of hormone secretion by cells of glandular tissues such as pancreatic islet cells, maturation of T lymphocytes and the flow of information in the nervous system.

In excitable tissues such as the nervous system and muscle ion channels are especially critical for the rapid transmission of signals for animals to react with agility either to avoid danger or procure resources essential for survival. Speed can be a matter of life and death, exerting substantial evolutionary pressure. Although muscle contraction itself is a relatively slow process not requiring coding on a precision scale, the initial command to contract must often be brisk. For the correct motor response to be selected, considerable computation may be required involving communication between a plethora of distant neurons, not to mention for the output to be coordinated finely in both speed and timing relative to other movements. Rapid transduction of nerve impulses into muscle contraction, rapid transmission of information from the brain to the musculature, and rapid transmission of information in the brain are crucial. The insulation of neuronal axons by myelin, or alternatively their substantial width, attest to the evolutionary need for speed. Ion channels can be divided into classes that include channels that are slowly modulated, ligand-gated ion

channels and voltage-gated ion channels, with some responding to a combination of influences. Critical for speed are the ligand-gated and voltage-gated channels. Ligand-gated channels allow for rapid neurotransmission and, at the neuromuscular junction, depolarization of muscle in response to neural commands. Voltage-gated ion channels are essential for the production of action potentials which allow expedited transmission of signals between distant organs on a millisecond timescale.

The ligand-gated and voltage-gated channels are mainly comprised of huge superfamilies of related proteins. Pentameric ligand-gated channels include nicotinic acetylcholine, GABA-*A*, glycine and 5-HT_3 receptors. Glutamate receptors belong to a smaller family composed of tetramers. TRP channels, IP_3 receptors and ryanodine receptors make up still other families. Diversity is increased by differential mRNA processing. In contrast, metabotropic, G protein-linked receptors often for the same ligands mediate signals on the timescale of seconds, minutes or even longer, often ultimately modulating ion channels as their downstream effectors among other targets. Voltage-gated ion channels largely appear to descend from a common ancestor, with calcium channels likely the oldest. These channels comprise sodium, calcium and potassium channels, as well as channels with mixed sodium-potassium conductances such as cyclic-nucleotide gated (CNG) and hyperpolarization-activated, cyclic-nucleotide gated, cation non-selective (HCN) channels.

Molecularly, sodium and calcium channels are composed of four concatemerized transmembrane domains each containing six transmembrane helices or segments, S1-S6. Potassium channels and close relatives such as HCN channels exist instead as four separate subunits that are assembled together as tetramers or, if they are from the same subfamily (Xu et al., 1995), heterotetramers containing structurally different subunits. All three main families are encoded by a number of genes, but the diversity is most vast by far in the case of potassium channels, where further diversity results from extensive use of differential mRNA processing into splice and other variants. Potassium channels

are the best characterized by molecular biology historically since they are encoded by shorter sequences that lack the repeated domains of the other major families that confounded subcloning as repeats are prone to DNA rearrangement. The three fundamental voltage-gated channel families work together to produce neuronal and myocyte action potentials.

Action potentials (Fig. 1.1) serve as discrete signals encoding information in neurons at a high bandwidth so long as the postsynaptic cell, or presynaptic terminal, can distinguish differences in frequency. These all-or-none signals trigger presynaptic calcium influx through high-voltage activated calcium channels that selectively respond to depolarization attained during action potentials. Calcium influx in turn gates neurotransmitter release. The longer the membrane potential dwells at a level that opens calcium channels, the more transmitter is released, in proportion to the third to fifth power of the free calcium concentration.

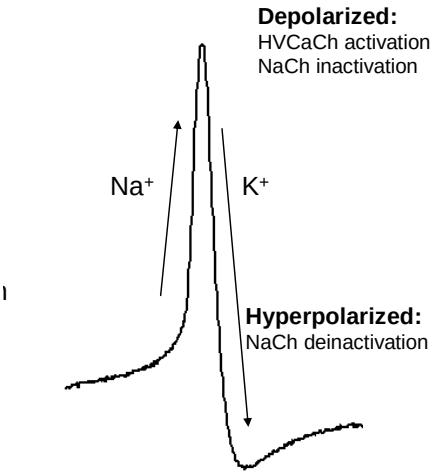

Figure 1.1. The action potential. Sodium channels open during the upstroke as depolarization increases together with, at a delay, potassium channels that repolarize the action potential during the downstroke or decay. Both channel types close once the membrane is repolarized.

The Kv3 subfamily activates and deactivates 10x faster than other voltage-gated K^+ channels

Dissecting the ionic contributions to action potentials, sodium channels passing cation current inward initiate the depolarization by progressively and regeneratively recruiting still more sodium channels as depolarization increases once other factors allow the membrane potential to approach a threshold value where a critical number of sodium channels open to begin the chain reaction. The voltage-dependence of the channel is such that the probability of opening increases with depolarization. Channel behavior is stochastic, entailing that there is always

some percentage of channels in a given state based on the probability of that state under certain conditions like voltage. As soon as the voltage is depolarized enough to trigger a sufficient percentage of the channel population to enter the open state to induce a collective conductance strong enough to augment the depolarization further in a self-reinforcing manner threshold is reached. The membrane potential then rises toward the equilibrium potential for sodium and the conductance decreases as it is approached due to the diminishing driving force. In addition, two factors also slow the rise as the peak is approached, the opening of potassium channels mediating a repolarizing outward cation current and the voltage-dependent inactivation of sodium channels. Potassium channels of the delayed-rectifier type open with depolarization at a delay after the sodium channels create it. Inactivation is a process separate physically and conceptually from channel deactivation, the mere reverse of activation. Inactivated channels cannot be activated again unless they are first deinactivated, a process that accelerates with increasing hyperpolarization after action potentials. Some potassium channels are only weakly voltage-sensitive and rather gated by the calcium concentration, which increases rapidly near high-voltage activated calcium channels opened by action potentials. Namely, large-conductance BK- and small conductance SK-type potassium channels are weakly sensitive or insensitive to voltage respectively but gated quite rapidly by calcium. The downstroke of the spike occurs when potassium channels gain the upper hand over sodium channels, aided by the strong driving force of potassium, far from its hyperpolarized equilibrium potential (E_{K+}). This action potential repolarization continues toward E_{K+} often beyond the resting potential resulting in an afterhyperpolarization, which can be divided into distinct fast and slow components sometimes when delayed rectifiers are present with different kinetics. Closer to E_{K+} the potassium conductance diminishes from both the driving force reduction and closing of potassium channels due to deactivation or, in the case of calcium-activated potassium channels, eventually calcium extrusion and buffering. Many delayed rectifiers can also eventually enter an

inactivated state like sodium channels. In myocytes, which function on the slower timescale of contraction, sodium channels only initiate the rising phase normally while calcium channels, which have slower kinetics, activate to produce the broad shoulder of depolarization that is not suppressed by fast potassium channels.

Voltage-gated potassium channels also influence spike rate. Specialized voltage-gated potassium channels can only open once the membrane potential has hyperpolarized due to fast inactivation at the depolarized potentials that initially activate them but deactivate slowly enough to exert an effect on the membrane potential before closing that mediate the “A-type” current. Typically channels of the Kv4 (*Shal* in fly) subfamily are the origin of this current. Such channels contribute nominally to repolarization but greatly to setting the interspike interval that determines spike frequency. Calcium-activated potassium channels can also lengthen the interspike interval depending how long calcium continues to flow through slow calcium channels yet to close or lingers after the spike. Delayed rectifiers control the interspike interval based on how quickly they make way for the next spike by deactivating. After repolarization Kv1 (*Shaker* in fly) and Kv2 (*Shab* in fly) subfamily members remain open for milliseconds whereas Kv3 (*Shaw* in fly) subfamily members deactivate, as well as activate, faster than any other subfamily in fractions of a millisecond.

Kv3-type channels facilitate high-frequency firing of action potentials by both rapid activation and deactivation because another determinant of the interspike interval is the number of available sodium channels that have not undergone inactivation. By keeping spikes brief through fast activation, less sodium channels enter the inactivated state than otherwise if the membrane potential dwelt longer in a depolarized range. A robust, deep afterhyperpolarization induces more efficient recovery from inactivation because deinactivation is faster at more hyperpolarized voltages. The large conductance of Kv3 channels may help in this regard.

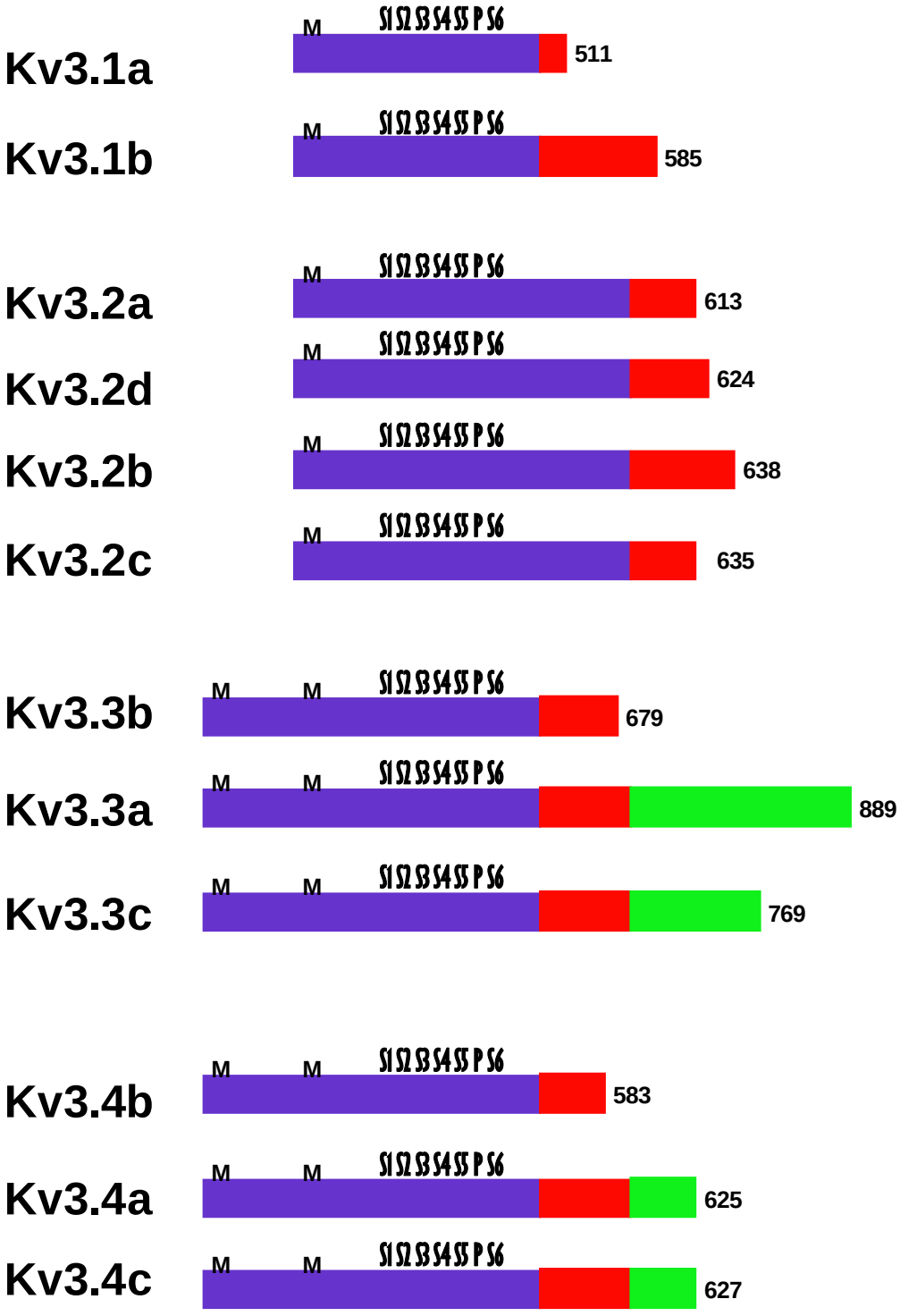
Kv3.1a
M
S1 S2 S3 S4 S5 P S6
511
Kv3.1b
M
S1 S2 S3 S4 S5 P S6
585
Kv3.2a
M
S1 S2 S3 S4 S5 P S6
613
Kv3.2d
M
S1 S2 S3 S4 S5 P S6
624
Kv3.2b
M
S1 S2 S3 S4 S5 P S6
638
Kv3.2c
M
S1 S2 S3 S4 S5 P S6
635
Kv3.3b
M M
S1 S2 S3 S4 S5 P S6
679
Kv3.3a
M M
S1 S2 S3 S4 S5 P S6
889
Kv3.3c
M M
S1 S2 S3 S4 S5 P S6
769
Kv3.4b
M M
S1 S2 S3 S4 S5 P S6
583
Kv3.4a
M M
S1 S2 S3 S4 S5 P S6
625
Kv3.4c
M M
S1 S2 S3 S4 S5 P S6
627

Figure 1.2. Coding regions of Kv3 channel genes and splice variants thereof, based on Rudy et al., 1999. The methionines, including internal and alternative methionines, are indicated with an M. Exons on which coding regions are present appear in different colors. Protein lengths are denoted at right. The core transmembrane segments (S1-S6) and pore region (P) are in the first coding exon.

1.1.1. Kv3 Channel Properties

1.1.1.1. Genes

The four Kv3 subunits are designated Kv3.1-4 and encoded by the genes *Kcnc1-4* in rodents or *KCNC1-4* in humans (Fig. 1.2). *Kcnc1* and *Kcnc3* are located within ~0.5-1 cM of one another on murine chromosome 7 syntenic with human chromosome 11p15 and human 19q13.3-13.4. The *Kcnc3* gene is very GC-rich and contains elaborate, stable secondary structures in the long 3'UTR. The DNA is very prone to rearrangement and relatively recalcitrant to PCR. *Kcnc2* is at mouse 10qD2 syntenic with human 12q21.1, while *Kcnc4* is at 3qF2.3 syntenic with human 1p13.3. All of the *Kcnc* genes are subject to splice variation that is likely not yet fully characterized. Variation mainly occurs at the 3' end of the gene typically affecting the C terminus of the protein. 5' end variation has been reported but only alters the 5'UTR (Rudy et al., 1992, Weiser et al., 1994). *Kcnc1* has at least two known variants that change the C terminus of the protein designated Kv3.1a and Kv3.1b (Luneau et al., 1991a, Luneau et al., 1991b, Ozaita et al., 2002, Perney et al., 1992). *Kcnc2* has three variants and *Kcnc4* has four 4 known variants. *Kcnc3* has 3 published and more unpublished variants affecting the 3'UTR (Pyle D. and McMahon A., unpublished).

1.1.1.2. Proteins

Like all of the delayed rectifier voltage-gated potassium channels, Kv3 channels are tetramers composed of subunits (Fig. 1.3). Each canonical channel subunit of these channels has a stereotyped topology where the N and C termini are intracellular sandwiching six transmembrane segments, S1-S6. The fourth

segment has positively charged residues that move the alpha helix upward or downward to control activation/deactivation responsible for voltage-dependent gating. Inactivation is imparted by the N terminus blocking passage of ions beyond the pore formed by the four S5-S6 linkers bearing polar amino acids at the filter to attract and select potassium ions. Kv3.3 and Kv3.4 have alternative initiator methionines that can extend the N terminus and render the otherwise non-inactivating channels inactivating (Desai et al., 2008, Fernandez et al., 2003). Also in the N terminus is the T1 domain essential to forming tetramers.

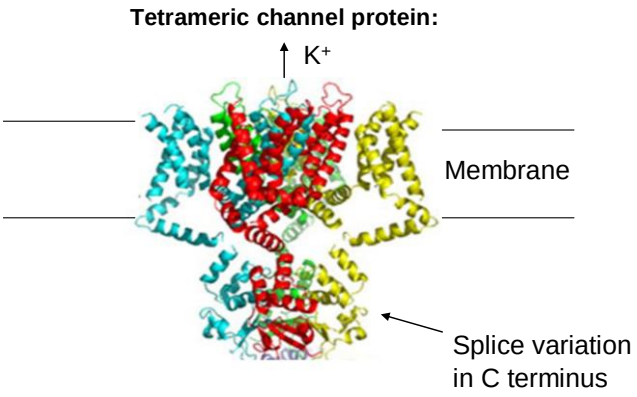

Figure 1.3. The Kv channel protein based on the structure of KcsA elucidated by Doyle et al., 1998. Individual subunits comprising the tetramer are shown in different colors.

In Kv3 channels diversity is imparted by heterotetramerization and splice variation impacting the C terminus. N and C termini provide a surface facing the cytosol along which posttranslational modification can be applied to modulate the channel. Also, the termini seem to be responsible for subcellular localization. Kv3.3 in the weakly-electric fish requires certain C terminal residues to localize properly in dendrites (Deng et al., 2005). C terminal splice variants of Kv3.1 exhibit differential subcellular localization (Ozaita et al., 2002) such that Kv3.1a must heterotetramerize with Kv3.1b to enter axons *in vitro* (Xu et al., 1995). Heterotetramerization has been shown to indeed exist by co-immunoprecipitation in the rodent brain in the case of Kv3.1b and Kv3.3b (Chang et al., 2007), Kv3.1 and Kv3.4 (Baranauskas et al., 2003) as well as Kv3.1 and Kv3.2 (Rudy et al., 1999). Kinetic properties can be affected such that they are intermediate between homomers of the two subunits. Diversity is further enhanced by

association with auxiliary subunits like MiRP2 which alter biophysical properties (McCrossan et al., 2003).

1.1.1.3. Biophysical Properties

The acute function on a millisecond timescale of Kv3 channels is in passing ions it is generally safe to assume. Nonetheless many proteins are multifunctional. Voltage-gated ion channels are known to participate in cell-cell interactions by acting as adhesion molecules which can function in organizing nodes of Ranvier (Chen et al., 2004, Kaczmarek, 2006). To date, however, the most parsimonious explanation for the effect of Kv3 expression on neurons is however mediation of the voltage-dependent flow of potassium in the voltage range pertaining to spikes.

As explained in the above overview for section 1.1, the most notable feature of Kv3 channels is rapid activation and deactivation. The voltage-dependence of activation is high among the Kv subfamilies, restricting the influence of the channels more to the domain of action potentials rather than on subthreshold activity, at least directly. A high single-channel conductance may support faster repolarization and a greater afterhyperpolarization if the number of docking sites for channels at the membrane is limited, constraining how much conductance can be obtained collectively by mere upregulation.

Inactivation is only present in Kv3.3 and Kv3.4 channels. It is contingent upon the translation via an upstream alternative methionine of an extended N terminus (Fernandez et al., 2003). A structurally-distinct mechanism, inactivation is very slow for Kv3.3 compared to other potassium channels. Sustained, high-frequency firing might be necessary for a significant fraction of Kv3.3 channels to enter the inactivated state. Kv3.4 however inactivates in tens of milliseconds during constant depolarizing voltage steps (Martina, Yao and Bean, 2003, Martina, Metz and Bean, 2007).

1.1.1.4. Modulation

Voltage-gated ion channels are known to be modulated by a plethora of molecules both soluble and in the membrane as well as posttranslational modifications. Through these routes neurotransmitters can modulate the excitability of neurons, synaptic plasticity and neurotransmitter release at terminals. By delimiting spike width at terminals Kv3 channels have been shown, using the Calyx of Held synapse where presynaptic recording is possible, to regulate neurotransmitter release (Nakamura and Takahashi, 2007, Ishikawa et al., 2003, Nakamura and Takahashi, 2007, Ishikawa et al., 2003, Ishikawa et al., 2003). Kv3.1 is modulated negatively by PKC (Critz et al., 1993, Kanemasa et al., 1995, Macica et al., 2003, Song et al., 2005). An exception is Kv3.3, the current of which is facilitated by PKC (Desai et al., 2008). Protein kinase A also modulates Kv3 channels (Moreno et al., 1995). The channels are in addition sensitive to oxidative stress (Rudy et al., 1992, Rettig et al., 1992, Duprat et al., 1995). Less acute modulation also is exerted through association with auxiliary subunits (McCrossan et al., 2003).

1.1.1.5. Pharmacology

First, it should be noted that the IC_{50} may differ between channels of different composition among neuronal cell-types. The classic blocker for Kv3 channels has been tetraethylammonium (TEA), which blocks ~90% of Kv3 current at 1 mM where it has weak effects on calcium-activated potassium channels. ~0.2 mM TEA is selective for Kv3 channels (McKay and Turner, 2004) but only blocks a fraction of the current. 4-aminopyridine (4-AP) is fairly selective for Kv3 at 20-600 µM however the variable responsiveness due to complex interactions with different channel states undermines its utility (Rudy et al., 1999). The sea anemone toxin blood-depressing substance I (BDS-I) specifically blocks the Kv3 subfamily at ~500 nM (Yeung et al., 2005). Originally it was believed to be selective for Kv3.4 (Diochot et al., 1998) with a 47 nM IC_{50} however other groups failed to replicate the result (Yeung et al., 2005). The drugs riluzole at an IC_{50} of 121 µM (Ahn et al., 2005), bupivacaine at 46 µM (Nilsson et al., 2008, Friederich,

Benzenberg and Urban, 2002), streptomycin (Liu and Kaczmarek, 2005), Sibutramine at 33 μM (Kim et al., 2007), flouxetine (Prozac™) at 13 μM and its metabolite norflouxetine at 0.8 μM (Choi et al., 2001, Sung et al., 2008) also block human Kv3.1 channels. Block by therapeutically relevant concentrations of the latter two drugs is intriguing in light of the hyperactivity of *Kcnc1*-null mice and classification of fluoxetine as an "activating" antidepressant capable of inducing iatrogenic hypomania as well as akisthesia (a type of restlessness characterized by an urge to incessantly move; spelling in medical literature varies also akasthisia) (Akagi and Kumar, 2002, Messiha, 1993, Vanderhoff and Miller, 1997). PKC, which inhibits these channels, has been implicated in mania, where a blocker had an anti-manic effect (Einat et al., 2007, Zarate et al., 2007).

1.1.2. Expression Pattern

Kv3 channels occur across the CNS. A general theme naturally is expression in fast-spiking neurons, which attain frequencies in excess of ~300 Hz at physiological temperature, near 37°C. A lot of fast-spiking neurons in the brain express the calcium-binding protein parvalbumin and develop perineuronal nets that unfortunately render patch-clamping in mature animals difficult (Morales et al., 2004, Hartig et al., 1999, Hartig et al., 2001). Most of these populations are GABAergic, expressing either GAD67, GAD65 or both, including projection and, more commonly, GABAergic interneurons. A few populations of glutamatergic projection neurons are fast-spiking. Among the subunits, Kv3.2 tends to be found rostrally in large part in forebrain structures. Kv3.3 and Kv3.4 are more often found in cells in caudal structures such the hindbrain, which includes the cerebellum (for the cerebellum see also section 1.4). Kv3.1 is distributed more evenly across structures from the forebrain to the hindbrain. Outside the CNS *Kcnc4*, and possibly at low levels *Kcnc1* and *Kcnc3*, are found in sympathetic ganglia. Skeletal muscle expresses some *Kcnc1* and substantial *Kcnc4* (Dixon and McKinnon, 1996). Cardiac muscle may express all subunits albeit at low levels. *Kcnc3* is also found in lung and kidney. T lymphocytes at least express

Kcnc1 (Grissmer et al., 1992). Finally, Kv3.4 has been verified at the protein level (Veh et al., 1995) and received some attention in myocytes where interactions with MiRP2 have been best studied that may also generalize to the CNS (McCrossan et al., 2003, Abbott et al., 2001).

Subcellularly Kv3 subunits differ in their localization, sometimes by splice variant (Ozaita et al., 2002, Xu et al., 2007). Kv3 subunits can be found in all neuronal compartments, with the least expression in distal dendrites normally. In given types of neurons a particular subunit may prefer a certain compartment. It remains unknown exactly how different subunits determine the distribution of each other in different compartments via heterotetramerization although this seems to occur (Xu et al., 2007). A preparation used to study this is Madin-Darby canine kidney (MDCK) cells, a polarized cell-type that models trafficking to axonal and dendritic compartments fairly reliably by their apical and basolateral membranes, respectively.

1.1.2.1. Kv3.1

Kcnc1 mRNA is expressed at high levels in forebrain and certain cerebellar neurons primarily. Forebrain structures with Kv3.1 include the cortex, hippocampus, and striatum, where GABAergic interneurons account for expression. In monkey at least Kv3.1b is found in cortical pyramidal neurons (Ichinohe et al., 2004), which ought to express Kv3 channels in some cases such as the chattering cells recorded in ferret that burst at a gamma frequency (~30-80 Hz) with intraburst frequencies of hundreds of Hertz (Brumberg, Nowak and McCormick, 2000). GABAergic neurons of the reticular thalamic nucleus are rich in Kv3.1. Ventral to this nucleus Kv3.1 is found in the zona incerta. GABAergic neurons co-mingled with cholinergic neurons in cholinergic nuclei in the basal forebrain on through the medial septum express Kv3.1 as well (Chang et al., 2007), along with pallidal GABAergic neurons. Apparently glutamatergic neurons pervasive in the subthalamic nucleus and, perhaps at low levels, some glutamatergic thalamocortical relay neurons also express *Kcnc1*. Midbrain

structures including the substantia nigra reticulata, red nucleus and very prominently the inferior colliculus contain the subunit. Several brainstem nuclei have *Kcnc1* mRNA including the medial nucleus of the trapezoid body (MNTB) and the vestibular nuclei (for cerebellar detail see section 1.4). In the olfactory bulb mitral cells express *Kcnc1* (Weiser et al., 1994).

Kcnc1 represents a unique case among the subunit genes where the differential distribution of splice variants has been mapped (Ozaita et al., 2002, Perney et al., 1992). Kv3.1a is enriched in axons and terminals (Ozaita et al., 2002, Xu et al., 2007). Kv3.1b is present throughout the cell albeit less so in distal dendrites. Kv3.1b, but not Kv3.2 or Kv3.3b concentrates at nodes of Ranvier (Chang et al., 2007) and co-immunoprecipates with ankyrin G, a constituent of nodes (Devaux et al., 2003).

1.1.2.2. Kv3.2

Kv3.2 is most prominent in glutamatergic thalamic relay nuclei and GABAergic interneurons that express parvalbumin throughout the cortex and in the hippocampus (Chow et al., 1999, Lau et al., 2000). *Kcnc2* mRNA is expressed in the forebrain also like Kv3.1 in the zona incerta, subthalamic nucleus and in pallidal neurons. In the midbrain Kv3.2 mirrors Kv3.1 except it is additionally found in a layer of the superior colliculus. Unlike Kv3.1, Kv3.2 is very sparse in the brainstem (for cerebellar detail see section 1.4;Weiser et al., 1994). Kv3.2 does not appear to concentrate at nodes of Ranvier (Chang et al., 2007). Splice variants have yet to be explored at the protein level since antibodies recognize the invariant N terminus however in polar MDCK cells Kv3.2a and b distribute differentially in subcellular compartments (Rudy et al., 1999).

1.1.2.3. Kv3.3

Kv3.3 expression in the midbrain resembles Kv3.1 in most respects except the level is lower in structures other than the thalamic reticular nucleus and subthalamic nucleus. Expression is pronounced in posterior areas such as the

brainstem and cerebellum (for cerebellar detail see section 1.4). Like Kv3.1 it is in mitral cells of the olfactory bulb. Where assessed, Kv3.3b expression is mainly restricted to all areas except distal dendrites where in Purkinje cells it is present at a low level. A Northern blot suggested *Kcnc3b* was highest in the cerebellum (Goldman-Wohl et al., 1994). Kv3.3 does not appear to concentrate at nodes of Ranvier (Chang et al., 2007).

1.1.2.4. Kv3.4

Of all the subunits Kv3.4 remains the least understood. It is mostly expressed in skeletal muscle. mRNA levels even detected by radiolabeling (Weiser et al., 1994) are low and difficult to detect. The Allen Brain Atlas using non-radioactive methods barely detects it at all (for cerebellar detail see section 1.4). Weiser et al. 1994 using radioactivity detected *Kcnc4* mRNA in scattered pallidal neurons, the dentate gyrus, the subthalamic nucleus and pontine nuclei. It should be noted that antibodies used in different studies either detected all splice variants (Martina, Yao and Bean, 2003) or potentially Kv3.4a preferentially (Veh et al., 1995, Laube et al., 1996) given divergence in the epitope (Vullhorst, Jockusch and Bartsch, 2001).

1.2. KV3 CHANNEL FUNCTION

With the exception of one recently described human disease, Kv3 channels have only been explored functionally at the behavioral level by null mutant mouse models. At the cellular level many insights have been gained from TEA but there are as of yet no specific drugs that can really probe function *in vivo* non-invasively without toxicity. Prior to this thesis work, I developed a dominant negative Kv3.1 subunit that will be useful in the future. This approach works in Kv channels capable of heterotetramerization, and has been fruitful in unraveling the function of other potassium channels *in vivo* (Shakkottai et al., 2004, Peters et

al., 2005) potentially in select cell-types, ablating the function of all Kv3 subunits simultaneously. Null mutants are available for all subunits except Kv3.4. By virtue of being subtle historically null phenotypes were not immediately obvious for *Kcnc1* and *Kcnc3* however the creation of double-knockout (DKO or -/-;-/-) mice with more severe phenotypes made the affected parameters more apparent (Espinosa et al., 2001). *Kcnc1* and *Kcnc2* double mutants have only been analyzed *in vitro* based on published work (Goldberg et al., 2005). As a subfamily, the range of functions channels in essence tend to be involved in include sleep/arousal, activity levels (related to the latter), preventing epileptiform activity, and motor function.

1.2.1. Kv3.1

The most profound abnormality of the *Kcnc1*-null mice (or -/-;+/+) is reduced total slow wave sleep duration and fragmentation of slow wave sleep, a phenotype even more marked in *Kcnc1*/*Kcnc3* double-null (-/-;-/-) mutants which also have less delta power. -/-;-/- mice have a 40% decrease in total sleep during the light phase, which is perhaps the greatest reduction seen to date among null-mutant mouse models with sleep phenotypes. Moreover rebound sleep after sleep deprivation is impaired in mice just lacking *Kcnc1* and abolished in -/-;-/- mice (Espinosa et al., 2001, Espinosa et al., 2004a, Espinosa et al., 2008, Joho, Ho and Marks, 1999, Joho et al., 2006). Together with decreased slow wave sleep, outbred -/-;+/+ mice and -/-;-/- mice are hyperactive as indexed by ambulatory and stereotypic activity in the open field especially during the light phase (Espinosa et al., 2004b). 129Sv null mice did not display hyperactivity (Ho, Grange and Joho, 1997) probably because they have low activity levels and are considered generally a poor strain for behavioral testing. The hyperactivity can also readily be observed by eye and likely is not strictly a result of less time spent sleeping. There is an apparent attenuation of the circadian distribution of sleep and overall activity that is corroborated by other recent preliminary data.

The +/-;+/- and -/-;-/- mice lacking *Kcnc1* alleles additionally tend to spend more time in the center of the open field compared to wildtype controls, suggesting decreased anxiety. The mice just lacking *Kcnc1* have been described qualitatively by observers as feisty, emotional and sometimes agitated with a greater tendency to vocalize when handled or jump. Parenting is somewhat impaired and even mice heterozygous for the null allele display these traits, at least on some genetic backgrounds. Null mice are more sensitive to the disruptive effect of alcohol on coordination or balance such that they have an increase in sideways falls (Joho R.H., unpublished) that is more severe in DKO mice (Espinosa et al., 2001).

An effect of Kv3.1 on high-frequency firing has been described in the medial nucleus of the trapezoid body that functions in sound localization (Macica et al., 2003). Modulation of the channel here by PKC adjusts the firing frequency according to the acoustic milieu (Song et al., 2005). Further, a role for Kv3.1 in high-frequency spiking was shown in the thalamic reticular nucleus which may contribute to sleep deficits that worsens in parallel in -/-;-/- mice (Espinosa et al., 2008, Porcello et al., 2002). Spikes were broadened 20% in mice just lacking *Kcnc1* and 60% in -/-;-/- mice, measuring halfway between the threshold and the peak.

1.2.2. Kv3.2

The only clear phenotype discovered in *Kcnc2*-null mice was an increased susceptibility to phenylenetetrazole-induced seizures (Rudy et al., 1999). Spontaneous seizures occurred rarely and seizures were only induced during procedures in <20% of mice on a congenic C57/BL/6 inbred background but not during routine handling. Decreased power in low frequency ranges (~3.25-6 Hz) using fast Fourier analysis was reported during sleep however the durations of total sleep or sleep phases were normal in *Kcnc2*-null mice (Vyazovskiy et al., 2002) . The battery of tests used to first characterize the mutant (Rudy et al., 1999) included a general neurological screen for severe sensory and motor

abnormalities, the open field test for exploratory activity and anxiety-related responses, the light-dark test for anxiety-related responses, the rotarod test for motor coordination and skill learning, acoustic startle and prepulse inhibition of the acoustic startle response for sensorimotor gating, habituation of the acoustic startle response for sensorimotor adaptation, contextual and auditory-cued freezing to assess conditioned fear, and the hotplate test for analgesia-related responses.

1.2.3. Kv3.3

Kv3.3 is related primarily to cerebellar functions such as motor coordination based both on a null-mutant mouse model and a human disease, spinocerebellar ataxia type 13 (*SCA13*) (Waters et al., 2006). The role of Kv3.3 in motor coordination will be explored in detail in section 2.1.4 below. Congruent with disturbed cerebellar function, harmaline-induced tremor, thought to reflect intact function of the olivo-cerebellar loop, is virtually abolished in the null mutant (McMahon et al., 2004). Sleep phenotypes of *Kcnc1*-null are worsened by loss of *Kcnc3*, as discussed in section 1.2.1 above (Espinosa et al., 2004a, Espinosa et al., 2008). The +/+;-/- mice also displayed lethal seizures when excited by being transported in a cart on the 129Sv inbred background (Chan, 1997). Breeding onto an outbred background eliminated the seizures. Interestingly a null mouse from a recently derived congenic line on the 129Sv background in the lab was reported to have had seizures. At one point in the laboratory -/-;-/- mice started having similar seizures induced by transport on an outbred background that was becoming inbred. Crossing the breeding stock with outbred ICR, C57/BL/6 and 129Sv mice on a regular basis from the vendor alleviated and prevented this (Espinosa F., unpublished). Another *Kcnc3*-null phenotype is myoclonus (Espinosa F., unpublished) which like ataxia is markedly worse in -/-;-/- mice (Espinosa et al., 2001). Myoclonus is of intermediate severity in *Kcnc3*-null mice additionally lacking a *Kcnc1* allele (or +/-;-/-; Espinosa et al., 2004b). A tendency toward hyperexcitability when suspended by the tail that might be described

more aptly as dyskinesia and hyperactivity has also been observed (Chan, 1997).

A role for Kv3.3 in high-frequency firing has been evidenced in Purkinje cells where spike width is sensitive to 150 µM TEA, a dose specific for Kv3 channels (McKay and Turner, 2004) and broadens 100% in +/+;-/- mice (McMahon et al., 2004). Block by TEA triggers strong sodium-calcium spike bursts, which raised the possibility that Kv3.3 suppressed bursts in general (McKay and Turner, 2004) although the channel deactivates rapidly at subthreshold voltages. The effect, if attributable to Kv3, would result from increased calcium influx during broader spikes perhaps.

1.2.4. Kv3.4

Essentially nothing is known about the actual function of Kv3.4 *in vivo*. One study (Baranauskas et al., 2003) attempted to elucidate the role of this subunit using the ostensibly specific toxin BDS-I that was subsequently shown not to be specific (Yeung et al., 2005).

1.3. PHYSIOLOGY OF CEREBELLAR CIRCUITRY

Synthesizing the literature, the role of the cerebellum at large in a general sense it seems is to smooth, pace and coordinate information processing and behavioral output based on continuous, rapid feedback while serving as an associative substrate where a progressive fine-tuning of these processes for repeated tasks can reside. The cerebellum is not solely dedicated to motor function and posture; it modulates cognitive and emotional processing as well (Schmahmann, 2002). What is special and unique about the cerebellum is how it processes information rather than exactly what specific information it processes. The deficits seen in patients with cerebellar damage outside the motor realm (see section 2.1.1) are in keeping with this conception.

The cerebellum consists of an exquisitely structured, highly organized repetition of the same fundamental circuit connected to different afferent and efferent input concerned with respective modalities and related information. Complete loops are formed between the cerebellum and connected structures in the brainstem. To understand how just one loop performs related to one specific function, such as motor coordination, might then be to uncover the essence of how the other loops modulate other functions, such as working memory.

Though the beauty of Purkinje cells and remarkable organization of the relatively expansive cerebellar cortex have garnered much attention since the time of Ramon y Cajal, it is actually the more irregularly organized and difficult to study deep cerebellar nuclei that form the essential, primordial core of the cerebellum (Fig. 1.4). In phylogenetically older animals the cerebellar cortex is relatively small and rudimentary (Ito, 2000). The cerebellum began with the deep

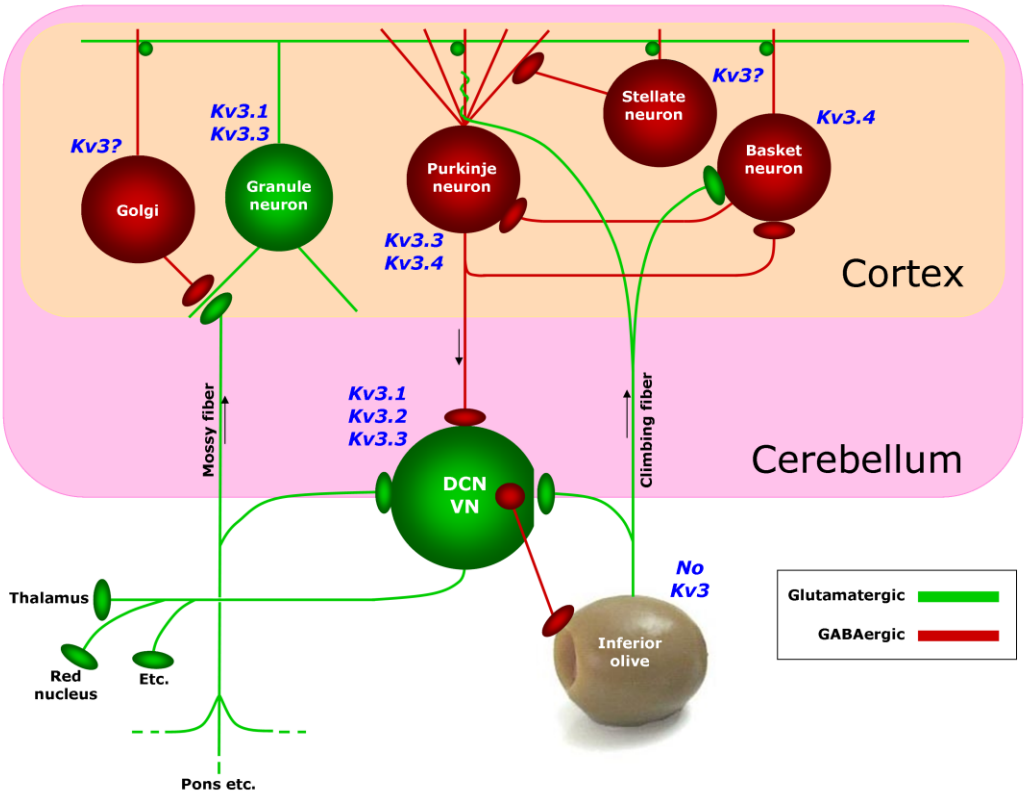

Figure 1.4. Cerebellar circuitry and distribution of Kv3 subunit expression therein.

nuclei, and the cortex evolved later perhaps to support more complex, finer processing and provided a vast number of additional connections for learned associations. Alongside the deep nuclei are the vestibular nuclei which hodologically, genetically and physiologically mirror the deep cerebellar nuclei (DCN) in most respects but are located in the dorsal brainstem. Importantly, to influence the rest of the brain and behavior the output of the cerebellar cortex, conveyed exclusively by Purkinje cells, must impinge on the deep or vestibular nuclei, for there are no other efferent structures. Without these nuclei there is no cerebellar output.

Just like the cerebellar cortex, the more primitive DCN receive input in parallel from mossy and climbing fibers that emanate from pontine nuclei, mainly, and neurons of the inferior olive, respectively. These excitatory inputs both drive DCN neurons simultaneously along with separate populations of cortical neurons. Specifically, mossy fibers drive only granule cells, while climbing fibers drive Purkinje cells, stellate cells and basket cells. The latter two are local-circuit inhibitory interneurons that in turn synapse on Purkinje cells. The climbing fiber synapse made onto Purkinje cells is a unique structure from which the fiber derives its name. Numerous synaptic contacts are made as the fiber ascends along around the Purkinje cell proximal dendrites providing collectively one of the most reliable synapses known, producing a robust excitatory postsynaptic potential (EPSP) that is crowned with a composite spike burst called the complex spike that attains a high intraburst frequency exceeding ~600 Hz (Fig. 1.5). Mossy fiber input is graded and fairly continuous whereas climbing fiber input occurs sporadically at rest or in rhythmic bouts at low frequencies around 1 Hz when the cortex is engaged by processing relevant to the local circuitry. Climbing fibers emanate in a fan-like formation in the sagittal plane from topographically organized segments of the olive to innervate cortical areas along the plane (Fukuda, Yamamoto and Llinas, 2001). Granule cells convey the mossy fiber input to Purkinje cells via parallel fibers that extend hundreds of microns in the

coronal plane perpendicular to the climbing fiber ramification in the molecular layer that houses the extensive, highly ramified, spiny Purkinje cell dendrites. In addition, Golgi cells (not shown in figure) are contacted by parallel fibers that provide inhibitory feedback onto mossy fiber terminals to gate excitation of granule cells, as well as stellate and basket cells. Finally, Purkinje cells integrate input from climbing fibers, mossy fibers and interneurons, providing GABAergic output to the DCN neurons which in turn generate cerebellar output evoked by mossy and climbing fibers with cortical processing taken into account. Purkinje cell output also feeds back to other Purkinje cells. The loops are closed by GABAergic projections back to the olive and pontine nuclei. *In vivo*, the cerebellum receives innervation from several diffuse, paracrine neuromedulatory systems including cholinergic, noradrenergic, serotonergic and histaminergic but not dopaminergic systems.

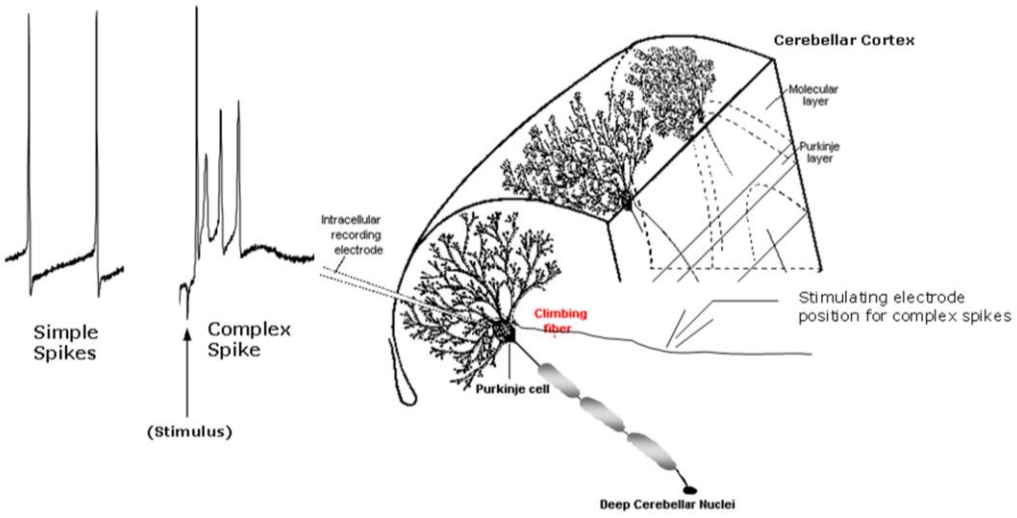

Figure 1.5. Experimental setup for intracellular recording of climbing fiber responses in parasagittal cerebellar acute slices *in vitro*. Purkinje cell illustrations adapted from those of D.P. van Lieshout.

1.3.1. Cerebellar Cortex

1.3.1.1. Granule Cells

The firing of granule cells is frequency-modulated by mossy fiber input. Recently burst firing has been described but not a high intraburst spike frequency (Steuber et al., 2007). The narrow action potentials of granule cells excite Purkinje cell dendritic spines throughout the dendrite, basket cells, stellate cells and GABAergic Golgi cells in the granule cell layer that in turn exert an inhibitory feedback effect on the mossy fibers presynaptically in synaptic glomeruli. Golgi cells also appear to be fast-spiking, extrapolating to physiological temperature from data collected at room temperature (Forti et al., 2006).

1.3.1.2. Purkinje Cells

The input to Purkinje cells from the parallel fibers of granule cells undergoes short-term plasticity in the form of paired-pulse facilitation as well as long-term depression (LTD) and long-term potentiation (LTP). Synapses are made by parallel fibers onto a profusion of spines that are thought to be the substrate of learned associations. Eyeblink conditioning and motor skill learning have received much scrutiny with regard to this synapse based on the Marr-Albus-Ito model of cerebellar learning (Albus, 1971, Ito, 1984, Kleim et al., 1998, Marr, 1969). In this model calcium influx triggered by the climbing fiber input, and in recent adaptations, from local, calcium-permeable AMPA receptors postsynaptic to parallel fiber terminals, elicits LTD at synapses that are inappropriately strong to weaken them in order to improve motor output (Denk, Sugimori and Llinas, 1995, Jorntell and Ekerot, 2002, Tempia et al., 1996). Climbing fibers fire in relation to motor errors according to this model. The precise role of LTD remains unresolved despite decades of work (Welsh et al., 1995), and some reports suggest complex spiking is more prominent after acquisition rather than before learning (Catz, Dicke and Thier, 2005).

At the resting potential even devoid of input Purkinje cells are spontaneously active. In addition to the complex spikes elicited by climbing fiber input, ~50-200 Hz tonic spikes christened simple spikes in early *in vivo* extracellular unit recordings produce a canvas of veritably constant activity upon

which complex spikes are painted. The frequency of simple spikes is modulated continuously by mossy fiber input by way of granule cells. Occasionally pauses in simple spike activity are observed (Steuber et al., 2007) of unknown significance that may be elicited by the inhibitory interneurons. Pauses in simple spikes also occur after each complex spike, and there is much cross-talk between the occurrence of simple spikes and complex spikes (Barmack and Yakhnitsa, 2003, Yakhnitsa and Barmack, 2006, Heck, Boughter and and Bryant, 2006, Miall et al., 1998, Sato et al., 1992, Servais et al., 2004). In some bistable neurons and in acute brain slices *in vitro*, complex spikes can toggle the cell between active up states and quiescent, silent down states (McKay and Turner, 2004). Whether bistability happens *in vivo* is controversial (Schonewille et al., 2006). Recent data suggest it is only seen in a subset of Purkinje cells *in vivo* (Yartsev et al., 2007). Furthermore, synchronized fast oscillations have been recently described that appear to depend on the interconnections between Purkinje cells and gap junctions (Cheron et al., 2004, Cheron et al., 2005, de Solages et al., 2008, Middleton et al., 2008). Since the DCN can facilitate such high-frequency, synchronized oscillations in forebrain structures (Timofeev and Steriade, 1997) and might enhance the impact of input to the DCN through synchronizing simple spikes (Shin et al., 2007a) the oscillations in Purkinje cells may be of great physiological significance, especially given the hypothesized role of fast oscillations in higher functions including attention and conscious perception (Engel and Singer, 2001, Llinas et al., 1998).

The function of the complex spike output has been a topic of great interest eluding explanation for over 40 years since their discovery by Eccles et al., 1966 (Eccles, Llinas and and Sasaki, 1966). Motor coordination, eyeblink conditioning and vestibular reflexes have proven the most amenable to study. A plethora of studies have been published correlating Purkinje cell activity to behavior in awake or anesthetized animals yet few conclusive cause-and-effect studies have emerged.

While some investigators have contended complex spikes appear randomly and just provide some modulatory influence (Miall et al., 1998) others have emphasized their temporal organization over spatial domains, synchronizing related ensembles in a meaningful way in relation to behavior (Welsh et al., 1995), as reviewed by Kitazawa and Wolpert (Kitazawa and Wolpert, 2005). Timothy Ebner's group has explored a role in correcting ongoing errors in motor speed or velocity even after a task has been acquired while simple spikes directly encode velocity (Coltz, Johnson and Ebner, 1999, Ebner, 1998, Ojakangas and Ebner, 1994). Velocity denotes movement in a certain direction, which is sensible if Purkinje cells are connected in such a way ultimately by several synapses to the musculature that output favors movement in a particular direction. Others have seen a similar relation between complex spikes, acute behavior and learning (Kitazawa, Kimura and Yin, 1998). Extensive interactions between complex and simple spikes as well as other effects (Balaban, 1985, Benedetti, Montarolo and Rabacchi, 1984) confound interpretation of simple lesion experiments removing the olivary input. Such studies nevertheless support a role for complex spikes in motor coordination.

Axonal propagation of complex spike spikelets remains enigmatic since it is difficult to study *in vitro* where curved axons are nearly always severed. Studies to date recording cell-attached from thin myelination after the first node of Ranvier in the cerebellar cortex suggest that some spikelets propagate at high frequencies but in a stochastic manner determined by rise time and amplitude (Khaliq and Raman, 2005, Monsivais et al., 2005). Converging, synchronized input to DCN neurons may allow the low percentage of axons propagating spikelets to nonetheless exert strong effects on DCN neurons.

Simple spikes have been posited to play roles similar to complex spikes in regulating the basic function of motor parts of the cerebellum to smoothly accelerate and decelerate movements of an appropriate steady speed. Simple spike rate seems related to speed (Coltz, Johnson and Ebner, 1999, Yamamoto

et al., 2007), directly or inversely, presumably, for a given cell depending on whether extensor or flexor muscles are controlled.

Whether simple spikes fire in synchrony like complex spikes under certain conditions and what it entails is unclear. Theoretically precise temporal coherence of simple spike activity might create windows in between IPSPs during which DCN neurons could fire in turn, and DCN neurons are capable of responding in this way *in vitro* (Gauck and Jaeger, 2000). Alternatively, asynchronous simple spikes across Purkinje cells converging on DCN neurons would result simple in tonic inhibition, decreasing the firing rate of DCN neurons. There is some *in vivo* evidence that at times, more than previously thought, Purkinje cells fire quite regularly with a very consistent interspike interval as seen in slices (Shin et al., 2007b).

The synapse made by Purkinje cells onto DCN neurons is subject to synaptic depression thought to stem from transmitter depletion (Pedroarena and Schwarz, 2003, Telgkamp and Raman, 2002). Higher-frequency output would depress faster to a lower steady state level of inhibition. The net effect of depression is to render postsynaptic neurons less sensitive to tonic, invariant input and conversely more acutely sensitive to changes in the frequency of input.

Purkinje cell collaterals also would be expected to inhibit interneurons along with other nearby Purkinje cells. Little is known about this output.

1.3.1.3. Basket Cells

All the cerebellar interneurons remain far less characterized than Purkinje or granule cells and basket cells are no exception. Fast-spiking basket cells in the Purkinje cell layer or vicinity receive input from granule cells and direct climbing fiber innervation, providing inhibitory input to Purkinje neurons via pinceaux contacts which are pericellular basket terminals concentrated around the axon hillock, poised to powerfully gate Purkinje cell output, as well as to stellate cells (Jorntell and Ekerot, 2002, Barmack and Yakhnitsa, 2008, Palay and Chan-Palay, 1974).

1.3.1.4. Stellate Cells

Fast-spiking stellate cells are quite numerous in the molecular layer where they innervate Purkinje cell dendrites, receiving input from the climbing fiber, Purkinje cell collaterals and granule cells. They outnumber Purkinje cells by 10:1 in rodents and 50:1 in humans (Suter and Jaeger, 2004). Stellate cells as well as basket cells have been implicated in the antiphasic modulation of complex spikes and simple spikes via Purkinje cell recurrent collaterals (Barmack and Yakhnitsa, 2008).

1.3.1.5. Golgi Cells

Golgi cells are fast-spiking interneurons that receive input from granule cells and stellate cells. They are thought to be involved in filtering and attenuating mossy fiber input by forming inhibitory presynaptic contacts (Marr, 1969, Gabbiani, Midtgaard and Knopfel, 1994). Specific ablation of Golgi cells using a transgenic approach in mice sufficed to cause ataxia (Watanabe et al., 1998).

1.3.2. Deep Cerebellar Nuclei

1.3.2.1. Large Neurons

The large DCN neurons refer to the spiny, glutamatergic projection neurons that carry input out of the cerebellum primarily to motor centers, namely the red nucleus, ventral thalamus, intralaminar thalamic nuclei and pontine nuclei. Each large DCN neuron receives input from ~30 Purkinje cells (Chan-Palay, 1977), the inferior olive, mossy fiber collaterals and interneurons. Action potentials occur spontaneously and are modulated by rather constant inhibition from Purkinje cells during simple spiking. Climbing fiber stimulation *in vivo* can lead to large IPSPs and rebound excitation in the DCN in the form of fairly discrete bursts or accelerated spiking that undergoes more gradual frequency adaptation (Armstrong, Cogdell and Harvey, 1973, McCrea, Bishop and Kitai, 1977, Kitai et

al., 1977). A recent study just stimulating Purkinje cells in a circumscribed area saw rebounds in only 15% of 109 DCN neurons recorded extracellularly (Alvina and Khodakhah, 2008), probably because of diversity in cell types, such as weak and strong burst large neurons (Molineux et al., 2006) or small neurons (Uusisaari, Obata and Knopfel, 2007) however it suggests brief trains may not be enough in large neurons. Climbing fiber input may recruit more Purkinje cells. Perfusion of harmaline, which evokes synchronized olivary neuron firing, through an acute explant of the cerebellum and brainstem induced strong, rhythmic IPSPs in DCN neurons (Llinas and Muhlethaler, 1988). Recordings of awake behaving monkeys confirm that DCN activity is reciprocal to tonic Purkinje cell activity (Ghez and Thach, 2000). DCN neurons from genetically dystonic rats exhibit bursts but little definitive data are available as to their exact function. Removal of inhibition by the cerebellar cortex resulted in compensatory changes in the strength of inhibition by glycinergic interneurons (Linnemann et al., 2004, Sultan et al., 2002) suggesting homeostatic plasticity may occur chronically.

1.3.2.2. Small Neurons

The physiology of these neurons is almost totally unknown aside from a few investigations of firing properties. They are comprised of GABAergic, glycinergic and possibly dual GABAergic/glycinergic interneurons (Chan-Palay, 1977) and GABAergic projection neurons closing the loop with the inferior olive. These neurons receive input from Purkinje cells (De Zeeuw and Berrebi, 1995, Teune et al., 1998). Based on the many analogous relationships with the vestibular nuclei, where potentially cognate small and large neurons are found (Bagnall, Stevens and du Lac, 2007, Gittis and du Lac, 2007), some of the glycinergic small neurons may project to the contralateral DCN. Older intracellular recording studies could only differentiate DCN neurons based on size and morphology via biocytin fills. Since small neurons are more difficult to impale by sharp microelectrodes or patch, data are relatively scant (Aizenman, Huang and Linden, 2003, Czubayko et al., 2001). Recently Uusisaari et al., 2007 used mice

with green fluorescent protein (GFP) knocked-into the GAD67 locus to illuminate GABAergic neurons. Both small GABAergic and non-GABAergic neurons resembled each other but not large neurons in that these small neurons had broader but still narrow action potentials and fired at relatively lower frequencies. These neurons had larger input resistances, especially GABAergic ones, and longer rebound depolarizations. They differed amongst themselves in the duration of the depolarizations, with GABAergic neurons showing longer ones.

1.3.3. Vestibular Nuclei

Although these nuclei are not formally part of the cerebellum, hodologically and functionally they are analogous to the DCN with the difference that they are concerned with maintaining balance and eye movements rather than motor coordination. The cellular electrophysiology has been explored by Sacha DuLac's group (Bagnall, Stevens and du Lac, 2007, Gittis and du Lac, 2007, Sekirnjak et al., 2003) and resembles that of DCN neurons.

1.4. KV3 CHANNELS IN THE CEREBELLUM

Cerebellar neurons are mostly fast-spiking in contrast to other brain areas intersperced with a subset of fast-spiking neurons that are more the exception not the rule. Afferents to the cerebellum, mossy and climbing fibers, lack Kv3 channels (Figure 1.1). Pontine nuclei that give rise to most mossy fibers do however express them, just apparently not in axons. The neurons of the inferior olive from which climbing fibers emanate does not express Kv3 channels. These expression data are challenging to reconcile with physiological data *in vitro* (Mathy et al., 2007) and *in vivo* (Ito and Simpson, 1971) citing high-frequency transmission of action potentials in putative olivary axons. If spikes can be initiated at the first node of Ranvier as claimed it cannot be argued based on somatic protein expression that Kv3 channels are absent, however that no

mRNA was detected in the olive is still problematic. Thus far no empirical data support high-frequency firing taking place independent of Kv3 channels. In all of the cases below it should be borne in mind that *in situ* probes and antibodies do not always detect all splice variants.

1.4.1. Cerebellar Cortex

1.4.1.1. Granule Cells

Kcnc1a and *Kcnc1b* mRNA has been detected in rodent granule cells (Weiser et al., 1994, Perney et al., 1992). Kv3.1a and Kv3.1b proteins are accordingly detected in parallel fibers (Ozaita et al., 2002, Sekirnjak et al., 1997) . Kv3.2 and Kv3.4 are consistently absent using antibodies that detect all variants. *Kcnc3* mRNA is reliably detected along with Kv3.3b protein mainly in parallel fibers (Chang et al., 2007). In summary, granule cells and parallel fibers express Kv3.1a, Kv3.1b and Kv3.3b, with Kv3.1 at a higher level.

1.4.1.2. Purkinje Cells

Purkinje cells can be distinguished by expression of the calcium binding protein calbindin, which localizes near the membrane in these cells, and their very distinctive morphology. *Kcnc1* mRNA may have been present at low levels in the work of Weiser et al. The authors felt that signal in the flocculus and paraflocculus, ventrolateral lobes of the cerebellum involved in vestibular function and eye movements, was real (Weiser et al., 1994). Perney reported Kv3.1a as absent (Perney et al., 1992). Meanwhile the Allen Brain Atlas suggests it is expressed in all Purkinje cells. Neither Kv3.1a nor Kv3.1b protein has ever been detected (Ozaita et al., 2002, Sekirnjak et al., 2003). As with many cell-type specific genes, the specific expression of Kv3.1 protein may be determined in part at the RNA level by cell-type specific miRNAs that can suppress translation (Mattick and Makunin, 2005).

Expression of Kv3.3b reaches its zenith in Purkinje cells. *Kcnc3* mRNA is present at high levels (Weiser et al., 1994, Goldman-Wohl et al., 1994) along with the protein primarily in somata and proximal dendrites with lower levels in axons and distal dendrites (Chang et al., 2007, Martina, Yao and Bean, 2003). Kv3.2 is absent using antibodies detecting all variants (Rudy et al., 1999). *Kcnc2* mRNA likewise was absent in rat in Weiser et al. and a single-cell RT-PCR study but detected in the Allen Brain Atlas *in situ*. Conversely, *Kcnc4* mRNA was present at low levels in Weiser et al. but essentially absent in the Allen Brain Atlas *in situ*. In mice nonetheless Kv3.4 protein is expressed in Purkinje cells. Martina et al., 2003 detected somatic and curiously rather punctate, discontinuous labeling in the dendrite. An earlier study by Veh et al., 1995 evidenced weak labeling in their figure using an antibody that may prefer certain splice variants. Together, data suggest Kv3.3b and Kv3.4 are expressed in Purkinje cells.

1.4.1.3. Basket Cells

Because of their position in the cortex, the labeling of basket cells is difficult to distinguish from granule cells, especially in the cases of Kv3.3 and Kv3.1. Physiological data using the blockers 4-AP and TEA suggest Kv3 channels are present in basket or stellate cells which are fast-spiking interneurons. The absence of Kv3.2 is more readily asserted since no other cerebellar cortical neurons express it. Kv3.4 immunolabeling revealed expression in the cerebellar pinceaux, the form taken by the basket contact of basket cells in the cerebellum which envelops the axon hillock along with part of the soma in GABAergic contacts. To summarize, Kv3 expression in basket cells remains partially obscure.

1.4.1.4. Stellate Cells

Definitive *Kcnc1a* mRNA (Perney et al., 1992) signal was seen in what could be stellate cells in the molecular layer. *Kcnc1b* and *Kcnc3* have not been detected in the molecular layer. Kv3.1a and Kv3.1b proteins are in parallel fibers rendering it

difficult to exclude expression in stellate cells as with Kv3.3b (Weiser et al., 1994, Luneau et al., 1991b, Chang et al., 2007, Sekirnjak et al., 1997, Weiser et al., 1995). Holes can be seen likely corresponding to stellate cells in immunolabeled sections but it cannot be determined whether channels might be present in the periphery or at a low level not detected with the settings on the microscope optimized to see cells with high expression levels using immunofluorescence (Weiser et al., 1994). Kv3.2 expression can be excluded because antibodies detect all variants and there is no signal throughout the cortex (Lau et al., 2000). Kv3.4 however did appear weakly in the figure shown by Veh et al., 1995 though they made no remarks on it. Thus, like basket cells stellate cells, which are fast-spiking, may yet have Kv3 channels and likely have at least Kv3.4.

1.4.1.5. Golgi Cells

Kv3 subunit expression in Golgi cells has never been described, possibly because they are immersed in granule cells expressing Kv3.3 and Kv3.1. Kv3.2 can be ruled-out based on its clear absence in the cortex. *Kcnc4* mRNA by contrast is virtually detected exclusively in what appear to be scattered Golgi cells in the Allen Brain Atlas.

1.4.2. Deep Cerebellar Nuclei

1.4.2.1. Large Neurons

Kv3.1b and Kv3.1a have been found at both the protein and mRNA levels (Weiser et al., 1994, Weiser et al., 1995) in large neurons. In stark contrast to the cortex, Kv3.2 is detectable at the mRNA and protein levels. A low level of *Kcnc4* mRNA has been detected possibly attributable to large neurons, however the protein may not have been detected. Martina et al., 2003 did not examine the DCN.

1.4.2.2. Small Neurons

Only one recent study (Alonso-Espinaco et al., 2008) has addressed Kv3 expression at the level of small neurons by assessing whether neurons were GABAergic. Many GABAergic interneurons are highly variegated in their gene expression within most brain structures. Results of Alonso-Espinaco et al., 2008 along these lines suggest heterogeneity. A subset of GABAergic neurons expressed the subunit in the case of Kv3.1b and, evaluated separately, in the case of Kv3.3b. These subpopulations could represent interneurons or those supplying feedback to the olive. There are no data regarding Kv3.2 or Kv3.4 reported at a sufficient resolution to infer presence in small neurons.

1.4.3. Vestibular Nuclei

The physiologically and hodologically similar vestibular nuclei roughly parallel the DCN in terms of *Kcnc* mRNA expression and protein.

CHAPTER TWO
Review of the Literature

2.1. ATAXIA IN KCNC MUTANT MICE AND HUMANS

2.1.1. Cerebellar Ataxia

Ataxia is essentially incoordination, although it does not emphasize movement of muscles in relation to one another. The nuance is that it is more general. It is defined as disorder of movement without loss of strength or sensation. Gait ataxia, though what most often comes to mind, is but one manifestation. As with most of the nosology in neurology, the exact definitions of ataxia and cerebellar ataxia are vague and inconsistent (Schlaggar and Mink, 2003).

Cerebellar ataxia is that which was originally described observing the sequelae of cerebellar lesions. As Babinski described, “Rapid, exaggerated movements maintain their directional orientation” (Barboi, 2000). The most marked, general symptom is a dysregulation of the speed of movements that typically does incorporate the relative timing and speeds of movements too. Relative timing problems manifest as non-alternating gait. This facet of cerebellar ataxia is believed to be dissociable from altered movement speed and has been referred to as asynergia. Consequently movement is not smooth and rather broken down into isolated movements. The excess speed that results in exaggerated movements has been called hypermetria, under the umbrella term of dysmetria. Hypometria, or excessively low velocity, is also seen. Hypermetria can disrupt the speed of alternating movements as well, contributing to alternating gait deficits along with asynergia. Alternating movement disturbances of this kind have been called adiadochokinesia or dysdiadochokinesia. Both the initiation and cessation of movements are delayed together with impairments in smooth acceleration and deceleration of movement. The net result is for movement to take on a jerky and oscillatory character. Oscillations result from overshooting the target and then overly compensating by moving the limb back. The cycle repeats until the target is reached as the amplitude progressively

diminishes. Cerebellar intention tremor results when patients with cerebellar damage try to reach an object, and postural instability leading to oscillatory head bobbing and difficulty standing known as titubation may occur. Saccadic dysmetria also may be present causing difficulty maintaining a fixed gaze. In keeping with the role of cerebellar processing in more than just motor function, patients with cerebellar lesions also present with cognitive and psychiatric symptoms (Schmahmann, 2002, Barboi, 2000, Mariotti, Fancellu and Di Donato, 2005, Stolze et al., 2002).

In addition to lesion-induced ataxia, several genetic diseases cause it as well as autoimmune diseases such as paraneoplastic disorders when Purkinje cell antigens are expressed ectopically by tumor cells. Others are metabolic in etiology. Many act by causing progressive Purkinje cell degeneration. Some arise from X-linked, mitochrondrial or recessive mutations but most are autosomal dominant progressive ataxias classified as spinocerebellar ataxia (SCA). A number of SCAs continue to be discovered and in nearly half of these cases the gene responsible remains elusive. Most result from genetically unstable CAG repeat expansions causing polyglutamine tracts as with the huntingtin gene in Huntington's disease (Mariotti, Fancellu and Di Donato, 2005).

2.1.2. *SCA13*

SCA13 represents the first human disease linked definitely to a *Kcnc* gene (Waters et al., 2006, Waters et al., 2005). Unlike most SCAs, *SCA13* results from dominant negative point mutations. Two affected pedigrees have been found each with different mutations in *KCNC3*. A Filipino pedigree carried a R420H mutation affecting one of the positively charged residues in the voltage sensing (see section 1.1.1.3) S4 segment that acted as a potent dominant negative eliminating all current when co-expressed with wildtype Kv3.3. The other F448L mutation located in the pore-forming S5 segment at the cytoplasmic end involved in translating changes in voltage detected by S4 into pore opening in a French pedigree renders the gating similar to that of Kv1 channels. In particular fast

deactivation, essential for high-frequency firing, is removed. In fact, most voltage-gated potassium channels that close more slowly than Kv3 channels have a leucine at that position; the mutation strikes at the very essence of what distinguishes Kv3 channels that endows them with their unique physiological role.

Patients display cerebellar ataxia and mild mental retardation in the French family. Onset is in childhood in the Filipino family and adulthood in the French family where progression is slower. The Filipino mutation further causes cerebellar atrophy. Gait ataxia and dysmetria tended to be the most severe among affected family members. Titubation was also present. It is interesting that the mutation that abolishes all current results in earlier onset and cell death, whereas the mutation that mainly just slows deactivation does not in theory broaden spikes but just decreases spike frequency. The authors speculated that neurodegeneration might result in the Filipino pedigree because spike broadening would increase calcium influx. Assuming Kv3.3 heterotetramerizes with all the other subunits, the dominant negative would eliminate all Kv3 current in cells that express Kv3.3, leading to greater broadening than might be seen ablating one or two subunit genes.

2.1.3. *Kcnc1*-Null Mutant Mice

Cerebellar ataxia might be anticipated in -/-;+/+ mice considering the abnormal parallel fiber drive onto Purkinje cells that can be inferred from decreased paired-pulse facilitation, which is thought to reflect higher baseline neurotransmitter release closer to saturation. Action potentials monitored optically in parallel fibers are significantly broadened. A mere 50% increase in spike width is capable of inducing a 300% increase in postsynaptic current in Purkinje cells (Matsukawa et al., 2003).

The most widely-used method to measure limb ataxia and motor skill learning is the accelerating rotarod. In this test rodents are placed on a slowly-rotating, horizontal, elevated rod in a narrow space between two walls that

gradually accelerates and latency to fall is measured. Typically the rod is ~3 cm wide, and, unless the impairment is profound, most mice are able to remain on the rod at the initial speed of 5 rpm. Ataxic mutants however fall at a reduced latency compared to wildtype controls. Often the test is not extended beyond a set, maximal duration.

Ataxia has been suggested for -/-;+/+ mice by the rotarod test (see section 3.3.1.3) however the penetrance on different genetic backgrounds varied (Ho, Grange and Joho, 1997, Sanchez et al., 2000). Subtle motor coordination abnormalities were initially suggested using the sensitive force plate actometer (see sections 3.3.1.1 and 3.5.2.1). The device measures lateral deviation as the mouse ambulates across a plate mounted on force transducers to track the center of gravity essentially, reflecting both the position of the mouse and forces exerted by paws in contact with the plate at any given moment. Greater deviation raises the area of triangles formed by every three consecutive measurements of the center of gravity and this is indexed to the total distance traveled. Lateral deviation tends to correlate to the total distance traveled. Even though it is measured by indexing to the distance traveled, it could still be affected by motor drive rather than coordination or gait pattern. Thus plotting the LDI itself against the distance traveled to obtain a slope derives a more pure measure of lateral deviation due to abnormal rather than merely heightened movement. Although the raw LDI measure was significantly increased in -/-;+/+ mice (Espinosa et al., 2001), this slope is not significantly different from wildtype mice (Joho et al., 2006). The -/-;+/+ mice did not make significantly more slips traversing a 2-cm or 1-cm narrow beam. In this test mice traverse a 100-cm long beam five times a day for five days (Joho et al., 2006; see sections 3.3.1.2 and 3.5.2.2). It is interesting that these mutants have little or no ataxia indexed by the beam despite the abnormally strong parallel fiber input to Purkinje cells (Matsukawa et al., 2003). The observation suggests the synapse made by parallel fibers onto Purkinje cells, highly subject to plasticity, may adjust with learning to compensate for the excess excitatory drive. Overall data suggested that *Kcnc1*-null mice have

either mild cerebellar ataxia only evident on the rotarod with poor penetrance or are free from ataxia if the criteria of detection in multiple behavioral assays is a requisite.

2.1.4. *Kcnc3*-Null Mutant Mice

The +/+;-/- mice have broadened spikes in Purkinje cells despite co-expression of Kv3.4 in these cells that do not broaden further upon loss of *Kcnc1* in DKO mice. Accordingly there is no broadening in -/-;+/+ mice (McMahon et al., 2004). Parallel fiber input is inferred to resemble that of -/-;+/+ mice because loss of *Kcnc3* alleles intensifies the defect in paired-pulse facilitation suggesting more glutamate release. The +/+;-/- mice make significantly more slips on the 1-cm beam than wildtype mice even after five days of training that persists even if the test is extended to 10 days and have significantly increased lateral deviation that is true also examining the slope of area plotted against distance. On the less challenging 2-cm beam +/+;-/- mice improve by day five to the performance level of wildtype (Joho et al., 2006).

2.1.5. DKO Mice

Despite altered paired-pulse facilitation LTD is unaltered however in -/-;-/- mice (Matsukawa et al., 2003). LTP induction is blocked possibly due to saturation prior to slice preparation. One would expect alterations in LTD in -/-;-/- mice to be if anything more severe than that of -/-;+/+ mice. That LTD was normal in -/-;-/- mice suggests it is in *Kcnc3* single-null mice, but whether LTP is blocked with less glutamate release than in -/-;-/- mice is uncertain. The ability of parallel fibers to sustain high-frequency firing was studied in -/-;-/- mice which have the greatest broadening compared to the two single-null mice (deductively inferred or directly measured). Axons were able to propagate sustained compound action potentials at 100 Hz with mild attenuation but not at 200 Hz, however this is the upper boundary of the range at which granule cells normally fire. Net effects of a potentially decreased rate of firing in mutants *in vivo* with a given strength of

mossy fiber input and increased glutamate release may either increase or decrease parallel fiber drive onto Purkinje cells.

The -/-;-/- mice cannot stay on the rotarod significantly to obtain meaningful results (Espinosa et al., 2001). When compared by slope (see section 2.1.4), -/-;+/- mice have more lateral deviation than -/-;+/+ mice, while +/-;-/- mice have more than +/+;-/-. Loss of both subunits leads to a much greater increase in the LDI/distance traveled slope in -/-;-/- mice. On the 2-cm and 1-cm beams, the aforementioned genotypes perform for the most part like +/+;-/- mice. The beam test has not been performed with DKOs because they typically fell quite promptly, as on the rotarod, on the genetic backgrounds tested. No effort was made to give them repeated chances. Use of a 0.5-cm beam in contrast uncovers a difference between the mice lacking three alleles and +/+;-/- mice. The former are much worse. Here falls are counted because slips are too numerous (Joho et al., 2006). These data reinforce the notion that Kv3.3 is most involved in coordination but that a latent role for Kv3.1 is revealed in the absence of Kv3.3, suggesting functional redundancy in functionally related neuronal cell-types.

2.2. OTHER MUTANT MOUSE MODELS OF CEREBELLAR ATAXIA

2.2.1. *Pcd* Mice

A natural mutation in the *Nna1* gene leads to quite selective Purkinje cell degeneration in *pcd* mice. Granule cells are lost but are upstream of Purkinje cells, and just a few thalamic neurons eventually. Indeed, a recent study introduced wildtype Nna1 in a cell-type specific manner to Purkinje cells and fully rescued motor coordination (Chakrabarti et al., 2008, Wang et al., 2006). Because Purkinje cells are necessary for cortical output, the mutant is essentially decorticated in the cerebellum. *Pcd* mice surprisingly have relatively moderate cerebellar ataxia compared to mice with alterations in DCN output discussed below, as well as -/-;-/- mice (Joho RJ, unpublished observation). This

establishes the importance of the cortical output and Purkinje cells in motor coordination, and suggests the DCN may only adapt to a loss of inhibition by Purkinje cells to a limited extent.

Other natural mouse mutants exist where Purkinje cells are lost fairly specifically albeit less than *pcd*. These include *Lurcher* mice. All have ataxia.

2.2.2. Natural and Engineered Channelopathies

Given the prominent, decisive role of ion channels in determining neuronal excitability and transmitter release in a key downstream position in many signal transduction cascades it is perhaps not surprising that ion channel genes form the basis of a number of severe neurological disorders, referred to today collectively as channelopathies (Cannon, 2006, Bernard and Shevell, 2008). Ataxias are no exception.

2.2.2.1. Voltage-Gated Potassium Channels

The first channelopathy to be identified in humans was episodic ataxia type-1 resulting from a mutation in *KCNCA1* encoding Kv1.1 (Browne et al., 1994). Cerebellar cortical interneurons such as basket cells express the subunit. A mouse model was generated and used to show that input from basket cells onto Purkinje cells is abnormally strong, causing excess inhibition (Herson et al., 2003). Blockade of Kv3 channels with TEA interestingly has similar augmenting effects *in vitro* (Southan and Robertson, 2000).

SCA1 is caused by a repeat expansion affecting Ataxin-1, a protein involved in transcriptional regulation (Emamian et al., 2003, Zoghbi and Orr, 2008). Recent data suggest Kv4 channels are upregulated in Purkinje cells causing excessive A-type current to decelerate spontaneous simple spiking. The deceleration was also seen *in vivo* and injection of the blocker 4-AP rescued coordination in a mutant mouse model using the rotarod test. Oddly the physiological abnormalities preceded symptoms, however this may reflect the

sensitivity of the rotarod in detecting subtle ataxia (Hourez et al., 2007). In a similar vein, expression of Ataxin-3, the causative gene in *SCA3*, in PC12 cells resulted in a hyperpolarizing shift in the activation curve of delayed-rectifier potassium current (Jeub et al., 2006).

2.2.2.2. SK channels

Shakkottai et al., 2004 produced transgenic mouse lines using the Thy1.1 promoter where a dominant negative SK channel subunit was expressed in circumscribed neuronal cell populations mainly in the red nucleus, pons and DCN. Severe cerebellar ataxia including gait ataxia resulted that correlated best with DCN expression. Balance based conjecturally on loss of equilibrium on a stationary rod and grip strength based on the hanging wire test appeared to be affected while ataxia was clear on the rotarod and in the footprint test. Firing was accelerated in this case recording DCN neurons.

2.2.2.3. BK channels

A BK channel null mutant with ataxia was analyzed by Sausbier et al., 2004 that had a reduced area and amplitude of the afterhyperpolarization of evoked Purkinje cell spikes but not spike broadening at the soma in slice recordings. Spontaneous spiking was abrogated. As expected at the Purkinje cell synapse in the DCN if spikes are broadened at the terminal, paired-pulse depression was enhanced (Sausbier et al., 2004). The overall mutant phenotype is consistent with the notion that loss of fast repolarization in Purkinje cells leads to ataxia. *In vivo* the lack of spontaneous activity should reduce overall Purkinje cell output unless afferent input is much greater. Synaptic depression was also augmented at DCN synapses.

Ataxia was measured by the footprint test, the rotarod and the beam test measuring falls. Fore paws were inked blue to differentiate prints from those made by hind paws inked red. Null mice performed worse on these tests than wildtype mice, making shorter strides and showing paw discordance or abduction

referring to a failure to place the hind paw over the fore paw print as normal mice do. Swimming speed was also reduced.

2.2.2.4. Calcium Channels

Several calcium channel mutations give rise to ataxia (Miki et al., 2008, Erickson et al., 2007, Ovsepian and Friel, 2008). *Cacna1a* and *Cacna2d*, the auxiliary subunit of the latter, are affected by the *leaner* and *ducky* mutations, respectively. *Cacna2a* encodes Cav2.1. Mutations in the human gene form the basis of episodic ataxia type 2 (Riant et al., 2008). The two above mouse mutants exhibit increased simple spike irregularity in slices. More precisely, the coefficient of variation of the interspike interval is increased. Enhancing calcium-activated potassium currents in the cerebellum *in vivo* with an agonist drug alleviated the ataxia along with the spike irregularity, leading the authors to conclude it was the cause (Walter et al., 2006). Complex spikes, which P/Q type calcium channels such as these help shape, were not examined.

The *tottering* mutant also harbors a mutation in the *Cacna1a* gene, as well as the *rocker*, *rolling Nagoya*, and *groggy* mutants. *SCA6*, a CAG repeat SCA, also results from mutations in this channel that cause excessive accumulation with age sparing electrophysiological properties in a mouse model (Watase et al., 2008).

2.2.2.5. Sodium Channels

Among the few experiments addressing the role of an ion channel in Purkinje cells was the cell-type specific ablation of the sodium channel gene *Scn8* encoding Nav1.6 that participates in action potential generation and contributes to subthreshold excitability using the *Cre-lox* system (Levin et al., 2006). The ablation was sufficient to elicit an ataxic phenotype as in the conventional *Scn8*-null mutant (Raman et al., 1997) and humans carrying a loss-of-function mutation (Trudeau et al., 2006). It was known from studies of dissociated cells that spontaneous spiking is eliminated and bursts argued to be akin to complex

spikes triggered by current injection[1] displayed fewer spikes and a lower intraburst frequency (Raman et al., 1997). Cell-type specific ablation in granule cells produced similar effects on behavior (Levin et al., 2006).

Ablation of the gene encoding Nav1.1, another sodium channel prominent in Purkinje cells, also led to ataxia (Kalume et al., 2007). In this case spontaneous spiking remained in dissociated Purkinje cells but was decelerated. Here it is unclear if the loss of the channel in Purkinje cells is causative.

2.2.2.6. HCN channels

In Nolan et al., 2003, decreased performance on the rotarod only at high speeds and altered timing of the conditioned eyelid response in *Hcn1*-null mice suggested cerebellar pathology. Purkinje cell recordings revealed that spontaneous activity in slices, with little or reduced inhibitory interneuron input, was normal but subthreshold properties had changed. After hyperpolarization below threshold and subsequent depolarization using a zig-zagging ramp protocol, there was an increased latency to resume spiking. This suggested that Purkinje cells might remain hyperpolarized after inhibition and not bounce back to baseline readily, rendering the effect of subsequent inputs dependent on past inputs that determined what state the cell was in (Nolan et al., 2003). The study did not definitively link Purkinje cells per se to the phenotype causatively, however the data are consonant with the idea that Purkinje cell firing must be normal for normal motor coordination.

2.2.3. Calcium-Binding Protein Mutants

Calcium-binding proteins seem to serve as buffers of intracellular calcium which may protect neurons and compartmentalize calcium entry into the cytosol. Ultimately calcium levels can impact firing through calcium-activated potassium channels, like the BK channels discussed above, among other routes. Ablation of

[1] Dissociated Purkinje cells lack the enormous dendritic conductance and so have a high input resistance, reacting dramatically to the slightest depolarizing current as it is essentially undiluted by the currents of the now reduced cell membrane area.

calretinin leads to electrical abnormalities in Purkinje cells and granule cells accompanied by ataxia (Schiffmann et al., 1999). Restoration of calretinin exclusively in granule cells yielded a rescue of motor coordination (Bearzatto et al., 2006). Intriguingly, spiking phenotypes in Purkinje cells *in vivo* were rescued cell non-autonomously as well. Complex spike burst and pause durations were decreased and the simple spike frequency increased in null mice, presumably due to altered parallel fiber input to Purkinje cells directly by way of interneurons.

2.2.4. MGluR1

The role of Purkinje-cell expression of mGluR1 metabotropic glutamate receptors in motor coordination was shown by cell-type specifically restoring expression in Purkinje cells using the tetracycline-regulated system (Nakao et al., 2007). Conventional mGluR1 null mice which have ataxia were bred with mice carrying an mGluR1 transgene that requires co-expression of the tetracycline transactivator (tTA) in the same cell. The transactivator was expressed selectively in Purkinje cells using the L7-tTA line, and rendered inducible by using doxycycline to suppress expression in adulthood. Restoration only in Purkinje cells rescued coordination in the footprint test as well as on the rotarod and it could be reversed by doxycycline, suggesting it was through a fairly acute effect of mGluR1 expression. There was no electrophysiological analysis.

2.2.5. ROR-α

Mutation of the retinoid orphan receptor-α also causes ataxia in mice in this case by developmental effects (Steinmayr et al., 1998). Prior to identification of the genetic etiology the mouse was known as the *staggerer* mutant. Though expressed also in thalamus and hypothalamus these areas are morphologically normal. Purkinje cells in contrast are multiply innervated by climbing fibers.

2.2.6. *SCA8*

Deletion of the *Kelch-like 1* gene which may be suppressed by the dominant mutation at the *SCA8* locus either in the whole mouse or just in Purkinje cells was sufficient to cause progressive ataxia detectable by the rotarod (He et al., 2006). Expression levels of Kelch-like 1 can affect the level of P, Q-type calcium channels (Aromolaran et al., 2007) implicated in ataxia as discussed above in section 2.2.2.4. This mutant constitutes further evidence of the critical role of Purkinje cells as established by the *pcd* mouse.

CHAPTER THREE
Methods

3.1. GENERATION OF NULL MUTANT AND TRANSGENIC MICE

3.1.1. Null Mice

3.1.1.1. Generation and Genotyping of Kcnc1*-null allele*

Mice lacking *Kcnc1* were generated by homologous recombination by the usual methods in ES cells derived from mice of the 129Sv strain in the context of the dissertation of Dr. Chi Shun Ho, where detailed methods can be found that led to the initial report of the null mutant (Ho, Grange and Joho, 1997, Ho, 1996). The targeting construct ablated codons 273-285 5' to those encoding the pore and voltage gate essential to form a functional potassium channel subunit, leaving the mRNA 5' to this portion intact. Indeed, a Northern blot indicated persistence of the 5' sequence but not the sequence 3' to the deletion in null mice. It is unknown whether the N terminal part of the protein is translated and, if so, if it is stable, for all Kv3.1 antibodies target C termini. Using such antibodies a Western blot confirmed the loss of Kv3.1 in null mice. The ablated region was replaced with a pgk-neo cassette in the same orientation as *Kcnc1* for screening ES cells for the targeting construct, the correct targeting of which was confirmed by a Southern blot. This cassette remains at the locus. *Kcnc1*-null alleles were subsequently discriminated from wildtype alleles during genotyping routinely by a multiplex PCR sharing a common forward primer,
5'-GCGCTTCAACCCCATCGTGAACAAGACC-3'. Reverse primers specific to wildtype and null alleles were 5'-GGCCACAAAGTCAATGATATTGAGGGAG-3' and 5'-CTACTTCCATTTGTCACGTCCTGCACG-3', respectively. Wildtype mice yield a 216 bp band, *Kcnc1*-null mice a 420 bp band and heterozygotes both bands (see diagram in Appendix A). PCR was performed on a PTC-100 Programmable Thermal Controller (MJ Research) as follows: 95°C for 3 minutes, followed by 35 cycles at 95°C for 1 min, 61°C for 1 min, and 72°C for 1.5 min,

and a final extension at 72°C for 3 min. Bands were observed on a 1.6% agarose 0.5 µg/ml ethidium bromide gel.

The *Kcnc1*-null allele was maintained on an outbred genetic background for several years prior to this study. The initial characterization of *Kcnc1*-null mice was performed on a 129Sv inbred genetic background.

3.1.1.2. Generation and Genotyping of Kcnc3-*null allele*

Mice lacking *Kcnc3* were generated by homologous recombination by the usual methods in ES cells derived from mice of the 129Sv strain in the context of the dissertation of Dr. Emily Chan in the laboratory of Nathaniel Heintz at the Rockefeller University, where detailed methods can be found that led to the initial report of the null mutant (Chan, 1997). The targeting construct ablated ~3 kb of the 5' promoter region along with the first two initiator methionines in the coding region on the first exon. The deleted sequence was replaced with a pgk-neo cassette in the opposite orientation with respect to *Kcnc3*. Correct targeting was verified by a Southern blot and loss of expression was confirmed by a Western blot. Subsequently mice were genotyped using a multiplex PCR sharing a common reverse primer for wildtype and null mice, however, even after several attempts at optimization, the DNA could not reliably be amplified without laborious Phenol:Chloroform extraction. Even then, bands were often weak. Therefore I redesigned the PCR.

I repositioned the genotyping primers to amplify sequences with less GC content and other features likely to hinder PCR with which the *Kcnc3* locus is replete, especially in the CpG island encompassing the basal promoter region at exon 1 where the deletion is located (see diagram Appendix A). I designed a completely separate primer pair, 5'- GCCCAGCAATGAGTGTCCTT -3' and 5'-TAGACCTGGGCGAAGAGGAT-3' to amplify a 227 bp band exclusively in wildtype mice, placing it in the deleted promoter region 5' to the CpG island. I retained the 5' null-specific genotyping primer in the pgk-neo sequence, 5'-TTCCATTTGTCACGTCCTGCACG-3' and moved the 3' primer, 5'-

TGCGGTAGTAGTTGAGCACG-3' closer to the edge of the neo cassette, producing a ~300 bp amplicon (the exact junction between the neo cassette and genomic DNA is unclear using the Celera 129Sv genome now on NCBI; the 129Sv genome of ES cells is slightly different from that of other 129Sv lines. Thus, the exact length is unknown). PCR was performed as with *Kcnc1* above except using 55 cycles. Further, I modified also the overall tail DNA preparation protocol of Malumbres et. al. 1997 to include a 15-minute 95°C incubation step to immediately inactivate DNase prior to proteinase K digestion. This dramatically improved subsequent PCR robustness and was a key innovation that enabled me to circumvent DNA purification for all genotyping in the lab.

The *Kcnc3*-null allele was maintained on an outbred genetic background for several years prior to this study. The initial characterization of *Kcnc3*-null mice was performed on a 129Sv inbred genetic background. Maintenance on an outbred background prevented seizures from occurring occasionally upon handling of the null mice.

3.1.1.3. Generation of Kcnc1/Kcnc3-*null allele*

Because the *Kcnc1* and *Kcnc3* genes are closely linked within ~1 centimorgan (cM) of one another, to obtain double-mutant mice it was necessary to first derive recombinants among single-null mice acquiring the other nearby null allele (Espinosa et al., 2001). After ~100 crosses, offspring were born of crosses between mice lacking *Kcnc1* and mice lacking one *Kcnc3* together with one *Kcnc1* allele on separate chromosomes. *Kcnc1*-null offspring (~50%) also carrying a *Kcnc3*-null allele were identified by genotyping as, by necessity, carrying a double-null allele. These double-heterozygous mice, with both null alleles now on the same chromosome, were maintained since around 1999 on a mixed background. Specifically, on a roughly annual basis C57/Bl/6/J, 129SvJ and ICR mice were obtained that were bred together to yield mice with 25% of the genome from the inbred strains and 50% from the ICR background. This mix

promoted maximal fecundity and overall vigor that was particularly beneficial in breeding -/-;-/- mice.

3.1.2. Transgenic Mice

3.1.2.1. Generation of pBIKcnc3b-eGFP *transgenic mice*

Mice that simultaneously express Kv3.3b and the fluorescent reporter enhanced eGFP in the presence of the tetracycline transactivator were generated using the pBI-EGFP bicistronic vector (Clontech). Here, two truncated CMV promoters are oriented in opposite directions with a TRE sandwiched between them to impart dependence on the tetracycline transactivator for expression. The murine *Kcnc3b* mRNA sequence containing the native Kozak sequence 5' to the first initiator methionine and ~0.4 kb of the 3'UTR was obtained by RT-PCR subcloned into a series of cloning vectors over a period of years and then transferred to pBI between the PvuII and MluI sites in the polylinker. The integrity of *Kcnc3b*, which is highly prone to recombination in *E. coli*, was confirmed by restriction digests and SURE™ cells (Stratagene) were used to greatly reduce the incidence of DNA rearrangement. The construct was linearized in the vector backbone and purified using the Elutip-d kit (Whatman) and submitted to the transgenic core, the UT Southwestern Medical Center Transgenic Technology Center. The transgenic construct was introduced to the germline by microinjection into C57/SJLF1 pronuclei. Dr. Anne McMahon screened the founders from the core and performed all of the work up until this point.

For genotyping I devised a set of primers to detect the transgene via the eGFP moiety, 5'-TGCTCAGGTAGTGGTTGTCG-3' and 5'-ACGTAAACGGCCACAAGTTC-3', yielding a 546 kb band, that was amplified directly from proteinase K digest using protocol I modified based on Malumbres M et al. 1997 detailed in Appendix A in a PCR performed as with *Kcnc1* above. Bands were visualized by means of 1.6% agarose gel electrophoresis.

3.1.2.2. Generation of L7-tTA/pBIKcnc3b-eGFP *bi-transgenic mice*

pBIKcnc3b-eGFP founders were crossed with transgenic mice carrying the *L7-tTA* construct obtained from Dr. Harry Orr at The University of Minnesota (Zu et al., 2004) to initially screen for expression in Purkinje cells, potential leaky transgene expression and ultimately assemble the transgenes necessary for the Purkinje cell rescue experiment. *L7-tTA* mice are a driver of tetracycline transactivator (*tet-off*) expression under the direction of the Purkinje-cell specific *L7/PcP2* promoter (Zhang et al., 2001). The line was generated on an inbred FVB/N strain background where the *L7-tTA* transgene had been homozygosed, as evidenced by test crosses. F1 offspring with the pBI construct, inevitably hemizygous for the *L7-tTA* transgene, were detected by genotyping for eGFP as described above. Double-transgenic F1 offspring were then crossed to mice carrying only the *L7-tTA* transgene, often F1 siblings or from other F1 crosses, to derive F2 offspring to screen for expression. I designed primers to amplify a 400 bp band from the tTA coding region of the transgene, 5'-GCTCGACGCCTTAGCCATTG-3' and 5'- TGGCTCTGCACCTTGGTGAT-3', that were multiplexed together with the pBI (eGFP) primers as described above.

Brains of double-transgenic F2 offspring were then screened for eGFP expression because by the F2 generation most individual transgene integrants at discrete chromosomal loci will have segregated. I screened acutely-dissected brains by manually cutting ~1 mm-thick slices from ice-cold tissue with a razor blade, placing them in Dulbecco's phosphate-buffered saline (1X DPBS, Sigma; in mM: 1.5 KH_2PO_4, 8.1 Na_2HPO_4, 136.9 NaCl and 2.7 KCl, pH7.4), and immediately assessing eGFP expression on a microscope equipped with a 40X water-immersion lens used for acute brain slice recordings (see below) with epifluorescence. Alternatively, I used immunofluorescence or highly-sensitive Ni-enhanced DAB immunohistochemistry using the ABC kit (Vector Labs, Burlingame, CA) following the manufacturer's instructions to detect eGFP using rabbit anti-GFP (Molecular Probes). Several additional mice were screened for eGFP expression to be sure the line used bred true and assess mosaicism which

can exhibit interindividual variability. Genotyping PCR proceeded directly from proteinase K digest of tail DNA using protocol I devised as described above for the null alleles detailed in Appendix A.

3.1.3. Breeding

Double-transgenic wildtype mice (50% FVB/N; 50% B6SJLF1) carrying the *pBIKcnc3b-eGFP (313 line)* and *L7-tTA* transgenes were crossed with outbred mice carrying the *Kcnc3*-null allele to obtain mice for restoration of Kv3.3 expression in Purkinje cells initially in *Kcnc3*-null mice and related controls. Next, I bred mice to restore Kv3.3 to Purkinje cells on a maximally similar genetic background that was *Kcnc3*-null and heterozygous for the *Kcnc1*-null allele by crossing wildtype mice with the *L7t-TA* transgene from the above single-null experiment with *Kcnc1*/*Kcnc3*-null double-heterozygous mice to obtain *Kcnc1*/*Kcnc3*-null double-heterozygous mice with the *L7t-TA* transgene. These mice were then crossed with *pBIKcnc3b-eGFP+ (396 line)***,** *L7-tTA+ Kcnc3*-null mice to yield mice lacking *Kcnc3* as well as one *Kcnc1* allele, rescue mice with the latter genotype except bearing both transgenes and mice heterozygous for *Kcnc3* as controls. Offspring of mice from this experiment and their parents were used to derive mice double-heterozygous for *Kcnc1* and *Kcnc3* carrying the two transgenes were bred together to generate -/-;-/- mice, -/-;-/- rescue and wildtype control mice. Mice were bred and maintained on 4% fat chow (Harlan) unless otherwise specified.

Separate control groups were used for each mutant because it is essentially impossible to derive all three types of mutants from the same breeding pairs along with either wildtype or *Kcnc3*-null allele heterozygote controls. I however minimized the genetic distance between these groups by deriving them from breeders largely culled from the other groups.

3.2. CHARACTERIZATION OF GENE EXPRESSION

3.2.1. Western Blot Analysis

3.2.1.1 Preparation of Protein Samples

Brains were dissected from adult mice anesthetized with avertin (1.25% tribromoethanol in *t*-amyl alcohol) and separated into cerebellum, brainstem and forebrain/midbrain (tissue anterior to the pons). Frozen tissue was homogenized rapidly in cold lysis buffer (in mM: 1.5 KH_2PO_4, 8.1 Na_2HPO_4, 136.9 NaCl and 2.7 KCl, pH7.4, 1% Triton X-100) to which 1 Mini Protease Inhibitor™ cocktail tablet (Roche, Indianapolis, IN) per 10 ml lysis buffer was added. Tissue was deemed homogenized upon obtaining an even opacity and centrifuged at 13,000 rpm in a microfuge for 5 minutes at 4°C. The BCA kit (Pierce, Rockford, IL) was used to measure protein concentrations. Supernatant was stored as aliquots at -80°C.

3.2.1.2 SDS-PAGE and Transfer to Blot

Protein samples were separated by electrophoresis in 8.0% SDS-polyacrylamide at 100V in a BioRad Mini Protean apparatus (BioRad, Hercules, CA) and transferred to nitrocellulose membranes. The transfer was performed in the apparatus at 30V overnight at 4°C.

3.2.1.3 Immunoblotting and Imaging

Blots were blocked in 0.1% TBS-T (100 mM Tris, 1.5 M NaCl, 0.5% MgCl, 1% Tween-20, pH 7.4) with 5% dry milk (Sanalac, Conagra, Irvine, CA) for 3-4 hours with gentle agitation. Kv3.3b protein was detected with rabbit anti-Kv3.3b antibody (Alomone Labs, Jerusalem, Israel) at 1:1200 and mouse anti-actin (Sigma) at 1:800 in 0.1% TBST-T with 1% dry milk overnight at 4°C with gentle agitation. Blots were given five 10-minute washes in 0.1% TBST-T followed by peroxidase-conjugated goat anti-rabbit IgG antibody at 1:1500 (Pierce, Rockford, IL) in 0.1% TBS-T with 0.1% dry milk. After four 10-minute washes blots were treated for enhanced chemiluminescence according to the manufacturer's

instructions (Pierce, Rockford, IL).

3.2.2. Immunofluorescence

3.2.2.1. Characterization of Kv3 Expression

Adult mice anesthetized with avertin were transcardially perfused with cold Dulbecco's phosphate-buffered saline (1X DPBS, Sigma; in mM: 1.5 KH_2PO_4, 8.1 Na_2HPO_4, 136.9 NaCl and 2.7 KCl, pH7.4) followed by 4% paraformaldehyde in 1X DPBS. Brains were dissected, post-fixed for 1 hour at 4^oC, followed by cryoprotection in 40% sucrose in DPBS at 4^oC. The tissue was embedded in OCT, sectioned at 20 µm coronally or sagittally, stored at -20°C in storage buffer (80 mM DPBS, 30% glycerol and 30% ethylene glycol) until free-floating immunohistochemistry was performed. Sections were protected from light whenever quenchable fluors were present.

Frozen sections in storage buffer were first given three 10-min washes in 1X DPBS followed by a 2-3 hour incubation with blocking solution (4% goat serum, 5% BSA, 0.3% Triton X-100, 0.05% Tween-20 in 1X DPBS). Gentle agitation was used during all incubations. Primary antibodies including rabbit anti-Kv3.3b (1:650; Alomone), mouse anti-Kv3.1b (1:50; Antibodies Inc., Davis, CA), rabbit anti-Kv3.2 (1:500; Alomone), rabbit anti-Kv3.4 (1:200; Alomone), mouse anti-Kv3.4 (1:50; Antibodies Inc.), mouse anti-SMI-32 (1:1000; Covance, Princeton, NJ), mouse (IgG_{2a}) anti-GAD67 (1:2000; Chemicon/Millipore, Temecula, CA), mouse anti-calbindin (1:750; Swant, Switzerland) were applied overnight in blocking solution at 4^oC with gentle agitation followed by four 10-minute washes in 1X DPBS. Goat anti-rabbit Alexa568-, Alexa488- or Alexa633, or anti-mouse Alexa568-, Alexa488- or Alexa647-conjugated secondary antibodies (Molecular Probes/Invitrogen, Eugene, OR) were applied in blocking solution at 1:400 at room temperature for 3-4 hours followed by three 10-min rinses in PBS Sections were mounted on Probe-On™ Slides (Fisher) and dried. Slides were dried in graded ethanols and defatted in xylene.

3.2.2.2. Post-Hoc Identification of Alexa488-filled Neurons from Patch-Clamp Recordings

Transcardial perfusion of mice with aCSF before slice preparation (see section 3.4.1.1) was necessary to eliminate autofluorescence from blood vessels for post-hoc immunofluorescence. Slices were placed in 4% paraformaldehyde in 1X DPBS on ice within 2 minutes of seal loss for 1-1.5 hours until stored in 40% sucrose in 1X DPBS with sodium azide at 4°C protected from light at least overnight to several weeks. Slices were resectioned at 40 µm or processed without sectioning. The above immunohistochemistry protocol in section 3.2.2.1 was used except unsectioned slices were incubated in the blocking solution with the Triton X-100 elevated to 10%.

3.3. BEHAVIORAL ANALYSIS

3.3.1. Analysis of Motor Coordination

3.3.1.1. Force Plate Actometer

Individual, naïve mice were allowed to freely explore a lightweight, rigid platform (28 x 28 cm) resting on four sensitive force transducers covered by a Plexiglas enclosure suspended just above the plate (Fig. 3.1). The walking trajectory during epochs of linear ambulation on the plate is represented by connections of temporally consecutive centers of force (COFs), which are essentially the center of gravity determined by which paws are on the plate, how far paw placements are from each other and how much force is applied during stepping. COFs are

Figure 3.1. (Below) Mouse ambulating freely on the force plate actometer. Normally the plate is covered with a plexiglass box that has been removed here for better visualization. Force transducers can be seen in each corner.

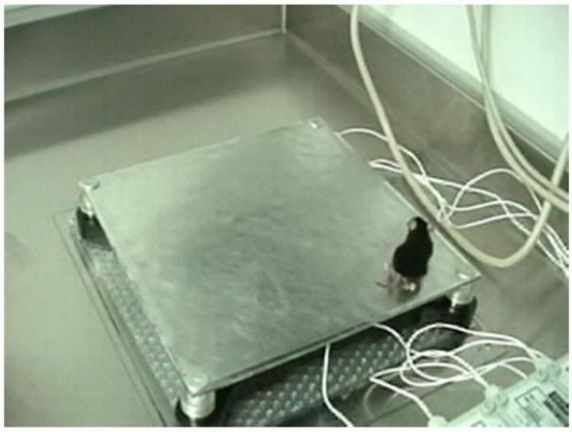

sampled at 20 ms intervals at high spatial resolution (< 1 mm). The total distance traveled is the sum of the linear distances (Σd_i) between consecutive COFs. The area measure corresponds to the sum of all triangular areas (Σa_i) defined by every three consecutive COF measurements (Joho et al., 2006, Fowler et al., 2001). For a quantitative measure of lateral deviation from the main walking trajectory, the summed areas (Σa_i) generated during the 6-min test are divided by the total distance traveled (Σd_i) to obtain the lateral deviation index (LDI = $\Sigma a_i/\Sigma d_i$). The LDI would equal zero if the walking trajectory were a straight line (area measure equals zero). The LDI (in mm) increases with increasing lateral deviation of the COFs from the main trajectory of movement and corresponds to the 'relative amplitude' of deviation from the mean path, representing an operational measure for motor coordination during ambulation.

For the force plate experiment, mice were maintained on a 12/12 light/dark cycle and tested during the latter half of the light phase. Males and females were used because the lab did not observe gender differences in previous work (Joho et al., 2006). In the DKO rescue experiment mice were kept on 11% fat chow (Harlan) from weaning onwards to reduce mortality and better equalize body size to that of wildtype controls by the time age-matched control groups were tested at 3-6 months of age. Testing occurred on the first day of the beam test (see below) for a duration of 6 minutes.

3.3.1.2. Beam Test

The same mice used on the plate above were on the same day started on the 5-

day beam test (see section 3.3.1.1 above for age, photoperiod and other subject parameters). Males and females were used because we did not observe gender differences (Joho et al., 2006).

Figure 3.2. Mouse traversing the 1-cm beam in the midst of making a slip with its right hind limb.

The protocol was based on that of Goldowitz et al., 2006 (Goldowitz, Moran and Wetts, 1992). Mice were placed at the end of a narrow (2-cm, 1-cm or 0.5-cm wide) 100-cm long Plexiglas beam with a smooth, flat surface and 1-cm tall vertical sides suspended 10 cm above a surface and allowed to traverse the beam five times per day on five consecutive days. Forelimb and hind limb slips on the 1-cm beam and sideway falls on the 0.5-cm beam were counted by two observers on each side blind to genotype (nearly all slips were by hind legs), namely Dr. Joho and myself consistently. In the -/-;-/- rescue experiment the 2-cm beam was used and falls were counted because of the severe ataxia of -/-;-/- mice virtually precludes counting of slips. After falling mice were placed back on the beam where they fell and released once they regained their footing. If -/-;-/- mice fell promptly after 15 attempts to place them on the beam they were deemed unable to perform. When mice lacking one *Kcnc1* allele as well as *Kcnc3* were tested on both the 1 and 0.5-cm beams, a 2-day hiatus separated the two tests. Process NPD, and ammonium quat disinfectant (Steris), was used to clean the beam between mice. The average numbers of slips and sideway falls per 100 cm traveled each day were used for data presentation and analysis.

3.3.1.3. Rotarod

Largely the same mice used in the above studies were tested on an Economex (Columbus Instruments, Columbus, Ohio) accelerating rotarod at 8-11 months of age. Mice were kept on a 12/12 light/dark cycle, tested during first half of dark phase in very dim light. The width of the rod covered in a longitudinally-grooved plastic casing was ~3 cm and it rotated such that mice must move forward to remain on in the orientation they are initially placing, facing away from the experimenter. I gave the mice 4 trials separated by ~1-hour intervals on each of 4 days, based on the method of Nolan et al., 2003. Rotation began at 5 rpm and accelerated at 10 rpm/minute. The latency to fall was noted for each mouse. Obese mice and mice not remaining on the rod on day 4 for >10 seconds on average over the last 4 trials were excluded from the analysis. The maximal latency to fall among all mice was nearly 7 minutes.

3.3.2. Gait Analysis

3.3.2.1. DigiGait™ Analysis

Mice used for DigiGait™ analysis largely overlapped those used for the above tests. For the pilot *Kcnc3*-null experiment, mice were 10-12 months old and the same mice used for the rotarod test, where most wildtypes were albino and most agouti mice were pigmented. All mice used in the experiment examining +/-;-/- mice were agouti males, and 3-6 months of age, with the majority 4-6 months. In this experiment, mice heterozygous for the *Kcnc3*-null allele served as normal controls.

Data were acquired by first painting the paws of mice with a red, and extraneous reddish parts of the mice with a blue Betty Crocker Easy Writer cake decorating marker and placing the mice on the stationary DigiGait™ treadmill (Mouse Specifics, Boston, Massachusetts). Paws are detected as red color contacting the belt and blue is ignored. The treadmill is equipped with a Plexiglas chamber mounted over the area monitored by the camera to keep the mouse running in place and in view. I removed the curved bumper accessories and

added a dropped ceiling made of Scotch tape to prevent rearing. The belt was turned on at an initial speed of 5-10 cm/second to keep the mouse from grooming away the red coloring from its paws as well as acclimate the mouse to the treadmill. Excess food coloring that came off at first on the belt was wiped away as the belt moved past the Plexiglas box. The speed was then increased in increments of 5 cm/seconds, and each stepwise increase lasted for ~5 seconds until the speed was increased again. Recordings for gait analysis were made once the mouse was able to reach 25 cm/second consistently to produce 10 suitable consecutive strides uninterrupted by pauses causing backward drifting on the belt. Using the DigiGait imager (Mouse Specifics), .XVF video files were acquired of 1000-3000 frames from which smaller .AVI video clips could be selected for analysis.

3.3.2.2. Footprint Analysis

The paws of adult mice largely overlapping those used in the above studies were dipped in India ink and the mice were allowed to ambulate at will on bench paper to the end of a one-liter graduated cylinder laid horizontally that was covered in tin foil. When *Kcnc3*-null compared to wildtype control mice were tested, a longer cardboard poster tube with an autoclave glove over the end was used. Both tunnels were ~3.5 inches in diameter. Fore paws were inked blue while hind paws were inked red. Mice were held in one hand along the entire scruff while the other hand was used to press the overturned cap of the India ink containing a puddle of ink held firmly against the bottom of a paw. The most regular, consistent samples of gait uninterrupted by pauses spanning three consecutive strides were selected for analysis from each mouse. Mice that never produced such samples of gait after three trials were excluded from the analysis. The distances between the centers of (sole defined as center) of three consecutive hind paw prints on one side of the body were averaged and taken as the stride length. Stance width was taken as the average of distances separating every four opposing hind paw print centers. Gait was defined as 100% alternate if each paw

print was equidistant between preceding and succeeding opposite paw prints or 0% if exactly opposite a contralateral paw print (hopping). The distance between each of the consecutive paw prints and the closest, preceding or succeeding, opposite paw print was multiplied by 200%, and the product divided by the distance between preceding and succeeding opposite paw prints (stride length) to obtain the percent value quantifying alternate gait. Values from three consecutive strides were averaged. Paw discordance was taken as the average of the distances between the centers of each hind paw print and the nearest fore paw print for each of eight pairs of fore and hind paw prints from consecutive strides.

3.3.3. Other Motor Phenotypes

3.3.3.1. Twitching Score

During the 5-day beam test, mice were observed every day for the presence of subtle, highly-localized twitches that were best observed when mice paused on the beam. Twitches were most evident on the back of the mouse and the ears. Mice were rated as 0, 1, 2 or 3 (twitch score) according to frequency and strength of twitches by two observers that were blind to genotype. The averaged twitch scores for 5 days were used for data analysis.

3.3.3.2. Electromyography (EMG) Recordings

Mice were anesthetized with 50 mg/kg ketamine (Fort Dodge)/ 25 mg/kg acepromazine (Vetus) diluted in 25% ethanol (ethanol 2 mg/kg), shaved over the neck and monitored by a bipolar EMG electrode placed just subcutaneously. The electrode was moved around until locations were reached where motor unit activity was observable. In some instances the electrode was left in a silent location and monitored for up to an hour until activity appeared. Bursting activity was only regarded as such if it was not in phase with respiration and therefore

potentially a mere artifact of the muscle moving with respect to the stationary electrode tip.

3.3.3.3. Grip Test

Individual mice were placed on the inside of an inverted Edstrom wire mesh cage top that was flipped once the mouse grabbed a hold and suspended ~4 feet above a surface. The latency was measured up to a maximum of 3 minutes.

3.3.3.4. Rocking Ball Test

A 6-inch diameter, clear, colorless round bottom Pyrex flask was suspended on the end of a horizontal 1-cm wide metal rod anchored in a rubber cork inserted into the opening in the middle of the flask. The rod was clamped ~7 inches high (determines amplitude of rocking) to a vertical ring stand apparatus affixed to the fulcrum of a variable-speed adjustable tilt Shaker 35 blot rocker (Labnet International Corp., Woodbridge, NJ) set at 7°. Beneath the ball (flask) a 63 x 37 cm wide 15 cm inch deep pool of room temperature water was made in a plastic tray. It was important to keep the walls of the tray far enough from the ball that the mouse did not attempt to escape from the ball, invalidating the test. I placed mice squarely on top of the stationary ball and immediately turned the rocker on speed setting of 5 (1 Hz) until mice fell into the water. This training session was necessary to ensure mice were motivated to stay on the ball in the future. Actual testing at 1.25 Hz commenced 1-2 hours after the initial dunk. Swimming ability was noted. The latency to fall was measured up to 1 minute. The number of seconds the mouse remained on the ball was subtracted from the maximal duration of 60 seconds to provide a measure proportionate to impaired postural control or balance.

These mice were kept on a 12/12 light/dark cycle and 2-4 months of age.

3.3.3.5. Harmaline Tremor

Harmaline tremor was induced in mice by injecting harmaline (Sigma) i.p. at 15 mg/kg in 0.9% NaCl (pH ~7.4 with NaOH). Tremor was measured for 12 minutes ~10 minutes post-injection on the force plate actometer (see section 2.1.3 above). Each recording was divided into 72 10.24-second epochs that were visually inspected and 6 epochs were selected for analysis by a Fast Fourier-algorithm.

3.4. BRAIN SLICE ELECTROPHYSIOLOGY

Unless otherwise indicated all chemicals were obtained from Sigma.

3.4.1. Purkinje Cells

3.4.1.1. Brain Slice Preparation

Mice aged P40-95 were anesthetized with 50 mg/kg ketamine (Fort Dodge)/25 mg/kg acepromazine (Vetus) diluted in 25% ethanol (ethanol 2 mg/kg by i.p. injection prior to decapitation. Artificial cerebrospinal fluid (aCSF) was (in mM): NaCl, 125; KCl, 3.25; $CaCl_2$, 1.5; $MgCl_2$, 1.5; $NaHCO_3$, 25; D-glucose, 25; preoxygenated by carbogen (95% O_2, 5% CO_2) gas. The cerebellum was rapidly exposed, cooled with ice-cold aCSF, excised together with the brainstem, and cut with a razor blade parasagitally for mounting on the cut surface with cyanoacrylate securely to a chuck in a Vibratome (Ted Pella, Redding, CA, USA). The brain was conveyed to the room temperature chuck with an ice-cold spatula that was dabbed against a paper towel to dry the brain somewhat before dislodging with a #1 fine sable paint brush onto the glue. Within 5-10 seconds the tissue was immersed in ice-cold aCSF. The glue must be warm to cure and the brain thoroughly chilled to stand firm against the blade. Warming should be minimized however to reduce injury, as well as the overall duration of the slicing procedure. 200 µm-thick slices were cut from the vermis in ice-cold, carbogen-

bubbled aCSF at speed 1.5-2 and an amplitude 5-8 with the dorsal surface facing the blade. Each slice was pinched free from non-cerebellar tissue with forceps, immediately transferred to an Edwards chamber submerged in carbogen-bubbled aCSF maintained in a 35 °C water bath and incubated for 30–45 min; upon removal from the water bath slices were allowed to cool and remain at room temperature (22 °C) until use in recording at least 45 minutes after slicing.

3.4.1.2. Whole-Cell Patch-Clamp Recording

Slices were recorded in a submerged chamber maintained at 35 +/-0.5°C anchored by a C-shaped piece of metal small enough to hold the parasagittal cerebellar slice. The temperature was monitored near the slice with a bead thermistor using a TC-344B heater (Warner Instruments, Hamden, CT). Osmolality was adjusted if needed with sucrose, and was ~305 mOsm. Neurons were visualized at 40x with an Eclipse 6600FN epifluorescence microscope (Nikon, Melville, NY) using differential interference contrast-infrared optics and a Hamamatsu C2400 camera (Hamamatsu Corp., Hamamatsu, Japan) linked to a video monitor (Sony, Tokyo, Japan).

Borosilicate glass recording pipettes (bath 2–7 MΩ) were pulled on a Sutter P-87 puller (Sutter Instruments, Novato, California) from thin-walled (1.2 mm O.D.; 0.68 I.D.) borosilicate glass with filament (Warner). The internal solution consisted of (in mM): K-methylsulfonate, 130; EGTA, 0.1; HEPES, 10; NaCl, 7; $MgCl_2$, 0.3; Di-Tris Creatine-PO_4, 5; Tris-ATP, 2; Na-GTP, 0.5 at ~290 mOsm. The stock solutions of the latter 3 phosphates was adjusted upon dissolution to pH 7.3 with HCl. The pH of the internal solution prior to the addition of 100X phosphate stocks was adjusted to 7.3 with KOH. The electrolyte for whole-cell current-clamp recordings was adjusted to closely approximate physiological thermodynamic potentials for key ion species at 35 °C: E_{Na} 55.9 mV; E_K−97 mV; E_{Cl}−76 mV. A liquid junction potential with the external bathing medium of ~11.6 mV was calculated for this electrolyte. Whole-cell current-clamp recordings were obtained using the Axoclamp 2B amplifier (Axon

Instruments / Molecular Devices, Sunnyvale, CA) filtering at 10 kHz in bridge mode. The intracellular pipette resistance was kept at 15-25 MΩ for spike waveform measures by monitoring the bridge balance. Data were collected at 40 kHz with pCLAMP 9.2 software (Axon Instruments), operating on a Dell Dimension 8250 (Dell Computer, Austin, Texas) interfaced with a Digidata 1322A (Axon Instruments). Only neurons capable of stable spontaneous spiking overshooting 0 mV resting more negative than ~-45 mV were recorded. Purkinje cells were easily identified by their distinct morphology and position within the cerebellar cortex, and selected primarily on the basis of membrane appearance. An average bias current of ~−1 nA was applied in current-clamp mode to stop spontaneous discharge and maintain all recordings at a baseline level of −70 mV except for brief periods to deliver stimulation at various holding potentials or rest.

3.4.1.3. Spontaneous Simple Spike Recordings

Recordings were made at the resting potential to measure the spontaneous spike rate and action potential waveform parameters. Measurements were taken after the spike rate settled to a steady-state yet within 2 seconds of turning off hyperpolarizing bias current. The simple spike rate was measured from the interspike interval immediately preceding the complex spikes, and the pause was taken as the interval between the last spikelet and first simple spike after the complex spike.

3.4.1.4. Spike Frequency as a Function of Injected Current (F-I) Relation

F–I plots were compiled from 1.2-second depolarizing steps delivered by the clamp every 5 seconds from a holding potential of -70 mV. After each step the magnitude of the injected current was increased by 200 pA.

3.4.1.5. Climbing Fiber Stimulation

Climbing fibers were stimulated by 100-µs stimuli from an A365 stimulus isolator (World Precision Instruments, Sarasota, FL) triggered by pClamp delivered via a

1.5 mm theta pipette in the granule layer pulled as above with the tip broke to ~10 µm filled with HEPES-aCSF (in mM: 150 NaCl, 3.35 KCl, 1.5 MgCl2, 20 D-glucose, 10 HEPES, 1.5 CaCl2, pH 7.4 with NaOH). Formvar-insulated tungsten 0.005 wires (Plastics One, Roanoke, VA) were inserted into each barrel with the insulation stripped 2 mm at the tip. These wires were connected by gold plugs to hi-flex, shielded wire (Cooner Wire, Chatsworth, CA) that blocked transmission of vibrations from the stimulus isolator to which it was connected outside the rig. Climbing fiber responses were distinguished by their all-or-none nature, were free from antidromic contamination and parallel-fiber evoked responses. Stimuli were delivered at 1 Hz only to avoid short-term plasticity at the climbing fiber synapse at minimal intensities.

3.4.2. DCN Neurons

3.4.2.1. Brain Slice Preparation

The methods were identical to those enumerated in section 3.4.1.1 above except for the following modifications. Mice aged P17-21 were used that were typically the offspring of mice used in behavioral experiments involving the +/+;-/- mice lacking one or both *Kcnc1* alleles. Perfusion was necessary to eliminate autofluorescence from blood vessels for post-hoc immunofluorescence. Under deep 100 mg/kg ketamine (Fort Dodge)/25 mg/kg acepromazine (Vetus) anesthesia diluted in 25% ethanol (ethanol 2 mg/kg), mice were perfused at 20 ml/minute with 23-30 ml of ice-cold aCSF. Artificial cerebrospinal fluid (aCSF) for preparing slices was (in mM): Sucrose, 228; KCl, 3.25; $CaCl_2$, 0.5; $MgCl_2$, 7; $NaHCO_3$, 28; D-glucose, 7; NaPyruvate, 3; ascorbic acid, 1; preoxygenated by carbogen (95% O_2, 5% CO_2) gas. Ascorbic acid and pyruvate were added fresh from frozen stocks. Osmolality was adjusted if needed with sucrose, and was ~320 mOsm. Completely-exsanguinated, cold brains were then used for dissection to prepare 300 µm slices principally including the medial nucleus. Slices recovered in normal aCSF.

For DCN recordings, normal or CsCl internal solution (see individual descriptions below) was used except Alexafluor488 was added at 68 µM to fill cells for post-hoc co-labeling with immunofluorescence. Recording pipettes were pulled on a P-87 or P-97 horizontal puller (Sutter) when using 1.2 O.D. 0.68 I.D. (Warner) or 1.5 O.D. 0.86 I.D. (Sutter) glass, respectively, as indicated in the sections that follow. Low-pass filtering was at 3 kHz via the Axoclamp 2B, for current clamp recordings, or 5 kHz for voltage clamp on the Axopatch 200A. Data were collected at 200 kHz to provide adequate resolution of fast spikes for measurement of waveform parameters in Minianalysis (See section 3.5.3.1).

3.4.2.2. Intrinsic Firing Properties

Normal aCSF was used except 25 µM D-(-)-2-Amino-5-phosphonopentanoic acid (D-AP5; Ascent Scientific) and 25 µM 6,7-Dinitroquinoxaline-2,3-dione (DNQX) were added to block glutamatergic inputs during stimulation and to minimize interference from spontaneous synaptic inputs. Action potential waveform measurements were taken from the resting potential 4-5 minutes after breaking into the cell. *F–I* plots were compiled from 1.2-second depolarizing steps delivered by the clamp every 5 seconds from a holding potential of -60 mV. After each step the magnitude of the injected current was increased by 100 pA.

3.4.2.3. Stimulation of Purkinje Cell Terminals in the DCN

Normal aCSF was used except 25 µM D-AP5 and 25 µM DNQX were added to block glutamatergic inputs during stimulation and to minimize interference from spontaneous synaptic inputs. Stimulation was delivered as 100 µs stimuli from an A365 stimulus isolator (World Precision Instruments) triggered by pClamp delivered via a 1.5 mm theta pipette (W.P.I) in the granule layer pulled as above with the tip broke to ~30 µm filled with HEPES-aCSF (in mM: 150 NaCl, 3.35 KCl, 1.5 MgCl2, 20 D-glucose, 10 HEPES, 1.5 CaCl2, pH 7.4 with NaOH). Formvar-insulated tungsten 0.005 wires (Plastics One) were inserted into each barrel with the insulation stripped 2 mm at the tip. These wires were connected

by gold plugs to hi-flex, shielded wire (Cooner Wire) that blocked transmission of vibrations from the stimulus isolator to which it was connected outside the rig. The stimulus electrode was placed >100 µm, typically 150 µm, dorsal or posterior to the patched cell. Deeper placements tended to be more effective. The distance was important to mitigate antidromic stimulation of axons that tend to course ventrally to exit the cerebellum. Nonetheless, antidromic stimulation was frequently a problem when the soma was depolarized. Also, the dendritic field of large DCN neurons in rodents can extend out > 300 µm. Apparent direct stimulation of the cell was evident in sudden depolarization of the membrane potential in some cases. On the other hand, larger responses could be elicited closer to the cell. Optimal responses were obtained from the most medial slices containing the medial DCN nuclei with the stimulating electrode placed in the white matter of folium VI adjacent to the dorsoposterior corner of the DCN, which was moreover most amenable to patching for the white matter was less dense here. Parasagittal slices at this level were indeed found to have the most intact connections using DiI tracing (Telgkamp and Raman, 2002). Often the position had to be adjusted to achieve usable responses.

3.4.2.4. IPSC Recordings

Inhibitory postsynaptic currents were recorded in voltage-clamp mode using an Axopatch 200A amplifier (Axon). The internal solution for these experiments was (in mM): CsCl, 126; EGTA, 9; HEPES, 9; NaCl, 6.2; $MgCl_2$, 1.8; Di-Tris Creatine-PO_4, 5; Tris-ATP, 2; Na-GTP, 0.5; QX-314 Br, 7 at ~290 mOsm (calculated E_{cl} +1mV). The calculated liquid junction potential was -6 mV. Gabazine (SR-95531; Tocris) was applied when indicated at 10 µM in HEPES aCSF (See above section 3.4.1.5) with 0.01% phenol red using a puffer pipette consisting of a patch pipette broke to ~100 µm placed upstream with respect to the direction of bath perfusate pressed into the surface of the slice controlled by a 1 cc syringe. Pipettes were kept below a bath resistance of 4 MΩ and intracellular resistance of 20 MΩ, most often <15 MΩ. 95% prediction and 50% compensation was used.

Recordings were rejected if the access resistance drifted >20% or input resistance decreased below 50 MΩ. Stimulation trains were delivered at 15-second intervals. Between trains cells were held at -6 mV (-6 mV correcting for junction potential) to allow binding of the use-dependent sodium channel blocker QX-314, which proved essential for blocking contaminating action potentials triggered by the largest eIPSCs that were of sufficient magnitude to escape the clamp. Otherwise cells were held at -60 mV, for holding the cell near the resting potential is thought to extend the duration of stable whole-cell recordings. Protocols were also executed from -60 mV, yielding eIPSCs of sufficient magnitude while improving the space clamp by minimizing voltage error because this potential is close to the resting potential. The frequencies of the protocols used for voltage clamp were the same as those used in current clamp however the overall durations were kept constant; the wildtype protocol at 100 Hz delivered a total of 50 stimuli over 0.5 seconds whereas the null protocol was 33 stimuli over 0.5 seconds.

3.4.2.5. Post-Hoc Identification

When possible, 100-millisecond negative current injections were given at 1 Hz at the end of recordings for up to 5 minutes to aid in filling the cell with the positively-charged fixable polar tracer. Cells were retrieved after recording within 2 minutes, typically 1 minute, of completely breaking the seal. Often the pipette could be withdrawn slowly from the cell as though excising a patch with the resting potential remaining negative to -30 mV. Perfusion was stopped, the anchor was removed, sometimes with the help of a fine sable #0 paint brush, and the slice was retrieved by lifting the piece of lens paper or Kimwipe it was placed on with forceps. The slice was dropped into 5 ml ice-cold 4% paraformaldehyde in 0.1M DPBS that had been frozen promptly after and freshly thawed. In some cases it was thawed by a 10-second pulse in a domestic microwave (May be contraindicated as this seemed correlated to poor recovery). Slices were protected from light. Fixation proceeded 1-2 hours after which slices were

transferred to 40% sucrose in DPBS with sodium azide until resectioning (See section 3.2.2.2 above).

3.5. DATA ANALYSIS AND PRESENTATION

3.5.1. Characterization of Gene Expression

3.5.1.1. Imaging

Immunofluorescence was imaged using a Zeiss LSM 510 laser confocal microscope except that shown in Figure 4.2, which employed a Leica TCS SP2. Figures were made in Microsoft Publisher. With this microscope images were of sufficient quality to obviate the need for adjustments in Photoshop. Though by necessity laser confocal settings had to differ between slides and even regions of interest to optimize dynamic range, the strategy employed to optimize the image was very consistent. All images were scanned so that the gain and offset were set to limit saturation (red on lookup table) and not show signal in areas that are truly black yet minimize non-illuminated areas (blue on lookup table). It was often necessary to saturate the soma in images of Alexafluor-filled cells for the ratio of signal intensity in the soma compared to the dendrites was very high so that fine processes would otherwise be invisible. Background in some negative controls may seem higher because this same protocol was applied to those sections which in the absence of strong signals had maxima closer to background. This in turn elevated the overall intensity somewhat.

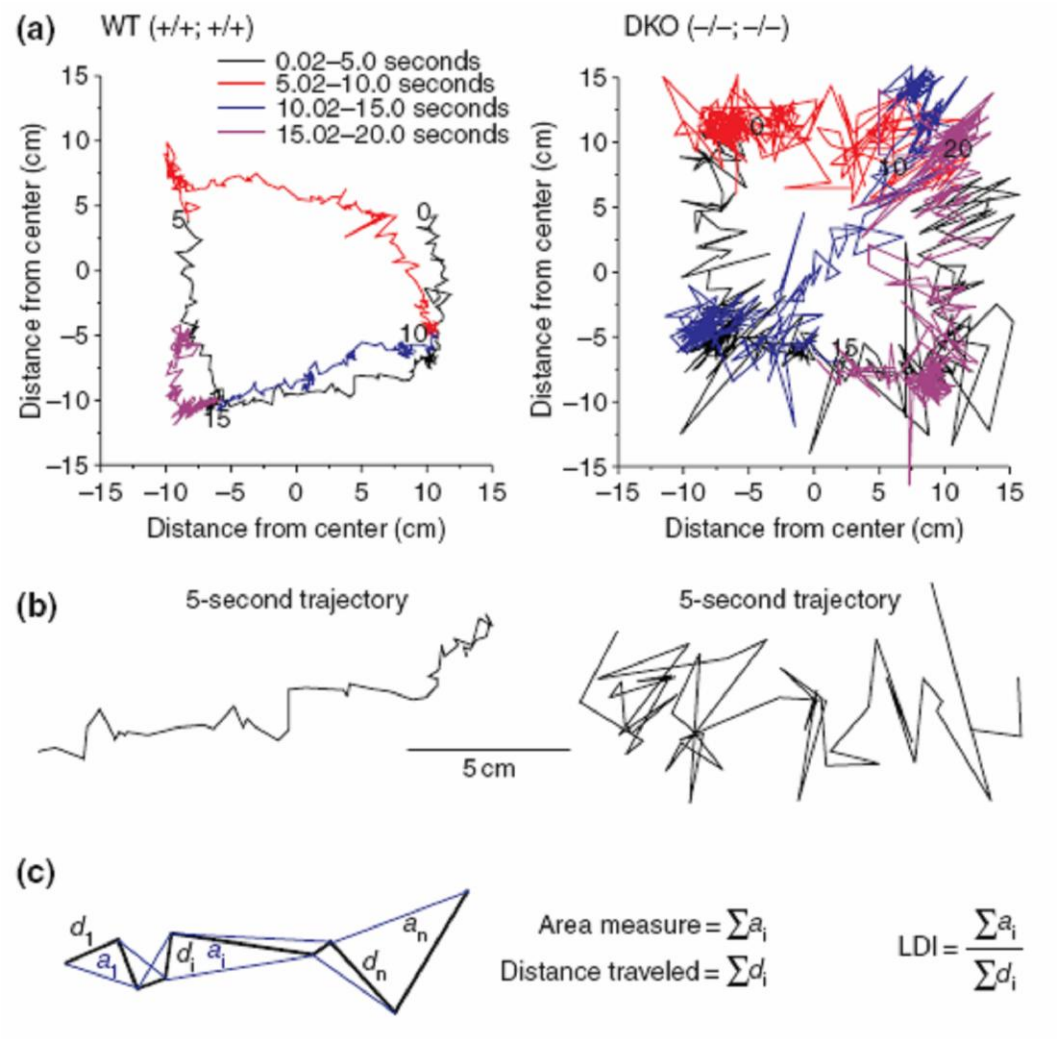

Figure 3.3. Calculation of the lateral deviation index. (***A***) Individual walking trajectories are identified and colored differently in the figure. (***B***) Examples of individual walking trajectories that are analyzed taken from a above. (***C***) Triangular areas denoted 'a' defined by every three, consecutive center of force measurements. Distances between consecutive points are labeled 'd'. The first and third points of every three, consecutive measurements are connected with blue lines. The walking trajectory is black. To derive the lateral deviation index the sum of the triangular areas is normalized to the total distance traveled along the black walking trajectory connecting consecutive center of force measurements.

3.5.2. Behavior

3.5.2.1 Analysis

Center of force (COF) data from the force plate actometer were examined in Origin (Origin Lab Corp., Northampton, MA) where walking trajectories were identified, lateral deviation was computed and ANOVA was performed. Area measures were taken from every three consecutive COF measurements and normalized to the total distance traveled to derive a lateral deviation index (see section 2.1.3). Slips and falls of each mouse were averaged over the 5 traversals of the narrow 100-cm beams from each of the 5 days. The means for each mouse were analysed by 1-way and 2-way ANOVA in Origin. For 2-way ANOVA, genotype was the between factor and days on beam was the within factor. DigiGait™ data were analyzed in DigiGait™ analysis software v. 6.0 in MatLab (The Mathworks, Natick, Massachusetts) by taking .AVI video files sampling the 300 frames containing the most consistent gait from each 1000-3000-frame .XVF file captured at acquisition were taken per mouse, which typically captured 10 strides. The snout-out feature was adjusted to ensure the red in the snout was not spuriously recognized as a paw. The red filter was set at 0.8 (just sufficient to avoid artifactual recognition of red in agouti coat and prevent fusion of recognized paw prints during frame-by-frame analysis) and the blue filter was kept at 2. Control brightness was set at 255 and control darkness at 0. All automated frame-by-frame analysis was monitored for artifacts. Data were of sufficient quality that correction provisions in the program were rarely needed and if so not more than one for every 10 steps. Footprint data were measured within 1-mm manually and means were computed in IgorPro v. 5.0.4.8 (Wavemetrics, Oswego, OR). ANOVA for gait tests and the rotarod was performed in Prism v. 5.01 (GraphPad Software, La Jolla, CA). Averaged twitch scores of each mouse over 5 days were analyzed by the Kruskal-Wallis test in Origin. Rocking ball data were analyzed by the Kruskal-Wallis test in Prism. Harmaline tremor epochs were analyzed by a fast fourier transform algorithm and ANOVA while frequency was analyzed with 2-tailed Student *t*-tests in Origin

(Microcal Origin, 7.0; Origin Lab Corp.). For ANOVA the Tukey post test was always used.

3.5.2.2 Presentation

Graphs of force plate and beam data were created in Sigmaplot v. 8.0, SPSS, Chicago, IL). Those of gait tests, rotarod and rocking ball were created in Prism (Graphpad Software). Means and standard error of means (S.E.M) were used.

3.5.3. Brain Slice Electrophysiology

3.5.3.1. Analysis

Complex spike parameters, including pause durations, as well as the simple spike frequency and action potential waveform data from Purkinje cells were measured in Clampfit v. 9.2 (Axon). The latter was used also to measure foot-to-peak IPSC amplitudes. Complex spikes were only measured if they were not preceded by a simple spike for at least 2 ms. Spikelets were considered to comprise a complex spike if the interspike interval did not exceed 75% of that of the surrounding simple spikes, though typically the need for this criterion was obviated by the significant pause following the complex spike. Action potential waveform data from DCN neurons and spike rate data from both Purkinje and DCN neurons were analyzed in Minianalysis v. 6.0.3 (Synaptosoft, Decatur, GA) using the following settings. In the main window:

- *Threshold* = 20
- *Period to search a local maximum* = 1000
- *Time before a peak for baseline* = 750
- *Period to search a decay time* = 1000
- *Fraction of peak to find a decay time* = 0.05
- *Period to average a baseline* = 200
- *Area threshold* = 3.5
- *Number of points to average a peak* = 3.

Spike rate data were compiled from the detected peaks by calculating interevent intervals and viewing the column statistics in Data Array menu. Spike waveform

measurements were then taken by marking the detected events as group 1 and clicking Group Analysis in the Events menu. In Group Analysis the gain was set at 20 and 4 blocks were analyzed per event. Events were analyzed as individual aligned at rise. Baseline was set to zero and threshold was used as baseline. Threshold was detected as the peak of the second differential using heavy filtering (smoothing set to 80 points). Data from 10 spikes were analyzed per cell and the average obtained from column statistics in the results menu.

Input resistances were measured by taking the linear slope of the plot of voltage as a function of injected current using 4-9 steps (including zero) of current injection, typically only in the negative direction but always where the response was linear (“ohmic”) from a subthreshold voltage of -60 mV. Amplitudes of the peaks of voltage steps from baseline were measured in Clampfit 9.2 (Axon). Input resistances were calculated by plotting the change in voltage as a function of injected current to derive a slope in Prism (Graphpad).

3.5.3.2. Presentation

Graphs from Purkinje cells were presented using Sigmaplot (SPSS Corp.) while DCN data were presented using Prism. Action potential data were presented using Igor Pro (Wavemetrics) and not corrected for the calculated for the junction potential.

CHAPTER FOUR
Results

4.1. A TRANSGENIC APPROACH TO RESTORE KV3.3 EXPRESSION IN PURKINJE CELLS OF MICE LACKING KCNC3

To bridge the gap from ion channel gene to acute behavior, analysis at the level of cellular electrophysiology is required, which requires knowledge of which cell types actually contribute to the behavioral deficits. The main hypothesis I sought to test in my dissertation work was the hypothesis that Kv3.3 expression in Purkinje cells is sufficient for motor coordination such that expression in other neuronal cell types is not absolutely necessary. A corollary of this hypothesis is that restoration of Kv3.3 expression in Purkinje cells should suffice to abolish ataxia in *Kcnc3*-null mice. Thus, I, with help from Dr. Anne McMahon, used a transgenic approach to restore Kv3.3 expression in exclusively in Purkinje neurons. I used a transgenic construct created by Dr. Anne McMahon to express Kv3.3 and eGFP selectively in Purkinje neurons by using a bidirectional promoter active only upon co-expression of the tetracycline transactivator protein (tTA). By crossing these mice with existing *L7-tTA* transgenic mice that express the tTA only in Purkinje cells on a *Kcnc3*-null background, I restored Kv3.3 expression only in Purkinje cells (Fig. 4.1). The tTA of the *L7-tTA* is of the "*tet-off*" variety with which transcription of the *tet*-regulated gene is constitutively active and potentially suppressed by doxycycline if desired.

4.1.1. Characterization of Transgenic Lines

4.1.1.1 Transgenic Construct Design

The design of the *pBIKcnc3b-eGFP* construct used to generate transgenic mouse lines featured the coding region of the b splice variant of *Kcnc3* along with the endogenous Kozak sequence and ~0.5 kb of 3'UTR

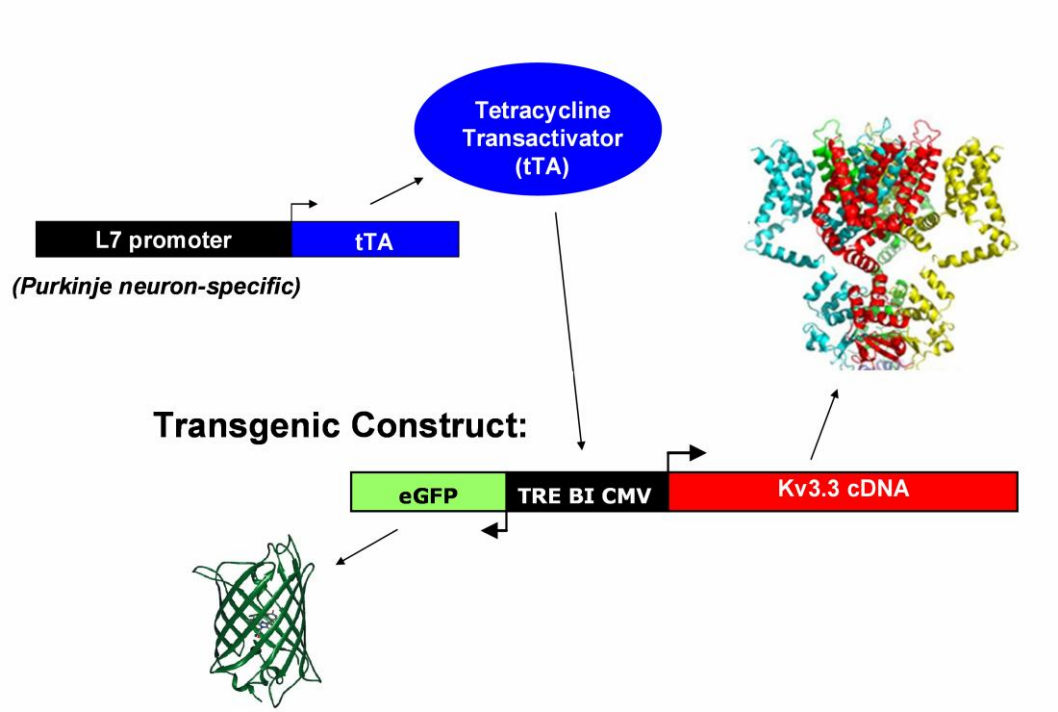

Figure 4.1. Transgenic approach to restore Kv3.3 expression specifically in Purkinje cells. The rectangles denote transgene constructs in two separate transgenic lines that are bred together. Hooked arrows signify promoters. Expression of the tetracycline transactivator in the same cell is necessary for transcription of Kv3.3 and eGFP. The protein structure at right depicts a tetrameric potassium channel based on the structure of KcsA.

transcribed in one direction and that of eGFP in the other. The b splice variant was selected because by Northern blot it is by far the most abundant variant in the cerebellum and has been verified to be expressed at high levels in Purkinje cells by (see sections 1.1.1.1 and 1.1.2.3). EGFP served as a marker during patch recordings to discriminate definitively between basket and Purkinje cells. The bidirectional promoter consisted of two minimal CMV promoters in opposite orientations flanking a tetracycline response element (TRE).

4.1.1.2 Screening of Transgenic Founders

pBIKcnc3b-eGFP founders were crossed with homozygous *L7-tTA+* transgenic mice to obtain bi-transgenic (*L7-tTA+;pBIKcnc3b-eGFP+)* F1 mice. The F1 mice

were then crossed with *L7-tTA+;pBIKcnc3b-eGFP-* mice to obtain F2 mice used to screen for transgene expression in the cerebellum to increase the chance of segregation of potential separate transgene integrants on different chromosomes. Screening took place by either inspecting acute slices for eGFP fluorescence or immunofluorescence using an anti-GFP antibody. Several lines were obtained, but most of them were scattered mosaics or quite sparse. Where one of these lines was maintained, the degree of mosaicism was found to vary between mice. Two lines, from founders 313 and 396, yielded expression in a majority if not all Purkinje cells.

Several offspring derived from the F1 parents of the 313 and 396 line F2 mice with good expression were additionally examined once they had bred to verify that they bred true. Consistent expression would suggest that any potential alternate integrants that produce PCR positives but do not yield expression have segregated away from the insert site with the expressed copy or complex concatemer of nearby copies. Neither this method nor Southern blots can establish whether there are multiple integrants present with perfect certainty. All 396 line bi-transgenic mice yielded expression of eGFP it seemed in all Purkinje cells. Mice from the 313 line usually expressed in what seemed to be upwards of 80-90% of Purkinje neurons but in these initial screens the extent of mosaicism varied considerably.

4.1.1.3 The Transgenes Are Expressed Exclusively in Purkinje Cells Throughout the Cerebellum

Several bi-transgenic mice of each line were examined for potential mosaicism using either acute slices, immunofluorescence with anti-GFP antibodies or native eGFP fluorescence in tissue fixed briefly. Since there are also pyramidal shaped albeit smaller basket cells also in the Purkinje layer, and the characteristic dendritic arbors of Purkinje cells are sometimes severed in sections, I also

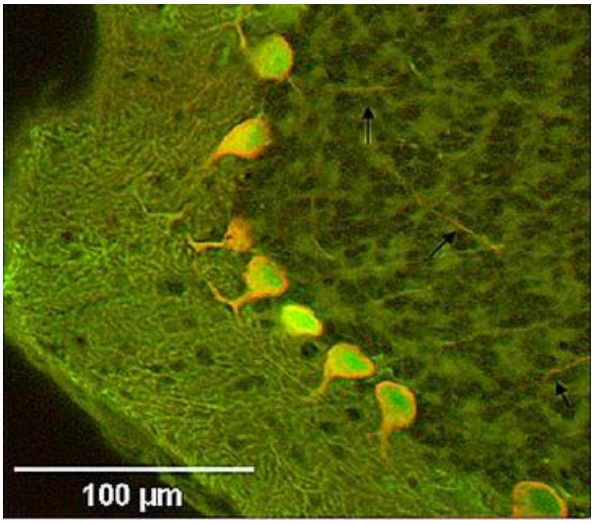

Figure 4.2. Immunofluorescent detection of Kv3.3b using Alexafluor 568 and native eGFP fluorescence in Purkinje cells in the cerebellar cortex. Three axons are indicated by arrows. Note the concentration of the channel in the membrane.

ultimately used calbindin immunofluoresence in bi-transgenic mice lacking endogenous Kv3.3b to distinguish Purkinje cells, which are calbindin+, from basket cells, which are calbindin-. These data verified that 100% of Purkinje neurons in the 396 line expressed the Kv3.3b transgene and native eGFP together (Fig. 4.2). Because of variability observed in the extent of mosaicism in the 313 line, I later screened 16 of the bi-transgenic *Kcnc3*-null mice used in the rescue experiment for behavior by immersion-fixing crude slices cut as each mouse was sacrificed at the end of the battery of tests. In 16/16 cases, 90% of calbindin+ cells in the Purkinje layer expressed the Kv3.3b transgene. Purkinje cells of the 313 line however did appear to express a relatively variegated level of eGFP fluorescence compared to the 396 line. In general the expression level of Kv3.3b restored by the transgenic lines tended to appear higher than that of wildtype Purkinje cells when sections were processed together. On the tissue level, however three 313 and three 396 cerebella yielded Kv3.3b signals of similar intensity on a Western blot mirroring the β-actin loading controls (Fig. 4.3).

Therefore, the 396 line produced reliable, even expression over all Purkinje cells and only in Purkinje cells, while the 313 line exhibited some mosaicism and variegation in expression level yet was for the most part reliably expressed in the vast majority of Purkinje neurons.

4.1.1.4. The Subcellular Localization of the Kv3.3b Splice Variant Used in the Construct Matches that of Endogenous Kv3.3b in the Absence of the Other Splice Variants

Altered subcellular localization of the Kv3.3b variant delivered by the transgene was a concern because not all portions of the UTRs are present that are known to regulate the subcellular localization of some neuronal genes through transport and local translation. In addition, because the channels can exist as heteromultimers, it was possible that the other variants might be necessary to convey Kv3.3b to certain subcellular locations.

In both transgenic lines used in the study the Kv3.3b transgene appeared in all the same subcellular locales on a *Kcnc3*-null background as endogenous Kv3.3b (Fig. 4.2 above). Expression was observed most prominently in the soma and proximal dendrite, fading with distance from the soma. There was low, even expression over the more distal dendritic tree and axon. Axon terminals in the DCN however were more intensely immunofluorescent. Although the level of expression could be higher restored by the transgenic lines, this did not apparently lead to ectopic accumulation of the channel at least at the plasma membrane. Thus, null phenotypes related to fast repolarization in all parts of cell should be restored in bi-transgenic null mice, insofar as the other variants are redundant or inconsequential to this property.

4.1.1.5. The tet*-Regulated Transgene Construct Is Not Leaky and Kv3.3 Is Absent Outside the Cerebellum*

Another concern surrounding the transgenic approach implemented here was the possibility that the *tet*-regulated promoter would exhibit leaky expression outside

Purkinje cells independent of the presence of the tTA. Since transgenes can be inserted essentially anywhere there are DNA strand breaks, there is always some potential for the position of insertion to confer unusual transcriptional regulation of transgenic constructs that are otherwise tightly-regulated. Leaky expression, however, more often tends to be seen with the reverse tTA *tet-on* system where tetracycline is necessary for transcriptional activity by virtue of a mutation in the tTA; the *tet-off* tTA of the *L7-tTA* line tends to be free of this problem. I therefore, with the technical assistance of Mitali Bose, assessed expression of Kv3.3b by Western blot.

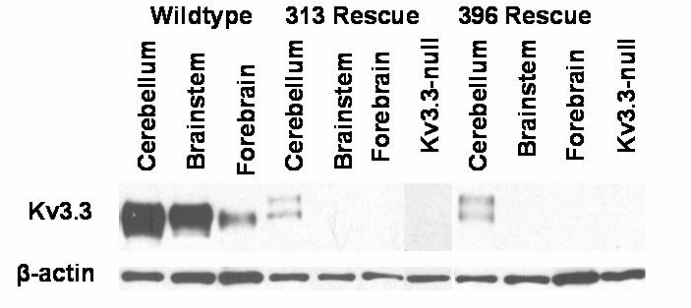

Figure 4.3. Western blot. Genotype is indicated above lanes. The numbers denote two independent transgenic lines. β-actin serves as a loading control. The Kv3.3-null control is from whole brain. Forebrain includes midbrain.

Leaky expression from the pBI TRE promoter would be expected to appear in mice with the *pBIKcnc3b-eGFP* transgene lacking the *L7-tTA*. Herein, I will refer to bi-transgenic mice lacking *Kcnc3* with Kv3.3b expression restored to Purkinje cells as “rescue” mice. Brains were dissected into the cerebellum, the brainstem and everything rostral, including the midbrain, referred to collectively for brevity as simply the forebrain. A β-actin loading control ensured that a comparable amount of protein was added to all lanes. A wildtype brain yielded as expected relatively little Kv3.3b in the forebrain but a strong signal in the hindbrain areas, cerebellum and brainstem (Fig. 4.3). In rescue mice of both lines, signal was observed only in the cerebellum, supporting the contention that the *pBIKcnc3b-eGFP* transgenes are not leaky and that the L7-tTA is faithfully expressed just in Purkinje cells, corroborating previous work employing the line. As anticipated, the signal is weaker because the channel has not been restored

in parallel fibers or DCN neurons. Curiously, an additional band of high molecular weight appeared which may reflect differentially-glycosylated channel subunit that accumulated in the ER due to overexpression, an impression congruent with the seemingly more intense Kv3.3b immunofluorescence in Purkinje cells of rescue mice compared to wildtype. Importantly, whole brains of mice that carried only the *pBIKcnc3b-eGFP* transgene from each line on a *Kcnc3*-null background did not express detectable Kv3.3b, which suggests that the construct was not leaky or the *pBIKcnc3b-eGFP* somehow intrinsically active in Purkinje cells (see "KO" lanes). Had the latter been the case, care would have needed to been taken to avoid using such mice to represent *Kcnc3*-nulls.

In addition to the Western data, I also sectioned brains of bi-transgenic mice in both the coronal and sagittal planes at ~1-mm intervals to examine eGFP expression by immunofluorescence as described in section 3.2.2.1 above. In every case I only saw expression in Purkinje cells in the brain posterior to the olfactory bulb and anterior to the spinal cord. In theory the Western blot, even using chemiluminescence rather than radiolabeling, is more sensitive or at least easier to interpret unequivocally when there are low levels of expression potentially buried in the noise of the higher background frequently seen with immunofluorescence.

4.2. KV3.3 EXPRESSION IN PURKINJE CELLS IS SUFFICIENT TO RESCUE MOTOR COORDINATION IN *KCNC3*-NULL MICE

With a transgenic line that expressed the channel in Purkinje cells, I tested the hypothesis that Kv3.3 expression in Purkinje cells is sufficient for motor coordination such that expression in other neuronal cell types is not absolutely necessary. A corollary of this hypothesis is that restoration of Kv3.3 expression in Purkinje cells should suffice to abolish ataxia in *Kcnc3*-null mice. Thus, I put mice

with Kv3.3 restored in Purkinje cells through a battery of behavioral assays to test this hypothesis.

The +/+;-/- mice on this genetic background displayed the readily-observed traits noted previously as well as a yet to be described phenotype that potentially surfaced only on this background. Increased lateral deviation on a force plate actometer and slips on a 1-cm beam were seen, confirming previous work in the lab. Also the dramatic reduction in harmaline-induced tremor and the ability to elicit it in mice lacking *Kcnc3* was confirmed (see sections 1.2.3 and 2.1.4).

When +/+;-/- mice were initially characterized, “trembling and hyperexcitability when picked up by the tail” was noted (Chan, 1997). Normal mice will attempt to grasp and look around for something to get a hold of when suspended by the tail, whereas the null mice tend to make relatively stereotyped, repetitive, rapid flailing movements that often culminate in limb clasping. In addition to this overt phenotype, I noticed both +/+;-/- and +/-;-/- mice exhibited frequent, localized muscle twitches that were especially overt when mice stood still that were most pronounced in the latter genotype. Both of these phenotypes persisted in rescue mice, affording a control for specificity that would support the notion that Purkinje cell Kv3.3 functions in motor coordination specifically. I chose to use the twitching phenotype as control for specificity presumably unrelated to the cerebellum because it was more readily scored and quantified.

When tested for a rescue of wildtype behavior I found that mice with Kv3.3 restored in Purkinje cells indeed did not differ significantly from wildtype mice. The twitching phenotype by contrast was not corrected, serving as a control for specificity. That it was not alleviated yet beam performance and lateral deviation were indicates twitching was not the cause of the deficits in these tests. As the force plate and beam could be measuring various manifestations of cerebellar ataxia, specifically jerky movements (hypermetria), loss of balance or altered gait, I tested independently whether gait and balance or postural control were altered to determine more precisely what was rescued. These tests

suggested Kv3.3 function in Purkinje cells specifically pertains to regulating movement speed, with loss of the channel engendering hypermetria.

I further tested whether the rescue of coordination extended to +/-;-/- mice. Kv3.1 is expressed in the cerebellum in granule cells, deep nuclear neurons and possibly interneurons, but not Purkinje cells. The rescue was still effective for the beam test but only partially regarding lateral deviation in +/-;-/- mice. There was no detectable rescue of wildtype behavior in DKO mice entirely lacking both channel genes. Moreover, additional phenotypes appeared. When just one allele of *Kcnc1* was lost on top of both *Kcnc3* alleles, a subtle gait abnormality appeared. Additional loss of both *Kcnc1* alleles resulted in the full spectrum of cerebellar ataxic signs, encompassing severe gait abnormalities and grossly impaired balance. These data suggested that impaired fast action potential repolarization appeared at additional nodes in the cerebellar circuitry with loss of *Kcnc1* that must be functional for restoration of fast repolarization in Purkinje cells to be effective in rescuing mutant behavior.

4.2.1. Motor Coordination

To test whether motor coordination was rescued in mutants lacking *Kcnc3* I employed three tests. Because virtually any behavioral test is sensitive to multiple parameters and therefore convergent data from multiple assays yield greater confidence, I tested mice for performance in the narrow beam test, on the force plate actometer and on the rotarod (see section 2.1.3). I began with line 313 to breed with +/+;-/- mice because it was the first suitable line to be uncovered during screening. The risk of obtaining a false negative or uninterpretable result due to unreliable expression in 100% of Purkinje cells was greater with +/-;-/- and -/-;-/- because motor phenotypes are more severe. As the expression characteristics of the 396 line were of better quality I later tested +/-;-/- as well as -/-;-/- mice using this line. The results of the force plate and beam tests from the rescue experiment are published in Hurlock et al., 2008.

4.2.1.1. Force Plate Actometer

Lateral deviation on the force plate actometer (see section 2.1.3) was measured in +/+;-/- mice, wildtype controls and rescue mice (Fig. 4.4). The plate essentially tracks the center of gravity determined by which paws are on the plate, how far paw placements are from each other and how much force is applied during stepping. The lateral deviation index (LDI) is the ratio of the sum of the triangular

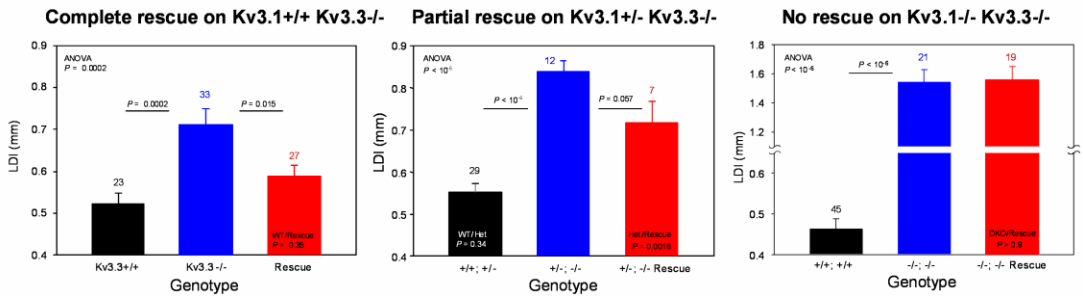

Figure 4.4. Ability of Kv3.3b restoration in Purkinje cells to rescue normal lateral deviation on the force plate actometer. The sample sizes are indicated above the bars. Error bars are S.E.M.

areas formed by every three consecutive center of gravity measurements to the total distance traveled during ambulation (Fig. 3.1). The LDI is used to exclude artifactual increases if the area measure was considered alone merely resulting from summation over a longer distance rather than genuine increases in deviation per se. Confirming previous observations in the lab (Joho et al., 2006), +/+;-/- mice exhibited a significantly greater lateral deviation index than wildtype mice (p = 0.0002). Rescue mice showed a significantly reduced LDI compared to null mice (p = 0.015), while the LDI of rescue mice was not significantly different from wildtype mice (p = 0.35), indicating a full rescue of normal lateral deviation.

The +/-;-/- had a higher LDI when compared directly to +/+;-/- mice using the same population of mice where the single-null mutant allele was derived by recombination from the double-null allele as recently as possible in generations before breeding for the experiment (Joho et al., 2006). Consonant with this observation, using mice of different genetic backgrounds that were only partially related by using one parent from the single-null experiment to breed all mice

tested, the LDI is considerably higher with one allele of *Kcnc1* absent than in +/+;-/- mice (Fig. 4.4, middle bars of left and middle graphs). Mice heterozygous for the *Kcnc3*-null allele did not have a significantly higher LDI than wildtype mice when genetically related mice were used previously (p = 0.34). Thus, I used +/+;+/- mice as normal controls in the +/-;-/- experiment which were expedient to breed. Indeed, +/+;+/- mice still exhibited a significantly lower LDI than +/-;-/- mice ($p < 10^{-6}$; Fig. 4.4, middle graph). Corresponding +/-;-/- bi-transgenic rescue mice had an LDI intermediate between the control and mutant mice that differed from wildtype mice (p = 0.002) and was on the cusp of differing from that of mutants (p = 0.057). The data suggested that a normal LDI was partially rescued in +/-;-/- mice by reintroduction of Kv3.3b in Purkinje cells.

The LDI of -/-;-/- mice was roughly 3 times that of wildtype control mice, replicating previous results from the lab (Fig. 4.4, right graph; $p < 10^{-6}$; Joho et al., 2006). In contrast to mutants retaining at least one *Kcnc1* allele, -/-;-/- mice exhibited absolutely no rescue of a normal LDI. Rescue mice were not significantly different from -/-;-/- mice ($p > 0.9$), and remained significantly different from the wildtype controls.

In sum, a normal LDI is rescued in mice just lacking *Kcnc3*, partially rescued in +/-;-/- mice, and not rescued in -/-;-/- mice.

4.2.1.2. Beam Test

As described above (see section 2.1.3), the beam test measures motor coordination by assessing the ability of mice to traverse a narrow beam without slipping or falling. The mice are tested on 5 consecutive days over which they learn a motor skill and become habituated to the test situation. Thus the first days could be conceived of as habituation and training days, where day 5 represents the actual test day, however trends observed on multiple days also likely reflect performance and can be taken into account to increase the sensitivity of the test. Analysis of each day was performed by one-way ANOVA whereas analysis taking all 5 days into account was carried out by using repeated measures ANOVA.

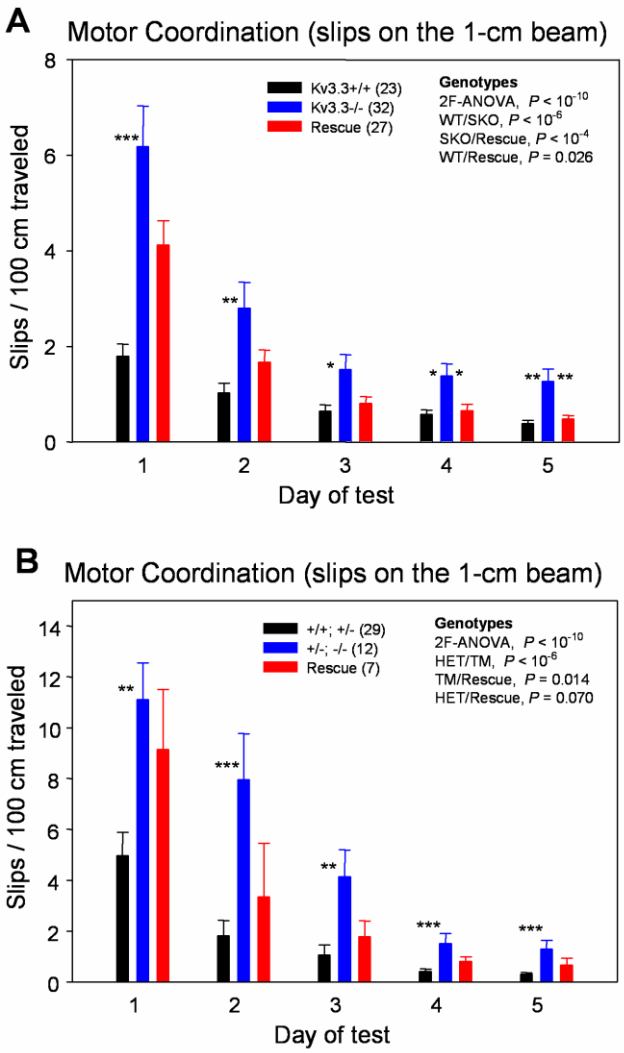

Figure 4.5. Ability of Kv3.3b restoration in Purkinje cells to rescue motor coordination on the narrow beam. (***A***) Restoration in mice lacking just *Kcnc3*. (***B***) Restoration in +/-;-/- mice. Asterisks indicate significance on single days using one-way ANOVA (*p < 0.05; **p < 0.01; ***p < 0.001). Error bars indicate S.E.M. Sample sizes are listed beside color codes, top, center.

On day one, +/+;-/- mice displayed significantly increased slips over wildtype mice on the 1-cm beam that persisted through day 5, essentially in agreement with earlier work (Fig. 4.5A; Joho et al., 2006). All genotypes are capable of improvement as learning presumably takes place over the 5 days. Interestingly, when fit with an exponential function the learning curves of wildtype, +/+;-/- and rescue mice appear to reach an asymptote at a similar latency. Thus the learning of a motor skill requiring coordination seems to be unaffected by loss of *Kcnc3*. Previous work extending the test out 5 additional days indicated that by day 5 improvement plateaus (Joho et al., 2006). Rescue mice did not differ from either null or wildtype mice on day 1. By day 4, presumably after learning, habituation or both had taken place, rescue mice made significantly less slips than +/+;-/- mice ($p < 0.05$). The number of slips made by rescue mice never differed from that of wildtype mice on any individual day, in contrast null mice made significantly more slips on all 5 days. Further, by 2-way ANOVA, taking repeated measures across all 5 days into account, null mice made significantly more slips than wildtype mice ($p < 10^{-6}$) while rescue mice made both significantly less slips than null mice ($p < 10^{-4}$) yet still significantly more than wildtype mice ($p = 0.026$), probably due to performance on the first days. Overall, both types of analysis indicated that motor function in the beam test was rescued by restoring Kv3.3b in Purkinje cells, with the null deficit only remaining evident on training days that likely account for the persisting difference between wildtype and rescue mice by 2-way ANOVA. Rescue mice moreover learned at a rate similar to the other two groups.

On the 1-cm beam +/+;-/- mice lacking one *Kcnc1* allele also improved with Kv3.3b restoration to Purkinje cells. Looking at individual days, the previously demonstrated increase in slips made by +/-;-/- mice compared to mice heterozygous for the *Kcnc3* null allele remained significant on all days despite improvement by both groups. Intriguingly, the degree of improvement is greater than that which occurs in mice just lacking *Kcnc3* because those additionally lacking *Kcnc1* begin by making more slips, consonant with previous work.

Although this is comparing across two different populations of mice, that it replicates previous work using a different outbred population and that I bred them such that half of the genetic material of one is derived from the other increases my confidence. Once learning and habituation have taken place, levels of slips appear to reach an asymptote at a quite similar latency across these mutants despite the initial difference in severity. Rescue mice, in this case using the 396 line, do not differ from mutant mice on any of the 5 days taken individually. It is noteworthy that in this test the mutant and rescue groups are considerably smaller than when mice just lacking *Kcnc3* were tested above. A trend toward a rescue however is clear and supported by two-way ANOVA comparing mutant and rescue mice across all 5 days (p = 0.014). Using *Kcnc3*-null allele heterozygote controls, rescue mice do not make significantly more slips than the control (p = 0.07). The rescue is potentially partial in nature though like that of lateral deviation considering the small sample size and that heterozygote controls may have more slips than wildtype mice, mitigating the difference between control and wildtype mice. In previous work the heterozygotes trended toward having slips than wildtype mice but it did not quite reach significance. That caveat notwithstanding, restoring

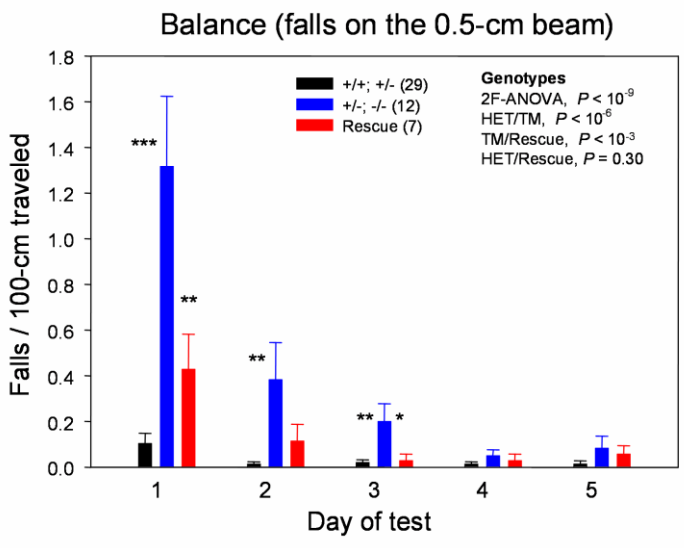

Figure 4.6. Ability of Kv3.3b restoration in Purkinje cells to rescue motor coordination or balance on the narrow beam. Asterisks indicate significance on single days using one-way ANOVA (* $p < 0.05$; ** $p < 0.01$; *** $p < 0.001$). Error bars indicate S.E.M. Sample sizes are listed beside color codes, top, center.

Kv3.3b in Purkinje cells also overall significantly improved beam performance in these mice.

To further ascertain whether beam performance was rescued in +/-;-/- mice I additionally counted falls on a 0.5-cm beam, a more robust phenotype exhibited by this mutant (Joho et al., 2006). Falls could be caused by impaired coordination, balance or both, however it seemed falls in these mice tended to occur in conjunction with slips. A rescue is clear by both repeated measures and considering individual days. Like wildtype mice examined by Joho et al., 2006, +/+;+/- mice make very few falls and have acquired performance after one day of training (Fig. 4.6). By day 4, all groups did not differ from each other significantly in terms of falls. On days 1 through 3, mutants fall significantly more than heterozygote controls. Rescue mice fall significantly less than mutants on days 1 and 3. The difference between wildtype and rescue mice was not significant on any day. As with slips all genotypes show improvement. Taking all 5 days into account, the mutants fall significantly more than heterozygotes and the rescue is apparent in both respects; rescue mice fall significantly less than mutants and at a rate not significantly different from heterozygote controls. Insofar as falls originate from the same underlying deficit as slips, these data reinforce those obtained counting slips to support the notion that motor coordination is rescued by replacing Kv3.3b in Purkinje cells.

An intriguing observation I made during the beam tests was that +/+;-/- mice and even more so in those additionally lacking a *Kcnc1* allele was that slips tended to occur in paroxysmal bouts. In some cases mice would traverse the beam upright making few if any slips but then during a consecutive 100-cm traversal would suddenly have more difficulty, often culminating in a total loss of grip in the hind quarters while the fore limbs did not loose footing. Upon loss of grip the hind limbs would kick rather frantically to regain footing on the beam. The movement had a striking jerky quality to it reminiscent of a cardinal sign of cerebellar ataxia, hypermetria, where excess speed is imparted to movements. Acceleration and deceleration of limb movement is no longer smooth but rather

jerky in character. Another observation I noted was that mice lacking *Kcnc3* seemed to poorly make use of their tails to balance themselves on the beam although the effect, if real, is quite subtle. Mice are said to use their tails to maintain balance on the narrow beam (Siegel, 1970). If so, ataxic tail movement could affect balance, precipitating slips. Finally, I occasionally noticed +/-;-/- mice had isolated incidents of hopping on the beam with their hind limbs. During normal ambulation however I never observed hopping. This could be a subtle manifestation of non-alternate gait emerging as *Kcnc* alleles are lost.

The -/-;-/- mice cannot perform on any beam except the widest, the 2-cm beam. Even here falls must be counted rather than slips because the impairment of -/-;-/- mice is so severe. The -/-;-/- mice in many cases must be initially placed on the beam numerous times because they are frequently so agitated that they leap away or attempt to bound across the beam, inevitably falling when they do. If mice could not be placed on the beam or fell 15 times before reaching the other end they were deemed unable. Falls were not strictly linked to obvious myoclonic jerks. On day 1 and day 5, 11/21 and 13/21 -/-;-/- mice were unable compared to 11/21 and 14/21 rescue mice, respectively. These rates are clearly not different and 49/49 wildtype mice by contrast were all able. Among mutant mice able to traverse the beam, -/-;-/- rescues and -/-;-/- mice did not differ significantly in the rate at which they fell on either day 1 or 5 ($P > 0.8$). Thus, on the -/-;-/- background Kv3.3b re-expression in Purkinje cells was unable to rescue beam performance.

Taken together, the beam test data indicate that restoration of Kv3.3b in Purkinje cells rescues motor coordination in mice lacking *Kcnc3* fully, +/-;-/- mice additionally lacking *Kcnc1* partially, and in DKO mice not at all.

4.2.1.3. Rotarod (Pilot Study)

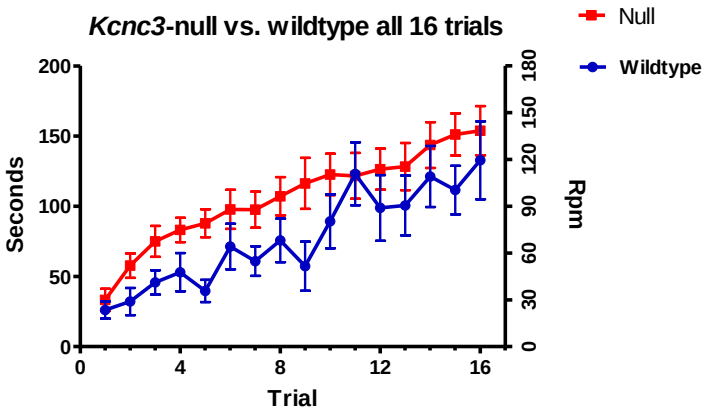

Figure 4.7. *Kcnc3*-null mice learn on the accelerating rotarod and do not become impaired preferentially at high speeds. Wildtype *n* = 11; Null *n* = 22. Error bars indicate S.E.M. Mice underwent 4 trials on each of 4 days.

To further elucidate the nature of the ataxia that is alleviated by restoring Kv3.3b to Purkinje cells, I tested *Kcnc3*-null and wildtype mice, a subset of those used for the latter two studies above, on the accelerating rotarod. Although the rotarod is regarded as a fairly easy motor task that might not detect subtle ataxia, the difficulty can be varied by allowing the mice to continue on to ever higher speeds. Indeed, as discussed in the review of the literature above (section 2.2.2.6), when Nolan et al., 2003 tested *Hcn1*-null mice, which have Purkinje cell firing alterations, they did not uncover a phenotype except at high speeds. Therefore, I allowed the mice to remain on the rod as long as they were able. I gave the mice the usual 4 days of testing for learning to take place with 4 trials on each day. Looking across all 16 trials, aside from perhaps the first trials, the performance of wildtype mice is significantly different (2-way ANOVA, P <0.0001). Surprisingly, null mice perform better than wildtype mice, and this becomes clear on the first day. In the beam test, improvement with learning usually mitigated the difference between wildtype and null mice. Here the deficit likely stems from the fact that, unfortunately, the subset of mice tested on the rotarod that were not too obese to perform by the time I added this test were very skewed in terms of how many albino mice were present. The wildtype group was nearly all albino whereas the null mutant group was nearly all agouti or black. Albino mice are known to develop visual deficits,

and this really seemed to be the case when I attempted to use the pole test to assess equilibrium (data not shown). I could not use the test because many mice I had available were albino and remarkably indifferent to heights. When placed ~5 feet above a surface atop a ~3.5 cm-wide vertical extendable shower rod pigmented mice were reluctant to climb down but albino mice often showed little hesitation to attempt to climb plummet 5 feet to a cushion. Therefore, I cannot draw conclusions as to whether there are any static differences in rotarod performance between these groups of mice.

I decided to include these data nevertheless because there are two conclusions that can still be drawn. First, if Kv3.3 has a role in fine motor timing, as with *Hcn1* a phenotype might only manifest itself at higher speeds but not lower speeds. This would be expected to lead to a ceiling where improvement with further trials in the +/+;-/- mice begins to taper off whereas it does not with wildtype mice once they attain equivalent speeds. Instead I saw that the rate of improvement of null mice did not decline relative to wildtype mice over the trials. Insofar as a sufficiently high speed was reached by the last trial, the data suggest that fine motor timing of limb movements is not part of the ataxic phenotype of in +/+;-/- mice. Second, the rates of improvement over the trials after the first three remain the same between wildtype and *Kcnc3*-null mice corroborates, together with the beam data, that motor skill learning is intact upon loss of *Kcnc3*.

4.2.2. Gait

One aspect of motor coordination is gait. As it is unclear exactly what lateral deviation reflects and why mice make slips on the beam, I decided to investigate further what aspect of the ataxia in +/+;-/- mice is related to Kv3.3 expression in Purkinje cells, as revealed by the fact that restoration of the channel here rescued performance in these tests. The increased lateral deviation and beam slips in +/+;-/- mice could arise from increased force application due to hypermetric, jerky movements, irregular paw placement due to gait ataxia, wobbling from a deficit in balance or muscle twitches. Here I examined gait using

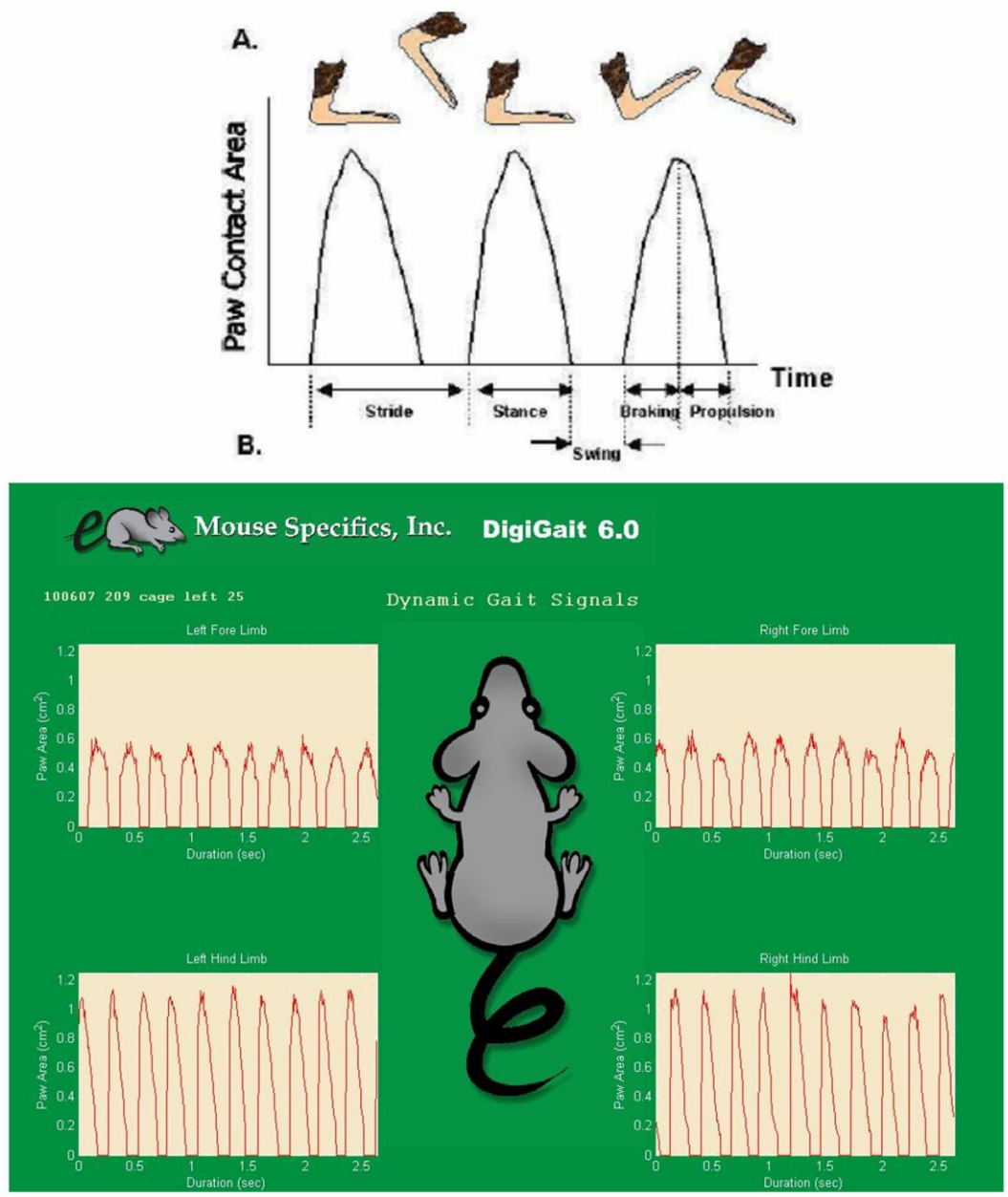

Figure 4.8. DigiGait™ apparatus. (***A***) The DigiGait™ treadmill derives gait parameters from traces of the total paw area detected in films of the paws on a transparent belt from underneath. The paw area increases as the foot is set down and decreases as it is lifted. (***B***) Data from mice in my study from each of the four paws. Note the near total absence of artifactual signals. The traces are separated into discrete paw prints by the software.

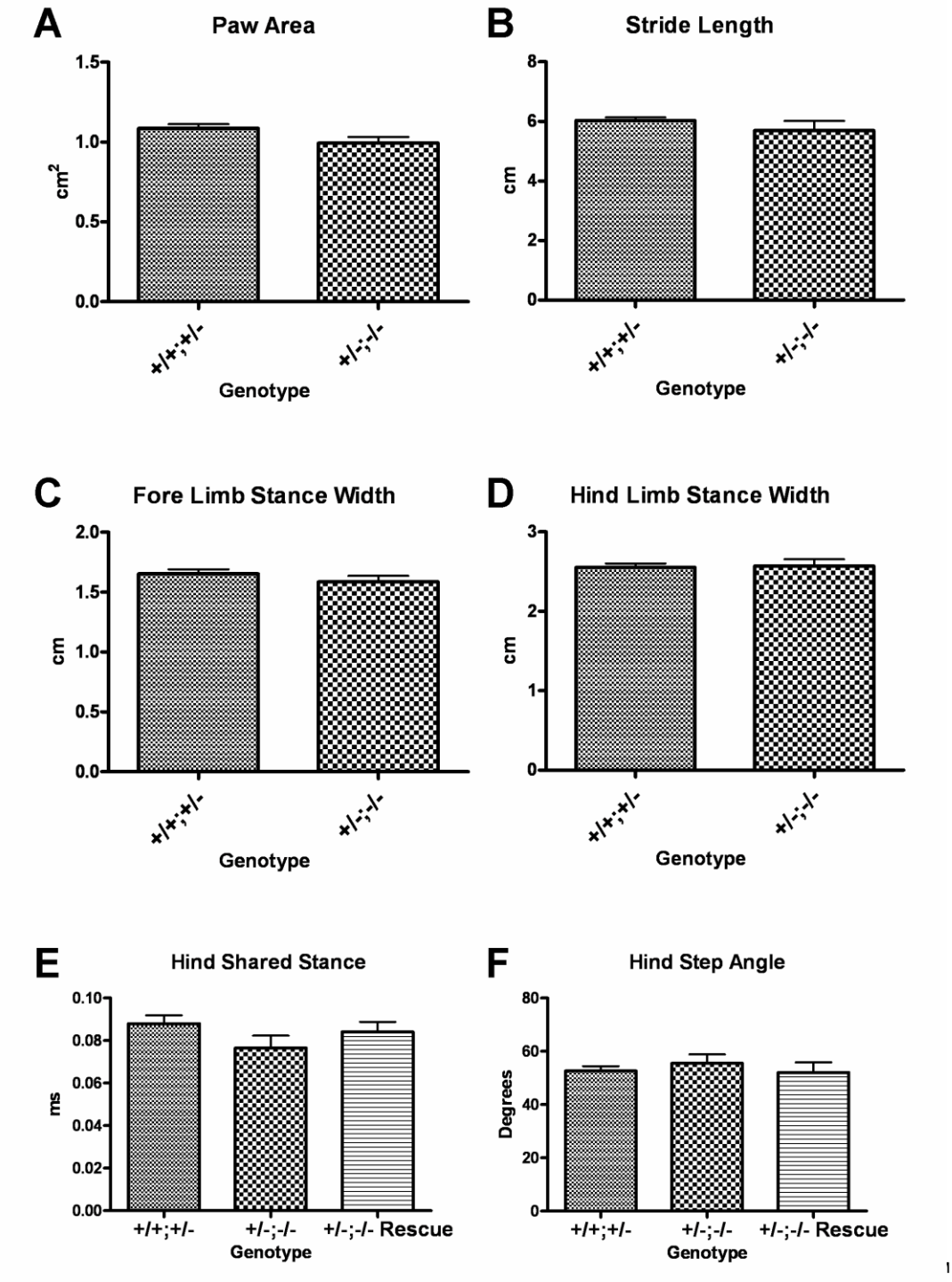
A
Paw Area
1.5
1.0
0.5
0.0
cm2
+/+;+/-
+/-;-/-
Genotype
B
Stride Length
8
6
4
2
0
cm
+/+;+/-
+/-;-/-
Genotype
C
Fore Limb Stance Width
2.0
1.5
1.0
0.5
0.0
cm
+/+;+/-
+/-;-/-
Genotype
D
Hind Limb Stance Width
3
2
1
0
cm
+/+;+/-
+/-;-/-
Genotype
E
Hind Shared Stance
0.10
0.08
0.06
0.04
0.02
0.00
ms
+/+;+/-
+/-;-/-
+/-;-/- Rescue
Genotype
F
Hind Step Angle
80
60
40
20
0
Degrees
+/+;+/-
+/-;-/-
+/-;-/- Rescue
Genotype

Figure 4.9. (above) Results of DigiGait™ analysis for right hind limb are shown (all limbs yielded no significant differences) unless otherwise specified. Error bars are S.E.M.

DigiGait™ analysis, a semi-automated computer-assisted analysis of videos of paw prints made at a forced fast pace on a treadmill, as well as traditional footprint analysis of self-paced gait.

4.2.2.1. DigiGait™ Analysis

The DigiGait™ treadmill measures numerous gait parameters by computer-assisted analysis of video recordings of paw placements made through a transparent belt (see section 3.3.2.1). An initial pilot test was carried out to determine the optimal parameters for the treadmill. In doing so, I also tested the maximal speed at which wildtype and +/+;-/- mice could run, for I wanted to determine the fastest speed at which I could test the mice without too many of them failing to complete the test. The mouse was started at 10 cm/second and the belt speed was increased in increments of 5 cm/second, with each stepwise

Figure 4.10. *Kcnc3*-null mice do not exhibit an impairment in running at high forced speeds on the DigiGait treadmill. Bars are S.E.M.

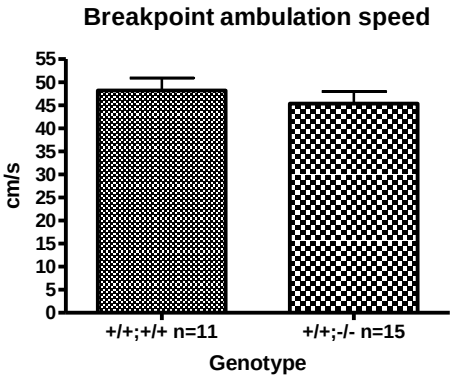

increase lasting for ~5 seconds until the speed was increased again, without intervening rest periods. Although the mean speed at which null mice could no longer run without hitting the rear bumper was lower than that of wildtype mice, the difference did not reach significance (Fig. 4.10). The higher the speed, the more precise fine motor timing needs to be, rendering higher-speed motor tasks theoretically more sensitive to fine timing deficits. Thus, in this task at least, +/+;-/- mice do not exhibit a deficit in fine motor skill timing that precludes running at high speeds.

Initially, I used the group of +/+;-/- mice I had used for the rotarod above that were imbalanced in terms of coat color composition with respect to genotype. Wildtype mice were nearly all albino. This was a serious problem for DigiGait™ analysis because the computer recognizes paws by detecting red signals. Even when paws were painted red the paw area of albino mice was registered as larger and detected for a longer duration as the paw neared and moved away from the surface of the belt. This led to likely artifactual differences in gait parameters sensitive to paw area. These +/+;-/- experiment data are not shown because of this confound. It is nonetheless worth mentioning that parameters such as stride length likely insensitive to this problem did not differ between wildtype and control males. Paws could not be painted entirely red because of technical limitations that restricted me to the use of cake decorators.

I had +/-;-/- mice and +/+;+/- controls that were all pigmented. Accordingly paw areas for the most part did not differ between mutant (*n*=7) and heterozygote control mice (*n*=17), however both mutant and rescue mice tended to be smaller due to slight runting which caused their paw areas to tend to be reduced. The reduction did not reach significance for any side-by-side comparisons of genotypes though (ANOVA). The gait of male mutants did not differ from that of heterozygote males (Fig. 4.9) despite the fact that mutants of this kind appear to remain just slightly smaller as adults. The most basic gait parameters, stride length and stance width, did not differ for any limb or pair of limbs, despite the fact that mutant mice appeared to be slightly smaller on average. A few +/-;-/- rescue mice were analyzed. Step angle of hind limbs[2], a parameter that can increase with ataxia (Hannigan and Riley, 1988), and hind limb shared stance means exhibited a pattern suggestive of a rescued null mutant phenotype that was not significant (rescue *n* = 5). That hind limb shared stance[3] was unaltered

[2] Increases as stride length decreases and stance width increases. If a right triangle is drawn from the stride length and stance width, and a line drawn from the midpoint of the hypotenuse to the right angle vertex, the angle formed between this line and the side corresponding to the stride length is the step angle

[3] Duration over which both hind paws contact belt

suggested alternating gait might be intact even at high speeds where cerebellar deficits in timing coordination might be most readily detected. Together DigiGait™ treadmill data suggested that gait ataxia was absent in +/-;-/- mice at a forced, high speed. The phenotypes of these mutants on the beam and plate is greater than that of mice just lacking *Kcnc3*, so if there were any gait phenotype in the latter mice it should have been apparent in the former.

4.2.2.2. Footprint Analysis

To assess gait alterations at a self-paced speed, such as paw discordance and alternation, that are not obtainable as continuous measures using the DigiGait™, footprint analysis was performed by painting fore paws and hind paws with blue and red India ink, respectively. Moreover, -/-;-/- mice are clearly too impaired to run at speeds required to keep normal controls from pausing on the treadmill, precluding analysis. Subject to footprint analysis mice with cerebellar ataxia typically display shorter strides, wider stance, decreased alternation of gait, veering from a straight path and paw discordance. The latter refers to the distance between the corresponding fore and hind paw prints, which usually is minimal in normal, wildtype mice.

Here, I measured stride length, stance width, the extent to which gait was alternate and paw discordance, noting qualitatively if veering was present. It is noteworthy that I always compared the best obtainable gait sample of each mouse capable of producing at least four strides of uninterrupted ambulation. Gait quality was determined by regularity and consistency. Undoubtedly this method will likely underestimate, if anything, the severe deficits of -/-;-/- mice, which most of the time produced gait that was frankly chaotic. Often -/-;-/- gait included extra fore paw prints that exceeded the number of hind paw prints. Most likely these were produced by the prominent myoclonic jerks that occur frequently in -/-;-/- mice.

I performed footprint analysis on +/+;-/- mice with wildtype controls, +/-;-/- with +/+;+/- as controls and respective Purkinje cell rescue mice, and finally -/-;-/-

mice with wildtype controls and respective -/-;-/- rescue mice (Fig. 4.11). The mice were almost entirely the same used for the other tests of motor

Figure 4.11. Self-paced gait patterns of mice lacking *Kcnc3* and *Kcnc1* alleles. The degree of impairment increases as *Kcnc1* alleles are ablated. Hind paws and fore paws are painted as indicated and mice are allowed to walk through a tunnel on paper. Wildtype, *n* = 17; *Kcnc3*-null heterozygote, *n* = 4; *Kcnc3*-null, *n* = 5; *Kcnc3*-null also lacking a *Kcnc1* allele, *n* = 10; *Kcnc3*-null also lacking a *Kcnc1* allele rescue, *n* = 9; DKO, *n* = 9; DKO rescue, *n* = 3.

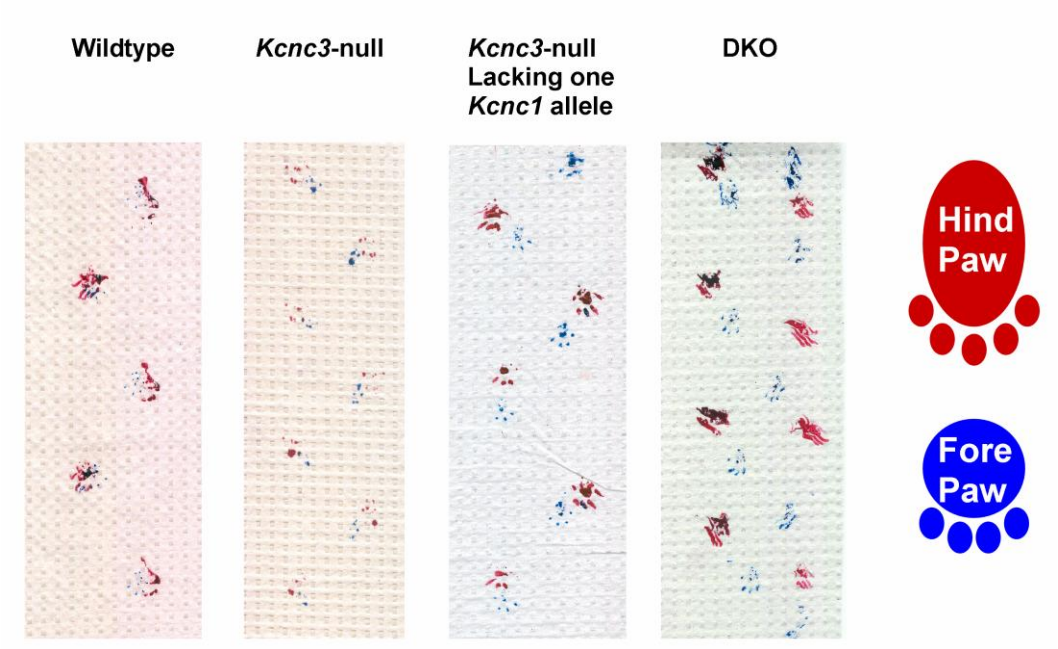

coordination. Separate control groups were used for each mutant because it is impossible to derive all three types of mutants from the same breeding pairs along with either wildtype or *Kcnc3*-null allele heterozygote controls. I however minimized the genetic distance between these groups by deriving them from breeders largely culled from the other groups. Indeed, none of the control groups differed from each other in terms of any gait parameter (Fig. 4.12). As discussed in the introduction, mice +/+;+/- also do not differ from wildtype controls in terms of lateral deviation or slips on any narrow beam. Results will be discussed comparing both to respective controls as well as when wildtype mice from both the +/+;-/- and -/-;-/- experiments are pooled with all genotypes being compared

alongside each other as a group. Only data from male mice are shown except for paw discordance. For all other parameters, inclusion of females in the groups in which they were sampled did not impact which parameters reached significance. All groups were of sufficient size using just males to apply the D'Agostino-Pearson omnibus K2 test for normality except the +/+;+/-, +/+;-/- and -/-;-/- rescue groups. The heterozygote sample was small and varied greatly in this parameter and was affected by an outlier (Fig. 4.12). For all parameters all groups of sufficient size passed, suggesting all parameters are normally distributed, and so ANOVA was used to assess differences.

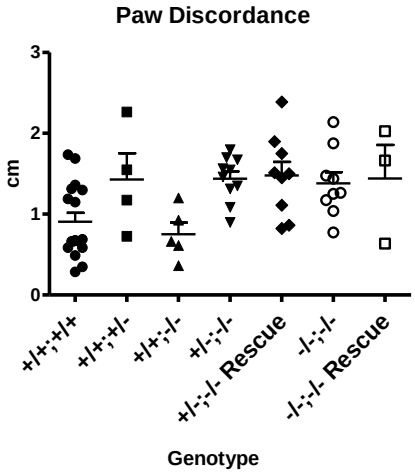

Figure 4.12. Scatter plot of paw discordance data from figure 4.11.

Given the posited role of the cerebellum in motor timing, particularly the coordination of timing across different limbs, alternation of gait between right and left limbs was of particular interest. As discussed in the above review of the literature, mouse mutants with cerebellar ataxia indeed display disturbances in alternating gait, referred to as asynergia or adiadochokinesia depending on the cause. Because most slips in +/+;-/- mice on narrow beams are made by the hind limb, I measured alternation of hind paw prints (red), where, if the beam performance phenotype is related to gait, differences should be most readily detected. I defined perfectly alternate gait, where each paw print would be equidistant between opposite prints made by the corresponding hind paw, as 100% alternate whereas totally non-alternate gait, where prints of both hind paws are separated by zero distance along the trajectory of ambulation, is 0% alternate. Wildtype mice exhibited 89% alternate gait. The +/+;+/-, +/+;-/-, +/-;-/-, and the Purkinje cell rescue counterpart of the latter, did not differ from wildtype mice in terms of alternating gait, however -/-;-/- and -/-;-/- rescue mice both

differed significantly from all other genotypes (Fig. 4.13A). The -/-;-/- mice exhibit a mean of 61% alternate gait, roughly one-third less than wildtype mice (p < 0.001). Considering that the most regular, alternate gait was analyzed, the difference likely represents a minimum difference. I noted that +/-;-/- mice occasionally show isolated, single instances of hopping traversing the 1-cm beam. It is interesting that these mice have the lowest mean in terms of alternating gait however it is not significantly lower than that of wildtype. In sum, only -/-;-/- mice show a disturbance in gait alternation and this is not remedied by restoring Kv3.3 in Purkinje cells.

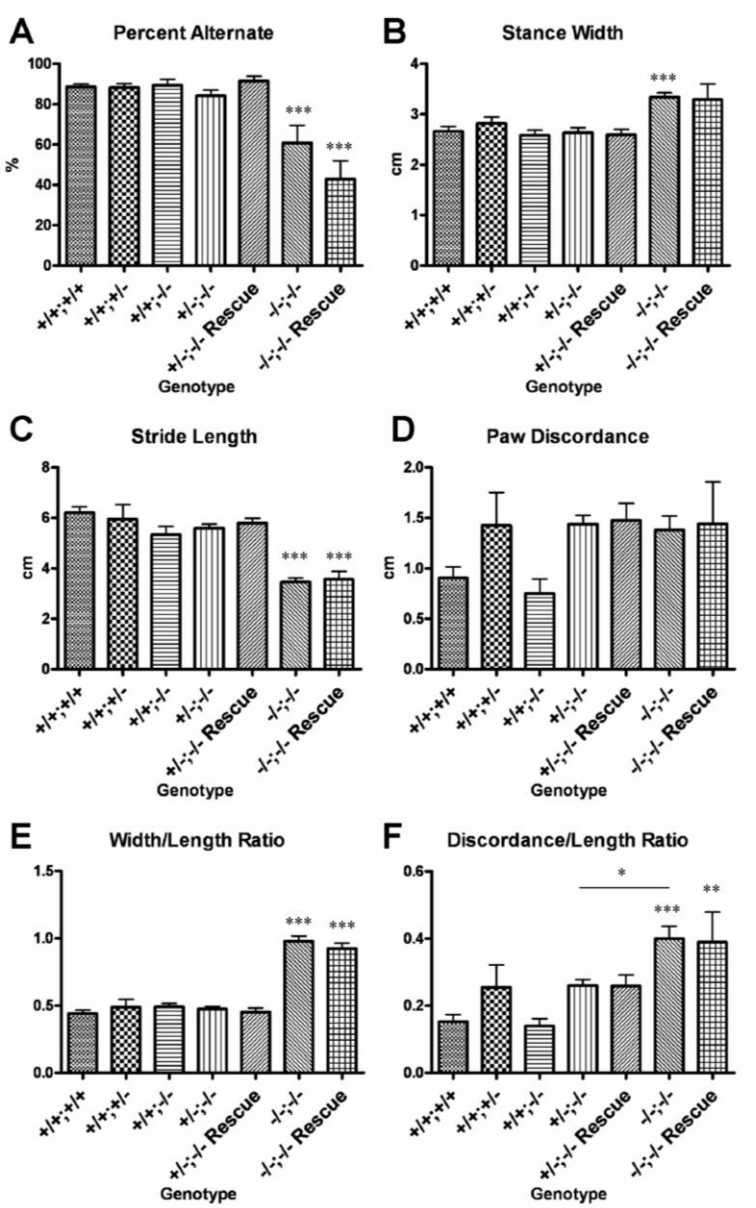

Figure 4.13. Results of footprint analysis of mice lacking *Kcnc3* and mice additionally lacking *Kcnc1* alleles. The data indicate gait ataxia is present in mice lacking *Kcnc3* if and only if *Kcnc1* alleles are lost. * p < 0.05; ** p < 0.01; *** p < 0.001. Horizontal bar compares +/-;-/- to -/-;-/-. All other comparisons are with reference to +/+;+/+.

Cerebellar ataxia also typically presents with a widened stance and shorter strides. I therefore measured stance width and stride length, as I did on the DigiGait™ treadmill using only +/-;-/- mice. In agreement with the DigiGait™, +/+;+/-, +/-;-/- and Purkinje cell rescue mice of the latter type did not differ from each other (Fig. 4.13B, C). As with alternating gait, -/-;-/- mice differed significantly from +/+;+/+, +/+;-/- and +/-;-/- mice. The -/-;-/- mice exhibited a wider stance width. That the stance width is greater concurs with what one can surmise just from qualitative observation. The -/-;-/- rescue mice did not differ from -/-;-/- mice however the small sample was quite variable. The data suggest that increased stance width is not corrected by the rescue. The stride length was significantly decreased in -/-;-/- and -/-;-/- rescue mice to nearly half that of +/+;+/+, +/+;+/-, +/+;-/-, +/-;-/- mice and their respective rescue line whereas the latter groups did not differ significantly from one another (Fig. 4.13C). The -/-;-/- and -/-;-/- rescue mice did not differ from each other significantly in stride length. Since the magnitude of the decrease in stride length in -/-;-/- mice exceeds the apparent difference in body length the difference likely at least in part reflects a real difference related to gait. In fact, when 5 wildtype and 4 -/-;-/- mice were held by the entire scruff and measured from the base of the tail to the ear the means suggested -/-;-/- mice might be 6% smaller however the difference was not significant (P>0.079). The apparent difference between these groups at maturity is likely an illusion due to the relative leanness of -/-;-/- mice. Whatever the cause of the decreased stride length, there is clearly an abnormal stepping pattern in addition to decreased gait alternation for the ratio of stance width to stride length is nearly one in -/-;-/- mice whereas in the other mutants and wildtype mice it is always around 0.5 (Fig. 4.13E). In this regard -/-;-/- mice and all rescue mice differ very significantly from the other genotypes tested, while -/-;-/- mice did not differ from -/-;-/- rescue mice.

Finally, paw discordance or abduction was measured, which is the distance separating otherwise overlaid fore and hind paw prints that has been observed to increase in other ataxic mutants as discussed in the literature

review. A normal, wildtype mouse will tend to place its hind paw directly over its fore paw print. In -/-;-/- mice, visual inspection revealed that the placement of the hind paw was often perfectly opposite in phase with respect to the fore paw, being placed exactly between successive fore paw prints. Indeed, paw discordance appeared to be greater in -/-;-/- mice as well as in +/-;-/- mice compared to +/+;-/- and +/+;+/+ control mice, however the differences were on the cusp of significance using only the male mice except when +/+;+/+ was compared to +/-;-/- rescue mice (Fig. 4.13D). When the females were included in the analysis to augment the sample size, the differences between wildtype and -/-;-/- as well as +/-;-/- mice reached significance, as was the analogous case with +/+;-/- mice which did not differ significantly from +/+;+/+ mice (data not shown). Differences in paw discordance could be obscured by differences in overall stride length such that the error in paw placement would be expected intuitively to increase in terms of absolute distance if the strides are longer. Therefore I re-examined paw discordance by rendering the measure ratiometric, dividing by the stride length. In particular this approach would be anticipated to better extricate potential differences in paw discordance in -/-;-/- mice merely stemming from their smaller size from those related to actual gait. Interestingly this analysis yielded, even when restricted to males, significant differences between +/+;+/+ mice and -/-;-/- mice, but also to lesser extent between the latter and +/-;-/- mice (Fig. 4.13). Thus, there appears to be an incremental gradient of this phenotype as *Kcnc1* alleles are lost on a *Kcnc3*-null background. Paw discordance is the only parameter evaluated by footprint analysis that was abnormal in +/-;-/- mice if we consider it intermediate between +/+;+/+ and -/-;-/-.

Together, the footprint data suggest that the pattern of gait is normal in +/+;-/- mice despite the fact that lateral deviation is increased, suggesting that increased lateral deviation arises from another abnormality, such as hypermetria, in these mice. The footprint data additionally are congruent with those from the DigiGait™ treadmill taken at high speeds that suggest gait pattern abnormalities, including abnormalities in right-left alternation, are absent in +/-;-/- mice with the

exception of increased paw discordance. Further, the footprint data reveal that the marked ataxia of -/-;-/- mice manifests not only as increased lateral deviation and poor narrow beam performance but also as altered gait. The -/-;-/- mice exhibit all the cardinal signs of the full extent of cerebellar ataxia, including decreased gait alternation and stride length along with increased stance width and paw discordance, with a veering ambulatory trajectory that is readily apparent upon visual inspection of most footprint samples. In general, there is a striking difference in terms of gait pattern between +/-;-/- mice and -/-;-/- mice completely lacking *Kcnc1*, alongside a graded increase in paw discordance as *Kcnc1* alleles are lost and a total absence of gait abnormalities in mice just lacking *Kcnc3*.

4.2.3. Other Motor Phenotypes

4.2.3.1. Twitching

One possible explanation for the ataxia is that highly localized postural instability results in essentially localized negative myoclonus, the sudden loss of tone, resulting in muscle jerks. Considering the role of Purkinje cells in maintaining posture it is conceivable at least that this could be the cause. If this was the case, restoring Kv3.3b to Purkinje cells should eliminate twitches as well as beam slips and increased lateral deviation. In this sense the beam and force plate phenotypes might not really be ataxia in the strict

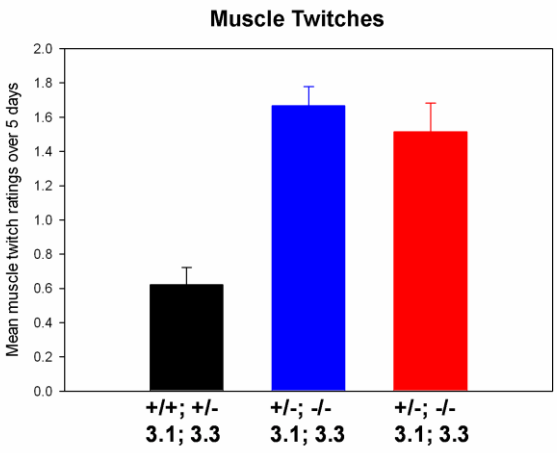

Figure 4.14. Restoration of Kv3.3b to Purkinje cells does not rescue increased muscle twitches in +/-;-/- mice. Error bars are S.E.M.

sense. Alternatively, the twitching represents an entirely independent, dissociable phenotype involving Kv3.3b function at a distinct anatomical locus.

To quantify twitching, Dr. Joho and I independently rated mice blind to genotype on a scale of 0-3. The +/-;-/- mice exhibited frequent localized muscle twitches, and our ratings confirmed this impression (Kruskal-Wallis, $p < 0.0001$; Fig. 4.14). Twitching in +/-;-/- was not rescued by restoring Kv3.3b in Purkinje cells. Beam slips therefore are not caused by twitching. That the twitching phenotype is independent of Purkinje neuronal expression of Kv3.3b suggests that expression in this cell type may indeed be specifically related to motor coordination.

4.2.3.2. EMG Recordings (Pilot Study)

To gain further insight as to the origin of the twitching I recorded the EMG of mice lacking *Kcnc3* and a wildtype controls under the guidance of Dr. Steven Vernino in the Department of Neurology. Because twitching is not corrected by restoration of Kv3.3b in Purkinje cells evidently the cellular locus underlying this phenotype lies outside Purkinje cells. As Kv3.3 is expressed in alpha motor neurons and patients with neuromyotonia, an autoimmune disease where anti-Kv channel antibodies block presynaptic Kv channels at motor neuron terminals, also exhibit twitching, it was conceivable that altered motor unit activity could explain the twitches. Fast repolarization at these terminals is sensitive to 1 mM TEA, consistent with loss of Kv3 function here being consequential for neurotransmitter release.

I observed motor unit waveforms in wildtype and *Kcnc3*-mutant mice under fairly deep anesthesia (Fig. 4.15). There was little or no twitching under this condition. Dr. Vernino considered the unit waveforms to be normal, based on his experience with rabbits. Spikes in multiunit EMG recordings reflect the depolarization of a group of fused myocytes that are excited together as a group or motor unit. This suggests the endplate potentials, muscle action potentials and neuromuscular junction are basically intact overall however it does not exclude

the possibility of a greater amplitude due to enhanced acetylcholine release upon spike broadening at terminals. What counts ultimately though is unit activity. Normal motor unit activity produces consistent tone by taking place repetitively at fairly regular intervals. Individual units, or units the same distance from the electrode, generate spikes of a particular amplitude. Perfect synchronization can result in summation. In the trace under deep anesthesia, we can see activity that would engender consistent tone.

Although myoclonus can be defined phenomenologically as any sudden muscle twitch regardless of origin, including localized jerks, typically myoclonus is accompanied by characteristic motor unit activity. Specifically, discrete bursts of activity are observed where unit activity occurs within a 100-ms brief window. Because muscle contraction takes place on a much slower timescale these action potentials are effectively synchronized as far as the muscle is concerned. The synchronized aspect of myoclonus is important for increased myoclonus is found in epilepsy. It therefore may be helpful to differentiate twitching due to synchronized activity identified by electrophysiology as myoclonic in nature from twitching due to other causes to bring nosology in line with biology. The +/+;-/- mice show whole-body myoclonic jerks very infrequently (see section 1.2.3). After monitoring a deeply-anesthetized null mouse EMG for an hour with the electrode placed in a virtually silent location I suddenly started observing occasional synchronized bursts (Fig. 4.15) that were not accompanied by whole-body jerks or twitching, however. Dr. Vernino considered this activity characteristic of myoclonus. Nevertheless myoclonus can also manifest as “negative myoclonus” where (presumably synchronized) lapses in excitatory input to muscles occur leading to brief, potentially localized, losses of tone and consequently posture.

As the acepromazine/ketamine (with ethanol) anesthesia lightened, both a +/+;-/- and rescue mouse displayed twitching that became more marked than normal once the anesthesia was very light. Notably the heads of the mice began to bob arrhythmically as though their posture was unsteady. The wildtype mouse

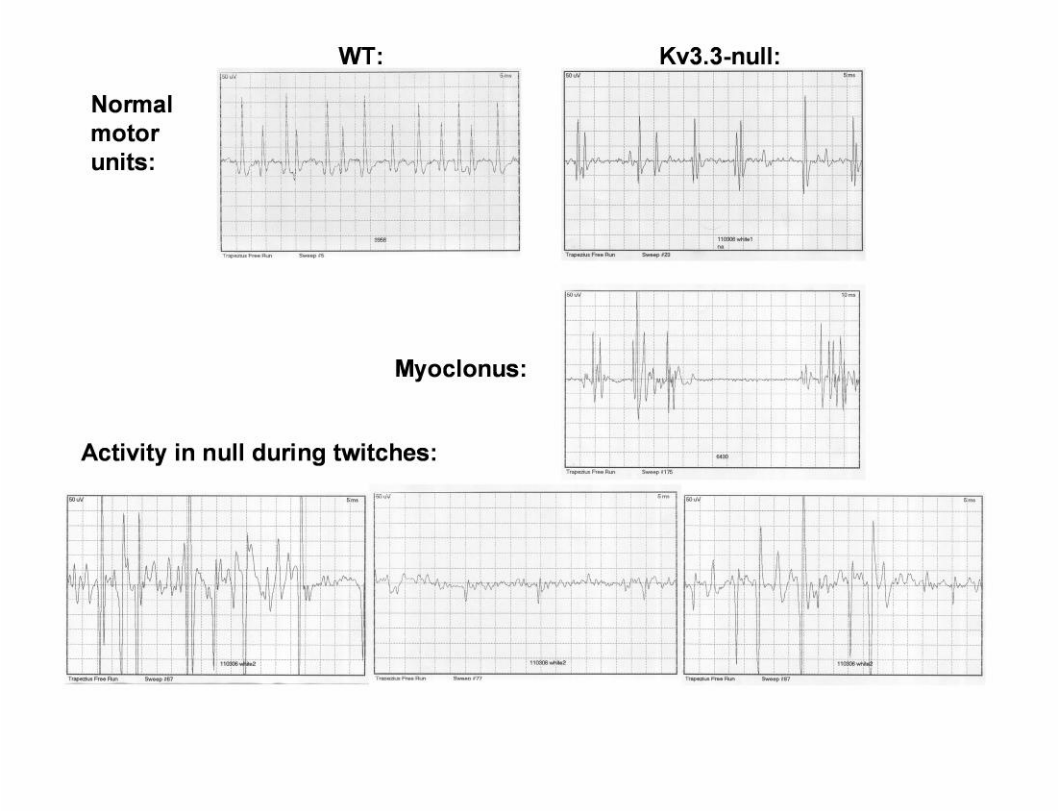

Figure 4.15. Abnormal EMG activity but normal motor units in *Kcnc3*-null mice during twitching. Multiunit recordings are from the trapezious muscle made with a subcutaneous bipolar electrode. Synchronized bursts typical of myoclonus (middle panel) were observed in *Kcnc3*-null mice but twitching was related to bursty activity and periods of synchronized silence, which could represent negative myoclonus (lower panels, which represent a continuous recording), while the unit action potential was normal.

did not display such a robust response when recovering from the anesthesia. Unit activity at this time was bursty and chaotic, however the short bursts distinguishing myoclonus were not observed. Rather, nearly complete lapses in multiunit activity within the range of the electrode were observed lasting >100 ms (Fig. 4.15, bottom). With this duration the pauses could affect the maintenance of posture and result in a twitch. That these were synchronized is potentially consistent with negative myoclonus but the irregular activity between the pauses

could just as well be involved. Interestingly, the observed activity is unlikely to arise from the types of intrinsic alterations one might expect to see in the firing of motor neurons without Kv3.3, which, in addition, is mainly expressed in the terminals rather than the soma. Though terminal expression likely has a function and neuromyotonia leads to twitching in humans, Kv3.4 is co-expressed there presenting the potential for functional redundancy. Thus it is likely that the twitching, though not rescued by replacing Kv3.3 in Purkinje cells, originates from the loss of Kv3.3 in another neuronal cell type elsewhere upstream in the brain.

The results of this pilot study further suggest the twitches are either non-myoclonic in nature or negative myoclonus. It is unclear whether the twitching phenotype shares a common anatomical origin with the infrequent, large myoclonic jerks already described in mice lacking *Kcnc1* and *Kcnc3* alleles.

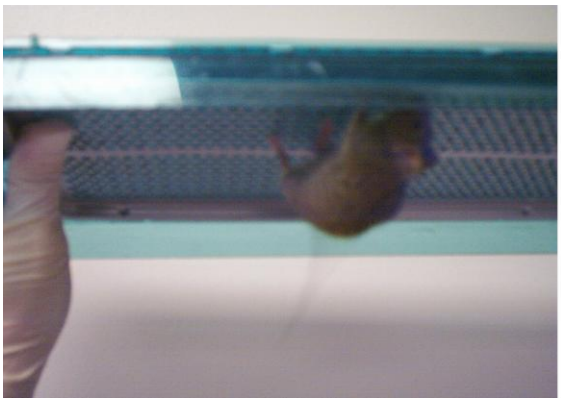

4.2.3.3. Grip Test

Another possible explanation of the beam slips is impaired grip strength. Expression of Kv3.3b in alpha motor neurons raises the possibility that muscle weakness leads to poor grip resulting in slips on the 1-cm beam and falls on the 0.5-cm beam. The

Figure 4.16. Mouse performing the grip test. Mice lacking *Kcnc3* and one *Kcnc1* allele have normal grip strength.

+/-;-/- mice used in the above studies were placed on the inside of a cage lid lined in wire mesh and the lid was inverted for 3 minutes. All mice were able to sustain their grip upside down on the cage lid. The mutant mice could even explore the underside of the lid, moving about. The -/-;-/- mice, in stark contrast, only remained on the lid a few seconds before falling. Poor beam performance therefore in the mutants is not merely due to impaired grip strength however in

-/-;-/- mice this may contribute. Because lateral deviation is also increased in -/-;-/- mice and myoclonic jerks are not frequent enough to account for the increase however poorer beam performance likely still reflects ataxia as well. It cannot be stated though that the increased LDI results from augmented hypermetria though because of the pronounced gait phenotype.

4.2.3.4. Equilibrium and Postural Control: The Rocking Ball Test (Pilot Study)

Beams slips and falls could both be due to a disturbance in balance or postural control rather than motor coordination, or a combination thereof. It is reasonable to expect postural adjustments to maintain balance to be potentially affected by cerebellar dysfunction, especially when visual cues as well as vestibular stimuli are involved since the cerebellum integrates these stimuli to maintain balance.

To directly measure balance and postural control there is an unfortunate paucity of options available to behavioral neuroscientists. For testing basic, gross equilibrium the contact righting test is available, however this test would not detect more subtle deficits or problems with postural control. Other such tests are assessment of negative geotaxis and swimming. The former refers to the fact that normal mice, when placed on a ramp on an incline, will climb upward. Mice with impaired equilibrium will climb down a ramp instead. When dropped in a pool of water, such mice will fall to the bottom rather than swim to keep their heads above water.

Figure 4.17. +/+;-/- mice are able to stay on the rocking ball suggesting posture and balance are intact. Data are the number of seconds the mouseremained on the ball subtracted from 60 to be directly proportional to impairment.

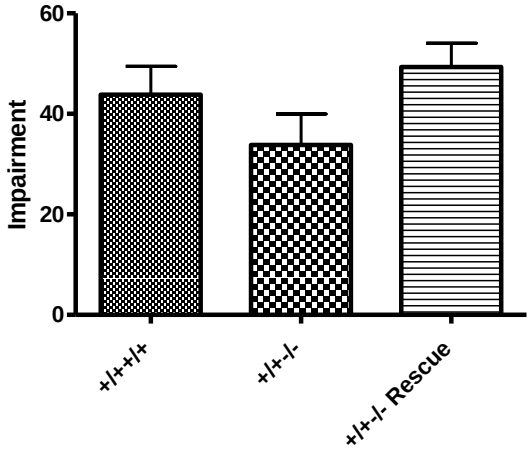

To test basic equilibrium I examined whether the +/+;-/- mice

would demonstrate negative geotaxis. I placed them on a textured slope and they did not climb downward but rather upward, indicating an absence of negative geotaxis and therefore gross equilibrium is intact. The elevated platform test where mice are placed on a small roost several feet above ground could not be performed because too many albino mice were in the group, which were not reluctant to jump down on purpose, invalidating the test. Because there is a lack essentially of sensitive tests that mostly measure postural control I resorted to devising a novel test.

I obtained pilot data comparing +/+;-/-, rescue and +/+;+/+ mice using the rocking ball test (Fig. 4.17). Briefly, in this test (see section 3.3.4.4) mice are placed on a smooth glass ball over a tub of water. The ball is rocked rapidly until mice fall into the water at which point swimming is also assessed. Neither +/+;-/- mice nor their cognate rescue mice fell in the water significantly sooner than wildtype controls. Further, +/+;-/- mice are able to swim, albeit less well, supporting the notion that their basic sense of equilibrium is intact. Again, during swimming the hind limb movement of null mutants has a jerky quality to it, as when they kick paroxysmally on the narrow beam after totally losing their footing. I also noted qualitatively that these mutant mice were abnormal in the use of their tails to aid in keeping their balance it seemed, as on the beam. The +/+;+/+ mice often wagged their tail in phase with the rocking of the ball.

The rocking ball test therefore suggests that +/+;-/- mice do not have impaired balance or fine postural control even when challenged with a demanding task. It should be emphasized though that this is not an established test, and there is no positive control with a known mild deficit in postural control to validate that the test is sensitive. Nonetheless, the results are quite striking. It was remarkable that some mice of the mutant and wildtype groups were able to remain standing on the rocking ball in excess of a minute, frequently correcting their position with agility whenever they began to slide down the ball.

4.2.3.5. Harmaline Tremor

As harmaline-induced tremor is believed to be an index of the functionality of olivo-cerebellar circuitry, harmaline was injected into +/+;+/+, +/+;-/- and rescue mice to determine whether Purkinje cells represented the critical link in the circuitry with regard to *Kcnc3* function. In particular, harmaline tremor had been posited to involve synchronized complex spike firing by Purkinje cells in response to olivary (climbing fiber) input. Harmaline tremor was not rescued. One possible explanation was that the 313 line used for the +/+;-/- rescue experiment did not consistently express in all Purkinje neurons in the mice sampled. This was the same population used for the force plate and beam test studies above, which by sampling 16 mice I confirmed expressed in >90% of Purkinje neurons. Nonetheless some +/+;-/- rescue mice bred using the 396 line were also tested which reliably express in virtually all Purkinje cells (see section 4.1.1). Still harmaline tremor was absent. That harmaline tremor was not at least rescued in +/+;-/- mice is intriguing and surprising. It suggests that another neuronal population in the olivo-cerebellar loop is affected by the loss of *Kcnc3*, neuronal populations in downstream target nuclei are affected, or the normal development of requisite connectivity is disturbed.

4.3. RESTORATION OF KV3.3B EXPRESSION IN PURKINJE CELLS RESCUES WILDTYPE OUTPUT TO DCN NEURONS WHICH EXHIBIT KCNC-ALLELE DEPENDENT SPIKE BROADENING

Above I established that expression Kv3.3 in Purkinje cells is involved in motor coordination by determining that selective restoration of Kv3.3b to Purkinje cells is sufficient to rescue motor coordination on a *Kcnc3*-null mutant background. With the functional relevance of expression in this cell type elucidated, I investigated what electrophysiological changes occur in null mice that are rescued in conjunction with behavior, and thereby bridge the gap between events in networks at the cellular level and behavior. As the only known physiological

role of axo-somatic Kv3 channels as of yet is to act upstream ultimately in spike repolarization, the most parsimonious explanation for the behavioral effect is the impact of the channel current on action potentials.

First, I further characterized the *Kcnc3*-null phenotype in Purkinje cells and tested for a rescue of normal spiking after Kv3.3b re-expression. These results are published in Hurlock et al., 2008. Secondly, I explored changes in the intrinsic firing properties of DCN in neurons in +/+;-/- mice, +/-;-/- mice, and -/-;-/- mice. For rescued Purkinje cell spiking to be able to correct cerebellar output the output of the DCN must in theory remain intact. Finally, I also assessed how the rescued changes I observed in Purkinje cell spiking in mice lacking Kv3.3 might affect DCN spiking, to the extent this can be addressed in slices *in vitro*.

4.3.1. Purkinje Cells

In +/+;-/- mice previous investigations had only addressed alterations in spontaneous simple spike width and frequency. High-frequency spiking, apt to be most affected by loss of Kv3 channels, such as that occurring during complex spikes elicited in response to climbing fiber input or when depolarized in a systematic, controlled manner, was not evaluated. I evaluated these parameters and found them to be altered in mice lacking Kv3.3. I further found that all of these parameters were rescued by re-introducing Kv3.3b using the 313 line, and found converging results with a recording from the 396 line.

4.3.1.1. Intrinsic Firing Properties

Figure 4.18. (below) Input resistance of Purkinje cells recorded in current clamp mode in the rescue experiment.

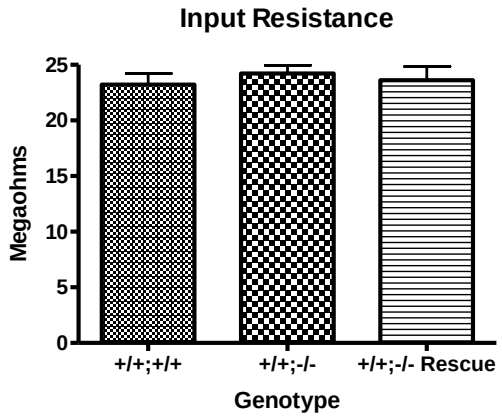

I recorded action potentials in current clamp mode in Purkinje cells from adult mice, often the same used for behavior, using whole-cell patch-clamp. The input resistances measured with current injections below threshold did not differ among wildtype, null or rescue groups (Fig. 4.18), congruent with the notion that Kv3 channels are only engaged at depolarized potentials above spike threshold. Importantly, the data suggest that any differences in spike rates among groups are not merely due to differences in the input resistance.

Replicating previous work in the lab (McMahon et al., 2004), I found that spikes were about twice as broad at half-height in +/+;-/- mice (0.26 ms, ANOVA, $p < 0.001$; Figure 4.21; Hurlock et al., 2008) compared to wildtype mice (0.15 ± 0.004 ms). Rescue mice (0.14 ± 0.006 ms) were indistinguishable from null mutants in this regard ($p > 0.05$). The mean width at half-height in a mouse heterozygous for the *Kcnc3*-null allele was 0.145 ms ± 0.015 (n=2). Considering the very low level of variation in this parameter between these two recordings, the data suggest, albeit weakly, that the width in heterozygotes is virtually unchanged, by contrast. When I applied 1 mM TEA to *Kcnc3*-null Purkinje cells, no clear additional broadening was observed (Figure 4.21), whereas spikes of wildtype Purkinje cells underwent a twofold broadening, a magnitude echoing that observed in the null mutant. As anticipated if the rescue of narrow spiking is through an acute, direct effect of restoration of Kv3.3, the spike width in Purkinje cells of rescue mice could be converted to that of null mice by 1 mM TEA, which should block the bulk of Kv3 current. That no further broadening is seen with 1 mM TEA than is seen in +/+;-/- mice suggests that somatic Kv3.4 expression does not contribute strongly to spike repolarization in Purkinje cells, at least in

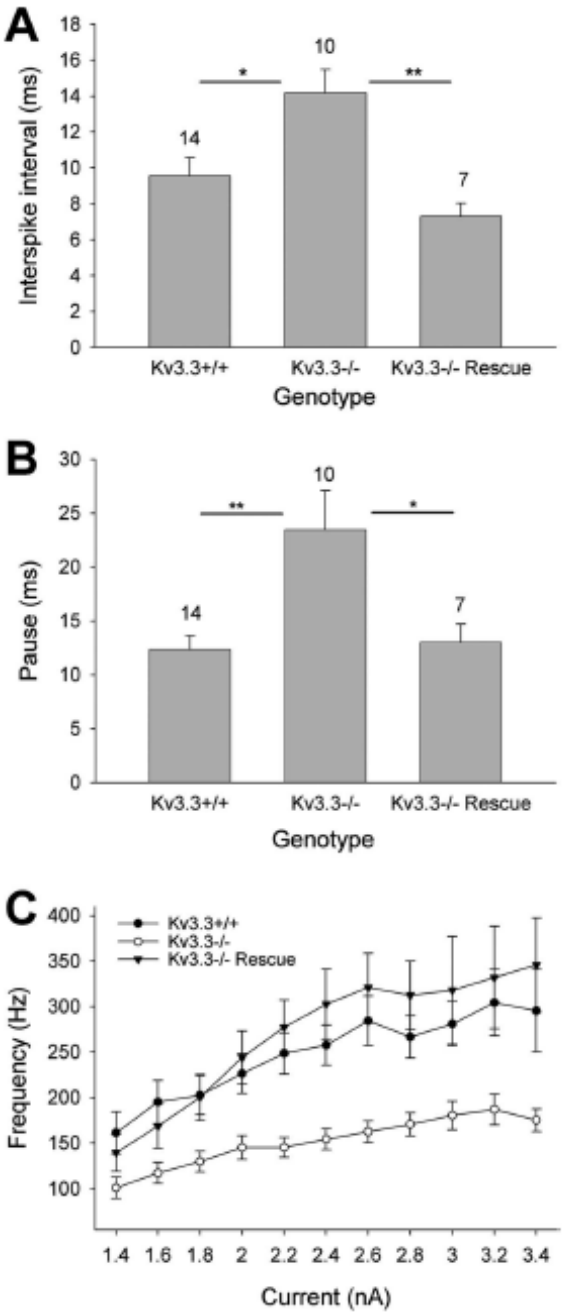

Figure 4.19. Spike frequency is slower in +/+;-/- mice especially at high frequencies. Interspike intervals. Data are from intracellular whole-cell patch-clamp recordings performed in current-clamp mode[4] (***A***), post-complex spike pause durations (***B***), and spike frequency as a function of injected current are all rescued to wildtype values with Kv3.3b restoration to Purkinje cells.

those sampled in this study in the vermis. In conjunction with spike broadening, removal of Kv3 current concomitantly abrogates the fast afterhyperpolarization that immediately follows the spike, caused when rapid hyperpolarization mediated by Kv3 current quickly ceases before other delayed-rectifier or calcium-activated potassium channels have opened substantially. The slow afterhyperpolarization that follows reflects activity of those slower channels.

[4] In current clamp mode current is injected and the membrane voltage is allowed to dynamically respond based on the value of the membrane resistance and the dialog between voltage-gated conductances etc. Action potentials can occur freely in response to depolarization. In voltage-clamp rapid feedback allows for ongoing adjustments in injected current to clamp the voltage, allowing isolation of currents provided the electrical access is sufficient and the injected current can effectively spread to all compartments of the cell.

Since I was already recording Purkinje cells intracellularly I also had recordings of the spontaneous simple spike rate. Intracellular recording perturbs cells and increases the variability in this measurement as well as the difference between cells in the behaving mouse and in the acute preparation because whole-cell recording dialyzes the cytosol, rapidly diluting small solutes that diffuse readily. These caveats notwithstanding, I still replicated in my sample the general observation reported previously using extracellular recording that the interspike interval of spontaneous spikes of +/+;+/+ mice (9.56 ± 1.02) is increased ($p < 0.05$) in +/+;-/- (14.2 ± 1.3) Purkinje cells and restored to normal in those of rescue mice (7.31 ± 0.72; Fig. 4.19A).

If high-frequency firing is relatively more attenuated by loss of Kv3 channels, we would expect to see the difference in the frequency of firing as a

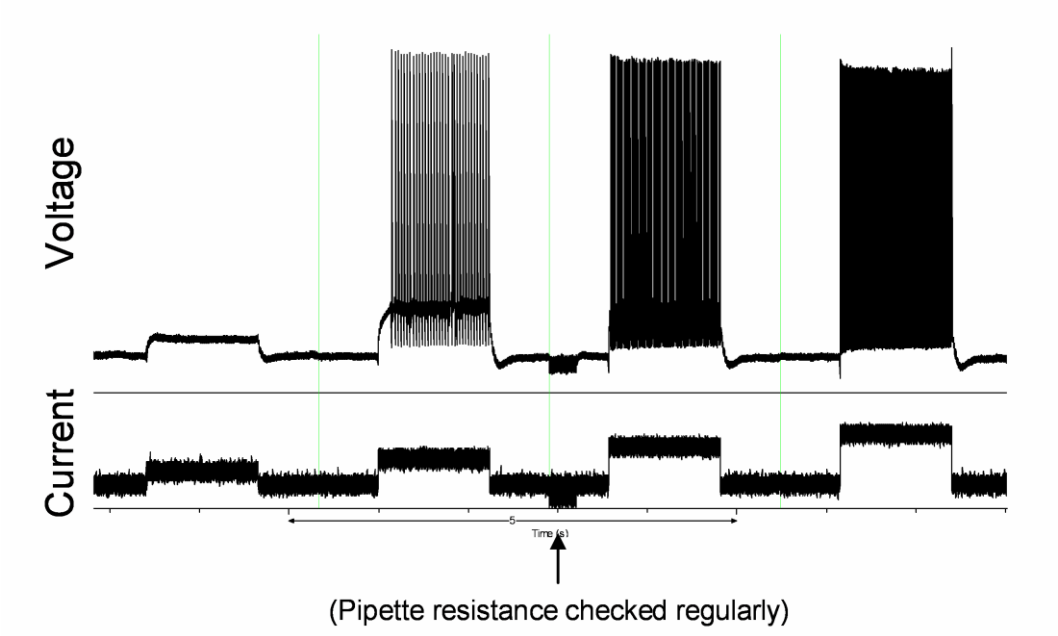

Figure 4.20. Square 1.2-second depolarizing current injection pulses to determine the relationship of spike frequency to injected current in Purkinje cells.

function of injected depolarizing current (*F-I* relation; Fig. 4.20) between +/+;-/- and +/+;+/+ mice to increase at higher frequencies. By 2-way ANOVA using repeated measures across all current steps +/+;-/- Purkinje cells spiked at 11.8 ±

2.55 Hz/200 pA a frequency significantly less than +/+;+/+ mice (29.3 ± 3.19, $p < 0.01$) while rescue mice did not differ significantly from +/+;+/+ mice (25.8 ± 3.42), consistent with the difference in spontaneous spike rates. The *F-I* plot (Fig. 4.19C) revealed that the slope of the relation was clearly decreased in null mice (ANOVA, $p < 0.01$) and normal in rescue mice, supporting the notion that high frequency firing is more susceptible to the loss of Kv3.3. This result suggested that complex spikes might be particularly affected by the null mutation.

4.3.1.2. Response to Climbing Fiber Input

To best model *in vivo* conditions relevant to behavior, climbing fiber responses were elicited with Purkinje cells at the resting potential (Fig. 4.21). In wildtype mice, complex spikes were comprised of an average of 2.61 ± 0.29 spikelets following the initial full spike. The number of spikelets in null mice was reduced roughly by a factor of two (ANOVA, $p < 0.001$; Fig. 4.21A). Measuring the first interspike interval to derive an instantaneous frequency, the frequency attained by wildtype complex spikes was roughly three times that of null mice (ANOVA, $p < 0.001$; Fig. 4.21A, B). In keeping with the notion that the main role of Kv3.3 is in supporting high frequency spiking, this three-fold difference contrasts with a less than two-fold difference in simple spike rates. Complex spikes of rescue mice did not differ significantly from wildtype controls in terms of spikelet number or frequency (Fig. 4.21A, C). The pause in simple spiking that typically ensues after a complex spike was about twice as long in +/+;-/- mice (ANOVA, $p < 0.01$). This parameter, likewise, was rescued in Purkinje cells of rescue mice (Fig. 4.19B). In summary, all spike parameters altered in Purkinje cells of +/+;-/- mice were rescued by Kv3.3 restoration at the soma. I did not endeavor to explore the mechanisms of complex spike attenuation in-depth, however some observations

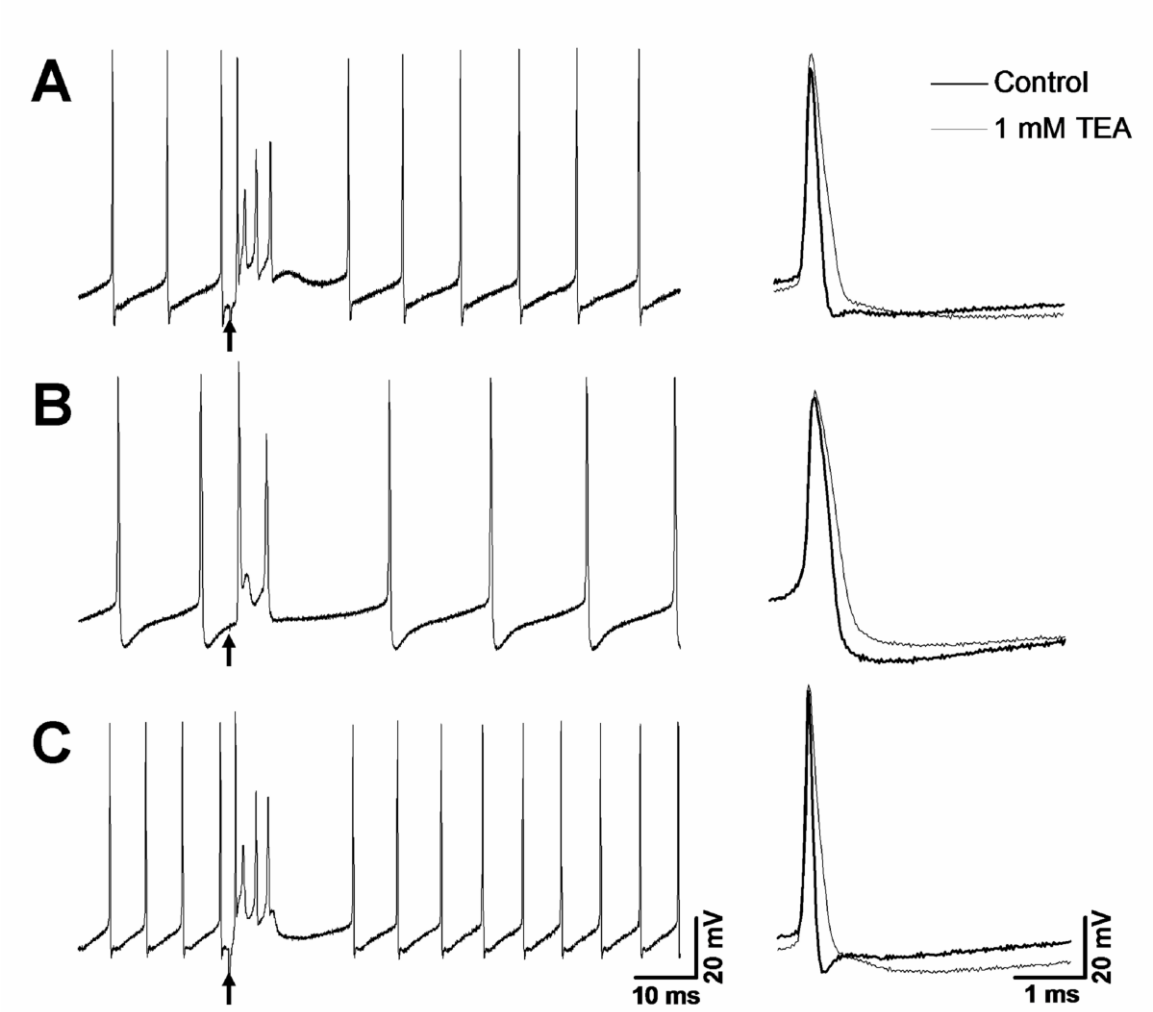

Figure 4.21. Purkinje-cell-targeted Kv3.3 expression restores normal action potentials and complex spikes in *Kcnc3*-null mutants. Complex spikes triggered by climbing fiber stimulation (arrow) in Purkinje cells at the resting potential in +/+;+/+ mice (***A***), +/+;-/- mutant (***B***), and upon restoration of Kv3.3b expression (***C***). At right, 1 mM TEA is able to reverse the rescue suggested that it Kv3-mediated and the spike-broadening effect is largely occluded by the null mutation in *Kcnc3*.

Figure 4.22. (below) Climbing fiber responses evoked from a hyperpolarized potential. Stimuli are delivered to the climbing fiber (arrow) in the absence of ongoing simple spiking by holding the membrane potential at -60 mV by injecting a constant, hyperpolarizing bias current. (***A***) +/+;+/+, (***B***) +/+;-/-, (***C***) Rescue.

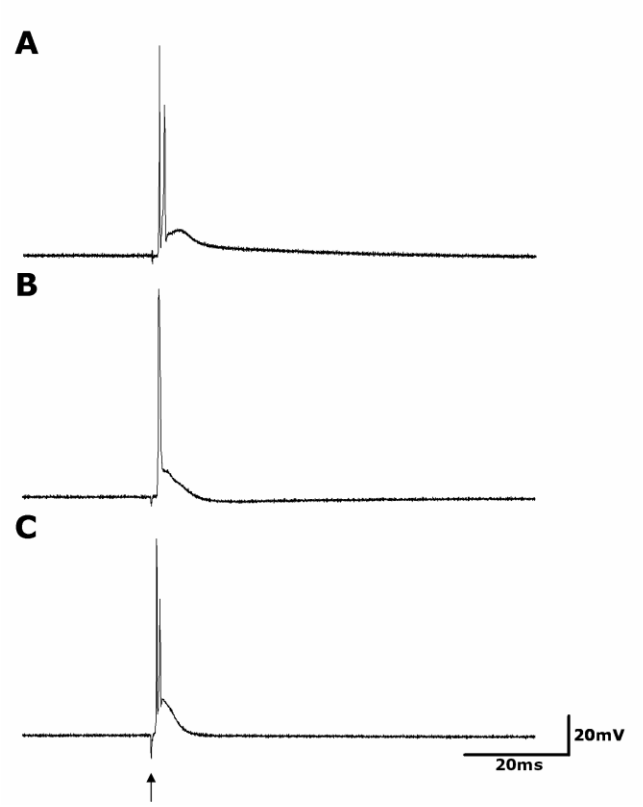

are worth noting. At non-physiological, hyperpolarized holding potentials in isolation without preceding, spontaneous simple spikes I arrived at the same conclusions in terms of the null phenotype. At -60 mV climbing fiber responses of wildtype Purkinje neurons quite consistently were crowned by one spikelet or, rarely, two (Fig. 4.22A). Null mice invariably just fired one spike without spikelets (Fig. 4.22B). Similar results were obtained at -70 mV, although here wildtype mice never had more than one spikelet. Rescue mice were indistinguishable from wildtype mice (Fig. 4.22C). The rescue of complex spikes therefore arose from intrinsic effects on the complex spike itself rather than somehow as an indirect result of effects on preceding simple spikes. Moreover, the rescue was likely attributable to the role of Kv3 channels in fast repolarization of action potentials facilitating high-frequency firing rather than a disturbance in climbing fiber input because injection of current waveforms simulating climbing fiber input of varying magnitude could not elicit instantaneous frequencies comparable to wildtype mice even at the highest strengths (data not shown).

4.3.2. DCN Neurons

For Purkinje cell output to influence motor skills, it must be conveyed to motor centers by way of DCN neurons. If the rescue of Purkinje cell action potential

firing corrects the motor coordination deficit of +/+;-/- mice but not mice lacking *Kcnc1* as well we would expect that perhaps DCN firing becomes significantly altered once *Kcnc1* alleles are lost. Kv3.3 and Kv3.1 subunits are both expressed by large DCN projection neurons that innervate motor centers raising the possibility that functional redundancy explains the pronounced cerebellar ataxia

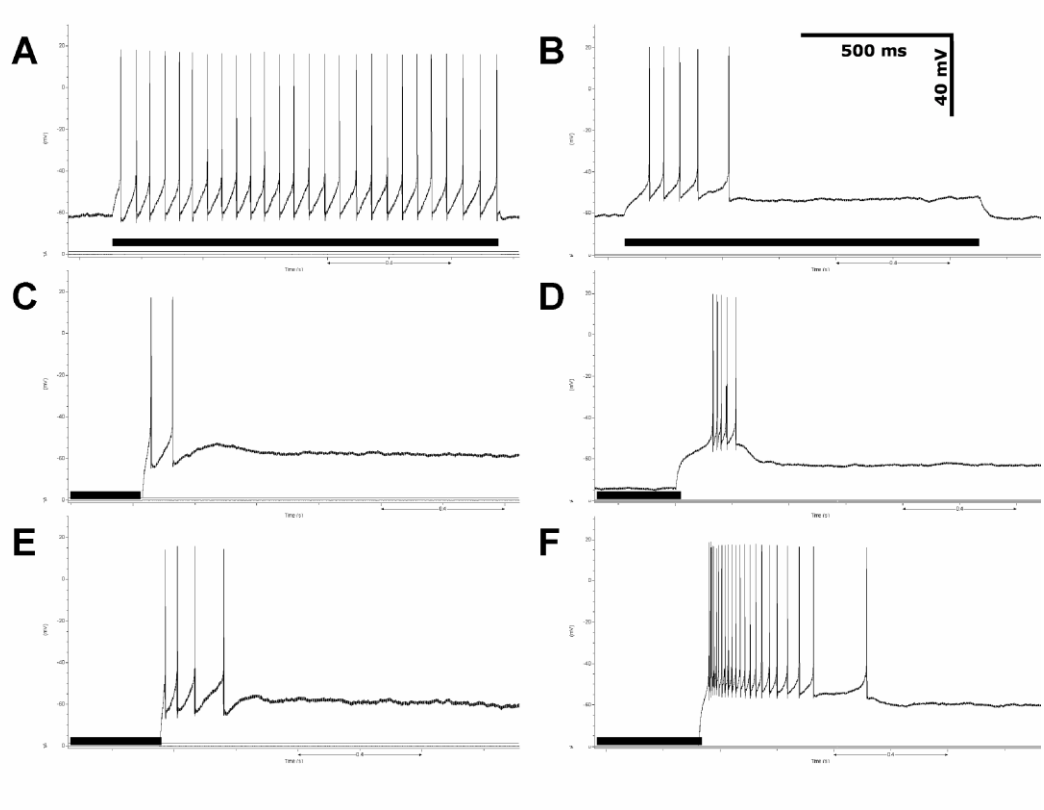

Figure 4.23. Electrophysiological signature of weak and transient, strong bursting neurons in the DCN. Current injection is indicated by a black line. A 100 pA depolarizing step is injected in A and B. In C, D, E, F a rebound burst response is shown upon relief of hyperpolarizaing current injection (or anode break). In E and F the current magnitude is more intense. A, C, E show a weak-burst neuron. B, D, F show a transient-burst neuron. Note the high-frequency firing at the leading edge of the rebound that appears to distinguish these neurons in mice. In rat the burst is more discrete. The morphology of the cell featured in B, D, F is shown in Figure 4.24C.

of -/-;-/- mice. Moreover, we would envision that Purkinje cell output to the DCN to be rescued too if the rescued parameters at the soma are to be consequential

for DCN firing. Of particular interest is the question of what aspects of Purkinje cell firing may account for the rescue. To this end I also collected whole-cell patch-clamp recordings of DCN neurons as above with Purkinje cells and assessed the response of DCN neurons to input from Purkinje simulated by stimulating axons in the slice.

4.3.2.1. Post Hoc Histology

Compared to Purkinje cells, DCN neurons are quite heterogeneous in their firing patterns and Kv3 channel expression. To make valid comparisons across genotypes accurate identification of neuronal cell types is potentially crucial. Although the effect of Kv3 channels on firing is generally confined to depolarized potentials, changes in calcium influx through high-voltage activated calcium channels due to broadened spikes, or, in the opposing direction, fewer spikes in null mice might conceivably effect changes in subthreshold properties. There is extensive overlap in the size distributions of the different cell populations. Therefore I drew from a combination of morphological and, when available, immunocytochemical, data in conjunction with electrophysiological characteristics to identify the large, non-GABAergic projection neurons on which I focused my study.

I chose to focus on the large projection neurons because these are the principal population known to express Kv3.1 and Kv3.3 in the DCN and the one that conveys information to motor centers likely relevant to motor coordination. I filled cells with Alexafluor 488 during recordings, a fixable polar tracer, and detected a marker for large glutamatergic neurons, SMI-32, and a marker for GABAergic neurons, GAD67, by immunofluorescence post hoc. SMI-32 is also known as neurofilament H and was shown to be co-expressed consistently with glutaminase but not GAD67 in the DCN (Hoshino et al., 2005). It is also expressed by Purkinje cells. In addition I noted the morphology and size of cells when making patch recordings. The Alexafluor reveals more detail of the dendrites and morphology than can often be seen using infrared DIC microscopy

during patching in the DCN, where myelination and perineuronal nets notoriously obscure them. Several examples of filled cells are shown (Fig. 4.24).

The cytological studies of Chan-Palay 1977 suggest long, fusiform cells may GABAergic or interneurons (Fig. 4.24E). In the literature large non-GABAergic relatively spiny projection neurons tend to be polygonal while aspiny

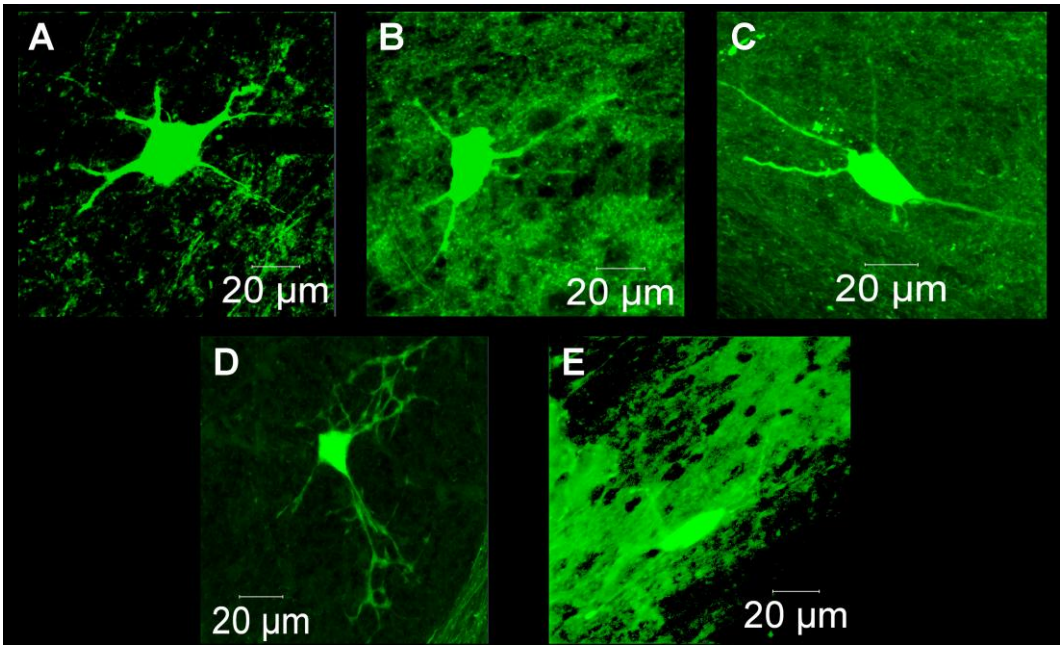

Figure 4.24. Alexafluor488-filled DCN neurons from whole-cell recordings. A, B, C are large, glutamatergic neurons. A and B are weak-burst and C is transient/strong burst. D is GABAergic. E is neither GABAergic or glutamatergic and likely an interneuron or glycinergic neuron. It resembled fast-spiking striatal interneurons which fire intermittently in bursts. Several of these neurons were recorded across genotypes. The diffuse label may have resulted from efflux of internal solution prior to establishing a seal.

neurons tend more rounded or pyriform or fusiform, but there is high variability (Aizenman, Huang and Linden, 2003, Czubayko et al., 2001). A transient-burst large non-GABAergic neuron was polygonal (Fig. 4.24C). For detailed characterization of Kv3 expression see section 4.4 below.

4.3.2.2. Intrinsic Firing Properties

The large, weak-bursting DCN neurons I focused on displayed graded differences in their action potential properties and ability to spike at high frequencies as function of genotype. The +/+;-/- mice showed only subtle alterations whereas mice additionally lacking *Kcnc1* exhibited more significant ones while DKO mice demonstrated pronounced alterations. Using hyperpolarizing steps otherwise as described for the *F-I* relation data below, I classified large neurons as transient or weak-bursting. Rebound bursts in murine DCN neurons may differ from those of rat. Though discrete transient bursts were absent in large neurons, I did see bursts where the initial spike frequency of the first three to five spikes was noticeably higher than the rest in the burst, which was generally larger than those of most large neurons but not quite as robust as those of small neurons. The abundances of these transient-burst neurons were as follows: +/+;+/+, 1/13; +/+;-/-, 4/10; +/-;-/-, 0/5; -/-;-/-, 1/9. These neurons were excluded from the analysis below.

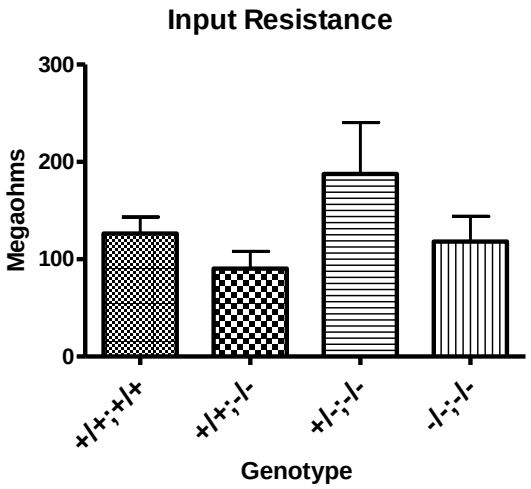

Figure 4.25. Input resistance of recorded large, glutamatergic DCN neurons across genotypes do not differ significantly (ANOVA). Error bars are S.E.M.

As in the case of Purkinje cells, input resistance measurements indicated that loss of Kv3 subunit genes did not affect this parameter and that recordings were comparable (Fig. 4.25). The variability was clearly higher not surprisingly given the diversity of neuronal sizes in the DCN within a given class. Resistance values were less than those of Uusisaari et al., 2007 probably because they used K-gluconate I used K-methylsulfonate as my electrolyte in my internal solution, which has been shown to block less conductances than the K-gluconate (Velumian et al., 1997), as

conductance is the inverse of resistance. Another difference was that Uusisaari et al., 2007 used NBQX as opposed to DNQX in the bath. NBQX blocks glycinergic input more, which, if it constitutes a sufficient conductance, could impact the input resistance. I measured action potential properties of spontaneous tonic spikes and the *F-I* relation.

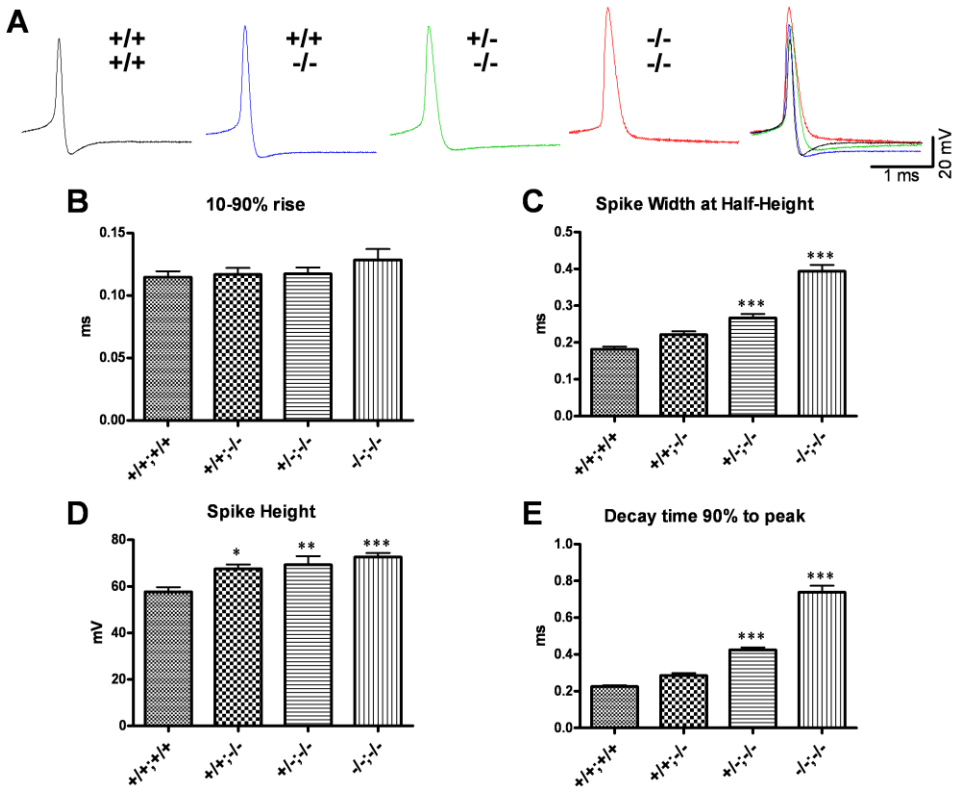

Figure 4.26. Action potential properties of large, glutamatergic DCN neurons across mutants lacking *Kcnc3* and *Kcnc1* alleles. Broadening becomes significant with loss of *Kcnc1* alleles. (***A***) Representative, individual action potential waveforms of each genotype indicated *Kcnc1* then *Kcnc3* below. An overlay is at right. (***B***) The time it takes the voltage to rise from 10-90% of the difference between the threshold and the peak. (***C***) The spike width measured halfway between the threshold and the peak. (***D***) The spike height measured from threshold to peak. (***E***) The time it takes for the spike to decay 90% of the distance between the peak of the spike to the peak of the afterhyperpolarization. +/+;+/+, n = 11; +/+;-/-, n = 6; +/-;-/-, n = 4; -/-;-/-, n = 8. All error bars are S.E.M. Asterisks are compared wildtype: * $p < 0.05$; ** $p < 0.01$; *** $p < 0.001$.

The mean action potential width at half-height was greater in the mutant DCN neurons than in wildtype, reaching significance in +/+;-/- mice lacking a *Kcnc1* allele (ANOVA, $p < 0.001$) where spikes were ~50% broader and in -/-;-/- mice ($p < 0.001$) where spikes were broadened in excess of ~100% (Fig. 4.26A, C). By the D'Agostino & Pearson test, wildtype data were not found to be normally distributed probably due to an outlier score. Using the Kruskal-Wallis test alternatively only the difference between wildtype and -/-;-/- mice was significant yet still yielded a p value of < 0.001. It is difficult however with the small sample sizes involved to determine normality for certain, and if the outlier is removed the distribution is normal. The width in -/-;-/- mice is moreover significantly greater than that of +/+;-/- mice ($p < 0.001$) or +/-;-/- mice ($p < 0.001$). Along with the spike width, the spike height is significantly greater in the mutants, and in this case the difference between wildtype and mice just lacking *Kcnc3* is significant ($p < 0.05$). The fast afterhyperpolarization amplitude also appears to diminish with decreased *Kcnc1/Kcnc3* gene dosage, while the time it takes for the membrane potential to decay to 90% of the difference between the action potential and afterhyperpolarization peaks significantly increases for all genotypes ($p < 0.001$) except +/+;-/- mice, in part reflecting the loss in -/-;-/- mice or reduction in +/-;-/- mice of the fast afterhyperpolarization. This decay time is significantly in slower in -/-;-/- mice than in mice just lacking

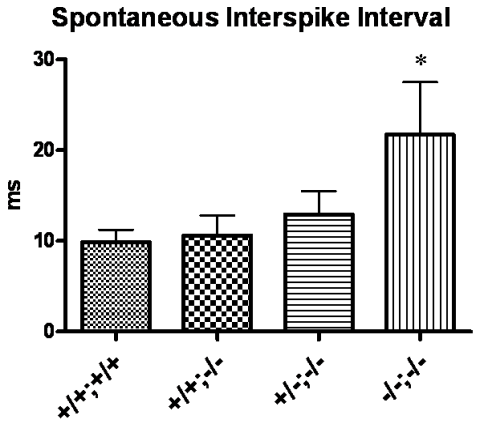

Figure 4.27. Intracellularly-recorded interspike interval at the resting potential in large, glutamatergic DCN neurons. The same cells were sampled as in the action potential waveform study in Figure 4.26. Error bars are S.E.M. * $p < 0.05$.

Kcnc3 ($p < 0.001$) and +/-;-/- ($p < 0.001$). The difference between mice just lacking *Kcnc3* and +/-;-/- mice is also significant ($p < 0.01$). Finally, the rise time of the action potential measured from 10-90% is not different among any of the genotypes. Among the limited number of transient-burst neurons that I sampled, there were no striking, obvious differences between this subtype and weak-burst large neurons. Values were within the same range observed for weak-burst neurons of the same genotype.

The mean spontaneous spike rate measured intracellularly was significantly ($p < 0.05$; Fig. 4.27) slower in -/-;-/- mice (~50 Hz) than is wildtype mice (~100 Hz). The two-fold difference in the spontaneous spike rate parallels the difference in spike width between wildtype and -/-;-/-. This was fairly similar to the situation in Purkinje cells lacking just *Kcnc3*. The coefficient of variance of the interspike interval was not increased over that of wildtype mice in -/-;-/- mice (ANOVA, overall $p = 0.2587$).

I took some pilot measurements to assess high-frequency spiking. The *F-I* relation also appeared to differ among genotypes such that mutants with greater spike broadening exhibited a more shallow slope on the *F-I* plot consistent with a relatively more severe impairment in firing at high frequencies (Fig. 4.28). These

Figure 4.28. Spike frequency as a function of injected current in large, glutamatergic DCN neurons lacking variable numbers of *Kcnc1* and *Kcnc3* alleles. (***A***) The *F-I* plot. (***B***) Average slopes of the *F-I* relation are shown. +/+;+/+, $n = 9$; +/+;-/-, $n = 4$; +/-;-/-, $n = 5$; -/-;-/-, $n = 6$.

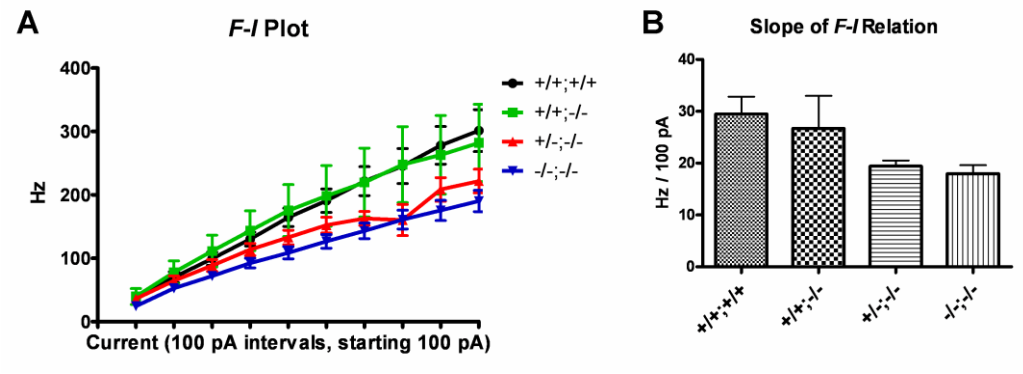

intuitive differences however were on the cusp of significance (ANOVA, overall *p* = 0.0523). Assessed by 2-way ANOVA again the differences were not significant except when the three most intense current injections were considered using multiple comparisons via the Bonferroni correction between wildtype and -/-;-/-. When the more variable, small +/+;-/- sample is removed, the effect of genotype, differences between -/-;-/- and wildtype, as well as differences between +/-;-/- mice become significant at the highest frequencies elicited by the strongest current injections. Although the small sample sizes render the conclusions tentative, it appears that higher-frequency firing is especially perturbed in -/-;-/- and +/-;-/- mice.

Taken together the intrinsic spike data suggest that the large, weak-bursting DCN projection neurons are only subtly altered by the loss of *Kcnc3*, more so by the loss of a *Kcnc1* allele and markedly, to an extent comparable to Purkinje cells upon loss of just *Kcnc3*, when both *Kcnc1* and *Kcnc3* are entirely ablated. The cerebellar output neurons downstream of Purkinje neurons are in essence normal in +/+;-/- mice, enabling normal Purkinje output restored in rescue mice to be faithfully transmitted to motor centers.

4.3.2.3. Depression of Input from Purkinje Cells to DCN Neurons (Pilot Study)

Loss of Kv3-mediated fast repolarization of action potentials at axon terminals leads to increased calcium influx through high-voltage activated calcium channels that in turn increases neurotransmitter release. At synapses made onto DCN neurons by Purkinje cells, short-term plasticity in the form of synaptic depression results due to progressive depletion of GABA. Since blockade of Kv3 channels principally by 1 mM TEA application augmented depression here (Telgkamp and Raman, 2002), I hypothesized that if Purkinje cell terminals rely on Kv3.3 like the Purkinje cell soma then loss of Kv3.3 expression would yield enhanced synaptic depression. A corollary would be that the basis of the rescue mediated by Kv3.3b, which is expressed at terminals (see sections 4.1.1.3 and

4.1.1.4) would potentially include a restoration of a normal level of synaptic depression.

DCN neurons can only be practically recorded by patch-clamp approaches without some tissue dissociation prior to P21. Fast repolarization, the cardinal sign of Kv3 channel expression, appears in Purkinje cells rather abruptly (McKay and Turner, 2005). In Purkinje cells Kv3 expression is first detectable postnatally and the protein accumulates thereafter. The latency between somatic expression and axonal transport to terminals remained unexplored. To ensure channel protein was actually present at terminals with assistance from Mitali Bose I examined sections processed in parallel from individual adult and P17 mice representing +/+;+/+, +/+;-/- and rescue genotypes. A low level of Kv3.3b subunit protein was detected by P17 in wildtype mice (data not shown).

The functional current magnitude generated by channels in the membrane cannot be inferred with certainty from expression levels, and it is not possible to make intracellular recordings of small axon terminals such as those of Purkinje neurons. Rescue mice had, if there was any difference, a higher level of Kv3.3b immunofluorescence at the terminal closer to that of adult wildtype mice (data not shown). Transgene expression should begin by P7 based on the activity of the L7 promoter (Zhang et al., 2001).

With the assistance of summer undergraduate student Ganon Pierce, Purkinje cell axons were stimulated in slices while eIPSCs were recorded in voltage-clamped DCN neurons using whole-cell patch-clamp recording (Fig. 4.30). 500-ms trains of stimuli were used to evidence depression of eIPSC foot-to-peak amplitude. Trains (Fig. 4.29) of two different frequencies characteristic of wildtype or null Purkinje cell simple spikes recorded in Hurlock et al., 2008 were delivered to either +/+;+/+ or +/+;-/-. The stimulation frequency was approximately matched to the spontaneous spike rate of Purkinje cells observed in slices (see section 4.3.2.3) in either wildtype or null mice. Depression measurements were taken at each frequency. Immediately following these trains, stimulation mimicking the average parameters of complex spikes were delivered

followed by a pause and then a resumption of the frequency prior to the simulated complex spike input for 500 ms. Next, the frequency was accelerated to 200 Hz for 500 ms, roughly twice the average wildtype simple spike frequency, to mimic the maximal frequency of simple spiking seen *in vivo*, and then returned to 100 Hz. Similarly, in the +/+;-/- frequency train, the average simple spike frequency was roughly doubled during this epoch of transient accelerated input.

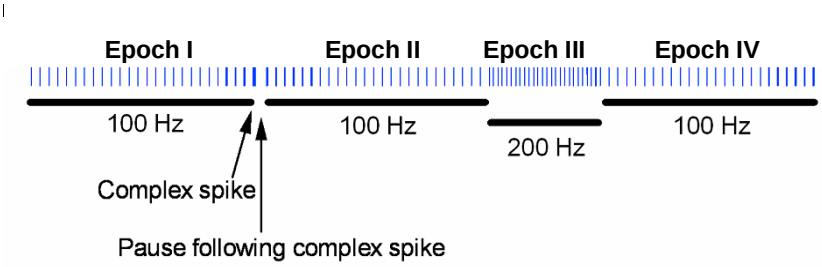

Figure 4.29. Stimulation train with frequencies approximating wildtype Purkinje cell spiking.

The fast epoch was included to assess whether depression increased and then diminished when the input frequency was increased and decreased, respectively. Very little summation of eIPSCs was observed during the simulated complex spike and no obvious recovery from depression occurred after the pause that follows the complex spike using either the wildtype or null simple spike frequency in either mice lacking Kv3.3 in Purkinje cells or wildtype mice. Likewise there were nominal if any effects on eIPSC amplitude when the simple spike input frequency was shifted within the physiological window between the mean and maximum. This does not exclude the possibility that recovery from depression could take place shifting between the low end of the spectrum of wildtype Purkinje cell output frequency (~50 Hz) or between longer pauses in Purkinje cell output and the maximum of 200 Hz. I chose then to focus on depression during epoch I of the protocol after a baseline of silence.

To be assured that eIPSCs were mediated by GABA-*A* receptors and that no other currents were elicited by the stimulation, SR-95531, a GABA-*A* blocker, was applied by a puffer at 10 µM while the stimulation trains were delivered at

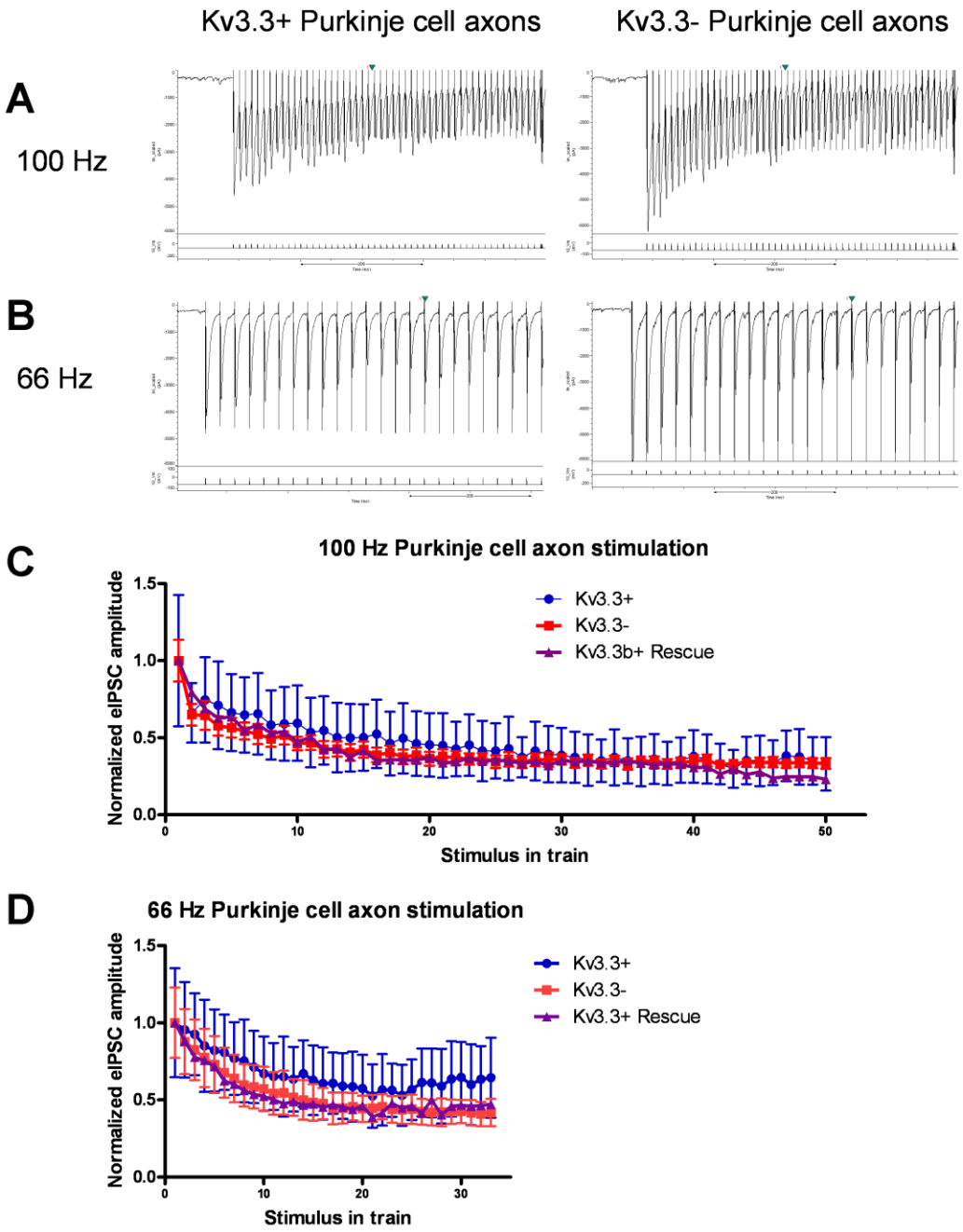

Figure 4.30. Synaptic depression at the synapse made by Purkinje cells on DCN neurons. eIPSCs were recorded in voltage-clamp after stimulating Purkinje cell axons near the DCN. Stimulation is indicated by negative-going stimulus artifacts prior to eIPSCs. (***A***) Purkinje-cell axonal stimulation trains delivered to either mice lacking or bearing Kv3.3 in Purkinje cell terminals at a frequency

roughly approximating the typical spike rate of wildtype Purkinje cells. (***B***) Trains delivered to both genotypes in the same manner except at a lower frequency more characteristic of mice lacking *Kcnc3*. (***C***) Plot of normalized averaged eIPSC amplitudes using the high-frequency wildtype-simulating protocol from A. (***D***) Conterpart plot of data from B. Wildtype, *n* = 3; *Kcnc3*-null, *n* = 5; Rescue, *n* = 1.

Figure 4.31. (below) Verification of the GABA-A-mediated nature of stimulated eIPSCs by puffer application of the GABA-*A* anatagonist SR-95531. 100 Hz stimulation is indicated by vertical lines caused by stimulus artifacts. Baseline (traces 1-4, going left to right), application (traces 5-12) and wash (traces 13-16) are shown. SR-95531 thoroughly and reversibly blocked the eIPSCs. Shown is the leading edge of the stimulation protocol used in Figure 4.30 above.

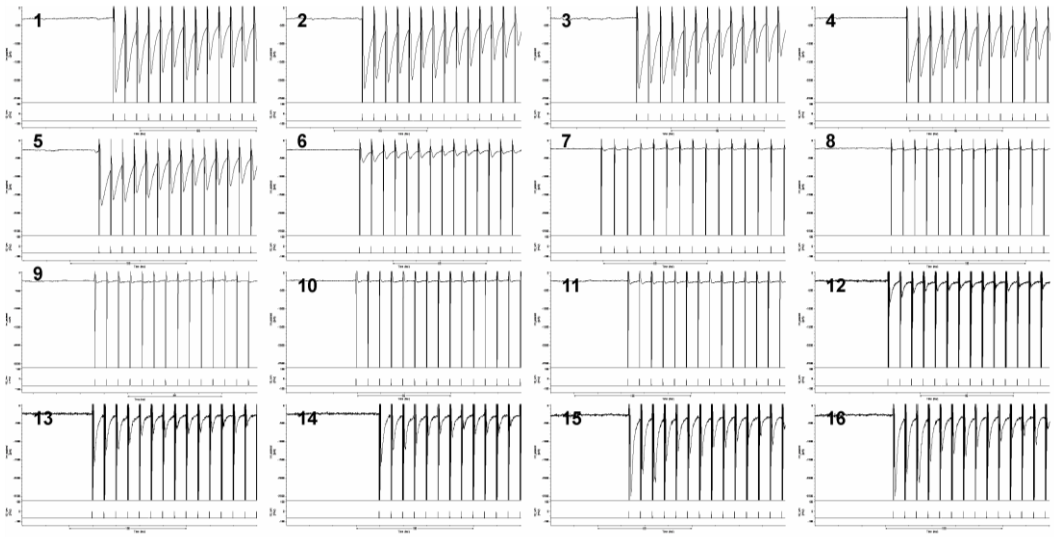

15-second intervals. During SR-95531 delivery eIPSCs were abolished and no synaptic currents insensitive to the blocker were evident. Glutamate blockers were present in the bath and interneuron stimulation was avoided by keeping the stimulation electrode at a distance in the white matter. GABAergic interneurons are also very rare in the medial nucleus (Molineux et al., 2006) where all cells were recorded for this part of the study. The eIPSCs therefore were most likely originated from Purkinje cell afferents to DCN neurons.

Wildtype mice as reported by Telgkamp and Raman, 2002 looking at mice younger than P17 exhibited depression (Fig. 4.30) that appears to be greater at steady state and more abrupt in its onset at higher frequencies. Purkinje-cell-to DCN synapses of mice lacking *Kcnc3* demonstrate the same pattern, and depressed more abruptly it seemed at either frequency than those of wildtype mice. The mutants seemed to have more depression at steady state than wildtype mice only at the null stimulation frequency, possibly due to saturation of the vesicle depletion effect at the higher frequency. In actual mutant mice, Purkinje cells might be expected to fire at the null frequency, so if this small pilot sample reflects true means the data suggest depression may occur both more rapidly and to a greater extent at steady state in *Kcnc3*-null mutants. One usable recording from a rescue mouse was analyzed. For both stimulation frequencies the mean eIPSC amplitudes tracked those of the 5 averaged null mice. The cell was recovered by histology and turned out to be GABAergic based on GAD67 immunofluorescence. eGFP+ axons can be seen in the white matter near the cell and genotyping confirmed that the mouse was a rescue (Fig. 4.24D). If the pilot recordings reflect the true means the data suggest that augmented depression is not rescued by restoration of Kv3.3b to Purkinje cells. To determine if any change in depression or other parameters of Purkinje cell output might be consequential for DCN firing I performed current clamp recordings.

4.3.2.4. Response to Input from Purkinje Cells (Pilot Study)

To characterize responses of DCN neurons to Purkinje cell input trains of stimuli mimicking the mean interspike intervals of simple spikes, complex spikes and the ensuing pauses in simple spike firing were delivered in current clamp mode. In addition, the effect of varying the frequency over the physiological range was examined (Fig. 4.31). The duration of and number of stimuli in simple spike trains

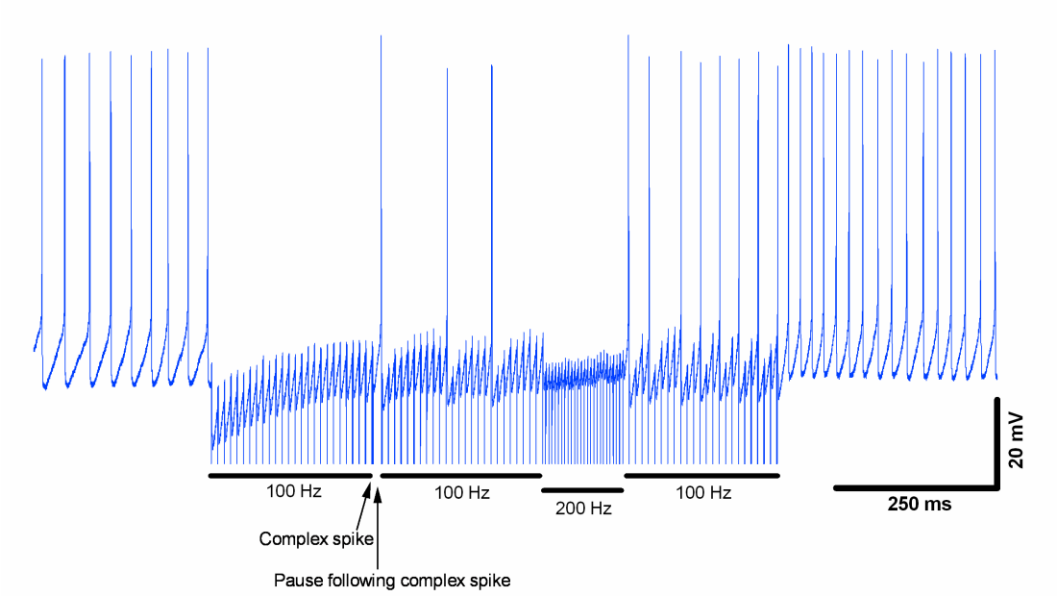

Figure 4.32. Annotated voltage trace of a DCN neuron in current clamp using a protocol developed to explore the effects of Purkinje cell input to the DCN that may be affected in *Kcnc3*-mutant mice explained in Figure 4.29. Stimulation frequencies during different epochs of the train are indicated. A complex spike input simulation comprised of the burst followed by the pause occurs after the first 100 Hz train (epoch I). I also developed a corresponding protocol that simulates input to the DCN from Purkinje cells lacking Kv3.3, as in the eIPSC recording experiment (see Figure 4.29). The vertical lines below are stimulus artifacts signifying the delivery of stimuli to Purkinje cell axons.

was sufficient for short-term plastic changes such as synaptic depression to reach steady-state based on previous work. By necessity, keeping the number of stimuli constant at different frequencies positioned later epochs within the train at different latencies after the onset of stimulation, which rendered traces collected with the two different frequencies difficult to compare with regard to the cumulative rebound depolarization that is very pronounced in DCN neurons. Nevertheless I persisted in an effort to be systematic. Only a few quality recordings were obtained across genotypes to provide a preliminary glimpse so I will give qualitative descriptions.

Cells were held using injection of constant current at various membrane potentials. The current often had to be varied to maintain a stable potential

because of the dynamic nature of the membrane potential below rest in DCN neurons. Despite keeping the stimulation electrode away from the ventral white matter surrounding the DCN that contains the efferent axons I nonetheless frequently encountered axons. Antidromic stimulation was especially rampant when the membrane potential was held at or more depolarized to the resting potential, possibly due to current spread into axons bringing them closer to threshold. I also saw this during climbing fiber stimulation in Purkinje cells. Consequently, only data acquired at potentials hyperpolarized to rest are shown, however it should be noted that the resting potential of DCN neurons varies *in vivo* and may be bistable, so at times these potentials may well be physiological. Had I kept the stimulating electrode strictly in medial slices I might have been able to avoid antidromic stimulation better because I would have been able to stimulate Purkinje cell axons effectively at a greater distance from the DCN but I realized this too late. Also noteworthy is that Purkinje cell axons were stimulated here in unison whereas *in vivo* activity in various afferent axons can be asynchronous, producing a smoothed, tonic IPSP.

In large neurons, the first epoch of the train was capable of halting spontaneous spiking at -55 mV (Fig. 4.33). Depending on the stimulation intensity, the first IPSP either reached the chloride equilibrium potential, at which there was saturation of the IPSP amplitude with increasing stimulation intensity, or a less hyperpolarized potential if milder. Despite the depressing nature of the synapse sub-saturating stimuli elicited temporal summation of IPSPs. Either because of synaptic depression or an accruing underlying rebound depolarization or, most likely, both, the membrane potential became depolarized returning back toward the resting potential by the time the first epoch was followed by the simulated complex spike input. With weaker stimulation, cells sometimes resumed spiking during the train. *In vivo* complex spikes occur in the context of ongoing simple spiking that is believed to shift in frequency in response to varying parallel fiber and interneuronal input. Thus, my protocol should serve as

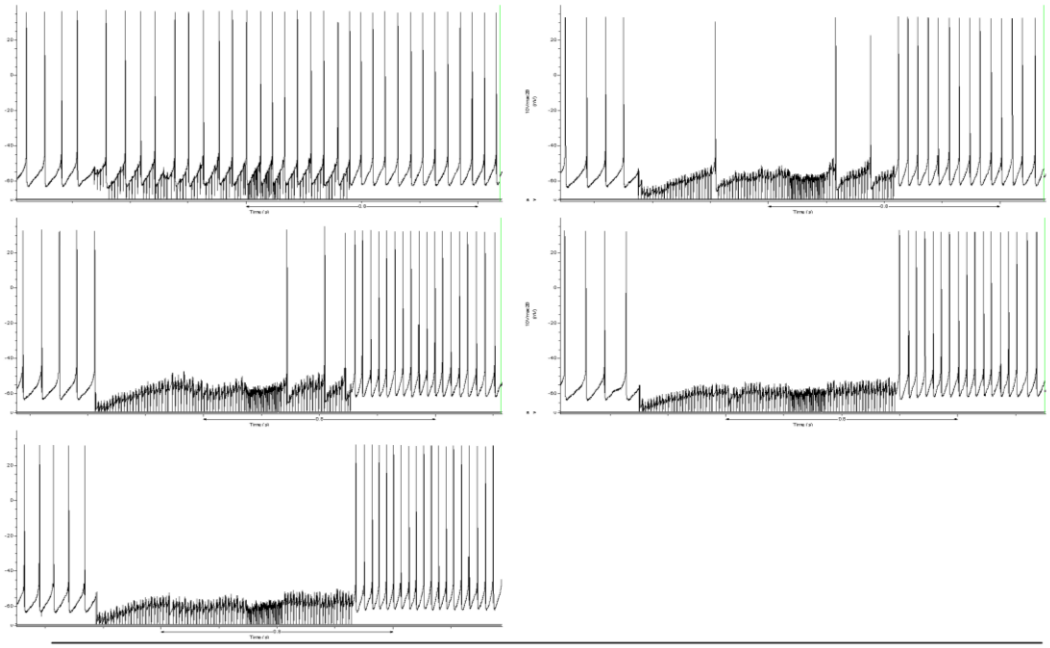

Figure 4.33. Stimulation as in Figure 4.32. (above) Response of a DCN neuron to Purkinje cell stimulation at -55 mV. Stimulus intensity is increased going left to right, top to bottom, in 200 µA increments. **Figure 4.34.** Stimulation as in Figure 4.32. (below) Response of a DCN neuron to Purkinje cell stimulation at -60 mV. Same cell as in Figure 4.33 above.

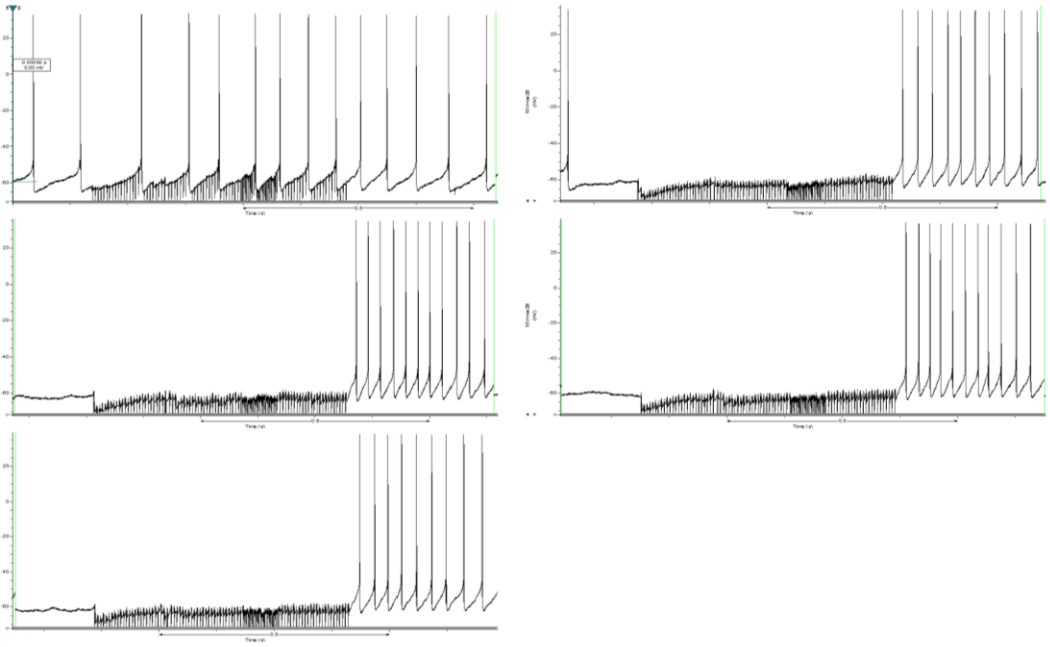

a valid representation of what might actually be happening after synaptic depression has reached steady state and the slow rebound depolarization has been engaged by IPSPs.

Surprisingly, despite suggestions by *in vivo* or explant preparation data to the contrary, the simulated complex spike input between epochs I and II even using the wildtype parameters in wildtype slices did not elicit a transient, discrete rebound burst or acute acceleration of firing at any potential or stimulation intensity. As seen in the depression recordings above, IPSCs that trigger the IPSPs are already suppressed once the complex spike stimuli arrive at the terminal on a background of simple spiking. Intriguingly, the simulated pause that follows the complex spike was in some cases capable of allowing the underlying rebound depolarization to drive the cell to threshold before stimulation resumed (Figs. 4.32 and 4.33). After the pause the depolarization was sustained, and spikes were more likely. Next the epoch of accelerated firing (III) typically resulted in somewhat enhanced hyperpolarization, as expected, which dissipated probably due to further rebound depolarization building since depression does not change much here. Indeed, following this high-frequency epoch the DCN neuron became more depolarized upon resumption of the previous stimulation frequency (epoch IV) than before the accelerated epoch (epoch III; Figs. 4.31, 4.32 and 4.34), suggestive of further rebound drive. The rebound depolarization was quite apparent after the end of the stimulation protocol as the spike rate was substantially accelerated over baseline. In some cases, the rebound potential presumably contributed to increased spiking not just by depolarizing the cell but also by decreasing the input resistance. Normally, decreasing the input resistance decreases excitability, however during repetitive IPSP trains from synchronized inputs, a subsequent shortening of the membrane time constant (time constant = resistance x capacitance) will allow the membrane to depolarize faster between IPSPs (Fig. 4.34).

At -60 mV the pattern was similar except the rebound depolarization actually depolarized the cells beyond the initial holding potential even while the

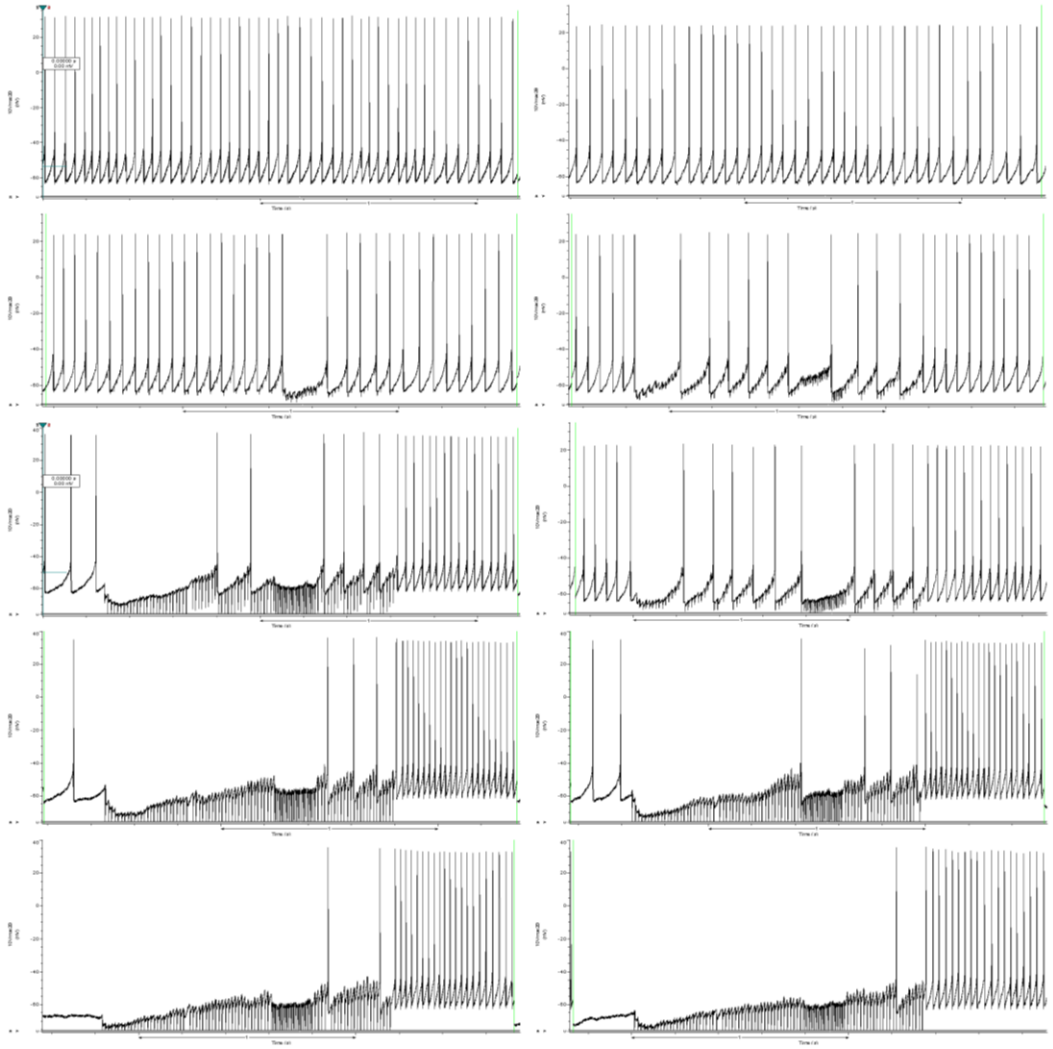

Figure 4.35. Stimulation of Purkinje cell axons according to the protocol in Figure 4.29 when the recorded DCN neuron is at a hyperpolarized potential is capable of leading to eventual net depolarization. Stimuli of increasing magnitude are given to Purkinje cell axons left to right, top to bottom. Note acceleration of membrane time constant as the rebound depolarization grows. In the first two trains stimuli are subthreshold.

barrage of IPSPs continued (Fig. 4.34). From hyperpolarized potentials below the chloride equilibrium potential (E_{Cl}) at the soma eIPSPs (or IPSPs in the electronically-distant dendrites) depolarized many cells, in some cases triggering a bistable shift to an up state. That occurred mostly in small neurons with high

input resistances that were more prone to spontaneous bistability in general, such as this GABAergic neuron (Figure 4.37) and another one below E_{Cl} (Fig. 4.36). This scenario may be physiological when bistable cells are resting in a down state.

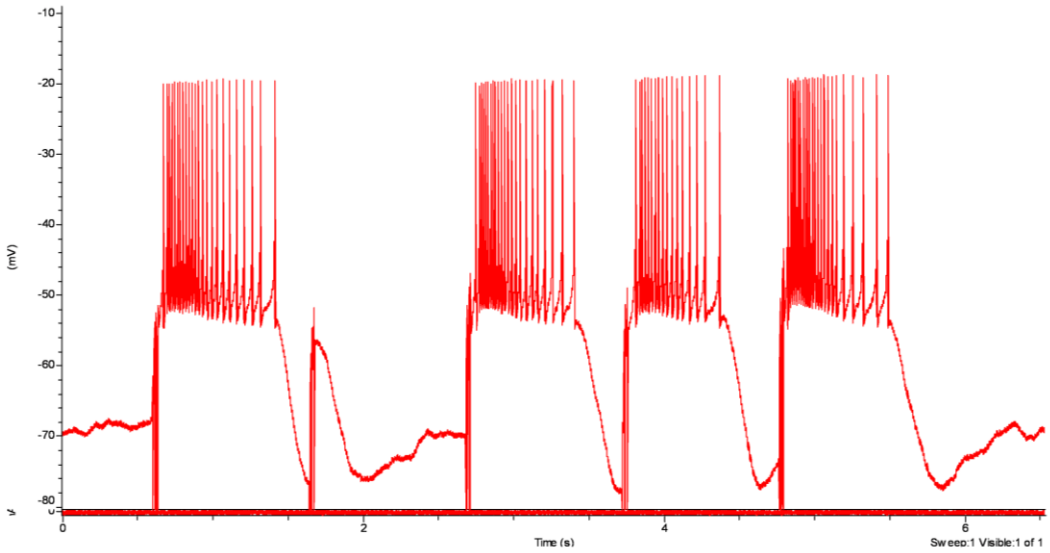

Figure 4.36. (above) GABAergic (GAD67+ and characteristic firing) DCN neuron responds to eIPSPs elicited by short trains of Purkinje cell axon stimulation from a hyperpolarized potential with bistable shifts to an up state lasting nearly one second. Pipette is blocked causing a high access resistance which filters the spike amplitude in this case.

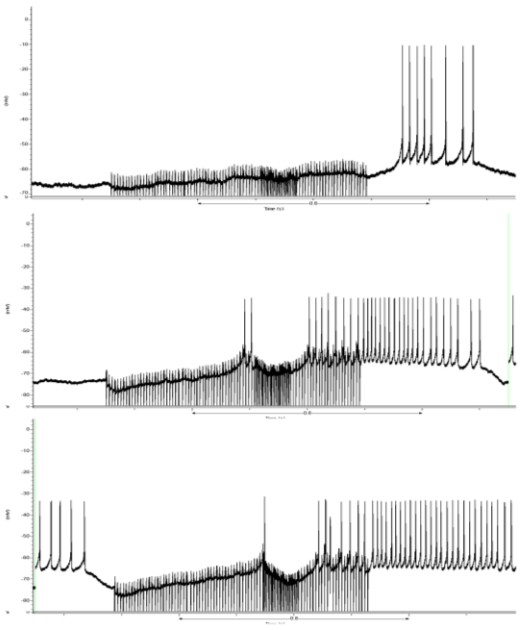

Figure 4.37. (right) Another GABAergic (GAD67+ and characteristic firing) DCN neuron responds to IPSPs elicited by short trains of Purkinje cell axon stimulation from a hyperpolarized potential with bistable shifts to an up state. This neuron exhibited

frequent bistability. Pipette is blocked causing a high access resistance which filters the spike amplitude in this case.

When the null frequency stimulation protocol was used with wildtype or +/-;-/- slices (no comparable pair of wildtype recordings was available at the two frequencies) overall inhibition was decreased as evidenced by more spiking during the trains. Whether Purkinje cell output is synchronized or asynchronous the net effect of a tendency toward a reduced simple spike frequency without Kv3.3 should then be to decrease inhibition of large, glutamatergic DCN neurons.

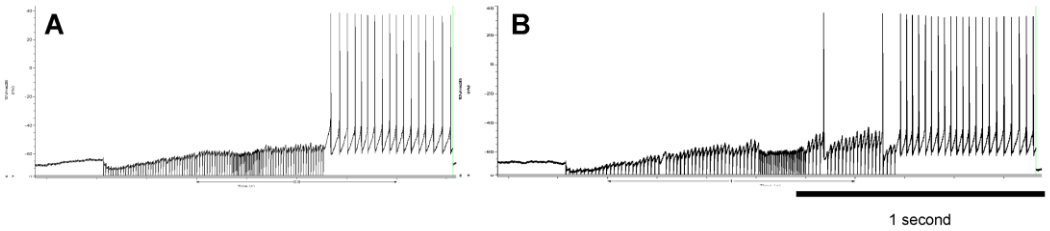

Figure 4.38. Comparable recordings of a DCN neuron responding to Purkinje cell stimulation at the frequency characteristic of wildtype or mice lacking Kv3.3 in Purkinje cells. Slices are from a +/-;-/- mouse. Just decreasing the frequency is sufficient to decrease the efficacy of inhibition by Purkinje cels to oppose the rebound depolarization it simultaneously fosters. That this is a slice that lacks Kv3.3 in Purkinje cells additionally indicates that frequency likely contributes to altered inhibition (***A***) Wildtype stimulation frequency. (***B***) *Kcnc3*-null Purkinje cell stimulation frequency. Note that null protocol takes longer because the frequency is lower yet the total number of stimuli is the same.

It remains unclear however whether overall inhibition of DCN neurons by Purkinje neurons during tonic spiking is increased or decreased at a given frequency. If synaptic depression is indeed enhanced in mutants lacking Kv3.3 in Purkinje neurons then neither would simply be true, for, initially, inhibitory drive would be greater due to more GABA release, whereas at steady state inhibition would weaken due to greater steady state depression. Further complicating this analysis is the inability to control how many axons are activated by the stimulation using intracellular recordings. Using extracellular recordings, a fiber volley directly proportional to the number of stimulated axons can be used to

normalize postsynaptic field responses to in order to remove this variable, even in disordered, non-laminar neural tissues (Dr. Donald Cooper, personal communication)[5]. IPSPs however cannot be observed with this method, only spikes. A very large number of these technically-challenging intracellular recordings would be needed to detect a difference in IPSP amplitude on average keeping stimulation intensities the same. Comparing a limited number of recordings all I could discern was that the diminution of inhibition transpired more quickly during trains in mice lacking Kv3.3. If true, it would be consonant with the anticipated effect of greater steady state depression and faster recruitment of the rebound depolarization by initially stronger inhibition.

Though it remains inconclusive whether tonic inhibition is altered when Purkinje neurons lack Kv3.3, I did reveal that the changes in spikelets are unlikely to have an impact on DCN neurons whereas the extended pause following the complex spike could. It may be quite clear that decreasing the frequency of input from Purkinje cells between null and wildtype frequencies decreases inhibition of the DCN, however if DCN neurons compensate for this in null mice by increased postsynaptic sensitivity to GABA it may be inconsequential.

The intrinsic firing data suggested that Kv3.3 and Kv3.1 are largely functionally-redundant in the DCN and that there is some haploinsufficiency when one Kv3.1 allele is lost when neurons evidently rely on Kv3.1 for fast repolarization. If we assume all Kv3 subunits are capable of repolarizing spikes with the same agility as Kv3.1 and Kv3.3, we would expect that Kv3.2 and Kv3.4 are absent in DCN neurons. If not, it is interesting that these subunits do not complement the function of Kv3.1 in -/-;-/- and *Kcnc3*-null mice lacking a *Kcnc1* allele. Previous expression studies suggested Kv3.2 was present in DCN neurons but did not determine which type(s). Meanwhile Kv3.4 protein is

[5] Typically, field recordings are performed in orderly, laminar tissues such as the hippocampus where potentials summate rather than cancel each other because the dipoles are aligned. Also neurons with long, apical dendrites produce more robust dipoles.

sometimes expressed where the mRNA is barely detectable. I therefore next examined co-expression of channel subunits in DCN neurons.

4.4. REDUNDANT EXPRESSION OF KV3 CHANNELS IN CEREBELLAR NEURONAL CELL TYPES

Understanding what neuronal cell types might account for the phenotypes seen with *Kcnc* subunit gene ablation calls for an assessment of the potential for functional redundancy at the anatomical and cellular levels. When two or more subunits are expressed in the same subcellular compartment, potential for functional redundancy exists. Co-expression of Kv3 subunits without functional redundancy is of interest regarding the respective functions of the individual genes for this bespeaks of non-overlapping roles. Though several studies have explored Kv3 subunit distributions in the cerebellum, as discussed in the introduction (see section 1.4) unanswered questions remained. For these reasons, I undertook some anatomical work with extensive technical assistance from Mitali Bose to take a closer look at the co-expression of the four Kv3 subunits in cerebellar neurons.

I availed myself of commercial antibodies that are either “pan” antibodies against all splice variants or just one. For Kv3.1, I used an anti-Kv3.1b antibody and for Kv3.3 I used an anti-Kv3.3b antibody, both reacting with the variable C termini of their respective targets. Antibodies I used for Kv3.2 and Kv3.4 bind to all subfamily members via the N terminus which is not subject to alternative splicing, except where otherwise specified. All antibodies were assessed for specificity using null-mutant tissue or preadsorption with antigen. The stranded appearance of some cells was likely due to light fixation used to preserve eGFP fluorescence for detection in the transgenics and I used light fixation as a general protocol.

Figure 4.39. Kv3.2 is not detected in wildtype cerebellar cortex. (***A***) Kv3.2. (***B***) GAD67, which marks Purkinje cells. (***C***) SMI-32, which marks Purkinje cells. (***D***) Overlay of A-C.

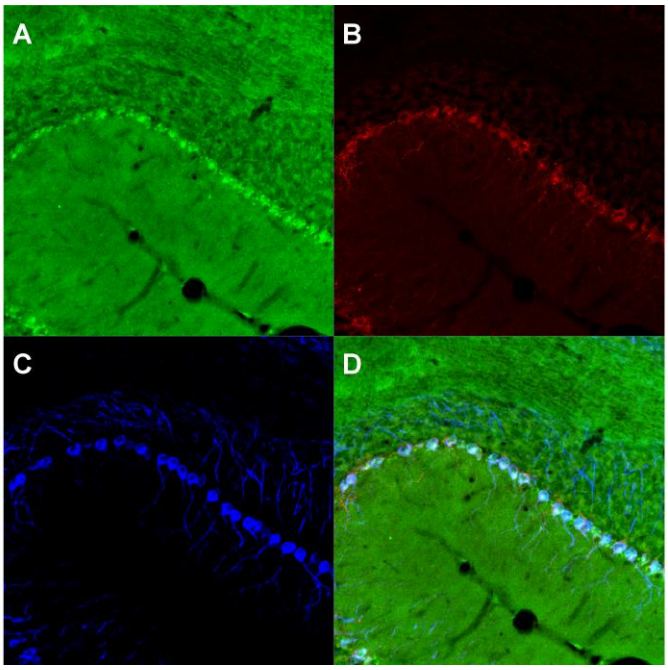

4.4.1. Cerebellar Cortex

Because our understanding of Kv3 subunit expression in fast-spiking inhibitory interneurons in the cerebellar cortex remained very sketchy and I had stained cerebellar sections at hand I also evaluated expression in the cortex.

4.4.1.1. Somata and Axons of Purkinje Neurons

The only Kv3 channel subunits detected in Purkinje cells to date at the protein level are Kv3.3b and Kv3.4. In agreement with these results, I did not detect Kv3.1b (data not shown) or Kv3.2 in Purkinje cells above background[6] (Fig. 4.39), where fluorescence did not differ from null-mutant or controls pre-adsorbed with antigenic peptide, respectively. Kv3.3b was co-localized with Kv3.4 in Purkinje cells at the cellular level using a monoclonal Kv3.4 antibody to the C terminus that may only

[6] It should emphasized that negative control images and images lacking the antigen in all cells were acquired according to the same algorithm as those with the antigen but not at the same absolute settings, which are virtually impossible to accurately recapitulate between sections using confocal microscopy. In all images the full dynamic range was used. For negative controls and tissue lacking the antigen this entails setting the strongest signal just below saturation. Consequently the background is higher. What is of significance is the relative difference between putative signals and background, not the absolute level.

recognize one splice variant (data not shown). The distributions diverged at the subcellular level such that Kv3.4 was spread throughout the dendritic tree in curious, almost punctate segments (see left, molecular layer, Fig. 4.40A, B and C, as well as F throughout in the molecular layer) and minimally at the soma whereas Kv3.3b was expressed predominantly in the soma and proximal dendrite, becoming very low but detectable in distal dendrites marked by calbindin as seen in wildtype (Fig. 4.40B, D, I & K) and more clearly in rescue mice lacking expression in granule cell somata and parallel fibers (Fig. 4.2,

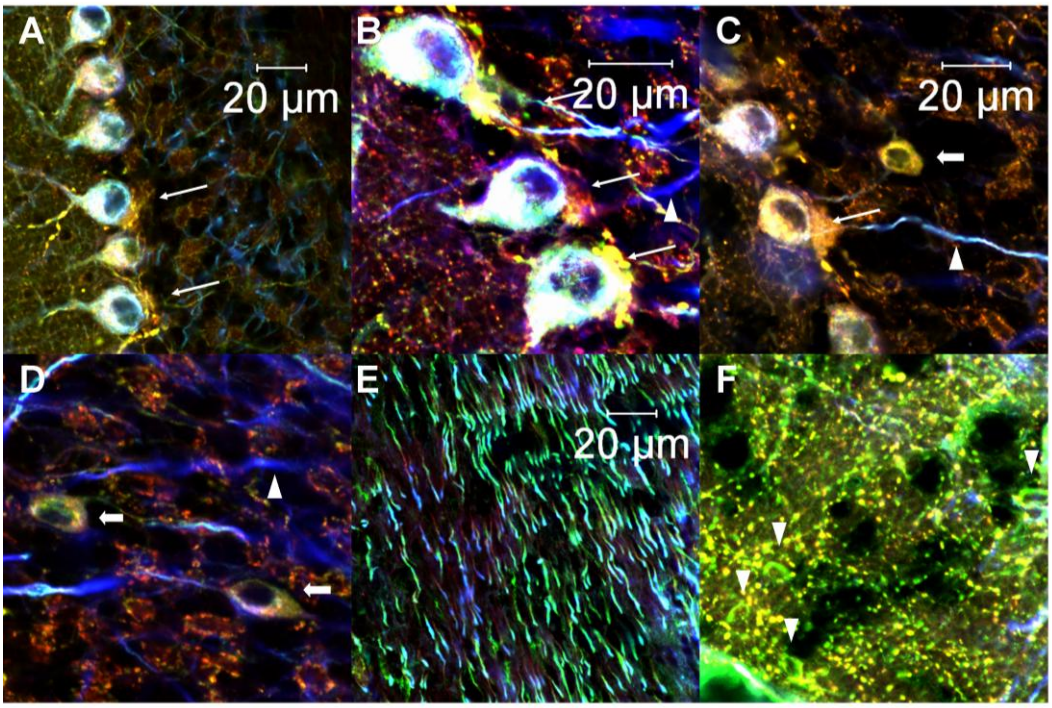

Figure 4.40. (above) Expression of Kv3.4 in Purkinje neurons, basket cell terminals, putative stellate and Golgi cells in wildtype cerebellar cortex. In all panels Kv3.4 is shown in green, SMI-32 in blue and GAD67 in red. Pinceauxs are indicated by arrows; putative Golgi cells by block arrows; putative stellate cells by downward arrowheads; Purkinje cell axons by upward arrowheads. Scale in panel F is similar to A; D is similar to B. (***A***) Purkinje cells with punctate Kv3.4 staining in the dendrites with pinceaux structures around axon hillocks. (***B***) Same as A. Axon shown with arrowhead. (***C***) Same as A and B except more of granule layer shown with putative Kv3.4+ Golgi cell indicated by block arrow. (***D***) More putative Kv3.4+ Golgi cells in the granule layer indicated by block arrows. Punctate Kv3.4 staining is likely derived from Golgi cell terminals in synaptic

glomeruli also composed of mossy fibers and granule cell dendrites. A Purkinje cell axon is indicated by the arrowhead. (***E***) Purkinje cell axons in the cortical white matter marked by GAD67 and SMI-32 express Kv3.4. (***F***) Putative stellate cells indicated by arrowheads in the molecular layer express Kv3.4 primarily in the somatic plasma membrane.

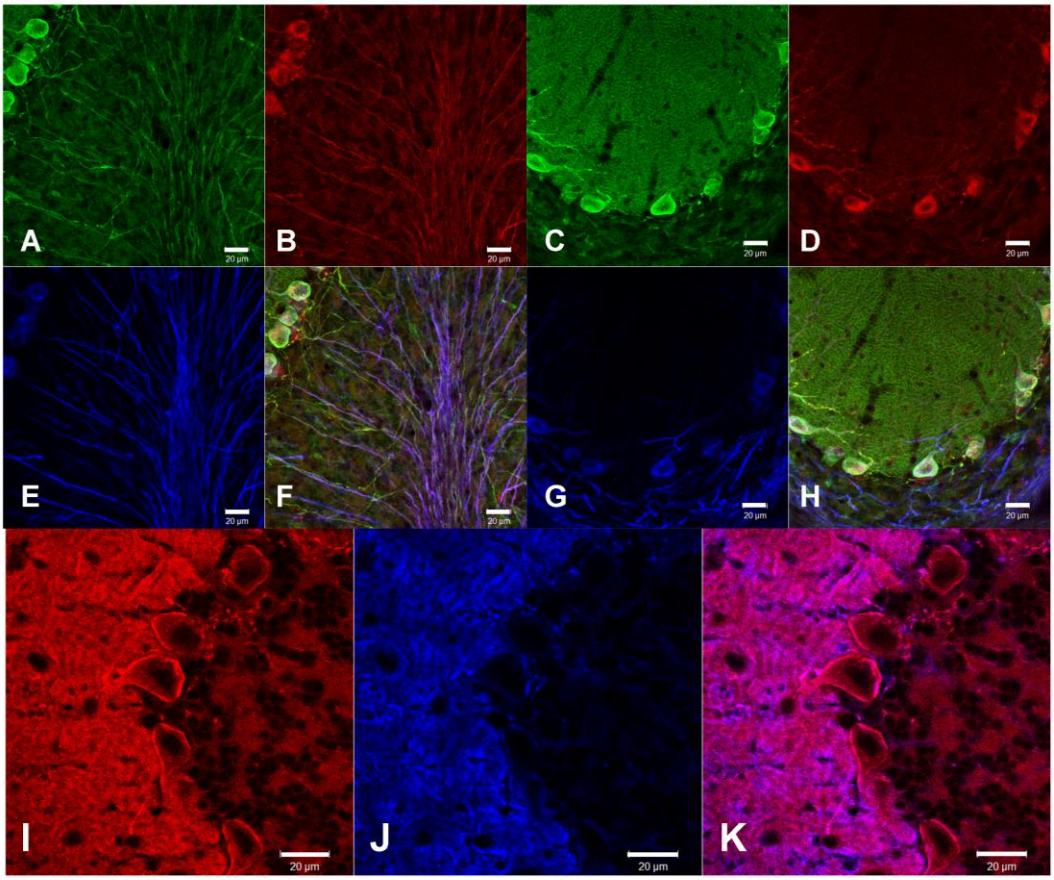

Figure 4.41. (above) Expression of Kv3.3b in the wildtype cerebellar cortex. Scale bars are 20 µm. A-H: Kv3.3b is visualized with green fluorescence, GAD67 with red and SMI-32 with blue. F and H are overlays. Note the clear lack of Kv3.3b in the pinceaux brightly stained with GAD67. (***A***) Kv3.3b. (***B***) GAD67. (***C***) Kv3.3b. (***D***) GAD67. (***E***) SMI-32. (***F***) Overlay of A, B & E. (***G***) SMI-32. (***H***) Overlay of C, D & G. I-K: Kv3.3b is red and calbindin blue. K is overlay. Kv3.3b is enriched in the Purkinje cell membrane. Parallel fibers account for some of the staining the the molecular layer. In Purkinje cells calbindin is also enriched near the membrane. (***I***) Kv3.3b. (***J***) Calbindin. (***K***) Overlay of I & J.

Novel observations that have not been noted thus far include the following. Kv3.3b can be seen in presumed terminal boutons of recurrent collaterals of

Purkinje neurons distinguished by calbindin just below the Purkinje cell layer manifest as sparse punctate labeling (Fig. 4.41I-J). Both subunits are distributed evenly in Purkinje cell axons (Figs. 4.40E and 4.41A, F). In the DCN, Kv3.4, as has been described for Kv3.3b, is concentrated at terminals on at least large neurons (Fig. 4.42A-B). The data indicate that Kv3.4 completely overlaps in its distribution with Kv3.3b in axons.

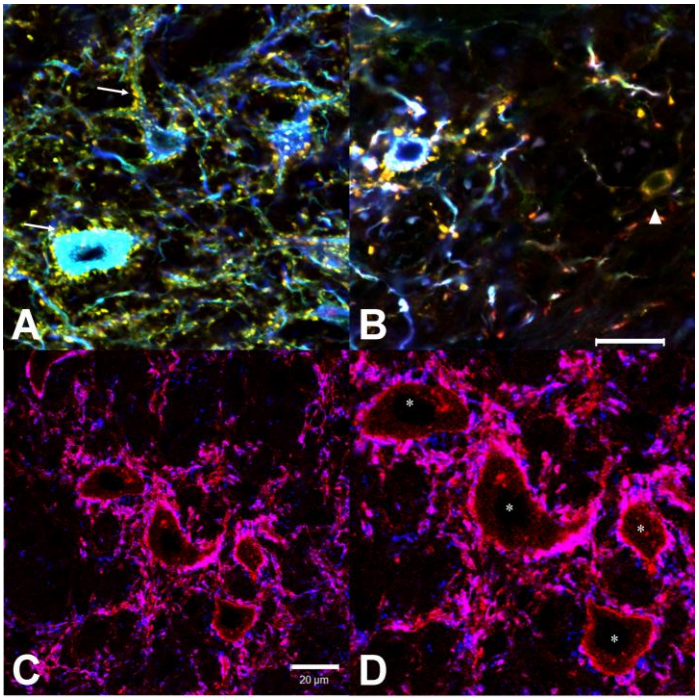

4.4.1.2. Granule Cells

Granule cells and parallel fibers had Kv3.1b and Kv3.3b expression. Kv3.2 (Figure 4.38) and Kv3.4 (Figure 4.40A-D) were clearly absent.

4.4.1.3. Basket Cells

Basket cells are known to be fast-spiking interneurons and spike brevity is sensitive to 1

Figure 4.42. Expression of Kv3.3 and Kv3.4 in Purkinje cell terminals in the DCN of wildtype mice. (***A-B***) Kv3.4 is stained green, GAD67 red and SMI-32 blue. Arrows indicate Kv3.4+ Purkinje cell terminals marked by GAD67 and SMI-32 on large DCN neurons and their proximal dendrites. Arrowhead indicates small Kv3.4+ GABAergic interneuron. (***C-D***) Kv3.3b is detected as red immunofluorescence and calbindin as blue. Large DCN neurons are indicated by asterisks and studded with numerous Kv3.3+/calbindin+ terminals, where Kv3.3b can be clearly seen enriched in the terminal membrane. D is a zoomed image of C.

TEA, however it was unclear whether Kv3.3 might contribute to fast repolarization in these cells. GAD67 immunofluorescence clearly demarcates cerebellar pinceaux formed by basket cells onto the axon hillocks of Purkinje

cells. Kv3.3b was absent from these structures. This does not exclude the possibility of expression of the low-abundance splice variants or restriction of expression to subcellular loci other than axonal plexes, but suggests that Kv3.3 most likely does not play a role in these inhibitory interneurons. I found no signal above background for Kv3.2, and Kv3.1b expression was difficult to conclusively exclude given the immersion in a sea of granule cells expressing this subunit. Kv3.4 immunofluorescence, however, as reported previously, was intense in the pinceauxs (Fig. 4.40A-C). Unless splice variants other than those detected by the antibodies are present, these data together suggest that Kv3.4 is solely responsible for Kv3 current in basket cells.

4.4.1.4. Stellate Cells

Like basket cells, stellate cells are fast-spiking interneurons. Although Kv3.3b is present in parallel fibers and Purkinje cell dendrites, sections were evidently thin enough to detect holes were stellate cells are located in sections treated with Kv3.3b antibody (Fig. 4.41C, I, K) suggestive of an absence of Kv3.3b when viewed against the contrast of another antigen in Purkinje cell dendrites, which allows one to exclude labeling potentially being circumscribed to a thin halo at the membrane. Similarly, Kv3.1b was excluded. There was no greater Kv3.2 signal in the vicinity of stellate cells above background. Kv3.4 again by contrast appeared to be present albeit at a low level (Fig. 4.40F, at downward arrowheads). That it was enriched in the membrane argues in favor of it being bona fide staining, although Kv3 channels are not universally overtly enriched in the membrane. Other types of interneurons could account for this signal however stellate cells are by far the most numerous. Thus Kv3.3 likely does not contribute to fast repolarization in cerebellar cortical interneurons in the molecular layer either, whereas Kv3.4 is present as in basket cells at least in a subpopulation of interneurons that most likely represents stellate cells.

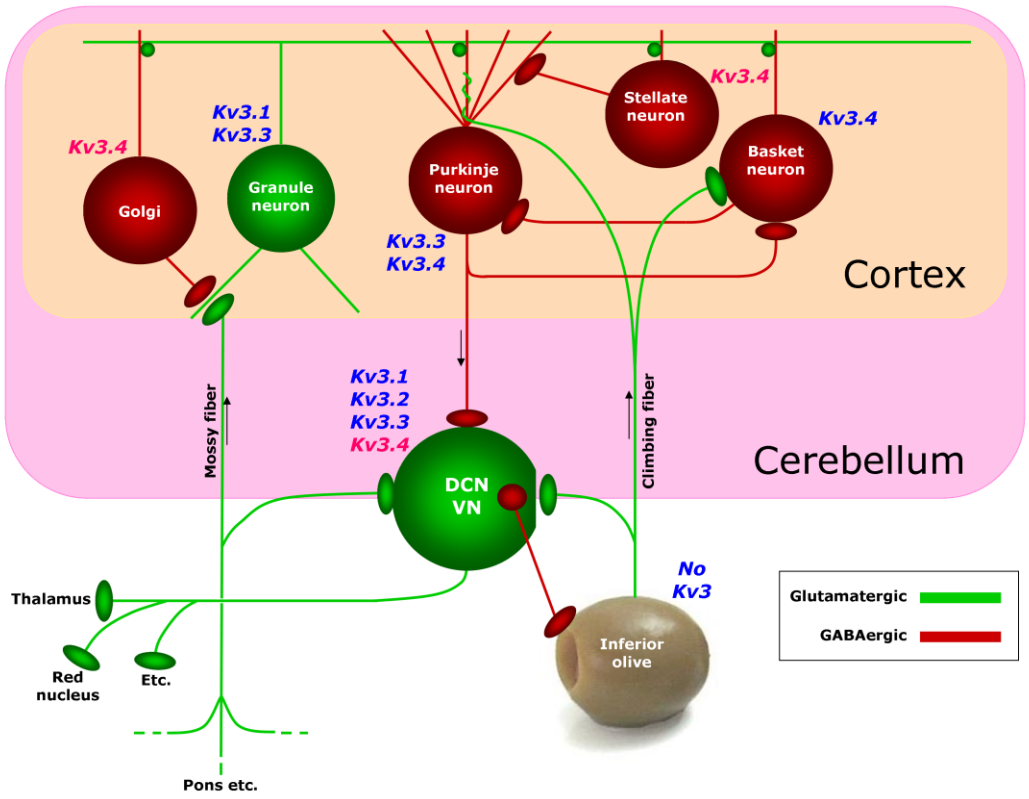

Figure 4.43. Revised diagram of cerebellar circuitry incorporating new information gleaned in this study. Not only was Kv3.4 detected in cortical interneurons but also the co-expression of all subunits in large DCN neurons was evidenced. Formerly the extent of co-expression and types of neurons wherein it occurred was unclear.

4.4.1.5. Golgi Cells

Although Kv3.4 was absent from granule cell somata, what could be seen were tiny puncta that, when viewed with perfect resolution by eye under epifluorescence, were configured as though they were part of the glomeruli that surround endings of granule cell and co-labeled with GAD67 (Fig. 4.40A-D, most apparent in D). Indeed a number of putative Golgi cells known to make such inhibitory contacts with granule cells were unequivocally labeled with anti-Kv3.4 antibody along with GAD67 (Fig. 4.40C, D, block arrows). No other subunit was detected in putative Golgi cells.

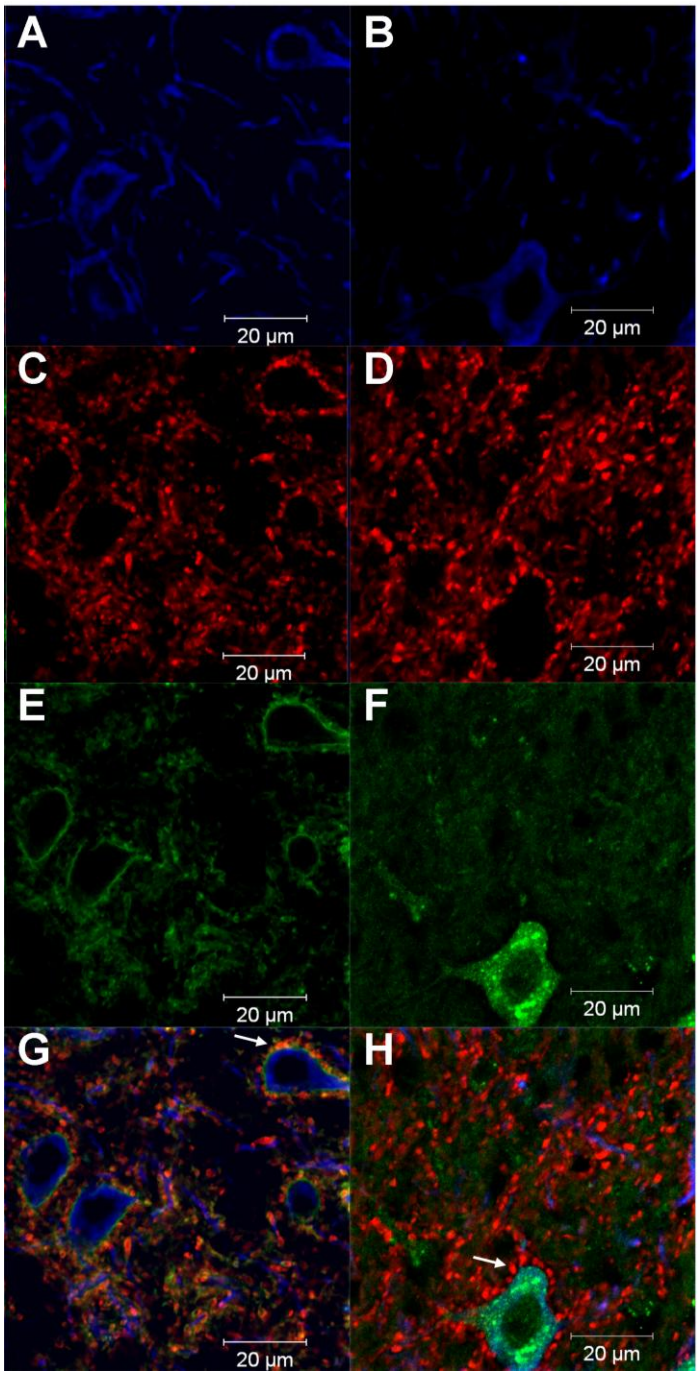

Figure 4.44. Kv3.3b and Kv3.2 are expressed in large, glutamatergic DCN neurons of wildtype mice. (***A-B***) SMI-32 in blue. (***C-D***) GAD67 in red. (***E***) Kv3.3b. (***F***) Kv3.2. Arrows indicate GABAergic presynaptic terminals largely derived from Purkinje cells. Kv3.3b localizes to terminals but not Kv3.2, which is absent in Purkinje cells. (***G-H***) overlays of the above panels.

4.4.2. DCN Neurons

Where host species compatibility allowed, subunit-specific antibodies were used to assess primarily co-expression of Kv3 subunits in DCN neurons to determine whether an anatomical, molecular basis exists for functional redundancy. Previous work found both Kv3.1 and Kv3.3 expression in large DCN neurons but had not directly demonstrated co-expression. I focused principally on large neurons.

GAD67 and SMI-32 were used to distinguish small GABAergic and large DCN neurons respectively however many small neurons are non-GABAergic. In

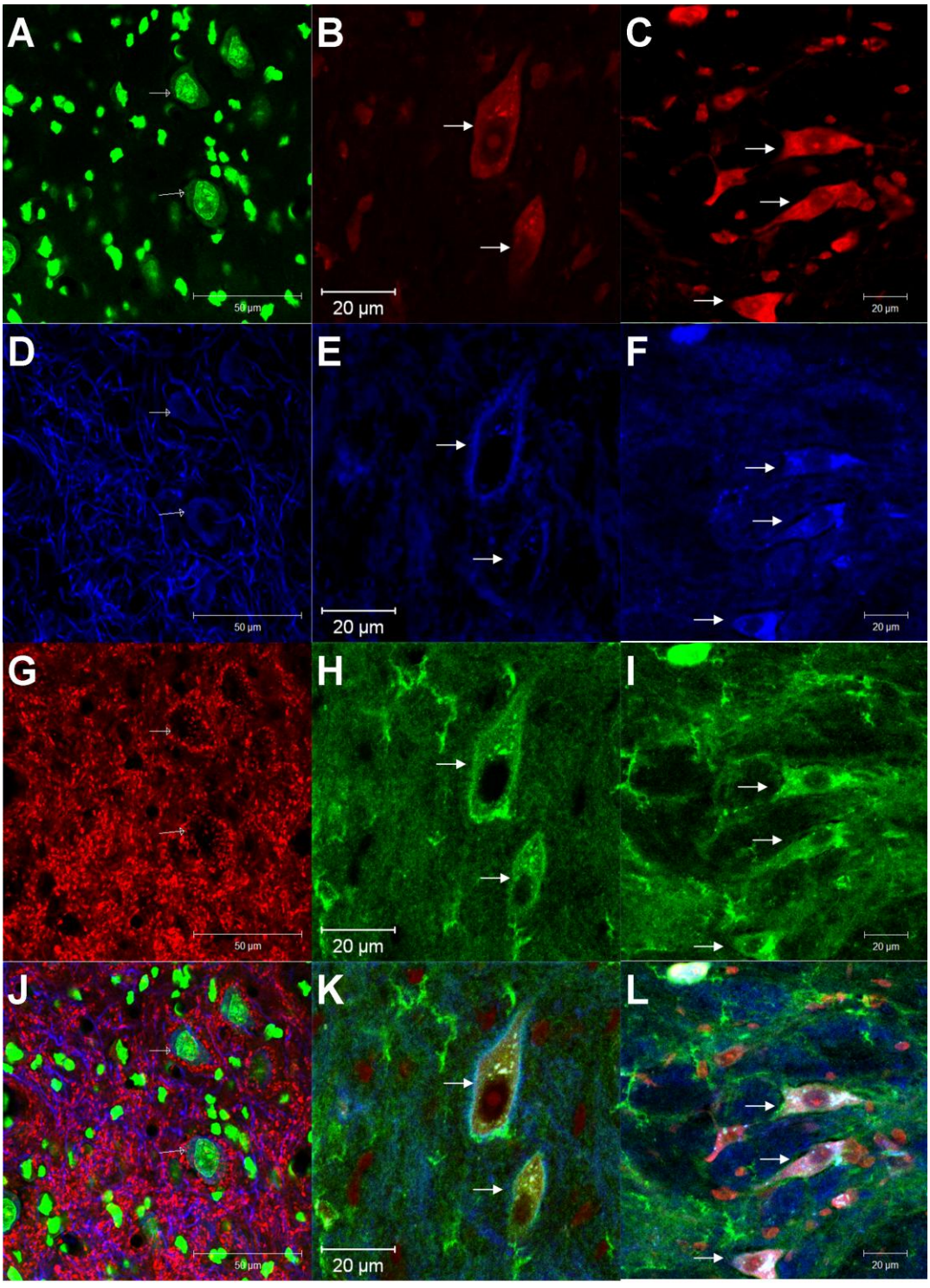
A
B
C
D
E
F
G
H
I
J
K
L
50 µm
20 µm

Figure 4.45 (above) Kv3.1b and Kv3.3b consistently are co-expressed by large glutamatergic neurons of wildtype mice. Column A, D, G, J shows that large SMI-32+ neurons have a characteristic appearance using Nissl staining (scale bars 50 µm). (***A***) Green fluorescent Nissl. (***D***) SMI-32 in blue. (***G***) GAD67 in red. (***J***) Overlay of A, D & G. Column B, E, H, K shows co-expression of Kv3.1b and Kv3.3b in large neurons and is corroborated by the experiment in column C, F, I, L using different antibodies. (***B, C***) Red Nissl. (***E, F***) Kv3.3b in blue. (***H, I***) Kv3.1b in green. (***K***) Overlay of B, E & H. (***L***) Overlay of C, F & I.

part to visualize these as well some sections were treated with fluorescent Nissl stain (Fig. 4.45A, D, G, J).

4.4.2.1. Large Glutamatergic Neurons

The large, glutamatergic neurons were identified by SMI-32 expression (Fig. 4.45A, D). Kv3.3b was universally expressed in such neurons and never in the small neurons sampled in this study (Fig. 4.44A, C, E, G). Kv3.3b was present in Purkinje-cell terminals marked by calbindin (Fig. 4.42C, D). Kv3.1b and Kv3.3b were co-expressed in all large neurons observed using fluorescent Nissl staining (Fig. 4.45K, L). All neurons that expressed Kv3.1b also expressed Kv3.3b. This result was confirmed with an independent pair of antibodies (Fig. 4.45L). Kv3.3b seemed to be relatively more enriched in the membrane than Kv3.1b using the Kv3.3b antibody with a greater signal-to-noise ratio. By deduction, therefore, because Kv3.3b is present in all large glutamatergic neurons Kv3.1b was present in all large, glutamatergic neurons. Unless other splice variants display a different expression pattern, an anatomical basis for functional redundancy does exist in large DCN neurons between Kv3.1 and Kv3.3. Kv3.3b seemed to be relatively more enriched in the membrane than Kv3.1b using the higher-quality Kv3.3b antibody.

In contrast to the aforementioned subunits, Kv3.2 was seen in essentially all large DCN neurons distributed evenly over the cytoplasm (Fig. 4.44H). All large neurons examined had Kv3.2 expression. Kv3.1b and Kv3.2 were in turn always co-expressed in large neurons (Fig. 4.46J). Kv3.4 was similarly expressed (Fig. 4.46K), and seemingly absent in small neurons (Fig 4.46K).

Finally, Kv3.3 and Kv3.4 could be seen together in large neurons (Fig. 4.46L). Together the expression data suggest that there is a potential for functional redundancy between all Kv3 subunits in large, glutamatergic DCN neurons marked by SMI-32.

4.4.2.2. Small Neurons

To my surprise, I did not observe GAD67+ DCN neurons among the sections I sampled despite vivid Purkinje cell terminal and soma labeling deep into the sections, though I did identify some in the course of recovering Alexafluor-filled cells from patch-clamp recordings. Molineux et al., 2006 did note that GAD67+ cells were rarely encountered at least in the medial nucleus from which parasagittal slices are obtained for recordings.

I never found Kv3 subunits in unequivocal small neurons lacking SMI-32 other than Kv3.4 (Fig. 4.42B). The theme that emerged from my data was expression in cerebellar neurons of potentially all Kv3 subunits in projection neurons, most prominently Kv3.3 and Kv3.1, and in interneurons Kv3.4. The fastest-spiking neurons invariably express Kv3.3 protein or a combination of Kv3.3 and Kv3.1. In the cerebellum small DCN neurons and cortical interneurons fire somewhat slower and seem to either exclusively express low levels of Kv3.4 possibly in combination with splice variants of Kv3.1 and Kv3.3, for which I only explored expression of the abundant b variants.

Figure 4.46 (below) Kv3.1b and Kv3.2 (column A, D, G & J), Kv3.1b and Kv3.4 (column B, E, H & K) as well as Kv3.3b and Kv3.4 (column C, F, I & L) all are co-expressed in large DCN neurons of wildtype mice. It is likely that these are the glutamatergic neurons because of the strong correlation that exists and distinctive Nissl staining that correlates well with SMI-32 staining in Figure 4.43J. Large neurons are indicated by arrows. (***A, B, C***) Red Nissl. (***D***) Kv3.2 in blue. (***E***) Kv3.4 in blue. (***F***) Kv3.4 in green. (***G***) Kv3.1b in green. (***H***) Kv3.1b in green. (***I***) is Kv3.3 in blue. (***J, K, L***) Overlays of the panels above. The Kv3.4 monoclonal antibody used for the co-expression experiments due to species constraints is weaker than that used in Figures 4.40 and 4.42 and binds the C terminus subject to splice variation.

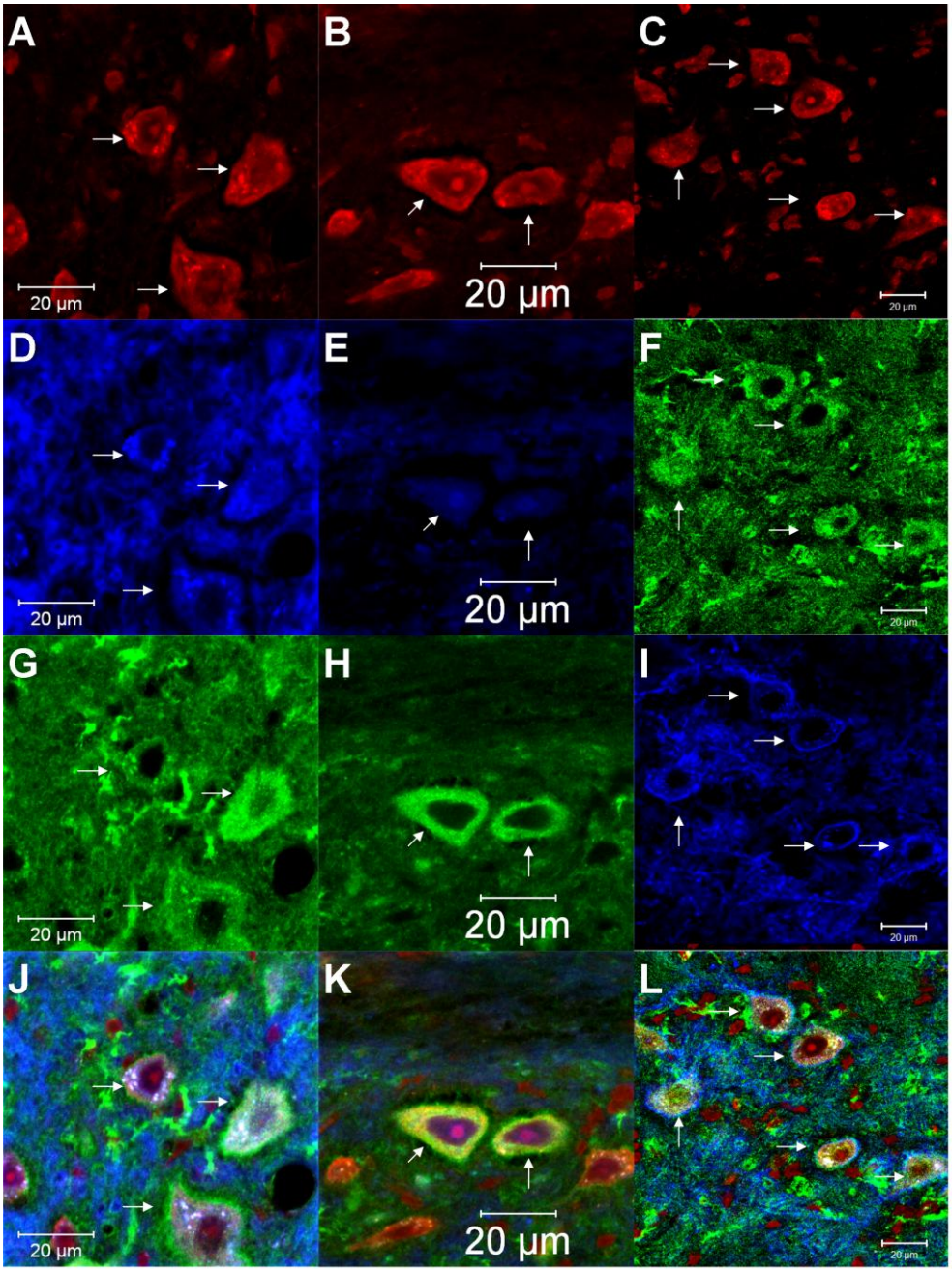
A
B
C
D
E
F
G
H
I
J
K
L
20 µm

CHAPTER FIVE
Conclusions and Recommendations

The results of the behavioral, electrophysiological and anatomical, molecular investigations support the main hypothesis that Kv3.3 expression in Purkinje cells is involved in motor coordination and can account for the ataxic phenotype of +/+;-/- mice. The mild ataxia specifically takes the form of hypermetria sparing gait. In addition to spike broadening and decelerated simple spiking described before I found that complex spikes are also markedly altered in mice lacking *Kcnc3*, while loss of *Kcnc1* alleles significantly affects action potentials of DCN neurons in parallel with coordination, yielding more marked phenotypes encompassing gait ataxia. Further, Kv3.1 and Kv3.3 are largely functionally redundant in large projection neurons in the DCN, however despite co-expression in these neurons, Kv3.2 and Kv3.4 by contrast do not complement the loss of Kv3.1 and Kv3.3.

While the behavioral rescue strongly implicates Purkinje cells as a locus where Kv3.3 exerts its effect on motor coordination, I formally show only that expression of Kv3.3 only in Purkinje cells is sufficient for normal motor coordination. I do not imply that it is necessary, although the rescue paradigm suggests expression in other cell-types is unnecessary. It could be that in neural circuitry single weak links where the channel is absent are tolerated such that loss of the channel in any one cell type would not yield a phenotype. Expression may be dynamically necessary, depending on the context of functioning of the rest of the network. Future work then will have to test necessity by ablating *Kcnc3* specifically in Purkinje cells perhaps with an L7tTA-promoter driven cre recombinase line and a floxed *Kcnc3* allele, or by using a dominant negative such as the one I created in the lab by site-directed mutagenesis prior to this thesis project in a transgenic approach analogous to that employed here for the rescue. The dominant negative however would also eliminate Kv3.4 current as well. Necessity might only be revealed for the reasons mentioned above however

when the channel is ablated in both granule and Purkinje cells, where a negative result ablating in just one cell type could be misleading.

5.1 RESTORATION OF KV3.3 FUNCTION IN PURKINJE CELLS CORRECTS HYPERMETRIA IN KCNC3-NULL MICE BUT NOT GAIT ABNORMALITIES THAT APPEAR AS KCNC1 ALLELES ARE ADDITIONALLY LOST

5.1.1. Expression of Kv3.3 Channels in Purkinje Cells Is Involved in Coordination of Movement Velocity

Subtle but significant deficits in motor performance of unknown origin had been described for +/+;-/- mice that became worse upon additional loss of a *Kcnc1* allele and severe when both *Kcnc1* alleles were lost. The deficits encompassed normal ambulation on a force plate actometer, measured as lateral deviation, and traversal of narrow beams without slips or falls. Motor skill learning was unaffected, as confirmed on the rotarod. Here, through restoring Kv3.3 expression exclusively in Purkinje cells, I was able to demonstrate a full recovery of function in +/+;-/- mice, and a partial rescue in +/-;-/- mice, establishing Kv3.3 function in this cell type as important for motor coordination and in the null phenotype. Other phenotypes present, including twitching, were not rescued arguing that expression in Purkinje cells was specifically related to coordination and that twitching did not interfere with beam performance. Testing this main hypothesis regarding function in Purkinje cells represented a significant step forward because then I then knew where to characterize electrophysiological changes that might explain how Kv3.3 expression supports motor coordination, bridging the gap between gene function at the molecular level to behavior.

5.1.2. Kv3.3b Delivered by A Transgenic Line Is Sufficient to Rescue Behavior

Selectively replacing the Kv3.3b splice variant intriguingly sufficed to rescue motor coordination completely in +/+;-/- mice despite the existence of several other splice variants, some of which even affect the coding region. In one respect it is not surprising. Kv3.3b is the most abundant variant in terms of mRNA level. Nonetheless it begs the question of what the function of the others might be. Evolutionarily speaking, it is possible that the function of these variants is redundant with Kv3.4 which is still expressed in null mice or they exist by chance, not having yet evolved a function.

It is also interesting that the level of expression in rescue mice did not either perturb cell function due to excess levels or fail to rescue function due to insufficient levels in both the 396 and 313 independent lines. The high-molecular weight bands on the Western blot and intensity of immunofluorescence when rescue mice were compared to wildtype mice suggested overexpression[7]. Moreover mean values for the spike width and spontaneous frequency alluded to a possible subtle gain-of-function but differences were not significant. This observation is of interest in terms of how ion channels are regulated. Limited essential docking sites for functional insertion at the plasma membrane or auxiliary subunits or posttranslational modification might delimit the amount of actual current regardless of the level of translation. Injection of simulated Kv3 current from a point source at the soma in fast-spiking interneurons was capable of rescuing fast repolarization during blockade of channels by TEA and excess Kv3 current initially accelerated but then blocked firing beyond a certain magnitude (Lien and Jonas, 2003). With genetic restoration throughout the cell either I was lucky with the level produced by the two lines or Purkinje cells are able to put a ceiling on Kv3 current.

Another noteworthy observation was that the 313 line, in spite of some mosaicism and variability in its extent, nevertheless rescued behavior. The

[7] If excess protein is retained in the endoplasmic reticulum, glycosylation may not be properly removed, resulting in an increase in molecular weight and corresponding upward shift on a gel.

rescue is not inconsistent with reports that rodents must lose >90% of Purkinje cells before there is any sign of motor impairment, at least on the rotarod (Martin, Goldowitz and Mittleman, 2003). Innervation of individual DCN neurons by multiple Purkinje cells is consonant with this, for as long as DCN neurons are sufficiently plastic to modulate responsiveness to inhibition, synapses made by surviving Purkinje cells might conceivably suffice. A rescue inspite of mosaicism also suggests the null mice lack firing properties necessary for normal function rather than that the abnormal firing actively disrupts normal function. Clearly, that the +/+;-/- mice were by all accounts fully rescued indicates that the mosaicism does not confound but rather strengthens my conclusions, for the rescue is evident even without 100% of Purkinje cells being restored. If only a few Purkinje cells expressed the transgene it would suggest however the rescue is related to an insertional mutation or background gene linked to the transgene insertion site. Though I did not determine the chromosomal location of the insertions, that both the 313 and 396 lines produced a rescue argues against this.

5.1.3. Hypermetria Is the Deficit Rescued in *Kcnc3*-Null Mice

The subtle phenotype of +/+;-/- mice afforded an invaluable opportunity to correlate specific changes in action potentials related to Kv3 expression, and in doing so, Purkinje cell firing, to a specific aspect of motor behavior. Although the effects of loss of Kv3.3 on Purkinje cell spiking are several-fold, because high-frequency spiking is most acutely affected the behavioral deficits might at least in large part reflect the role of complex spikes. Regardless of what specific aspect of Purkinje cell output is involved, observing what facet of motor coordination disappears first with a subtle alteration in spiking might uncover the main essence of the function of Purkinje cell output along with that of Kv3.3 in these cells. Given the above, I set out to systematically determine the specific origin of the deficits.

Ataxia is commonly thought of in the sense of gait ataxia. Investigators in the past have casually referred to ataxia presumably reflected in increased lateral deviation as abnormal gait. Here I tested explicitly whether gait was altered and it was actually normal in +/+;-/- mice using both a treadmill at high speed and the self-paced footprint test. Gait did show one type of abnormality in +/-;-/- mice, paw discordance, however these mice were only partially rescued on the plate and 1-cm beam. Moreover the paw discordance was not rescued by replacing Kv3.3b in Purkinje cells. Another explanation for increased lateral deviation on the force plate could be excessive force applied during steps side-to-side because the mouse is subtly tipping over during ambulation to an extent invisible to the eye due to defective maintenance of posture and balance. To directly test this, I conducted a pilot experiment using a novel test, the rocking ball, which incorporates an opportunity to observe swimming ability. That +/+;-/- mice were capable of performing this difficult task demanding rapid, fine postural adjustment based on vestibular and visual feedback as well as swim suggested balance and posture are intact. Although the test was pilot in nature, other more direct qualitative observations are congruent with the hypermetria hypothesis.

During swimming and on the beam, +/+;-/- mice manifested a striking tendency to make jerky kicking movements rather than exhibit smooth, coordinated acceleration and deceleration of movement with precision and finesse. Swimming and regaining of footing on the beam seemed to be impaired by this. Mice kick when trying to place their hind feet back on the beam and jerky movement would be expected to increase the chance of slipping, since mice grasp the side of the beam mostly when walking across. I also tested whether grip strength was normal and it was fully intact even in +/-;-/- mice that had worse lateral deviation and more beam slips. Taken together, the qualitative and quantitative data point to hypermetria, an abnormality prominent in cerebellar ataxia.

Other investigators suggested that beam performance might be affected by anxiety. The posture of mice was perturbed on the beam and this was

remedied by anxiolytic drugs which reduced slips (Lepicard et al., 2003). The +/+;-/- mice have not been tested for anxiety, and the cerebellum is involved in many brain functions, not just motor function. Novel environments are anxiogenic in rodents especially out in the open in bright light, as in the beam test. Indeed, often mice freeze on the beam but don't appear startled. A rescue of increased anxiety likely does not explain the results here though. Habituation likely progressively decreases anxiety on subsequent days of the beam test. The difference between null and rescue mice is not significant on individual days until the last two days, and by two-way ANOVA the rescue mice are still different from wildtypes taking all five days into account probably because of performance on day 1 chiefly which resembles that of null mice (Fig. 4.5). If increased anxiety is present in the null mice, it likely involves neuronal cell types other than Purkinje cells since poorer performance at the outset is not rescued and, importantly, one would expect improvement to be more marked at a time when anxiety is greater, unless it is a partial improvement that is only full when anxiety is diminished by habituation. Further support comes from the observation that wildtype mice are different in terms of kind rather than degree; wildtypes do not exhibit any of the jerky kicking episodes ever even on day one when they perform at their worst and are presumably most anxious over the novel test situation. This distinction was clear with the +/-;-/- mice where kicking bouts were more frequent. The reason they can be seen at all in rescue mice could stem from the fact that parallel fibers still lack Kv3.3.

The seemingly increased slipping on the training days that improves with learning and habituation in rescue and null mice could arise from a persistent lack of Kv3.3 in parallel fibers that learning eventually compensates for completely. The synapse made by parallel fibers onto Purkinje cells is highly plastic and this plasticity is thought to pertain to motor skill learning, primarily through LTD, which is normal even in -/-;-/- mice. It may be that LTD can gradually tune down this synapse to compensate for the increased glutamatergic

drive inferred from decreased paired-pulse facilitation, allowing the rescue of Purkinje cell Kv3.3 function to become evident on later test days.

Since beam performance is worse when the beam is novel another factor that may contribute is modulation. The cerebellum is innervated by monoamines such as norepinephrine which is influenced by behavioral state. Increased norepinephrine during anxiety could well alter the extent of the expression of the null phenotype at the cellular level.

5.1.4. Additional Loss of *Kcnc1* Leads to Gait Abnormalities

Kv3.1 is not expressed at the protein level in Purkinje cells but is present upstream in granule cells and downstream in large, glutamatergic DCN neurons. Interneuronal expression remains obscure but when detected appears to involve only a subclass in the DCN. In the case of parallel fibers, loss of individual *Kcnc1* alleles leads to significant but mild electrophysiological changes yet no significant behavioral changes on the beam or plate in mice solely heterozygous for *Kcnc1* or double-heterozygous mice that also lack a *Kcnc3* allele. Both beam performance and lateral deviation worsen when *Kcnc3* is absent in mice heterozygous for the *Kcnc1* allele, unmasking a haploinsufficiency effect.

Mice just lacking *Kcnc3* or heterozygous for the *Kcnc3*-null allele did not have abnormal gait, however upon additional loss of one allele of *Kcnc1, Kcnc3*-null mice exhibited paw discordance. Thus at some cellular locus, a reduced *Kcnc1* gene dosage is consequential for gait as well. The -/-;-/- mice completely lacking *Kcnc1* had by contrast all the characteristics of gait ataxia found in cerebellar ataxia. The gait aberrations are unlikely to be entirely explained by myoclonic jerks, tremors or twitches in -/-;-/- mice for the jerks, though of great magnitude, occur at a frequency lower than that necessary to account for altered gait and the other motor phenotypes do not produce deviations in paw placement of sufficient amplitude. These data suggested that *Kcnc1* is in large part functionally redundant with at least *Kcnc3* in one or several neuronal cell-types,

likely in the cerebellum or downstream in the motor circuitry. The same may be true of hypermetria but it is difficult to directly measure once gait abnormalities complicate the picture. Severe hypermetria might be capable of influencing gait pattern as well, at least paw discordance. Stride length, stance width and the relative timing of limb movement manifest in gait alternation as well as veering probably do not arise merely from jerky, hypermetric movements originating in uncoordinated movement speed, but a contribution cannot be categorically excluded.

5.2. COMPLEX SPIKES ARE ALTERED IN KCNC3-NULL MICE AND PURKINJE CELL FIRING IS RESTORED IN RESCUE MICE

The rescue of wildtype behavior highlighted Kv3.3 expression in Purkinje cells as important functionally in motor coordination. The most parsimonious explanation is that this occurs through the electrophysiological effects of the channel protein, so, with a relevant cell-type elucidated, I sought to characterize candidate electrophysiological mechanisms whereby Kv3.3 functions that could be involved in motor coordination. Previous investigations had revealed spike broadening and decelerated spontaneous firing of simple spikes in slices of +/+;-/- mice despite the co-expression of *Kcnc4* at the soma. I replicated these results and expanded our understanding by evaluating effects on high frequency firing, exploring the *F-I* relation, and eliciting climbing fiber responses. I found that complex spikes are more profoundly altered than simple spikes. The behavioral rescue was accompanied by a full restoration of Purkinje cell spiking parameters to those found in wildtype mice. In sum, I highlighted complex spikes as a potential contributor to the null phenotype, specifically hypermetria, in addition to spike broadening and slower simple spiking *in vitro.* Kv3.3 channels therefore function in regulating movement speed in Purkinje cells by supporting spike brevity and high-frequency firing, most markedly in the case of complex spikes.

5.2.1. Complex Spikes Are Altered in *Kcnc3*-Null Mice

My *in vitro,* intracellular brain slice recordings confirmed that spikes are doubled in their width at half height and that the spontaneous simple spike frequency is reduced by ~30%. Broader spikes would be expected to acutely increase synaptic depression at Purkinje cell terminals in the DCN (see section 5.4.1), as well as at synapses made by collaterals on cortical interneurons and other Purkinje cells. Inhibitory drive would increase early in a train or an acceleration of simple spiking and then decrease below that of wildtype mice after augmented depression set in. The lower frequency though would mitigate this effect since depression occurs more slowly at lower frequencies. It is very difficult to posit what the net effect might be of losing Kv3.3 *in vivo*. Parallel fibers undergo increased paired-pulse facilitation as *Kcnc3* alleles are lost, suggesting increased excitatory drive due to enhanced glutamate release onto Purkinje cells. Phasic increases in granule cell firing rate could thereby overcome the intrinsic tendency of *Kcnc3*-null Purkinje cells to fire at slower rates, driving them to perhaps fire at even higher rates. Future work should evaluate this *in vivo.*

At the resting potential and hyperpolarized potentials the number of spikelets in complex spikes was reduced by half or eliminated, respectively, while the intraburst frequency measured from the first interspike interval was only one-third that of wildtype mice in *Kcnc3*-null mice. Complex spikes were thus more affected than the simple spike rate. High-frequency firing, assessed by a plot of frequency as a function of injected current, was relatively more affected than low-frequency firing. Consistent with the explanation that an impairment in high-frequency firing produces the deficits in complex spikes rather than an alteration primarily in the underlying waveform, current injections simulating complex spikes could not elicit the high intraburst frequency or higher number of spikelets characteristic of wildtype mice in null mice.

Intriguingly, the post-complex spike pause that is also seen *in vivo* is longer in *Kcnc3*-null Purkinje cells. The pause is expected to produce synchronized disinhibition of DCN neurons after complex spikes that could facilitate rebound depolarization (see section 5.4.2). It could also impact effects of Purkinje cell collateral input onto other Purkinje cells and interneurons, an effect that may be difficult to study in slices because the connections are likely severed in most cases.

I did not observe bistable shifts between up and down states toggled by climbing fiber stimulation as McKay et al., 2007 did in rat using K-gluconate internal. In all my recordings I only saw this behavior once in a pilot study not included here. Based on *in vivo* data, only a subset of Purkinje cells may be prone to this. The propensity to shift Purkinje cells between states, if they do prove to be physiological, might be an interesting topic for future research. When Dr. McKay and I tried K-gluconate in mouse slices Purkinje cells were very prone to calcium spiking and less stable however.

In light of their use as normal controls in the behavioral studies of +/-;-/- mice, mice heterozygous for the *Kcnc3*-null allele were normal with regard to all Purkinje cell spike parameters. Again, the firing correlates to the motor phenotype. Evidently there is no haploinsufficiency in this cell type when one *Kcnc3* allele is ablated. Also, one Purkinje cell from a rescue mouse from the 396 line was indistinguishable from those of the 313 line used for analysis.

The laboratory of Dr. Bernardo Rudy was also investigating changes in climbing fiber responses in +/+;-/- mice simultaneously however that lab focused on the dendrite and at the soma only examined responses at a hyperpolarized potential. My manuscript reports data collected at the resting potential because it is more pertinent to the behavioral rescue but Zagha et al., 2008 made extracellular recordings *in vivo* (Zagha, Lang and Rudy, 2008). Our results were in agreement, with minor differences likely due to the difference in the ages of the mice. Namely, there were more spikelets in their wildtype mice probably because the input resistance should be higher in young mice extrapolating from the

maturation curve in rat slices reported by (McKay and Turner, 2005). Another factor is my use of K-methylsulfonate in my internal solution rather than K-gluconate, which blocks channels more and thereby raises the input resistance (Velumian et al., 1997). My use of K-methylsulfonate is if anything closer to natural conditions relevant to behavior.

Another study using K-gluconate in this case in young rat slices found that partial blockade of Kv3 channels at a dose of 150 μM that is ostensibly specific but not calcium-activated potassium channels led to the emergence of sodium-calcium spike bursts that were more intense at 1 mM (McKay and Turner, 2004). Although I could elicit bursting with TEA in adult mouse slices of +/+;-/- mice, I did not see these bursts at baseline in null mice, suggesting another mechanism was yet at play. Moreover, complex spikes, which are distinct, synaptically generated bursts that are partly sculpted by calcium currents were not augmented in the null. The effect McKay and Turner observed thus does not appear to bespeak of a general function of Kv3.3 in suppressing all types of bursts.

5.2.2. Normal Purkinje Cell Spiking Is Rescued by Restoring Kv3.3b to Purkinje Cells

Purkinje cells from rescue mice exhibited a concomitant cellular rescue of all spike parameters that were disturbed by ablation of endogenous *Kcnc3*, including spike width, spontaneous simple spike frequency, the *F-I* relation, and all aspects of complex spike firing including the lengthened pause that follows. Additionally responses to current injections simulating complex spikes returned to normal, suggesting the rescued abnormality is high-frequency firing rather than development of climbing fibers or other effects. The rescue could be reversed by TEA consistent with the notion that it was mediated by re-expression of the Kv3-type channel. Also, the diminution of the burst by TEA runs counter to the notion

that Kv3.3 suppresses bursts in general suggested by the effect on sodium-calcium spikes.

I was surprised that harmaline-induced tremor did not return in +/+;-/- mice with complex spikes rescued in Purkinje cells by Kv3.3. This result might entail that Kv3.3 must also be rescued downstream of the DCN in red nucleus neurons to adequately convey the synchronized output to effect movement or the GABAergic neurons of the DCN that close the olivo-cerebellar loop. Although these cells spike slower than the large, non-GABAergic neurons they are still fast-spiking by whole-brain standards and Kv3.3b has been reported to be expressed in some of them (Grandes et al., 2008).

5.3. FIRING IN DCN NEURONS DOWNSTREAM IS ALTERED UPON ADDITIONAL LOSS OF KCNC1

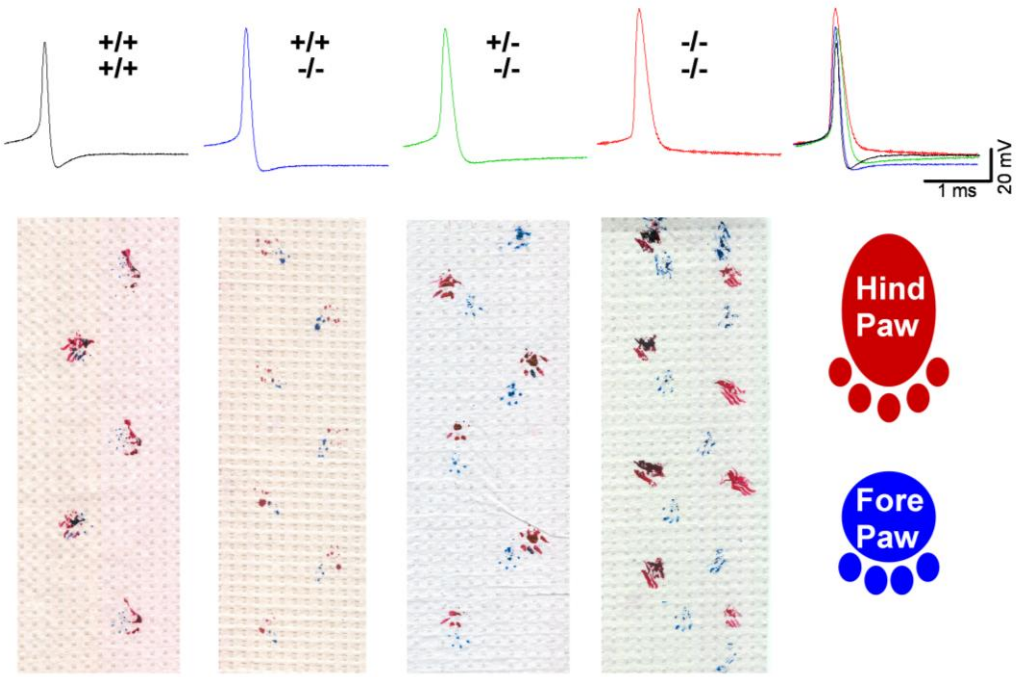

Figure 5.1. (above) The severity of gait ataxia correlates strikingly well with changes in the intrinsic firing properties of large glutamatergic DCN neurons.

In order for the rescue of Purkinje cell spiking to correct behavior presumably DCN firing must be normal in +/+;-/- mice. Also, it was not clear whether Kv3.1 and Kv3.3 might be functionally redundant in large glutamatergic DCN projection neurons. I recorded these neurons in +/+;+/+, +/+;-/-, +/-;-/- and in -/-;-/- mice. A graded slowing of action potential repolarization was evident as alleles were lost that was not quite significant in mice just lacking *Kcnc3*, suggesting that indeed DCN output is intact in single-null mutant rescue mice that achieve a full rescue of motor performance and lack gait abnormalities. Spikes were significantly broader in +/-;-/- mice that had only a partial rescue and a subtle gait disturbance. There was a considerable step up in spike width once both *Kcnc1* alleles were lost in -/-;-/- mice, which did not benefit at all from the rescue upstream in Purkinje cells and acquired the full spectrum of cerebellar gait ataxia (Fig. 5.1). The intrinsic firing properties mirror the gait phenotype and effectiveness of the Purkinje cell rescue, indicating that intrinsic changes in large DCN neurons in the cerebellum could underlie the gait phenotype and potentially explain why the rescue depends on the presence of *Kcnc1* alleles.

5.3.1. Action Potential Properties of DCN Neurons Become Significantly Altered As *Kcnc1* Alleles Are Ablated

Large, weak-burst DCN neurons of +/+;-/- mice had normal spike widths and decay times but the height of action potentials was significantly greater than that of wildtype mice. The *p* values for these parameters were suggestive of the possibility that a difference might surface with a larger sample size. Nonetheless the data indicated that action potentials are more or less normal in +/+;-/- mice, consistent with the notion that DCN spiking should be intact for the rescue of Purkinje cells to be expressed behaviorally. Additional lack of a *Kcnc1* allele broadened, heightened and slowed the rise and decay of action potentials, while

the lack of both *Kcnc1* alleles led to much greater differences. The spike width in -/-;-/- mice doubled relative to +/+;+/+ mice, whereas in +/+;-/- mice additionally lacking just one *Kcnc1* allele the width was 50% broader, changes that parallel both the loss of rescue efficacy and the appearance of gait ataxia. Spike broadening can have a non-linear effect on transmitter release if present also at axon terminals, for there is a third to fifth order dependence of transmitter release on calcium influx. If augmented transmitter release is a critical variable then in this respect the perhaps disproportionately lesser phenotype of *Kcnc3*-null mice with one wildtype *Kcnc1* allele (50% vs. 100% broader), and absence of a phenotype in *Kcnc3*-null mice with Purkinje cells rescued (~25% broader, if a larger sample shrinks the error without changing the now uncertain but almost significant mean), is sensible and does not argue against changes in the DCN accounting for the more marked phenotypes as *Kcnc1* alleles are lost.

Mechanistically speaking, the action potential rise time should have slowed significantly as spikes broadened but did not. Kv3 channels accelerate spike frequency ultimately by increasing the number of available, deinactivated sodium channels to reach threshold more readily. Concurrently the rate at which further sodium channels are recruited increases, in theory hastening the rise time. Perhaps because Kv3 channels open very quickly and have a large conductance, the fraction of channels that manages to open during the rise of the action potential is able to slow it slightly in wildtype mice. A reduction in Kv3 current magnitude in null mutants could potentially remove this stalling influence, thereby permitting the action potential rise time to decrease, canceling the stalling effect of fewer sodium channels being available to activate.

5.3.2. High-Frequency Firing of DCN Neurons Becomes Significantly Altered As *Kcnc1* Alleles Are Ablated

I strongly expected to see a decrease in the spontaneous spike rate in large DCN neurons in the mutants that had significantly broadened spikes. The spike rate is

indeed lower but statistical significance is only reached using intracellular recording with these sample sizes in -/-;-/- mice. At higher frequencies induced by current injection as revealed by the *F-I* plot pilot data from a small sample indicated DCN neurons from -/-;-/- mice showed a significant slowing. The slope of the plot was less in +/-;-/- and -/-;-/- mice with the *p* value on the cusp of statistical significance. As in Purkinje cells, the data pointed to a more marked deficit in high-frequency firing. In DCN neurons the spike frequency is higher during EPSPs and rebound depolarization following IPSPs. Transient-burst large neurons are apt to produce the highest frequencies during rebound bursts. My limited sample suggested spike properties of these neurons are affected in parallel with those of weak-burst neurons. Climbing fibers innervate DCN neurons as well but do not produce EPSPs of the same magnitude as with Purkinje neurons. Consequently, burst output of large DCN neurons would be diminished to an even greater extent than tonic excitation of downstream target neurons in the red nucleus and ventral thalamus. Of course the net effect of this combined with greater glutamate release is a potentially interesting topic for future empirical studies as the answer is non-intuitive.

I also examined the coefficient of variance of the interspike interval, a property that is disrupted in ataxic calcium channel mutants in Purkinje cells but normal in these neurons in +/+;-/- mice. Even in -/-;-/- mice which had the highest mean the difference was not even close to significant.

Together the spike data in the DCN elegantly track the changes in gait that appear as *Kcnc1* alleles are lost and offer an explanation as to why the rescue can occur without *Kcnc3* in DCN neurons but not without *Kcnc1* on a *Kcnc3*-null mutant background. Nevertheless alternative explanations exist and data for gait are only correlative. Parallel fibers also show graded changes in spike width and input to Purkinje cells as *Kcnc1* alleles are lost. The profile of this graded trend however does not match the behavioral deficits as well as that of DCN spike properties. Between mice lacking *Kcnc3* additionally lacking a *Kcnc1* allele and -/-;-/- mice there is a big jump in severity. This mirrors the considerable

broadening of large DCN neuron spikes better than the incremental increase in parallel fiber input to Purkinje cells seen as *Kcnc1* or *Kcnc3* alleles are lost. Downstream of the DCN, neurons in the ventral thalamus are likely unaltered because they chiefly rely on *Kcnc2*. It is not clear what Kv3 subunits the fast-spiking intralaminar and midline nuclear thalamic neurons express. An alternative candidate locus that cannot be ruled-out is the red nucleus in the midbrain where mRNA for all subunits has been reported but the fine cellular distributions of the channel proteins have yet to be described. On functional neuroanatomic grounds neurons within the cerebellum are the most likely candidates based on what is known from lesion studies to date since ataxic gait characteristic of cerebellar ataxia has only been reported after cerebellar lesions to my knowledge.

The ability of disruptions in DCN neuronal spike rate in general and impaired repolarization to elicit ataxia is evident in the report by Shakkottai et al., 2004, where although the red nucleus was also directly affected ataxia best tracked changes in the DCN.

5.4. INPUT TO DCN NEURONS FROM PURKINJE CELLS IS ALTERED IN KCNC3-NULL MICE

In these pilot studies I endeavored to discern what aspects of Purkinje cell input to DCN neurons is rescued and in turn related to hypermetria. For Purkinje cell activity to impact motor skills it must change DCN output, or vestibular nuclear output to the extent the task requires maintaining balance. Of particular interest was the question of whether complex spike changes wrought by the *Kcnc3*-null mutation are consequential for DCN output. This is primarily a section indicating future directions.

5.4.1. Synaptic Depression

Pilot data were consistent with increased synaptic depression in +/+;-/- mice. Only one rescue recording suggested normal depression may not be rescued by Kv3.3b restoration. If we assume this is variation about a mean and that normal depression was rescued, hypermetria could result from enhanced depression. Synaptic depression is believed to render the Purkinje cell-DCN neuron synapse more responsive to sudden changes in the frequency of input than steady inhibition. Despite the fact that broadened spikes would release more GABA acutely after a period of Purkinje cell silence or low-frequency spiking, once depression develops the overall tonic inhibition would be reduced. It is tempting to speculate that a synapse that overreacts to changes in input might amplify the effect of slight changes in Purkinje cell spiking triggered by parallel fibers and ultimately mossy fibers to cause hypermetric movements that would otherwise occur at a normal rate of acceleration and deceleration once the target limb position is reached.

The study by Sausbier et al., 2004 of mice lacking a large-conductance calcium-activated potassium channel gene also found spike repolarization deficits in Purkinje cells. In DCN neurons from these mice increased synaptic depression of input from Purkinje cells was observed along with ataxia. Decreased inhibition due to depression of inhibition by Purkinje cells of DCN neurons would presumably increase the frequency of firing. An increased firing rate of DCN neurons was also seen when a small conductance calcium-activated potassium channel was ablated functionally by a dominant negative approach. It is plausible that in all cases DCN output is increased in terms of spike rate, an effect that may be compounded by the fact that spikes are broadened, increasing glutamate release. Aberrantly increased DCN output to the red nucleus disrupts critical pauses in activity in animals lacking all inhibition from Purkinje cells (Tarnecki, 2003) suggesting this as a tenable mechanism.

The inability of restoring Kv3.3b to Purkinje cells to rescue coordination in -/-;-/- mice could parsimoniously result simply from DCN neuronal output being disrupted by spike broadening. If depression is greater without Kv3.3 and normal

with the rescue, rescuing input from Purkinje cells could actually make the -/-;-/- worse paradoxically. The tendency to spike slower in large -/-;-/- DCN neurons could be improved actually, at least during tonic inhibition at rest, by reducing inhibition by Purkinje cells. Increased steady-state depression then could actually mitigate dysfunction in -/-;-/- neurons, complementing the deficit. Unless there is a ceiling effect this is probably not true or inconsequential for DCN output ultimately in -/-;-/- mice because -/-;-/- rescues do not perform worse than -/-;-/- mice.

Augmented depression could also impact complex spikes. Since depression increases with increasing firing rates, high-frequency inputs during complex spikes might be diminished. Such an effect would be expected to attenuate the difference in complex spike instantaneous frequency between wildtype and +/+;-/- mice in terms of inhibiting DCN neurons.

Another attenuating influence might be the Purkinje cell axons themselves, as discussed in detail in the introduction (see section 1.3). We do not know whether Kv3.3b contributes to axonal propagation or is just in transit to axon terminals. Purkinje cell axons are myelinated and Kv3.3b does not show any enrichment in nodal structures. Moreover in wildtype murine and rat slices these axons do not reliably propagate sustained, high-frequency action potentials in the range attained by complex spike bursts. Though it may be that converging innervation by many Purkinje cells of DCN target neurons allows them to effectively experience burst input even though only a fraction of Purkinje cells propagate at any given latency after the first initial spike, the low-pass filtering effect of the axon might attenuate or erase the difference between +/+;-/- and wildtype complex spikes. The function of Kv3 channels in axonal propagation is a fertile future avenue of inquiry.

5.4.2. The Effect of Altered Purkinje Cell Input to the DCN on DCN Output

Here I was able to determine that the complex spike alterations except for the lengthened pause are unlikely to impact the DCN in a physiological context even if synchronized. Further, it was apparent that the lower frequency of Purkinje cell output in slices will disinhibit DCN neurons all other things being equal. The decreased simple spike frequency reduced DCN inhibition whether +/+;-/- or wildtype Purkinje cell axons were stimulated, but future work will have to determine with a very large sample size whether the net effect of spike broadening and a decreased spike frequency is to hyperpolarize or depolarize DCN neurons. Acute pharmacology may be misleading as to what is happening in the genetic model because of long-term adaptations that are known to take place in the DCN when deprived altogether of Purkinje cell-mediated inhibition.

To better recapitulate the *in vivo* situation I stimulated Purkinje cell axons after a simulated simple spike train that allowed steady state synaptic depression to be established, as *in vivo* Purkinje cells typically are spiking except during short pauses after complex spikes and occasional, longer pauses. By the time the simulated burst input of either wildtype or +/+;-/- mice reached the synapse the depression or other factors prevented any noticeable temporal summation of evoked IPSPs. During the pause however recovery from inhibition, in part driven by the accumulated rebound depolarization depolarized the membrane, led to at most one spike. Delivering stimulation at a frequency simulating that of mice lacking Kv3.3 in Purkinje cell axons compared to the corresponding wildtype frequency, the simulated longer pause seemed to increase the chance of a spike occurring as well as more significant recovery from inhibition that was not restored after the pause in either genotype. The complex spike input seemed to allow the DCN neuron to escape tonic hyperpolarization, which the ensuing simple spikes could not restore presumably due to depressed input. Based on these slice data the changes in complex spike bursts are virtually inconsequential while the pause might actually have an impact on DCN firing. According to some theoretical conceptions the pause could well be more important to the DCN than the complex spike burst (Armstrong, 1974).

The above conclusion on complex spikes is subject to the caveat that DCN neurons receive inhibitory contacts from ~30 Purkinje cells in rodents. Although I did deliver synchronized stimulation as might occur during certain behaviors *in vivo*, I cannot fully recapitulate the total number of inputs in 300 µm slices. Future work should address this question *in vivo*. Nonetheless it is difficult to imagine the input being robust if synapses are already depressed by prior simple spiking, suggesting complex spikes must occur after pauses or significant decelerations in Purkinje cell activity.

Under *in vivo* conditions neurons typically have a higher input resistance than *in vitro* and are subject to modulation by diffuse input from monoaminergic systems among others. The membrane potential is as a result more dynamic. As I saw in one GABAergic cell with a high input resistance, burst input from Purkinje cell axons, in that case after a baseline of silence, can toggle DCN neurons potentially between up and down states. In both Purkinje cells and DCN neurons complex spikes may function as a mechanism whereby cells are shifted between bistable states.

One aspect of complex spike function that has received much speculation and experimental attention is in timing. In +/+;-/- mice the ability of complex spikes to time DCN neuronal activity is likely unaltered based on my slice data where the pause remains and is if anything enhanced in its impact on DCN neuronal firing. Though I found movement velocity control was altered, a posited function for complex as well as simple spikes (see section 1.3), my work on the DigiGait™ and Rotarod suggested faster speeds did not differentially affect *Kcnc3*-mutant mice.

The ability of the complex spike to control fine timing of movement has

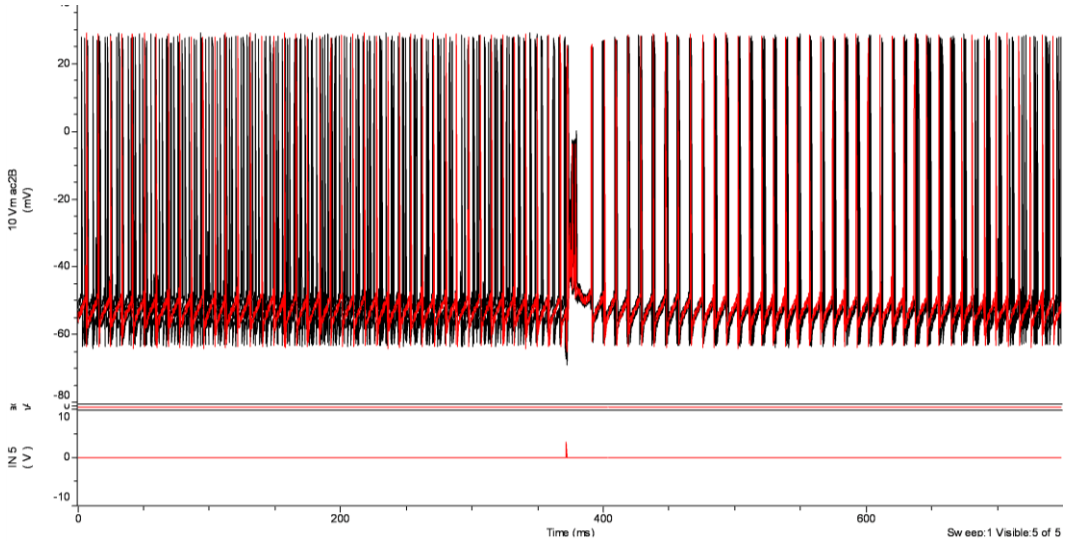

Figure 5.2. Simple spikes following complex spikes in the same cell are remarkably consistent in their phase. If this is true under some conditions across multiple Purkinje neurons it could powerfully synchronize simple spikes across the population after the occurrence of synchronized complex spikes. Here, an overlay of 5 traces is shown from a Purkinje cell stimulated at the notch in the middle of the lower trace.

been contested on the grounds that the low frequency of complex spikes (~1-4 Hz) is not fast enough to shape rapid movements. During my analysis of complex spikes at the resting potential I noticed that in overlays of 5 traces of climbing fiber stimulation simple spikes following complex spikes occurred at remarkably similar intervals (Fig. 5.2). If one imagines if these traces represented 5 different Purkinje neurons in a similar state of depolarization and modulation with similar input resistances it immediately becomes clear that the complex spike may not need to be elicited more frequently than 1 Hz to influence the timing of simple spikes up to 300 milliseconds later, at least in the slice. The recently described gap-junction mediated synchronized fast oscillations among Purkinje cells entrained by recurrent collaterals could help extend the duration of phase setting longer, allowing the simple spikes to ride on a harmonic of the fast oscillation. Also synchronizing simple spikes through persistent phase-locking might have

pivotal effects on DCN neurons since it would create windows during which the DCN neurons could fire action potentials also in synchrony, increasing the strength of output, in contrast to a tonic IPSP that would suppress output. If the complex spike can actually trigger large IPSPs under some conditions as suggested by some *in vivo* recordings where complex spikes were triggered by stimulation these too might be capable of temporal entrainment across DCN neurons if synchronized. If these *in vivo* recordings are representative of conditions where complex spikes can occur spontaneously and complex spikes in converging Purkinje cell terminals indeed elicit strong IPSPs this could be weakened in null mice. It is clear though that in null mutants such a phase-setting effect would persist. There was no indication of increased variability of the overall duration of the complex spike and pause that could disrupt it.

Although complex spikes are more affected than simple spikes, spikes are broadened in both cases and the results here only indicate that complex spikes are a potential mechanism through which Kv3.3 functions in motor coordination. The above data suggest only, and weakly given the caveats of slices, that the spikelet changes are superfluous. It is likely impossible to extricate effects of Kv3 on complex and simple spikes by other than correlational means. Changes in simple spike frequency, if they exist *in vivo* with inferred augmented parallel fiber drive in +/+;-/- mice could however be extricated from broadening perhaps by using Kv4 channels via a transgenic or gene transfer approach which, when overexpressed, decelerate spiking and, when blocked by a dominant negative, accelerate spiking leaving spike width more or less unaffected. The *SCA13* mutation that slowed deactivation would be expected to for the most part just affect spike rate without broadening spikes and sufficed to cause ataxia. This result suggests simple spike rate may contribute to motor coordination. However the dominant negative would likely decelerate spiking in many other neurons by removing all Kv3 function not just Kv3.3 which seems uniquely essential for narrow spikes in Purkinje cells based on what neuronal cell-types have been recorded so far. The finding of decelerated spiking in *SCA1*

is interesting in this regard as well but again there is no cell-type specificity to be sure it is attributable to Purkinje cells.

5.5. CO-EXPRESSION OF KV3 SUBUNITS DOES NOT IMPLY FUNCTIONAL REDUNDANCY

Functional redundancy has been invoked in the past to explain the mild phenotypes of the Kv3 single-null mutants in sharp contrast to the severe phenotype of the -/-;-/- mice. Early anatomical data relying on *in situ* hybridization suggested co-expression and potential heterotetramerization of subunits might be widespread. The cerebellar ataxia of mice lacking *Kcnc3* alone or along with *Kcnc1* alleles highlights neuronal cell-types in the cerebellum as likely cellular loci where functional redundancy explains the increased severity once *Kcnc1* is lost. Previous studies had not directly demonstrated co-expression of Kv3.1 and Kv3.3 in large, glutamatergic neurons. I found that these subunits were indeed co-expressed in all large, glutamatergic neurons marked by SMI-32 expression, indicating that Kv3.1b and Kv3.3b are not entirely redundant functionally considering that loss of one allele of *Kcnc1* led to significant spike broadening. Both Kv3.2 and Kv3.4 were also co-expressed in these neurons, interestingly, yet were incapable of complementing the loss of Kv3.1 and Kv3.3. Curiously, unlike Kv3.1 and Kv3.3, Kv3.2 and Kv3.4 did not exhibit enrichment in the membrane except in stellate cells. This may explain why these subunits make a lesser contribution to spike repolarization. The significance of this more homogenous, somatic distribution remains elusive.

It was also unknown whether Kv3.3 is expressed in cerebellar cortical interneurons. I found that stellate cells and basket cells, inferred from the pinceauxs revealed by GAD67 immunolabeling, lack expression of the most abundant splice variant, Kv3.3b. Thus the changes in complex spikes and

pauses seen in null mutants likely do not derive from changes in interneuronal input at least due to intrinsic alterations in action potentials in these cells.

5.5.1. Cerebellar Cortex

That re-expression of Kv3.3b in Purkinje cells of +/+;-/- mice sufficed to rescue motor coordination suggested that Kv3.3 expression upstream of Purkinje cells in the cerebellar circuitry was unnecessary for motor performance in the tests conducted. In the case of the beam, parallel fiber expression of Kv3.3 might only be important early in the 5-day test because the synapses made onto Purkinje cells are highly plastic and may adapt. Increased parallel fiber drive without *Kcnc3* alleles may not be causing the hypermetria detected on the force plate however because the rescue downstream in Purkinje cells is efficacious. Previous expression studies had neglected interneurons or yielded inconclusive data. I re-evaluated interneurons and found that Kv3.3b expression is absent in both stellate and basket cells, at least at the pinceaux. Kv3.3b is the most abundant variant by far. Therefore intrinsic electrophysiological changes in cortical interneurons most likely do not contribute to the null phenotype.

I also found that Purkinje cells express both Kv3.3b and Kv3.4 at the soma replicating previous work, however I further uncovered axonal expression. The even rather than beaded expression suggests there is no enrichment at nodal structures. In essentially all terminals in the DCN co-labeled with GAD67 and SMI-32, which is also found in Purkinje cells, Kv3.4 was highly concentrated raising the possibility that it functions in regulating neurotransmitter release however the lack of complementation regarding action potentials at the soma suggests it likely does not compensate for Kv3.3 loss. Heterotetramerization though could create channels with different properties when Kv3.3b and Kv3.4 subunits are co-mingled allowing Kv3.4 to still play a role in rapid repolarization.

5.5.2. DCN

To determine whether the alterations in spike properties seen as *Kcnc1* alleles are ablated in large DCN neurons were a result of limited complementation between *Kcnc1* and *Kcnc3* or non-overlapping expression in independent subsets of neurons I re-examined expression of these subunits. Although Kv3.1b and Kv3.3b have been described in separate experiments as confined to the large neurons, it remained unclear whether these neurons were the glutamatergic projection neurons and whether expression entirely overlapped. Action potentials of +/+;-/- mice tended to be slightly broader but only spike height reached statistical significance. Gene dosage effects were evident for *Kcnc1* comparing the different compound mutants when *Kcnc3* was ablated, a result that would make sense if the subunits are co-expressed rather than in separate cells, as mice just heterozygous for the *Kcnc1* allele with intact *Kcnc3* do not reliably exhibit motor impairment in all assays in all strains tested (Joho et al., 2006, Ho, Grange and Joho, 1997, Sanchez et al., 2000). A lack of functional redundancy could just as well result from some neurons expressing only Kv3.1 but not Kv3.3 as much as it could result from currents in the same cell failing to compensate.

Expression of Kv3.1b and Kv3.3b was completely overlapping and universally present in large, glutamatergic DCN neurons marked by SMI-32. Thus, the slight lack of functional redundancy in spike repolarization seen in mice lacking *Kcnc3* with intact *Kcnc1* does stem from co-expression not separate populations depending on one subunit gene. Curiously Kv3.2 and Kv3.4 were also present in large, glutamatergic neurons. Like in Purkinje cells, Kv3.4 does not complement the loss of other Kv3 subunits. Kv3.2 is known to be expressed in fast-spiking neurons such as thalamocortical relay cells, which have broader spikes and do not spike at as high of rates as large DCN neurons. To study the role of Kv3.2 in some neocortical interneurons, interestingly, a double-mutant had to be used encompassing the *Kcnc1* null allele, suggesting Kv3.2 loss is complemented by Kv3.1. Either Kv3.2 and Kv3.4 are expressed at lower

functional levels, resulting in a slower repolarization rate because the smaller conductance takes longer to change the membrane potential, or possess divergent, slower kinetics compared to Kv3.1 and Kv3.3. Together the expression and electrophysiological data from large DCN neurons buttress the notion advanced by findings from Purkinje neurons, thalamic reticular neurons and cortical interneurons that co-expression of Kv3 subunits does not imply functional redundancy with regard to somatic spike repolarization.

Again, the axonal function of Kv3 channels might be of immense interest. Aside from limited functional redundancy with respect to repolarization at the soma, Kv3.1 and Kv3.3 may differ crucially in their ability to support high-frequency propagation of action potentials, or still other functions, in the long axons of large, DCN neurons. In addition, the issue of glial expression of the channels should be considered, which had a mild but significant effect on myelination. A lack of both Kv3.1 and Kv3.3 in DCN neurons could exert complex effects at multiple cellular loci that together result in much more severe dysfunction. Work on Kv3 function in axons should be a high priority for future work on Kv3 channels that, while challenging, might yield insight into a novel and surprising roles for the channels beyond just action potential repolarization and delimiting neurotransmitter release.

Regarding -/-;-/- mice and mice lacking *Kcnc1*, the axonal role of the channels is especially enigmatic. Unless other splice variants not explored with available antibodies concentrate at nodes of Ranvier, it appears that myelinated axons rely on Kv3.1b to serve whatever function Kv3 current serves at nodes (Chang et al., 2007, Devaux et al., 2003). If expression here was critical for axonal function, one would anticipate motor phenotypes in mice lacking just *Kcnc1*. That -/-;-/- mice are much worse than +/+;-/- mice fits, however *Kcnc1*-null mice do not reliably show significant ataxia with good penetrance on all genetic backgrounds. Importantly, what has been detected is not present across multiple assays sensitive to ataxia. The paradox only adds interest to the question. The

effect may be subtle and require sensitive tests or special conditions to make it evident, but is interesting nonetheless.

APPENDIX A: Mouse Husbandry Manual

Joho Lab Mouse Husbandry Manual 6/24/07

By Ed Hurlock

This protocol is tailored to the Joho Lab using the NG vivarium at UTSW. Notes are included on other vivaria but they are not comprehensive.

Contents:

Remember always to think like a mouse. Mice perceive the world primarily through olfaction, and communicate by pheromones. They hear and communicate vocally in ranges we cannot hear, so equipment humming at these ultrasonic frequencies may agitate them, interfering with breeding etc. Educate yourself on the social behavior and natural history of mice; cultivating this awareness is *invaluable* and only touched upon here where directly relevant.

Knock-out or null alleles and transgenic lines need to be maintained, if not in "active duty" with ongoing breeding for experiments, every nine months if outbred or every 5 months if inbred (i.e. Kv3-null allele backcrosses). Waiting longer risks reproductive senescence. C57/BL/6 a.k.a "Black 6" females reputedly sometimes deplete their eggs by ~6 months. For maintenance, ideally two cages of five mice (NG facility) bearing the genes of interest should be kept, one cage of females and another of males. Every few generations these should be bred against outbred wildtype mice to prevent poor breeding, loss of fecundity (small litter size) and poor parenting that develops with inbreeding. Even in "inbred" strains (C57/BL/6, 129, FVB, etc.) there is still some diversity left so it can be beneficial to order mice from the vendor again to reinvigorate after breeding many generations a few mice within the colony. Keeping only one cage for maintenance (ideally females to avoid potential fighting) is risky because if that one cage floods (rare but happens), has water supply problems or is subject to an infectious disease outbreak (almost non-existent in clean facility) the line could be lost. If females or males have bred before at least once they may last longer before reaching reproductive senescence (Robert Hammer, pers. comm.).

Typically maintenance mice don't need regular attention from the lab. Vet techs will notify the lab of any mice that need to be sac'ed and place a card on cages where fighting is severe mandating separation. Initially, shepherd shacks and nestlets for distraction can be provided to mitigate violence. Mainly this is prevented by properly housing males and females as described further in the breeding section below.

If mice are culled for experiments or die and it is economical to consolidate them to fewer cages after P30 or so, note the following. Always at least give the new cagemates fresh bedding to eliminate territorial demarcation odors and preferably a shepherd shack. It may help to rub dirty bedding on the newcomers so they smell somewhat familiar. Males that have bred will almost certainly fight at least moderately, possibly viciously, after being removed from the female(s) and housed with males, even those that had been familiar prior to breeding. Males that have been bred can therefore only be used for further breeding, housed individually (potentially with sons) or sac'ed. Females with a litter should never have other females or males added to their cage, as it risks pups being bitten or eaten, stresses the mother, impeding proper care of the pups, and will result in fighting. Small females should not be placed with older, larger females for it risks fighting resulting in potentially severe wounds in the small mouse, although a shepherd shack may suffice to avert this. Genetic background strongly influences fighting probability. FVB mice and to a lesser extent outbred ICR mice are known to be more aggressive. For example, unfamiliar adult female FVB mice will fight aggressively. Eartags are often lost over time. To ensure positive identification, only house mice together that can be clearly differentiated by coat color, natural tail stripes, earpunches and or tags, unless mice are strictly for maintenance and all of the same genotype without a specific history to track, such as a genetic lineage.

For maintenance only, mice of genotypes known to be capable of breeding should be used. If null mice are more convenient to maintain since it obviates genotyping, first determine if they can breed, at least with one parent null so the line is not lost. In the Joho Lab this includes mice heterozygous for one or both Kv3 null alleles (Kv3.1 and Kv3.3). Transgenes thus far have no effect on breeding (pBIKv3.3b line 303, 313, 396; pBIKv3.1a A, pBIKv3.1b A and D, pBIKv3.1c, L7tTA and GAD67GFP (Parv. line). Kv3.3 SKO mice breed fairly well but Kv3.1 null females seem to take longer to get pregnant and mother less reliably (work in progress). Kv3.1 SKO males seem to breed fine but statistics are limited. +/-; -/- mice can breed but previous lab records indicate that both triple minus mice are contraindicated for breeding, possibly due to genetic background differences. In short it is more risky to breed null mice. -/-;-/- mice will consistently not breed. Nor will they fight, which makes housing more convenient (any male can be housed with any female or other male without concern of pregnancies and overcrowding). It is a good idea to save -/-;-/- mice on hand for unanticipated experiments, however there is an attrition of Kv3.1/3.3 -/-;-/- mice because of their seemingly shorter lifespan. Note that Kv3.1 SKO mice and even +/-;-/- mice are significantly more difficult to handle than wildtype or heterozygous mice.

1.2 Breeding

Breeding is the most arduous, complex, time-consuming aspect of colony management, for experiments or maintenance. Careful forethought and planning

are crucial, or at least will potentially save huge amounts of labor and resources, as well as avoid problems at publication time from concerns over effects of modifier genes. The latter have the greatest impact on behavioral studies, may affect electrophysiological studies and are likely to have relatively less impact on gene expression studies because behavior is a complex systems-level phenomenon known to be influenced by a myriad of genes. Keep a pedigree.

When mice are potentially going to give birth or “drop a litter” (as early as 17 days postpartum if the male was present during birthing), unless 1:1 harem ratios are used, the colony should be checked at least every couple days if not daily. If the birthdate is critical for experiments, mice should be checked daily. Early morning is most ideal because litters are usually born at night and overcrowded cages can be caught before they get tagged.

First, anticipate how much cage space will eventually be needed and arrange for it. Plan in detail crosses especially if it is important to control for modifying genes necessitating either use of pairwise comparisons of littermates or at least balanced culling of genotypes from related parents, ideally derived from a common breeding pair within a couple generations. Calculate Mendelian probabilities to determine how many mice to breed to have reasonable assurance of sufficient numbers of analyzable mice from each experimental group, or for maintenance, where a certain number of males or females might be sought (see section 1.1). Work backwards from the number of mice ultimately needed. It may be desirable or acceptable to breed the total number of mice needed over a few generations.

Thinking ahead about genetic caveats when breeding for experiments is crucial. The potential impact of modifier genes, linked genes and genetic drift should be considered. Ideally pairwise comparisons are made between littermate controls culled from litters from the same parents or additionally from closely-related parents to obtain reasonable sample sizes quickly. 25% wildtype, 25% null and 50% heterozygous mice should be obtained, so typically conventional null mutants can quite efficiently be bred with respective controls. If however further independently-segregating genes are involved, such as transgenes, the efficiency drops precipitously. With one additional gene it is still feasible to use littermates, but with two or more it becomes unrealistic or at least so exorbitant as to constitute questionable stewardship of grant money. Instead, a balanced breeding approach can greatly reduce the chances of genetic drift or modifier genes confounding results. To achieve this with one transgene and a null mutation, breed mice carrying the transgene (homozygous if possible) with null mice. Mate one pair of resulting heterozygous null mice carrying the transgene to obtain a number of null and wildtype mice carrying the transgene. Next, mate multiple pairs of these wildtype and null siblings that will produce essentially cousins to compare, 75% of which should carry the transgene. For larger sample sizes, use multiple heterozygous pairs bred as described but be sure to cross wildtype and null mice that are cousins to produce experimental mice, never siblings, to maximally mesh the genetic background. In fact, the more breeding pairs used with this paradigm the more evenly distributed the modifier genes will

be among experimental mice. Using this paradigm genetic drift is drastically reduced. To repeat the experiment >9 months later with young mice, again derive heterozygous null mice by crossing the wildtype and null breeders with each other, and then using these heterozygous mice to again generate wildtype and null breeders. This will reshuffle the genes, largely maintaining outbred vigor, and greatly reduce genetic drift or modifier effects appeared while maximally sustaining the genetic background. The problem of linked genes influencing a null phenotype can be excluded by analyzing heterozygous mice but only if there is no associated phenotype stemming from gene dosage effects. The only way to deal with this if it is observed is to breed the mice extensively and assess the heterozygous phenotype over several generations. Chances are that linked genes will eventually segregate by recombination. The same approach can be applied to transgenes. Where one transgene alone is insufficient to trigger the manipulated variable, double transgenics can be compared to single transgenics, or in the case of cre recombinase lines, the cre line with or without the floxed alleles. Alternatively, with transgenics different founder lines can be compared to exclude effects of linked modifier genes much faster.

Having maximally diversified coat colors aids in identifying mice, reducing the need for ear punches etc. to identify mice upon loss of tags. Preferentially breeding striped tails also aids in this. Color genes are dominant in roughly the following order: Agouti>white=black>hay/fawn[gold]=brown=light agouti=chinchilla[8]. Without a deliberate effort, all mice will eventually end-up agouti. Further, diversifying colors in a random way helps avoid distinguishing between mice of different genotypes in blind experiments. Therefore, try where possible to pair mice of dissimilar colors, with a slight but not absolute bias against agouti.

If sufficient males are available to be allocated to breeding (they cannot be housed with males other than sons afterward), the ideal harem ratio is 1:1. If cage space were no object, it would be best to remove the male prior to the birth of pups to maximize calm and avert the male potentially eating viable pups. A 1:1 harem ratio yields the best chance of rapid pregnancy since males have refractory periods after mating that may preclude inseminating another female in estrus at the same time. This is more marked in inbred males. Chances of pregnancy are further enhanced by using a male that is a proven breeder. When males of the right genotype are scarce, harem ratios of 1:2-1:4 can be used, and the male can even be rotated between cages every 4-5 days to encounter each female during at least one estrus phase. Frequently good outbred males will be

[8] Note that albino mice may have visual impairments affecting performance on behavioral tests requiring visual acuity. White however works best with the DigiGait system (Mouse Specifics), where pink pawprint videos are analyzed (other pink parts must be painted with a sharpie or food coloring pen, ideally blue), although this problem may be circumvented by painting paws red, removing the pigmentation variable.

able to handle this and (very approximately) up to 6 outbred females will get pregnant within a week or two.

When mice are setup for breeding[9], the female(s) should be introduced to the male's bedding or fresh bedding to avoid territorial conflict. A shepherd shack should be provided to mitigate conflict and it is rumored that these facilitate breeding. Observe mice for a minute. In rare cases aggression may be a problem and different prospective breeders will be needed. Good males will often immediately take an interest in the female(s) and attempt to mount after sniffing pheromones, particularly in the dark phase. Cross-out numbers of breeders on their former cages and create a new tag for the breeding cage. Write the purpose of the cross in the center at the top of the breeding cage card. Below, write the male on the left, indicating number and genotype and then a list of "X"s after which the tag number, genotype and markings of each female should follow. Finally, write the setup date below this information. If the male is switched, which is sometimes necessary due to poor performance, note the date because it may be important to know to keep track of the lineage or what genes require genotyping. A hiatus can be implemented to definitively know the lineage.

By consulting the setup date, check breeding cages 15-17 days after setting-up breeding. Only one litter is allowed per cage accompanied by up to three adults, including pre-weanling mice from the previous litter. Mice that show any clear sign of pregnancy (easiest in young, lean mice; difficult in older or obese mice) should be either noted if it is the only pregnant female among a total of three mice in the cage, or separated if there are more than two or more than two are pregnant. Take care not to apply pressure to the uterus when handling pregnant females; instead examine eartags of less or non-pregnant females and deduce by process of elimination the identity of the pregnant female using the list on the cage tag. The most pregnant female should be left in the old bedding if it appears that it doesn't need changing for several more days. This will minimize distress from new bedding. One nestlet should be provided (with two newborns often get lost in excess nest and die; one works best). Nesting material or at least a shepherd shack is important to ensure maximal survival of pups as the mother is stressed without a nest and, because pups are altricial, failure to maintain warmth can lead to a loss of viability. Cold pups are generally presumed non-viable and eaten[10]. Pups begin to maintain their own body temperature however once stubble appears around P5, and the nest gradually subsides in importance. A red special instructions card reading "No bedding change" should be conspicuously applied to the cage for bedding changes will distress the mother

[9] Whenever mice are handled in the NG clean facility using aseptic technique try to remember to wipe gloves with Process NPD disinfectant. Spray NPD in or near the hood to avoid breathing it (chronic breathing may lead to asthma) and take care to avoid eye contact. Do not get extensive NPD on the mice. Be sure to wipe cage lids before and after use them to grab mice.

[10] If pups are removed from the mother they need to be pre-warmed before they are returned.

perinatally and risk pup mortality (C57/BL/6 are especially susceptible). Changing the bedding before birth is not typically a problem since birth usually occurs deep into the dark phase that will occur at night with a conventional light dark cycle in the vivarium. As other females become pregnant in a harem, they can be separated from the others until only 3 adults remain and one nascent litter. In the latter case, the final female to get pregnant and the male should be moved to a fresh cage. There are pros and cons of a female giving birth in the continued presence of a male or additional female. Other mice can disturb the mother, and in the case of males, even the real father, may eat viable pups. An additional female is generally beneficial overall since she may help mother the pups and keep them warm. The male has a chance to inseminate the female again during postpartum estrus, which typically is the case. This is advantageous if a maximal rate of breeding is sought, although it can be inconvenient as it mandates early weaning to prevent overcrowding when the next litter arrives.

Check mice for pregnancies every 2-3 days. A good schedule to maintain is checking the colony Monday-Wednesday-Friday. The DOB can generally be judged accurately within 1 day this way when the appearance of neonates of different postnatal days is considered. If the nascent mother grows very large, becomes sluggish, and overall shows signs of pain or distress, it is likely dystocia. Usually the bulge will be lumpy. She must be sac'ed. Often by the time this is observed fetuses have died.

Unplanned pregnancies occur when males are inadvertently mixed with females and sometimes very small litters are dropped by females that did not appear pregnant. In these cases if pups are usable try to keep the mother in the familiar bedding if it is not too dirty to last a few days. Otherwise get a fresh cage. A nestlet should be provided and "No bedding change" special instructions card applied. The mother can often be determined by the extent to which the fur has cleared around her nipples, or observing nursing pups. Sometimes determining this is difficult since pups will latch onto other females albeit to a lesser extent. Up to three females can be kept with the pups just in case in that event. The difficulty in identifying the mother underscores the need to note which females are observed to be pregnant with planned pregancies.

If pups are born and the mother is not caring for them or is eating viable pups, the litter can be fostered to a mother with pups of roughly the same age. The total number of pups should remain close to that of the original litter, and a few pups from the original litter should be retained to ease the transition. Foster mothers preferably have pups visibly distinguishable from the fostered pups. Newcomers can be rubbed with bedding to discourage rejection. Good maternal care is indicated by visible milk within the semi-transparent newborns. Fostering can also be done at later ages. Keep red special instruction cards reading "No bedding change" on until about P5, when stubble appears, pigment reduces redness to a pink hue, digits separate, ears protrude laterally and the body becomes plump.

As pups mature, runts may appear. Check that functional teeth have emerged and sack or nurse (if valuable) any pups showing malocclusion. Runting

can be attenuated by removing robust pups from the mother for a few hours to allow the runt(s) to nurse, if it is feasible / worth the effort. -/-;-/- mice require special care because they have difficulty nursing in the presence of non--/-;-/- pups particularly in the case of backcrosses to inbred strains. After P10 -/-;-/- mice can be fairly easily identified, allowing the number of non--/-;-/- mice to be reduced by culling. If competition is not reduced to more than a couple non--/-;-/- mice to ensure free nipples by P14, -/-;-/- mice will likely perish. It is important to try to use a food hopper with young -/-;-/- mice with a round hole for one time an uncoordinated -/-;-/- mouse became stuck in the oval hole in one of the hopper types. Upon turning its head ninety degrees it could not go back through. The mouse lacked the insight and coordination necessary to emerge from the predicament.

If the male was present perinatally, there is a high likelihood that there was a conception during the postpartum estrus. Thus, when the litter reaches P17 check the mother for pregnancy and if she is pregnant the pups will have to be weaned early to prevent overcrowding, which risks trampling of the second litter. Early weaning (technically before P21) requires provision of food pellets, preferably wetted, on the floor, a Petri dish of water and placement of a red tag with a neon green charge lixit sticker that should request charging by the ARC tech for several days. The mother should be moved to fresh bedding with a nestlet and the red “No bedding change” tag should be applied. The entire litter can be kept in the same cage until P21. Before P28 mice are small enough that up to ~7 can be kept in the cage (exact rules regarding the weight of mice and limits on how many can inhabit a cage are complex, and whether this will pose a problem depends on your particular ARC tech’s meticulousness and interpretation of “the law”). Shepherd shacks should be removed around P13 once eyes open and pups begin to ambulate about the cage for this allows for the development of proper coordination during a critical period (per ARC vet techs).

A good time to tag and tail pups is between P18-P21. Although ears are somewhat smaller and tags slightly more likely to be removed, it is economical and efficient in terms of labor to genotype at this time because results can be obtained prior to the absolute weaning deadline of P28, obviating the need to sort mice twice (see section 2.1 for tailing details). It’s helpful to sprinkle food pellets on the floor to ease the transition to eating solid food. If there are >10 pups, it may be necessary to wean by P21 depending on how strictly this is enforced. Runts or the smallest mice in the litter are preferably kept with the mother until P28. DKOs should not be weaned until P28 or at the earliest P21. If weaned before P28, a water dish should be provided and food kept on the floor. DKOs from backcrosses to inbred strains may need more attention and soft food. Lixit charging tags should definitely be placed on the cage. Generally, because typically only 1-4 DKOs are born per litter, DKOs can be kept with the mother not exceeding 3 adults with one litter. Alternatively, newborns could be fostered if a foster mother happens to be available. Weaned DKOs can be housed in any combination desired because they cannot breed nor fight.

Once genotyping results are obtained prior to the P28 wean deadline, pups of unwanted genotypes of no potential miscellaneous use can be sac'ed and those of desired genotypes parsed into cages of no more than 5 mice. Requirements of specific experiments or line maintenance may differ, but there are a few good rules of thumb. Male mice can often be consolidated from different litters if united before P28. Afterward fighting is increasingly likely. Females can almost always be resorted later at will but males more or less need to remain with the same male cagemates for life. If males are removed from the group of five other males generally cannot be added because they will fight. Therefore one should plan to use multiples of 5 mice to prevent having one or two mice consuming potential space for 5 mice for long periods. Accordingly an effort should be made out of economics to either pare down the number of mice of a given sex to multiples of 5, if mice of the desired genotypes are abundant, or retain a few mice of potential miscellaneous use (so-called "scrub mice") to fill all cages with 5 mice.

Prevent adverse evolution by avoiding breeding offspring of poor parents (mating, fecundity or parental care) or highly aggressive mice (where aggression is part of the mutant phenotype, just don't select exceptionally aggressive ones).

1.3 Use in experiments

For behavioral experiments, mice can be taken to any common procedure rooms. Here they can be handled outside the hood, by necessity, but the area should be cleaned with NPD disinfectant before and after. Ideally one should wipe gloves and equipment between handling mice from different cages or at least racks to prevent potential spread of as-yet-undetected pathogens, although this is extremely rare in a clean facility.

Note that males removed from their cages housed with other males will entail fights for three principal reasons. First, the hierarchy and territorial distribution is disturbed, and males will attempt to establish a new order. Second, once a removed male is returned, the male may have smelled or worse acquired female urine during testing, which contains pheromones that elicit fighting. Third, if the reintroduced mouse merely smells unfamiliar from potentially any acquired scent or contact with unfamiliar males it will likely be assaulted. Females typically will not fight under these circumstances.

Mice can be identified using the Joho Lab system by eartags normally or if tags are lost which ear the tag was in as well as potentially punches. A tear should be evident on that side.

1.4 Imports and exports

On campus exports from NG can be executed within 72 hours as NG is a clean facility obviating the need for quarantine. There is an online animal transport form on the ARC website. Imports from other vivaria on campus require a ~6 week quarantine in NG if not also in their vivarium of origin if they were

infected with pathogens already. Serology is conducted by Joe Fields under the direction of Dr. Robert Lu. Once mice are seronegative in NG quarantine they can join the colony. The same is true for imports from other institutions. Mice can be ordered of specific strains (i.e. C57/BL/6) from outside vendors (i.e. Jackson Labs, C57/BL/6/**J** –even inbred strains differ slightly between vendors, so note the suffix. 129 mice have the most heterogeneity) through Dan Olsen in the ARC front office. One box costs ~$80.00. Males and females can be shipped in one box by requesting a divider, if it is desired that they not breed amongst themselves in transit. Mice are best ordered in spring or fall because of respiratory infections in the winter and the risk of overheating in the summer, especially in Dallas. Some feel that it is better to have mice shipped by air than truck but there are pros and cons. There may be better climate control during flights than in trucks but mice may sit at the airport with poor climate control, which can even be fatal.

2. Genotyping

2.1 Tailing

Usually it is most convenient to tail and tag at weaning (P18-P28). The ideal time however is P21 in terms of better tag retention, ease of tagging, minimizing distress to mice and ability to mix males of different litters without fighting. By genotyping before the P28 wean deadline, unwanted mice can be discarded upon obtaining results, minimizing the number of cages needed while awaiting genotyping results.

Have ready enough eartags, enough tail tubes, stainless nail-clipping scissors, tag applicator and ear puncher.

Separate males and females (useful convention is put males in fresh cage on right, females in empty food hopper, then put females back in original cage on the left. First tag males then females).

Enter litter DOB in excel sheet and copy-paste it into a total number of cells corresponding to the total number of pups. Copy-paste m's and then f's corresponding to the numbers of each sex, looking at the right and left cages conveniently. Then copy-paste from above, or type de novo, the coat colors (conventional order: Agouti, L [light] Agouti, Black, White, Gold aka Hay aka Fawn, Grey, Brown, Chinchilla). Note on the right in margin parents ("male tag#x female tag#") to keep track of family tree.

Put tag in applicator and position it poised upright ready to go in foam holder.

Label free-standing boil-proof 2 ml tube with alcohol-resistant marker on tethered screw cap (tubes: Corning 430915).

Tag ear by holding entire scruff of mouse (head to tail)[11], with tail held with the middle finger to restrain hindquarters, and letting mouse bite the edge of a cage (distraction) until an opportune moment arises when the tag can be inserted deeply into the ear (mitigates tag loss; ear lobe fills-out into it as it grows) but without hitting bone. Be patient. Hold applicator in right hand for right ear, left hand for left. Scruff mouse in opposite hand.

Before letting go of mouse punch or clip opposite ear if necessary.

Cut 0.25-0.75cm tail, close cap, tap sample down to bottom of tube to make sure it's there. Note: if tailing or retailing old mice (avoid if at all possible), put quick stop glob on cotton swab before tailing mouse to dab for several seconds onto tail immediately after cutting to stop bleeding and provide local anesthesia.

Pick up tip (not bloody end) of tail with ear puncher and drop into tube.

Arrange tubes in a row.

Look at row of tubes before placing them in a sealable bag. Ensure that all eartag numbers are there consecutively. An error will become immediately apparent by looking at tubes this way.

Do not let tails sit at room temperature for more than a couple hours; it is good idea to put tails in the freezer in the animal facility, if available, if a lot of tail cutting is yet to be done that may exceed 2 hours. DNA yield is important for the protocol used here to work.

Wipe down tools with NPD disinfectant, except near hinge of tag applicator to minimize rust. Spray foam holder copiously with NPD.

---

[11] The key things are to 1) Hold the tail far enough from the body to leave room for the other hand 2) Have relaxed, confident, resolute agility 3) Wait until the mouse is facing straight ahead, keeping glove nearby before lunging because the mouse can smell it approaching 4) Hold the entire length of one's thumb along the side of one's hand to apply instant pressure to the entire back of the mouse to restrain it, even the neck, pressing forward slightly 5) Pinch the scruff by rolling one's thumb tightly against the side of one's hand to hold the mouse. In general, minimize the time the mouse is restrained <100%, for it is restraint itself that provokes the mouse to bite. If the mouse is being restrained, it must be fully restrained. That's why resolve is important. If a mouse is poorly restrained, put it down and re-establish proper grip. If a mouse eases loose and is going to bite, immediate release will almost instantly abate the motivation of the mouse to bite.

2.2 DNA preparation

DNA is added directly to the PCR reaction from the proteinase K digest rather than purified by phenol:chloroform or salting-out. Generally, if primers and the chosen template are optimal, purification should be unnecessary (see section 2.3, PCR, and Appendix I). The hotshot method obviating the need for proteinase K digestion, that reputedly saves time and money, suffers from unreliability, often necessitating repetition. Here a modified version of the GNT-K buffer method (Biotechniques (1997) *22*:1114-1118) is used where additionally DNAse is heat-inactivated prior to proteinase K digestion ("Hurlock Modification"). There is no EDTA in the buffer but rather added Mg as well as various other components thought to foster the PCR reaction found in PCR buffers. Essentially the DNA is digested in a mild detergent that will not subsequently destroy Taq polymerase when added to the PCR reaction. In this same vein, heat inactivation of proteinase K is key to avoid destroying Taq.

DNA Preparation Protocol:

Remove tails from freezer, dump sealable bag on benchtop[12].

Stand up tubes to see numbered caps and then order them, spaced every other slot, in microcentrifuge tube racks, with tethered caps open.

Squirt 200ul GNT-K buffer (see Appendix III)[13] into each tube with a filter tip. Ensure tail is submerged.

Tightly close caps and place tubes on a heat block at 90-95C or boiling water for 15 minutes (at 30 minutes may start to see detrimental effect) to denature DNAse, which protects DNA from degradation during PK digest and may also help remove histones. This is a critical step that makes a night-and-day difference.

Let tubes cool on the benchtop until they are ~60C or cooler. At this point DNA will only slowly degrade, measured on a timescale of weeks.

Open caps. Add 2ul of 1230U/ml liquid proteinase K (i.e. Sigma P4850) using filter tips, close caps, and pulse on vortex for second to mix as well as collect condensation.

---

[12] A supply of tube racks and lids or boxes can be cycled between the lab and ARC but all materials must be cleaned with NPD; a matter of personal preference. Racks tend to spill.

[13] Another good option supposedly is the proprietary Direct PCR buffer by Viagen, or just use Tween-20. I have not tried these with the PCRs in the Joho Lab.

Place tubes overnight (12-18 hours) on orbital shaker in oven set at 55˚C, shaking fast enough to gently agitate the solution, ~30rpm. A four-hour incubation suffices at minimum, and another microliter of proteinase K can accelerate digestion.

Remove tails from oven and swish solution. The connective tissue skeleton should distintegrate to small bones, hair and debris if digestion is complete.

Spin tubes at ~10,000-13,000*G* for 5 minutes to pellet debris. Keep tubes at 4 C for a few weeks but freeze for long-term storage. Frost-free is OK since the DNA template for genotyping is typically short, so shearing by ice crystals is of minimal concern.

2.3 PCR

Although PCR has the potential to be highly sensitive, sensitivity depends on how many cycles are used, rounds of PCR and template purity. Contamination can be introduced by pipetting (use all filter tips for anything going into PCR reaction to be safe) or dirty tools during tailing (wipe blood), however usually substantial DNA needed using the number of cycles and one round used in genotyping PCRs. Negative controls lacking template can reveal contamination.

With genotyping yield is often more of a concern. Transgenes in particular often have no band signifying a genuine negative since a genomic integration site junction is typically not elucidated. A negative can be a true negative or mere failure to detect, a call aided by having a comparably-prepared positive control. Null alleles exist in single copies in heterozygous mice. Although here the junction is known (generally), and there are two bands involved, one may fail to amplify while the other still looks robust. The chance of this can be attenuated by fine tuning the relative concentrations of the two primer pairs to balance processivity. Nonetheless, the most frequent problem is obtaining bands at all with DNA samples that do not require a lot of time or hazardous, expensive reagents to prepare.

New PCRs should incorporate the design principles outlined here and existing PCRs adopted by the lab that are not compatible with the efficient DNA preparation methods outlined herein should be redesigned, unless the mice are only to be used for a few experiments such that the increase in efficiency gained does not compensate for time invested engineering. The PCR should amplify a region with the most suitable template for PCR. Genomic DNA is notorious bad PCR template in general, so if possible, coding regions of transgenes should be targeted. Problematic features of genomic DNA include GC-rich regions such as CpG islands (the rocky shoals that sinks the polymerase ship), repeats and secondary structures, especially GC-rich ones. Use of additives in the master mix, such as betaine or DMSO, can help melt GC-rich DNA to some extent and

should be tried at loci where primers cannot be repositioned. Once a promising template is found to generate bands ranging between 150bp-1kb, good 18-23bp primers should be selected from a large pool of potential pairs given the ever-lower cost of oligos designed to be cross-compatible having melting temperatures around 58C (see also Appendix I below). Design primers to all work well using single PCR program if possible for simplicity to avoid errors and for efficiency.

The optimal reaction conditions for different primers may differ but often it is possible to multiplex PCRs in the same reaction for efficiency. Raising magnesium or the primer concentration helps yield up to a point of diminishing return but at the cost of decreased purity; non-specific bands are more likely at higher concentrations. Enzyme concentration again can be raised up to a point of diminishing return. Intact dNTPs are crucial. These should be kept at -80C or otherwise in a non-frost-free freezer and aliquoted. They should be added just before enzyme given their expense. Always return dNTPs to the freezer as soon as possible and thaw them on ice or very rapidly by rubbing; do not leave on the benchtop. Taq can be made very economically in the lab using engineered bacteria and a protein purification column. RedTaq (Sigma) is more expensive but saves having to mix loading dye with samples and therefore time. Always add Taq last and do not vortex beyond “shake” settings to mix. Note whether it can be frozen or not, and at what temperature, in the buffer it is in. Frost-free freezers are not recommended.

Note that the nonlinear nature of PCR makes it potentially affected in all-or-nothing ways, and beyond a certain template concentration saturation of band intensity may occur.

PCR protocol:

Thaw primers, 25mM MgCl, 10X Red Taq buffer, and, on ice, 2.5mM dNTPs. dNTPs are unstable and should only be thawed immediately by hand or on ice. Do not leave them out on ice more than a couple hours and always store as aliquots (i.e. 200ul 2.5mM). Sigma sells 10mM dNTP sets that can be combined by making up 25% of the volume with each of the four dNTPs for a 2.5mM final concentration of each. Keep at -80C / not in frost-free freezer.

Go to excel sheet and count how many samples need to be run for each PCR. Write intervals i.e. 315 to 330, then add 1 to the interval (16 samples), then sum these for the total number of samples. Run though calculations on PCR worksheets described above.

Get out relevant tubes, including controls. Spin down debris if it is unsettled (1 minute 10,000*G* pulse is sufficient). Array tubes for PCR reaction in order in a tube rack leaving the first hole in the rack empty.

(While tubes thaw, if frozen, and/or spin) Open online archive of Word files of each PCR reaction made from adaptable templates for each set of primers (i.e. Kv3.1, Kv3.3, L7 & eGFP transgenes). Plug in total at the top and derive multiplier to multiply each reagent by. There should be enough excess for a couple controls. Try to run at least a positive control and negative control. An additional negative control that lacks template is beneficial to assess contamination of master mix/reagents.

Vortex all thawed reagents. The 10X buffer must always be vortexed to redissolve and/or distribute components that get separated when ice crystals form. For unknown reasons, not vortexing other reagents causes problems. Do *not* vortex the Taq enzyme.

Place reagents in ice bucket. Nearby place PCR 96-tube grids.

Assemble master mix in order in PCR worksheet by first pipetting 10X buffer into tube that will accommodate the full volume[14] *Always use filter tips for PCR reagents*. Do not pipette beyond the measured amount; the retentate in the tip is excess due to glycerol-containing solution clinging to the tip walls.

Next add the water. Should be autoclaved ddH2O, replaced regularly to avoid contamination.

Next add in any order the following reagents: MgCl2, primers and dNTPs. The latter are more expensive and best added last. Vortex ideally before adding enzyme so that the salt concentration is optimal since keeps the enzyme in good shape.

Finally, if everything else was added correctly, add the more precious reagent, Red Taq polymerase (Sigma).

Mix this master mix by vortexing gently on “shake” setting, and/or triturate. The red dye will indicate mixing, but mix more to be sure.

Arrange thick-wall 0.2ml PCR tubes[15] in grids on ice sufficient for anticipated number of samples.

Distribute 25ul of master mix to each tube.

---

[14] If 2ml is exceeded, can truncate 14ml culture tube with scissors. Also giant microcentrifuge tubes are sold that can be tightly closed.

[15] Changing suppliers risks necessitating adjustments to PCR program if primers are of borderline quality. Tubes should fit snug in the thermocycler and not spring upward when pressed down. We are currently using GeneMate from ISC Bioexpress.

Add 1ul of template without touching hair pellet to each PCR tube individually. Move tail DNA tube one space to the left, and transcribe the number to the PCR tube with sharp, alcohol-resistant marker.

Leftover reactions can be used for additional controls. Positive controls should at least include a sample where each multiplexed band is present. In addition, those with each of the multiplexed individually can be added to discriminate background/ghost bands. Negative controls can be the latter, mutually for individual multiplexed bands, or just a template sample that should yield bands, at least possible in the case of transgenes lacking a negative band. Also, to control for contamination of buffers, a control lacking DNA template just including master mix or GNT-K tail DNA buffer can be added if there is still room.

Load thermocycler and run PCR. Ideally, design primers so that they all are compatible with the same PCR program to avoid mistakes and maximize efficiency, obviating the need to wait for serial PCRs. If necessary, the reactions can wait several hours on ice, with little diminution in product observed even after sitting overnight. Be sure lid is heated. Keeping tubes a 4C overnight after the reaction is unnecessary and just wears-out the compressor.

Make 1.4-1.6% agarose gel >30 minutes before but not >1 week before thermocycling is complete. For model 75.2321 Continental Lab Products (CLP) gel apparatus, dissolve ~3g of fine powdered agarose in 200ml 1X TAE buffer[16] (without ethidium bromide) in Corning 500ml media jar with the cap loosened by microwaving ~2 minutes. Periodically swish every ~30 seconds. Add ***5ul of 10mg/ml ethidium bromide***[17] for every 100ml of gel (10ul) *after* microwaving. Swish to dissolve. Place 2 50-well combs into gel casting and then pour in gel at 4C[18]. Cooling is not necessary. Bubbles don't matter. The gel is ready to use in 30 minutes and will remain moist at 4C for hours. For longer storage periods wrap gel in casting tray in plastic wrap. Pull comb carefully.

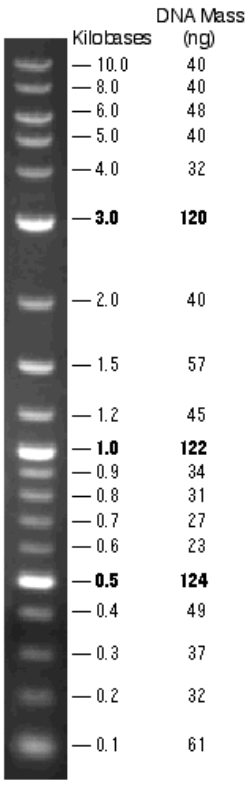

Place gel in tank with 1X TAE buffer with ethidium bromide added (***50ul/l or 10mg/ml stock per liter***).

e from 50X stock: For 1L, 242g Trizma base, 57.1ml
0.5M EDTA pH 8.0, and pH to 8.5 using HCl. To
consult Molecular Cloning. Used TAE remains good
nk. Condensed TAE may lead to blurry or smiling

itate forms at the bottom. Caution: carcinogen.
bottle by the cap as it is prone to being dropped if
rubber gripper to hold bottle, which is needed

Stir buffer between running gels. Do not touch things in the lab with gloves laden with ethidium bromide. Load gel with 17ul of each 25ul sample, starting actually with the lowest row so that any unused rows will remain uncontaminated at the top for later use. Load 5ul of 2 log NEB ladder solution[19] (see left) once per row. Run gel at 120V for ~30 minutes.

Transport gel to Alpha Innotech imager on a tray to prevent spillage of ethidium bromide. Bring compatible zip disk.

Carefully slide gel onto fluorescent lamp. Press out bubbles. A puddle of water helps to maneuver the gel. Make sure filter wheel is on ethidium bromide and turn it physically beneath camera if computer fails to control it. Click[20] expose preview (green button) with an exposure time of 1s and optimize zoom, light level and focus via black knobs on camera above box with the door open. Maximize the light level unless it is too much even with a 1s exposure, then optimize exposure time. The bands should be just visible not overexposed. Acquire image (red button). Set filtering to 4 by going to 3-D tab under filters tab in tools box. Acquire again if bands are now too intense. Save image as date followed by relevant genes in lab folder (i.e. “El Igor de Joho”). Copy tif file(s) to zip disk. Never touch zip disk with gloves.
Retain gel at 4C under plastic wrap until it is certain that it does not need to be scrutinized again.

2.4 Archiving of PCR data

Not only is heat sensitive film expensive, but there are also several key advantages to keeping a digital log of every PCR. Digital images can capture in a single image at high resolution the entire gel, can be arranged with neat labels in a layout using Microsoft publisher or Powerpoint or other software, can be archived to make extra copies readily, do not depend a continued supply of film with a functional printer, and can be conveniently accessed anytime from one’s laptop, including that which one brings to the vivarium in case a band must be double-checked, etc.

Tif images from the zip disk can be downloaded to the imaging computer with Photoshop and Microsoft Photo Editor. In Photoshop the image can be cropped and inverted by going to image, adjust, and invert. The image can then be opened in Photo Editor to save it as a tif that can be opened outside of Photoshop. Discard images on zip disk and periodically clean folder on shared computer used for image acquisition as a courtesy.

Insert each tif file into a Microsoft Publisher layout where they can be labeled with text boxes that one can copy-paste rapidly via control+C and

[19] 20% NEB 2-log ladder, 20% 5X loading dye (40% v/v glycerol with 0.25%w/v orange G) and 60% 1X TE pH 8.0; kept at 4C. Freeze ladder stock.
[20] Caution: Mouse and keyboard should be handled with gloves.

control+V, respectively. Excel files housing the mouse inventory can then be opened alongside the layout to type-in the genotypes. **Joho Lab bands**: Kv3.1: WT=216bp; null=420bp, Kv3.3: WT=594bp; null=~300bp[21], tTA=400bp (i.e. L7tTA transgenic), GFP=546bp (i.e. all pBI GFP/Kv transgenics), pBI[specific channels] not shown.

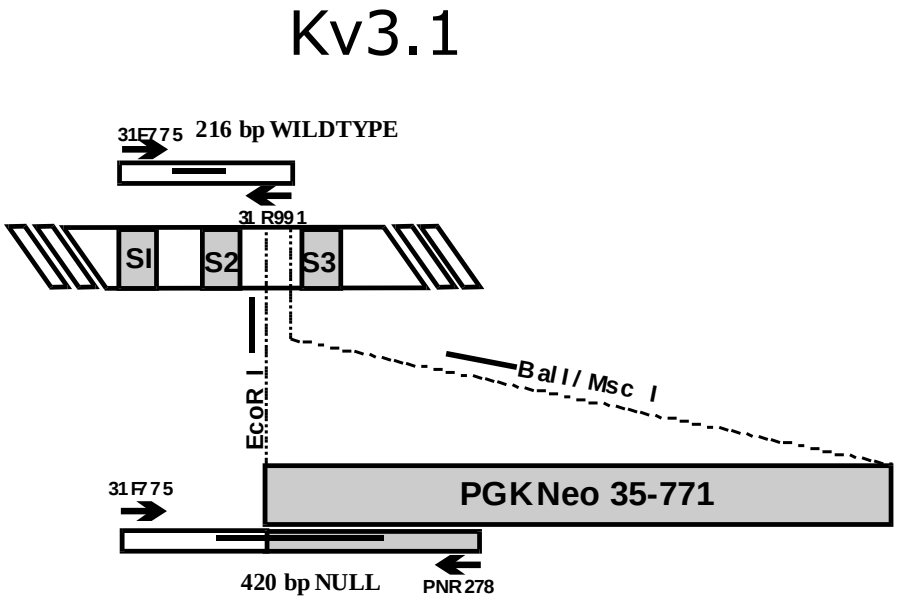

[21] The precise length will remain unknown until the junction between the neo insert and the genomic DNA is sequenced for the amplicon spans this junction. The wildtype band is located entirely in the deleted region 5' to Kv3.3. The null band spans the 3' junction of the neo insert with respect to the genome and the 5' edge of Kv3.3, exon 1. The neo cassette was inserted in reverse with regard to Kv3.3 to prevent inadvertent Kv3.3 transcription from the pgk promoter, so the 5' null genotyping primer is near the 5' end of the neo cassette with regard to the direction of neo transcription and the 3' end of the insert with regard to Kv3.3 transcription. Neo was inserted at the 5' end of Kv3.3, near the two alternative initiator methionines.

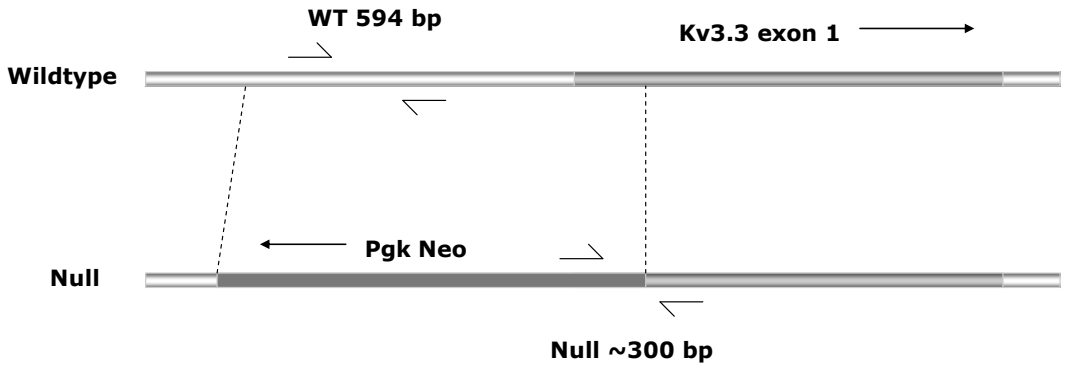

Appendix I:

GNT-K buffer:

50 mM KCl
1.5mM MgCl2
10mM Tris HCl, pH 8.5
0.01% v/v Gelatin
0.45% v/v Nonidet P-40
0.45% v/v Tween-20
For 500ml:

25ml 1M KCl
625ul 1.2M MgCl2
5ml 1M Tris, pH 8.5
2.5ml 2% Gelatin
22.5ml 10% NP-40
22.5ml 10% Tween-20

Keep at 4C. Prepare and handle only with filter tips.

REFERENCES

Abbott GW, Butler MH, Bendahhou S, Dalakas MC, Ptacek LJ, Goldstein SA (2001) MiRP2 forms potassium channels in skeletal muscle with Kv3.4 and is associated with periodic paralysis. Cell 104:217-231.

Ahn HS, Choi JS, Choi BH, Kim MJ, Rhie DJ, Yoon SH, Jo YH, Kim MS, Sung KW, Hahn SJ (2005) Inhibition of the cloned delayed rectifier K+ channels, Kv1.5 and Kv3.1, by riluzole. Neuroscience 133:1007-1019.

Aizenman CD, Huang EJ, Linden DJ (2003) Morphological correlates of intrinsic electrical excitability in neurons of the deep cerebellar nuclei. J Neurophysiol 89:1738-1747.

Akagi H, Kumar TM (2002) Lesson of the week: Akathisia: Overlooked at a cost. BMJ 324:1506-1507.

Albus JS (1971) A theory of cerebellar function. Math Biosci 10:26-27-61.

Alonso-Espinaco V, Elezgarai I, Diez-Garcia J, Puente N, Knopfel T, Grandes P (2008) Subcellular localization of the voltage-gated potassium channels Kv3.1b and Kv3.3 in the cerebellar dentate nucleus of glutamic acid decarboxylase 67-green fluorescent protein transgenic mice. Neuroscience 155:1059-1069.

Alvina K, Khodakhah K (2008) Selective regulation of spontaneous activity of neurons of the deep cerebellar nuclei by N-type calcium channels in juvenile rats. J Physiol 586:2523-2538.

Armstrong DM (1974) Functional significance of connections of the inferior olive. Physiol Rev 54:358-407.

Armstrong DM, Cogdell B, Harvey RJ (1973) Response of interpositus neurones to nerve stimulation in chloralose anesthetized cats. Brain Res 55:461-466.

Aromolaran KA, Benzow KA, Koob MD, Piedras-Renteria ES (2007) The kelch-like protein 1 modulates P/Q-type calcium current density. Neuroscience 145:841-850.

Bagnall MW, Stevens RJ, du Lac S (2007) Transgenic mouse lines subdivide medial vestibular nucleus neurons into discrete, neurochemically distinct populations. J Neurosci 27:2318-2330.

Balaban CD (1985) Central neurotoxic effects of intraperitoneally administered 3-acetylpyridine, harmaline and niacinamide in sprague-dawley and long-evans rats: A critical review of central 3-acetylpyridine neurotoxicity. Brain Res 356:21-42.

Baranauskas G, Tkatch T, Nagata K, Yeh JZ, Surmeier DJ (2003) Kv3.4 subunits enhance the repolarizing efficiency of Kv3.1 channels in fast-spiking neurons. Nat Neurosci 6:258-266.

Barboi AC (2000) Cerebellar ataxia. Arch Neurol 57:1525-1527.

Barmack NH, Yakhnitsa V (2008) Functions of interneurons in mouse cerebellum. J Neurosci 28:1140-1152.

Barmack NH, Yakhnitsa V (2003) Cerebellar climbing fibers modulate simple spikes in purkinje cells. J Neurosci 23:7904-7916.

Bearzatto B, Servais L, Roussel C, Gall D, Baba-Aissa F, Schurmans S, de Kerchove d'Exaerde A, Cheron G, Schiffmann SN (2006) Targeted calretinin expression in granule cells of calretinin-null mice restores normal cerebellar functions. FASEB J 20:380-382.

Benedetti F, Montarolo PG, Rabacchi S (1984) Inferior olive lesion induces long-lasting functional modification in the purkinje cells. Exp Brain Res 55:368-371.

Bernard G, Shevell MI (2008) Channelopathies: A review. Pediatr Neurol 38:73-85.

Browne DL, Gancher ST, Nutt JG, Brunt ER, Smith EA, Kramer P, Litt M (1994) Episodic ataxia/myokymia syndrome is associated with point mutations in the human potassium channel gene, KCNA1. Nat Genet 8:136-140.

Brumberg JC, Nowak LG, McCormick DA (2000) Ionic mechanisms underlying repetitive high-frequency burst firing in supragranular cortical neurons. J Neurosci 20:4829-4843.

Cannon SC (2006) Pathomechanisms in channelopathies of skeletal muscle and brain. Annu Rev Neurosci 29:387-415.

Catz N, Dicke PW, Thier P (2005) Cerebellar complex spike firing is suitable to induce as well as to stabilize motor learning. Curr Biol 15:2179-2189.

Chakrabarti L, Eng J, Martinez RA, Jackson S, Huang J, Possin DE, Sopher BL, La Spada AR (2008) The zinc-binding domain of Nna1 is required to prevent

retinal photoreceptor loss and cerebellar ataxia in purkinje cell degeneration (pcd) mice. Vision Res 48:1999-2005.

Chan E (1997) Regulation and function of Kv3.3.

Chang SY, Zagha E, Kwon ES, Ozaita A, Bobik M, Martone ME, Ellisman MH, Heintz N, Rudy B (2007) Distribution of Kv3.3 potassium channel subunits in distinct neuronal populations of mouse brain. J Comp Neurol 502:953-972.

Chan-Palay V (1977) Cerebellar dentate nucleus: Organization, cytology and transmitters. New York: Springer-Verlag.

Chen C, Westenbroek RE, Xu X, Edwards CA, Sorenson DR, Chen Y, McEwen DP, O'Malley HA, Bharucha V, Meadows LS, Knudsen GA, Vilaythong A, Noebels JL, Saunders TL, Scheuer T, Shrager P, Catterall WA, Isom LL (2004) Mice lacking sodium channel beta1 subunits display defects in neuronal excitability, sodium channel expression, and nodal architecture. J Neurosci 24:4030-4042.

Cheron G, Servais L, Wagstaff J, Dan B (2005) Fast cerebellar oscillation associated with ataxia in a mouse model of angelman syndrome. Neuroscience 130:631-637.

Cheron G, Gall D, Servais L, Dan B, Maex R, Schiffmann SN (2004) Inactivation of calcium-binding protein genes induces 160 hz oscillations in the cerebellar cortex of alert mice. J Neurosci 24:434-441.

Choi BH, Choi JS, Yoon SH, Rhie DJ, Min DS, Jo YH, Kim MS, Hahn SJ (2001) Effects of norfluoxetine, the major metabolite of fluoxetine, on the cloned neuronal potassium channel Kv3.1. Neuropharmacology 41:443-453.

Chow A, Erisir A, Farb C, Nadal MS, Ozaita A, Lau D, Welker E, Rudy B (1999) K(+) channel expression distinguishes subpopulations of parvalbumin- and somatostatin-containing neocortical interneurons. J Neurosci 19:9332-9345.

Coltz JD, Johnson MT, Ebner TJ (1999) Cerebellar purkinje cell simple spike discharge encodes movement velocity in primates during visuomotor arm tracking. J Neurosci 19:1782-1803.

Critz SD, Wible BA, Lopez HS, Brown AM (1993) Stable expression and regulation of a rat brain K+ channel. J Neurochem 60:1175-1178.

Czubayko U, Sultan F, Thier P, Schwarz C (2001) Two types of neurons in the rat cerebellar nuclei as distinguished by membrane potentials and intracellular fillings. J Neurophysiol 85:2017-2029.

de Solages C, Szapiro G, Brunel N, Hakim V, Isope P, Buisseret P, Rousseau C, Barbour B, Lena C (2008) High-frequency organization and synchrony of activity in the purkinje cell layer of the cerebellum. Neuron 58:775-788.

De Zeeuw CI, Berrebi AS (1995) Postsynaptic targets of purkinje cell terminals in the cerebellar and vestibular nuclei of the rat. Eur J Neurosci 7:2322-2333.

Deng Q, Rashid AJ, Fernandez FR, Turner RW, Maler L, Dunn RJ (2005) A C-terminal domain directs Kv3.3 channels to dendrites. J Neurosci 25:11531-11541.

Denk W, Sugimori M, Llinas R (1995) Two types of calcium response limited to single spines in cerebellar purkinje cells. Proc Natl Acad Sci U S A 92:8279-8282.

Desai R, Kronengold J, Mei J, Forman SA, Kaczmarek LK (2008) Protein kinase C modulates inactivation of Kv3.3 channels. J Biol Chem 283:22283-22294.

Devaux J, Alcaraz G, Grinspan J, Bennett V, Joho R, Crest M, Scherer SS (2003) Kv3.1b is a novel component of CNS nodes. J Neurosci 23:4509-4518.

Diochot S, Schweitz H, Beress L, Lazdunski M (1998) Sea anemone peptides with a specific blocking activity against the fast inactivating potassium channel Kv3.4. J Biol Chem 273:6744-6749.

Dixon JE, McKinnon D (1996) Potassium channel mRNA expression in prevertebral and paravertebral sympathetic neurons. Eur J Neurosci 8:183-191.

Doyle DA, Cabral JM, Pfuetzer RA, Kuo A, Gulbis JM, Cohen SL, Chait BT, MacKinnon R (1998) The Structure of the Potassium Channel: Molecular Basis of K^+ Conduction and Selectivity. Science 280: 69-77.

Duprat F, Guillemare E, Romey G, Fink M, Lesage F, Lazdunski M, Honore E (1995) Susceptibility of cloned K+ channels to reactive oxygen species. Proc Natl Acad Sci U S A 92:11796-11800.

Ebner TJ (1998) A role for the cerebellum in the control of limb movement velocity. Curr Opin Neurobiol 8:762-769.

Eccles JC, Llinas R, and Sasaki K (1966) The excitatory synaptic action of climbing fibres on the purkinje cells of the cerebellum. J Physiol 182:268-269-296.

Einat H, Yuan P, Szabo ST, Dogra S, Manji HK (2007) Protein kinase C inhibition by tamoxifen antagonizes manic-like behavior in rats: Implications for the development of novel therapeutics for bipolar disorder. Neuropsychobiology 55:123-131.

Emamian ES, Kaytor MD, Duvick LA, Zu T, Tousey SK, Zoghbi HY, Clark HB, Orr HT (2003) Serine 776 of ataxin-1 is critical for polyglutamine-induced disease in SCA1 transgenic mice. Neuron 38:375-387.

Engel AK, Singer W (2001) Temporal binding and the neural correlates of sensory awareness. Trends Cogn Sci 5:16-25.

Erickson MA, Haburcak M, Smukler L, Dunlap K (2007) Altered functional expression of purkinje cell calcium channels precedes motor dysfunction in tottering mice. Neuroscience 150:547-555.

Espinosa F, Torres-Vega MA, Marks GA, Joho RH (2008) Ablation of Kv3.1 and Kv3.3 potassium channels disrupts thalamocortical oscillations in vitro and in vivo. J Neurosci 28:5570-5581.

Espinosa F, Marks G, Heintz N, Joho RH (2004a) Increased motor drive and sleep loss in mice lacking Kv3-type potassium channels. Genes Brain Behav 3:90-100.

Espinosa F, Marks G, Heintz N, Joho RH (2004b) Increased motor drive and sleep loss in mice lacking Kv3-type potassium channels. Genes Brain Behav 3:90-100.

Espinosa F, McMahon A, Chan E, Wang S, Ho CS, Heintz N, Joho RH (2001) Alcohol hypersensitivity, increased locomotion, and spontaneous myoclonus in mice lacking the potassium channels Kv3.1 and Kv3.3. J Neurosci 21:6657-6665.

Fernandez FR, Morales E, Rashid AJ, Dunn RJ, Turner RW (2003) Inactivation of Kv3.3 potassium channels in heterologous expression systems. J Biol Chem 278:40890-40898.

Forti L, Cesana E, Mapelli J, D'Angelo Edgidio (2006) Ionic mechanisms of autorhythmic firing in rat cerebellar Golgi cells. J Physiol 574: 711-729.

Fowler SC, Birkestrand BR, Chen R, Moss SJ, Vorontsova E, Wang G, Zarcone TJ (2001) A force-plate actometer for quantitating rodent behaviors: Illustrative data on locomotion, rotation, spatial patterning, stereotypies, and tremor. J Neurosci Methods 107:107-124.

Friederich P, Benzenberg D, Urban BW (2002) Bupivacaine inhibits human neuronal Kv3 channels in SH-SY5Y human neuroblastoma cells. Br J Anaesth 88:864-866.

Fukuda M, Yamamoto T, Llinas R (2001) The isochronic band hypothesis and climbing fibre regulation of motricity: An experimental study. Eur J Neurosci 13:315-326.

Gabbiani F, Midtgaard J, Knopfel T (1994) Synaptic integration in a model of cerebellar granule cells. J Neurophysiol 72:999-1009.

Gauck V, Jaeger D (2000) The control of rate and timing of spikes in the deep cerebellar nuclei by inhibition. J Neurosci 20:3006-3016.

Ghez C, Thach W (2000) The cerebellum. In: Principles of neural science (Kandel E, Schwartz J, Jessell T, eds), pp832-833-852. New York: McGraw Hill.

Gittis AH, du Lac S (2007) Firing properties of GABAergic versus non-GABAergic vestibular nucleus neurons conferred by a differential balance of potassium currents. J Neurophysiol 97:3986-3996.

Goldberg EM, Watanabe S, Chang SY, Joho RH, Huang ZJ, Leonard CS, Rudy B (2005) Specific functions of synaptically localized potassium channels in synaptic transmission at the neocortical GABAergic fast-spiking cell synapse. J Neurosci 25:5230-5235.

Goldman-Wohl DS, Chan E, Baird D, Heintz N (1994) Kv3.3b: A novel shaw type potassium channel expressed in terminally differentiated cerebellar purkinje cells and deep cerebellar nuclei. J Neurosci 14:511-522.

Goldowitz D, Moran TH, Wetts R (1992)
Mouse chimeras in the study of genetic and structural determinants of behavior. In:
Techniques for the genetic analysis of brain and behavior (Goldowitz D, Wahlsten D, Wimer RE, eds), Amsterdam: Elsevier.

Grissmer S, Ghanshani S, Dethlefs B, McPherson JD, Wasmuth JJ, Gutman GA, Cahalan MD, Chandy KG (1992) The shaw-related potassium channel gene,

Kv3.1, on human chromosome 11, encodes the type l K+ channel in T cells. J Biol Chem 267:20971-20979.

Hannigan JH, Riley EP (1988) Prenatal ethanol alters gait in rats. Alcohol 5:451-454.

Hartig W, Singer A, Grosche J, Brauer K, Ottersen OP, Bruckner G (2001) Perineuronal nets in the rat medial nucleus of the trapezoid body surround neurons immunoreactive for various amino acids, calcium-binding proteins and the potassium channel subunit Kv3.1b. Brain Res 899:123-133.

Hartig W, Derouiche A, Welt K, Brauer K, Grosche J, Mader M, Reichenbach A, Bruckner G (1999) Cortical neurons immunoreactive for the potassium channel Kv3.1b subunit are predominantly surrounded by perineuronal nets presumed as a buffering system for cations. Brain Res 842:15-29.

He Y, Zu T, Benzow KA, Orr HT, Clark HB, Koob MD (2006) Targeted deletion of a single Sca8 ataxia locus allele in mice causes abnormal gait, progressive loss of motor coordination, and purkinje cell dendritic deficits. J Neurosci 26:9975-9982.

Heck DH, Boughter J, and Bryant J (2006) Inverted neuronal code in the cerebellum: Pauses in purkinje cell activity are correlated with rhythmic movements. Proc Soc Neurosci 32:.

Herson PS, Virk M, Rustay NR, Bond CT, Crabbe JC, Adelman JP, Maylie J (2003) A mouse model of episodic ataxia type-1. Nat Neurosci 6:378-383.

Ho CS (1996) Generation and characterization of a mutant mouse carrying the disrupted gene for the voltage-gated potassium channel Kv3.1.

Ho CS, Grange RW, Joho RH (1997) Pleiotropic effects of a disrupted K+ channel gene: Reduced body weight, impaired motor skill and muscle contraction, but no seizures. Proc Natl Acad Sci U S A 94:1533-1538.

Hoshino M, Nakamura S, Mori K, Kawauchi T, Terao M, Nishimura YV, Fukuda A, Fuse T, Matsuo N, Sone M, Watanabe M, Bito H, Terashima T, Wright CV, Kawaguchi Y, Nakao K, Nabeshima Y (2005) Ptf1a, a bHLH transcriptional gene, defines GABAergic neuronal fates in cerebellum. Neuron 47:201-213.

Hourez RH, Millard I, Servais L, Vig PJ, Orr HT, Gall D, Pandolfo M, Schiffmann SN (2007) Early electrophysiological anomalies of purkinje cells in a transgenic mouse model of spinocerebellar ataxia type 1 (SCA1). Proc Soc Neurosci 33:.

Hurlock EC, McMahon A, Joho RH (2008) Purkinje-cell-restricted restoration of Kv3.3 function restores complex spikes and rescues motor coordination in Kcnc3 mutants. J Neurosci 28:4640-4648.

Ichinohe N, Watakabe A, Miyashita T, Yamamori T, Hashikawa T, Rockland KS (2004) A voltage-gated potassium channel, Kv3.1b, is expressed by a subpopulation of large pyramidal neurons in layer 5 of the macaque monkey cortex. Neuroscience 129:179-185.

Ishikawa T, Nakamura Y, Saitoh N, Li WB, Iwasaki S, Takahashi T (2003) Distinct roles of Kv1 and Kv3 potassium channels at the calyx of held presynaptic terminal. J Neurosci 23:10445-10453.

Ito M (2000) Mechanisms of motor learning in the cerebellum. Brain Res 886:237-245.

Ito M (1984) The modifiable neuronal network of the cerebellum. Jpn J Physiol 34:781-792.

Ito M, Simpson JI (1971) Discharges in purkinje cell axons during climbing fiber activation. Brain Res 31:215-219.

Jeub M, Herbst M, Spauschus A, Fleischer H, Klockgether T, Wuellner U, Evert BO (2006) Potassium channel dysfunction and depolarized resting membrane potential in a cell model of SCA3. Exp Neurol 201:182-192.

Joho RH, Ho CS, Marks GA (1999) Increased gamma- and decreased delta-oscillations in a mouse deficient for a potassium channel expressed in fast-spiking interneurons. J Neurophysiol 82:1855-1864.

Joho RH, Street C, Matsushita S, Knopfel T (2006) Behavioral motor dysfunction in Kv3-type potassium channel-deficient mice. Genes Brain Behav 5:472-482.

Jorntell H, Ekerot CF (2002) Reciprocal bidirectional plasticity of parallel fiber receptive fields in cerebellar purkinje cells and their afferent interneurons. Neuron 34:797-806.

Kaczmarek LK (2006) Non-conducting functions of voltage-gated ion channels. Nat Rev Neurosci 7:761-771.

Kalume F, Yu FH, Westenbroek RE, Scheuer T, Catterall WA (2007) Reduced sodium current in purkinje neurons from Nav1.1 mutant mice: Implications for ataxia in severe myoclonic epilepsy in infancy. J Neurosci 27:11065-11074.

Kanemasa T, Gan L, Perney TM, Wang LY, Kaczmarek LK (1995) Electrophysiological and pharmacological characterization of a mammalian shaw channel expressed in NIH 3T3 fibroblasts. J Neurophysiol 74:207-217.

Khaliq ZM, Raman IM (2005) Axonal propagation of simple and complex spikes in cerebellar purkinje neurons. J Neurosci 25:454-463.

Kim SE, Ahn HS, Choi BH, Jang HJ, Kim MJ, Rhie DJ, Yoon SH, Jo YH, Kim MS, Sung KW, Hahn SJ (2007) Open channel block of A-type, kv4.3, and delayed rectifier K+ channels, Kv1.3 and Kv3.1, by sibutramine. J Pharmacol Exp Ther 321:753-762.

Kitai ST, McCrea RA, Preston RJ, Bishop GA (1977) Electrophysiological and horseradish peroxidase studies of precerebellar afferents to the nucleus interpositus anterior. I. climbing fiber system. Brain Res 122:197-214.

Kitazawa S, Wolpert DM (2005) Rhythmicity, randomness and synchrony in climbing fiber signals. Trends Neurosci 28:611-619.

Kitazawa S, Kimura T, Yin PB (1998) Cerebellar complex spikes encode both destinations and errors in arm movements. Nature 392:494-497.

Kleim JA, Swain RA, Armstrong KA, Napper RM, Jones TA, Greenough WT (1998) Selective synaptic plasticity within the cerebellar cortex following complex motor skill learning. Neurobiol Learn Mem 69:274-289.

Lau D, Vega-Saenz de Miera EC, Contreras D, Ozaita A, Harvey M, Chow A, Noebels JL, Paylor R, Morgan JI, Leonard CS, Rudy B (2000) Impaired fast-spiking, suppressed cortical inhibition, and increased susceptibility to seizures in mice lacking Kv3.2 K+ channel proteins. J Neurosci 20:9071-9085.

Laube G, Roper J, Pitt JC, Sewing S, Kistner U, Garner CC, Pongs O, Veh RW (1996) Ultrastructural localization of shaker-related potassium channel subunits and synapse-associated protein 90 to septate-like junctions in rat cerebellar pinceaux. Brain Res Mol Brain Res 42:51-61.

Lepicard EM, Venault P, Negroni J, Perez-Diaz F, Joubert C, Nosten-Bertrand M, Berthoz A, Chapouthier G (2003) Posture and balance responses to a sensory challenge are related to anxiety in mice. Psychiatry Res 118:273-284.

Levin SI, Khaliq ZM, Aman TK, Grieco TM, Kearney JA, Raman IM, Meisler MH (2006) Impaired motor function in mice with cell-specific knockout of sodium channel Scn8a (NaV1.6) in cerebellar purkinje neurons and granule cells. J Neurophysiol 96:785-793.

Lien CC, Jonas P (2003) Kv3 potassium conductance is necessary and kinetically optimized for high-frequency action potential generation in hippocampal interneurons. J Neurosci 23:2058-2068.

Linnemann C, Sultan F, Pedroarena CM, Schwarz C, Thier P (2004) Lurcher mice exhibit potentiation of GABA(A)-receptor-mediated conductance in cerebellar nuclei neurons in close temporal relationship to purkinje cell death. J Neurophysiol 91:1102-1107.

Liu SQ, Kaczmarek LK (2005) Aminoglycosides block the Kv3.1 potassium channel and reduce the ability of inferior colliculus neurons to fire at high frequencies. J Neurobiol 62:439-452.

Llinas R, Muhlethaler M (1988) Electrophysiology of guinea-pig cerebellar nuclear cells in the in vitro brain stem-cerebellar preparation. J Physiol 404:241-258.

Llinas R, Ribary U, Contreras D, Pedroarena C (1998) The neuronal basis for consciousness. Philos Trans R Soc Lond B Biol Sci 353:1841-1849.

Luneau C, Wiedmann R, Smith JS, Williams JB (1991a) Shaw-like rat brain potassium channel cDNA's with divergent 3' ends. FEBS Lett 288:163-167.

Luneau CJ, Williams JB, Marshall J, Levitan ES, Oliva C, Smith JS, Antanavage J, Folander K, Stein RB, Swanson R (1991b) Alternative splicing contributes to K+ channel diversity in the mammalian central nervous system. Proc Natl Acad Sci U S A 88:3932-3936.

Macica CM, von Hehn CA, Wang LY, Ho CS, Yokoyama S, Joho RH, Kaczmarek LK (2003) Modulation of the kv3.1b potassium channel isoform adjusts the fidelity of the firing pattern of auditory neurons. J Neurosci 23:1133-1141.

Malumbres M, Mangues R, Ferrer N, Lu S, Pellicer A (1997) Isolation of high molecular weight DNA for reliable genotyping of transgenic mice. BioTechniques 22:1114-1119.

Mariotti C, Fancellu R, Di Donato S (2005) An overview of the patient with ataxia. J Neurol 252:511-518.

Marr D (1969) A theory of cerebellar cortex. J Physiol 202:437-470.

Martin LA, Goldowitz D, Mittleman G (2003) The cerebellum and spatial ability: Dissection of motor and cognitive components with a mouse model system. Eur J Neurosci 18:2002-2010.

Martina M, Metz AE, Bean BP (2007) Voltage-dependent potassium currents during fast spikes of rat cerebellar purkinje neurons: Inhibition by BDS-I toxin. J Neurophysiol 97:563-571.

Martina M, Yao GL, Bean BP (2003) Properties and functional role of voltage-dependent potassium channels in dendrites of rat cerebellar purkinje neurons. J Neurosci 23:5698-5707.

Mathy A, Ho S, Davie JT, Clark BA, Hausser M (2007) Cerebellar climbing fiber axons transmit bursts of spikes. Proc Soc Neurosci 33:.

Matsukawa H, Wolf AM, Matsushita S, Joho RH, Knopfel T (2003) Motor dysfunction and altered synaptic transmission at the parallel fiber-purkinje cell synapse in mice lacking potassium channels Kv3.1 and Kv3.3. J Neurosci 23:7677-7684.

Mattick JS, Makunin IV (2005) Small regulatory RNAs in mammals. Hum Mol Genet 14 Spec No 1:R121-32.

McCrea RA, Bishop GA, Kitai ST (1977) Electrophysiological and horseradish peroxidase studies of precerebellar afferents to the nucleus interpositus anterior. II. mossy fiber system. Brain Res 122:215-228.

McCrossan ZA, Lewis A, Panaghie G, Jordan PN, Christini DJ, Lerner DJ, Abbott GW (2003) MinK-related peptide 2 modulates Kv2.1 and Kv3.1 potassium channels in mammalian brain. J Neurosci 23:8077-8091.

McKay BE, Turner RW (2005) Physiological and morphological development of the rat cerebellar purkinje cell. J Physiol 567:829-850.

McKay BE, Turner RW (2004) Kv3 K+ channels enable burst output in rat cerebellar purkinje cells. Eur J Neurosci 20:729-739.

McMahon A, Fowler SC, Perney TM, Akemann W, Knopfel T, Joho RH (2004) Allele-dependent changes of olivocerebellar circuit properties in the absence of the voltage-gated potassium channels Kv3.1 and Kv3.3. Eur J Neurosci 19:3317-3327.

Messiha FS (1993) Fluoxetine: Adverse effects and drug-drug interactions. J Toxicol Clin Toxicol 31:603-630.

Miall RC, Keating JG, Malkmus M, Thach WT (1998) Simple spike activity predicts occurrence of complex spikes in cerebellar purkinje cells. Nat Neurosci 1:13-15.

Middleton SJ, Racca C, Cunningham MO, Traub RD, Monyer H, Knopfel T, Schofield IS, Jenkins A, Whittington MA (2008) High-frequency network oscillations in cerebellar cortex. Neuron 58:763-774.

Miki T, Zwingman TA, Wakamori M, Lutz CM, Cook SA, Hosford DA, Herrup K, Fletcher CF, Mori Y, Frankel WN, Letts VA (2008) Two novel alleles of tottering with distinct ca(v)2.1 calcium channel neuropathologies. Neuroscience 155:31-44.

Molineux ML, McRory JE, McKay BE, Hamid J, Mehaffey WH, Rehak R, Snutch TP, Zamponi GW, Turner RW (2006) Specific T-type calcium channel isoforms are associated with distinct burst phenotypes in deep cerebellar nuclear neurons. Proc Natl Acad Sci U S A 103:5555-5560.

Monsivais P, Clark BA, Roth A, Hausser M (2005) Determinants of action potential propagation in cerebellar purkinje cell axons. J Neurosci 25:464-472.

Morales E, Fernandez FR, Sinclair S, Molineux ML, Mehaffey WH, Turner RW (2004) Releasing the peri-neuronal net to patch-clamp neurons in adult CNS. Pflugers Arch 448:248-258.

Moreno H, Kentros C, Bueno E, Weiser M, Hernandez A, Vega-Saenz de Miera E, Ponce A, Thornhill W, Rudy B (1995) Thalamocortical projections have a K+ channel that is phosphorylated and modulated by cAMP-dependent protein kinase. J Neurosci 15:5486-5501.

Nakamura Y, Takahashi T (2007) Developmental changes in potassium currents at the rat calyx of held presynaptic terminal. J Physiol 581:1101-1112.

Nakao H, Nakao K, Kano M, Aiba A (2007) Metabotropic glutamate receptor subtype-1 is essential for motor coordination in the adult cerebellum. Neurosci Res 57:538-543.

Nilsson JM, Madeja M, Elinder F, Arhem P (2008) Bupivacaine blocks N-type inactivating kv channels in the open state: No allosteric effect on inactivation kinetics. Biophys J .

Nolan MF, Malleret G, Lee KH, Gibbs E, Dudman JT, Santoro B, Yin D, Thompson RF, Siegelbaum SA, Kandel ER, Morozov A (2003) The hyperpolarization-activated HCN1 channel is important for motor learning and neuronal integration by cerebellar purkinje cells. Cell 115:551-564.

Ojakangas CL, Ebner TJ (1994) Purkinje cell complex spike activity during voluntary motor learning: Relationship to kinematics. J Neurophysiol 72:2617-2630.

Ovsepian SV, Friel DD (2008) The leaner P/Q-type calcium channel mutation renders cerebellar purkinje neurons hyper-excitable and eliminates Ca2+-na+ spike bursts. Eur J Neurosci 27:93-103.

Ozaita A, Martone ME, Ellisman MH, Rudy B (2002) Differential subcellular localization of the two alternatively spliced isoforms of the Kv3.1 potassium channel subunit in brain. J Neurophysiol 88:394-408.

Palay SL, Chan-Palay V (1974) Cerebellar cortex: Cytology and organization. New York: Springer-Verlag.

Pedroarena CM, Schwarz C (2003) Efficacy and short-term plasticity at GABAergic synapses between purkinje and cerebellar nuclei neurons. J Neurophysiol 89:704-715.

Perney TM, Marshall J, Martin KA, Hockfield S, Kaczmarek LK (1992) Expression of the mRNAs for the Kv3.1 potassium channel gene in the adult and developing rat brain. J Neurophysiol 68:756-766.

Peters HC, Hu H, Pongs O, Storm JF, Isbrandt D (2005) Conditional transgenic suppression of M channels in mouse brain reveals functions in neuronal excitability, resonance and behavior. Nat Neurosci 8:51-60.

Porcello DM, Ho CS, Joho RH, Huguenard JR (2002) Resilient RTN fast spiking in Kv3.1 null mice suggests redundancy in the action potential repolarization mechanism. J Neurophysiol 87:1303-1310.

Raman IM, Sprunger LK, Meisler MH, Bean BP (1997) Altered subthreshold sodium currents and disrupted firing patterns in purkinje neurons of Scn8a mutant mice. Neuron 19:881-891.

Rettig J, Wunder F, Stocker M, Lichtinghagen R, Mastiaux F, Beckh S, Kues W, Pedarzani P, Schroter KH, Ruppersberg JP (1992) Characterization of a shaw-related potassium channel family in rat brain. EMBO J 11:2473-2486.

Riant F, Mourtada R, Saugier-Veber P, Tournier-Lasserve E (2008) Large CACNA1A deletion in a family with episodic ataxia type 2. Arch Neurol 65:817-820.

Rudy B, Kentros C, Weiser M, Fruhling D, Serodio P, Vega-Saenz de Miera E, Ellisman MH, Pollock JA, Baker H (1992) Region-specific expression of a K+ channel gene in brain. Proc Natl Acad Sci U S A 89:4603-4607.

Rudy B, Chow A, Lau D, Amarillo Y, Ozaita A, Saganich M, Moreno H, Nadal MS, Hernandez-Pineda R, Hernandez-Cruz A, Erisir A, Leonard C, Vega-Saenz de Miera E (1999) Contributions of Kv3 channels to neuronal excitability. Ann N Y Acad Sci 868:304-343.

Sanchez JA, Ho CS, Vaughan DM, Garcia MC, Grange RW, Joho RH (2000) Muscle and motor-skill dysfunction in a K+ channel-deficient mouse are not due to altered muscle excitability or fiber type but depend on the genetic background. Pflugers Arch 440:34-41.

Sato Y, Miura A, Fushiki H, Kawasaki T (1992) Short-term modulation of cerebellar purkinje cell activity after spontaneous climbing fiber input. J Neurophysiol 68:2051-2062.

Sausbier M, Hu H, Arntz C, Feil S, Kamm S, Adelsberger H, Sausbier U, Sailer CA, Feil R, Hofmann F, Korth M, Shipston MJ, Knaus HG, Wolfer DP, Pedroarena CM, Storm JF, Ruth P (2004) Cerebellar ataxia and purkinje cell dysfunction caused by Ca2+-activated K+ channel deficiency. Proc Natl Acad Sci U S A 101:9474-9478.

Schiffmann SN, Cheron G, Lohof A, d'Alcantara P, Meyer M, Parmentier M, Schurmans S (1999) Impaired motor coordination and purkinje cell excitability in mice lacking calretinin. Proc Natl Acad Sci U S A 96:5257-5262.

Schlaggar BL, Mink JW (2003) Movement disorders in children. Pediatr Rev 24:39-51.

Schmahmann JD (2002) The role of the cerebellum in affect and psychosis. In: The cerebellum and its disorders The role of the cerebellum in affect and psychosis. pp136. Cambridge: Cambridge University Press.

Schonewille M, Khosrovani S, Winkelman BH, Hoebeek FE, De Jeu MT, Larsen IM, Van der Burg J, Schmolesky MT, Frens MA, De Zeeuw CI (2006) Purkinje cells in awake behaving animals operate at the upstate membrane potential. Nat Neurosci 9:459-61; author reply 461.

Sekirnjak C, Vissel B, Bollinger J, Faulstich M, du Lac S (2003) Purkinje cell synapses target physiologically unique brainstem neurons. J Neurosci 23:6392-6398.

Sekirnjak C, Martone ME, Weiser M, Deerinck T, Bueno E, Rudy B, Ellisman M (1997) Subcellular localization of the K+ channel subunit Kv3.1b in selected rat CNS neurons. Brain Res 766:173-187.

Servais L, Bearzatto B, Hourez R, Dan B, Schiffmann SN, Cheron G (2004) Effect of simple spike firing mode on complex spike firing rate and waveform in cerebellar purkinje cells in non-anesthetized mice. Neurosci Lett 367:171-176.

Shakkottai VG, Chou CH, Oddo S, Sailer CA, Knaus HG, Gutman GA, Barish ME, LaFerla FM, Chandy KG (2004) Enhanced neuronal excitability in the absence of neurodegeneration induces cerebellar ataxia. J Clin Invest 113:582-590.

Shin SL, Rotter S, Aertsen A, De Schutter E (2007a) Stochastic description of complex and simple spike firing in cerebellar purkinje cells. Eur J Neurosci 25:785-794.

Shin SL, Hoebeek FE, Schonewille M, De Zeeuw CI, Aertsen A, De Schutter E (2007b) Regular patterns in cerebellar purkinje cell simple spike trains. PLoS ONE 2:e485.

Song P, Yang Y, Barnes-Davies M, Bhattacharjee A, Hamann M, Forsythe ID, Oliver DL, Kaczmarek LK (2005) Acoustic environment determines phosphorylation state of the Kv3.1 potassium channel in auditory neurons. Nat Neurosci 8:1335-1342.

Southan AP, Robertson B (2000) Electrophysiological characterization of voltage-gated K(+) currents in cerebellar basket and purkinje cells: Kv1 and Kv3 channel subfamilies are present in basket cell nerve terminals. J Neurosci 20:114-122.

Steinmayr M, Andre E, Conquet F, Rondi-Reig L, Delhaye-Bouchaud N, Auclair N, Daniel H, Crepel F, Mariani J, Sotelo C, Becker-Andre M (1998) Staggerer phenotype in retinoid-related orphan receptor alpha-deficient mice. Proc Natl Acad Sci U S A 95:3960-3965.

Steuber V, Mittmann W, Hoebeek FE, Silver RA, De Zeeuw CI, Hausser M, De Schutter E (2007) Cerebellar LTD and pattern recognition by purkinje cells. Neuron 54:121-136.

Stolze H, Klebe S, Petersen G, Raethjen J, Wenzelburger R, Witt K, Deuschl G (2002) Typical features of cerebellar ataxic gait. J Neurol Neurosurg Psychiatry 73:310-312.

Sultan F, Konig T, Mock M, Thier P (2002) Quantitative organization of neurotransmitters in the deep cerebellar nuclei of the lurcher mutant. J Comp Neurol 452:311-323.

Sung MJ, Ahn HS, Hahn SJ, Choi BH (2008) Open channel block of Kv3.1 currents by fluoxetine. J Pharmacol Sci 106:38-45.

Suter KJ, Jaeger D (2004) Reliable control of spike rate and spike timing by rapid input transients in cerebellar stellate cells. Neuroscience 124:305-317.

Tarnecki R (2003) Responses of the red nucleus neurons to limb stimulation after cerebellar lesions. Cerebellum 2:96-100.

Telgkamp P, Raman IM (2002) Depression of inhibitory synaptic transmission between purkinje cells and neurons of the cerebellar nuclei. J Neurosci 22:8447-8457.

Tempia F, Kano M, Schneggenburger R, Schirra C, Garaschuk O, Plant T, Konnerth A (1996) Fractional calcium current through neuronal AMPA-receptor channels with a low calcium permeability. J Neurosci 16:456-466.

Teune TM, van der Burg J, de Zeeuw CI, Voogd J, Ruigrok TJ (1998) Single purkinje cell can innervate multiple classes of projection neurons in the cerebellar nuclei of the rat: A light microscopic and ultrastructural triple-tracer study in the rat. J Comp Neurol 392:164-178.

Timofeev I, Steriade M (1997) Fast (mainly 30-100 hz) oscillations in the cat cerebellothalamic pathway and their synchronization with cortical potentials. J Physiol 504 (Pt 1):153-168.

Trudeau MM, Dalton JC, Day JW, Ranum LP, Meisler MH (2006) Heterozygosity for a protein truncation mutation of sodium channel SCN8A in a patient with cerebellar atrophy, ataxia, and mental retardation. J Med Genet 43:527-530.

Uusisaari M, Obata K, Knopfel T (2007) Morphological and electrophysiological properties of GABAergic and non-GABAergic cells in the deep cerebellar nuclei. J Neurophysiol 97:901-911.

Vanderhoff BT, Miller KE (1997) Major depression: Assessing the role of new antidepressants. Am Fam Physician 55:249-54, 259-60.

Veh RW, Lichtinghagen R, Sewing S, Wunder F, Grumbach IM, Pongs O (1995) Immunohistochemical localization of five members of the Kv1 channel subunits:

Contrasting subcellular locations and neuron-specific co-localizations in rat brain. Eur J Neurosci 7:2189-2205.

Velumian AA, Zhang L, Pennefather P, Carlen PL (1997) Reversible inhibition of IK, IAHP, ih and ICa currents by internally applied gluconate in rat hippocampal pyramidal neurones. Pflugers Arch 433:343-350.

Vullhorst D, Jockusch H, Bartsch JW (2001) The genomic basis of K(V)3.4 potassium channel mRNA diversity in mice. Gene 264:29-35.

Vyazovskiy VV, Deboer T, Rudy B, Lau D, Borbely AA, Tobler I (2002) Sleep EEG in mice that are deficient in the potassium channel subunit K.v.3.2. Brain Res 947:204-211.

Walter JT, Alvina K, Womack MD, Chevez C, Khodakhah K (2006) Decreases in the precision of purkinje cell pacemaking cause cerebellar dysfunction and ataxia. Nat Neurosci 9:389-397.

Wang T, Parris J, Li L, Morgan JI (2006) The carboxypeptidase-like substrate-binding site in Nna1 is essential for the rescue of the purkinje cell degeneration (pcd) phenotype. Mol Cell Neurosci 33:200-213.

Watanabe D, Inokawa H, Hashimoto K, Suzuki N, Kano M, Shigemoto R, Hirano T, Toyama K, Kaneko S, Yokoi M, Moriyoshi K, Suzuki M, Kobayashi K, Nagatsu T, Kreitman RJ, Pastan I, Nakanishi S (1998) Ablation of cerebellar golgi cells disrupts synaptic integration involving GABA inhibition and NMDA receptor activation in motor coordination. Cell 95:17-27.

Watase K, Barrett CF, Miyazaki T, Ishiguro T, Ishikawa K, Hu Y, Unno T, Sun Y, Kasai S, Watanabe M, Gomez CM, Mizusawa H, Tsien RW, Zoghbi HY (2008) Spinocerebellar ataxia type 6 knockin mice develop a progressive neuronal dysfunction with age-dependent accumulation of mutant CaV2.1 channels. Proc Natl Acad Sci U S A 105:11987-11992.

Waters MF, Fee D, Figueroa KP, Nolte D, Muller U, Advincula J, Coon H, Evidente VG, Pulst SM (2005) An autosomal dominant ataxia maps to 19q13: Allelic heterogeneity of SCA13 or novel locus? Neurology 65:1111-1113.

Waters MF, Minassian NA, Stevanin G, Figueroa KP, Bannister JP, Nolte D, Mock AF, Evidente VG, Fee DB, Muller U, Durr A, Brice A, Papazian DM, Pulst SM (2006) Mutations in voltage-gated potassium channel KCNC3 cause degenerative and developmental central nervous system phenotypes. Nat Genet 38:447-451.

Weiser M, Vega-Saenz de Miera E, Kentros C, Moreno H, Franzen L, Hillman D, Baker H, Rudy B (1994) Differential expression of shaw-related K+ channels in the rat central nervous system. J Neurosci 14:949-972.

Weiser M, Bueno E, Sekirnjak C, Martone ME, Baker H, Hillman D, Chen S, Thornhill W, Ellisman M, Rudy B (1995) The potassium channel subunit KV3.1b is localized to somatic and axonal membranes of specific populations of CNS neurons. J Neurosci 15:4298-4314.

Welsh JP, Lang EJ, Suglhara I, Llinas R (1995) Dynamic organization of motor control within the olivocerebellar system. Nature 374:453-457.

Xu J, Yu W, Jan YN, Jan LY, Li M (1995) Assembly of voltage-gated potassium channels. conserved hydrophilic motifs determine subfamily-specific interactions between the alpha-subunits. J Biol Chem 270:24761-24768.

Xu M, Cao R, Xiao R, Zhu MX, Gu C (2007) The axon-dendrite targeting of Kv3 (shaw) channels is determined by a targeting motif that associates with the T1 domain and ankyrin G. J Neurosci 27:14158-14170.

Yakhnitsa V, Barmack NH (2006) Antiphasic purkinje cell responses in mouse uvula-nodulus are sensitive to static roll-tilt and topographically organized. Neuroscience 143:615-626.

Yamamoto K, Kawato M, Kotosaka S, Kitazawa S (2007) Encoding of movement dynamics by purkinje cell simple spike activity during fast arm movements under resistive and assistive force fields. J Neurophysiol 97:1588-1599.

Yartsev M, Givon-Mayo R, Maller M, and Donchin O (2007) Simple spike pauses in purkinje cells of the awake cat: Relation to behavioral events and complex spike activity. Proc Soc Neurosci 33:.

Yeung SY, Thompson D, Wang Z, Fedida D, Robertson B (2005) Modulation of Kv3 subfamily potassium currents by the sea anemone toxin BDS: Significance for CNS and biophysical studies. J Neurosci 25:8735-8745.

Zagha E, Lang EJ, Rudy B (2008) Kv3.3 channels at the purkinje cell soma are necessary for generation of the classical complex spike waveform. J Neurosci 28:1291-1300.

Zarate CA,Jr, Singh JB, Carlson PJ, Quiroz J, Jolkovsky L, Luckenbaugh DA, Manji HK (2007) Efficacy of a protein kinase C inhibitor (tamoxifen) in the treatment of acute mania: A pilot study. Bipolar Disord 9:561-570.

Zhang X, Baader SL, Bian F, Muller W, Oberdick J (2001) High level purkinje cell specific expression of green fluorescent protein in transgenic mice. Histochem Cell Biol 115:455-464.

Zoghbi HY, Orr HT (2008) Pathogenic mechanisms of a polyglutamine mediated neurodegenerative disease: SCA1. J Biol Chem .

Zu T, Duvick LA, Kaytor MD, Berlinger MS, Zoghbi HY, Clark HB, Orr HT (2004) Recovery from polyglutamine-induced neurodegeneration in conditional SCA1 transgenic mice. J Neurosci 24:8853-8861.

-